THE CONSTRUCTION AND APPLICATION OF METAL COMPLEXES FOR DNA STRAND SCISSION

Thesis by

Michael Pustilnik

In Partial Fulfillment of the Requirements

for the Degree of

Doctor of Philosophy

California Institute of Technology

Pasadena, California

1995

(Defended July 25, 1994)

ACKNOWLEDGEMENTS

I would like to thank my graduate advisor, Prof. Jacqueline Barton, for introducing me to a wonderful project that helped me develop as a scientist in so many ways, for her advice, encouragement, and for giving me her full support when I needed it the most.

I would like to thank Dr. Rick Cruse for training me in organic synthesis, and for his unmatched generosity. The Karlin group thinks the world of you, and deservedly so.

I would like to thank Dr. Lena Basile for her friendship, and for her generosity in spending countless hours helping me to get my project started. I would like to thank Donna Campisi for her friendship, and for making the years I spent here far more bearable then they otherwise would have been. I would like to thank Dr. Takashi Morii, for the training and encouragement that he gave to me and to others, which has been missed and will be missed for years to come. I would like to thank Niranjan Sardesai for his wise advice that will be sorely missed in the years ahead. I would like to thank Dr. Ayesha Sitlani for her caring friendship, and for being a wonderful listener.

I would like to thank the former members of the Barton group that have meant a lot to me: Dr. Alan Friedman, Dr. Scott Klakamp, Dr. Louis Kuo, Dr. Inho Lee, Dr. Ellen Levy, and Cathy and Bob Murphy. I would like to thank the members of the Barton group, both past and present, who have without exception been both free and generous with their advice and assistance: Michelle Arkin, Dr. Jeff Bocarsly, Debbie Brown, Dr. Christy Chow, Dr. Sheila David, Wayne Davis, Dr. Cindy Dupureur, Kitty Erkkila, Prof. Jim Finholt, Marilena Fitzsimons, Dan Hall, R. Eric Holmlin, Brian Hudson, Yonchu Jenkins, Tim Johann, Dr. Kevin Kingsbury, Dr. Mindy Kirshenbaum, Dr. Achim Krotz, Dr. Eric Long, Ai Ching Lim, Susanne Lin, Dr. Houng-Yau Mei, Tom Shields, Dr. Eric Stemp, Bob Terbrueggen, Prof. Kiyoshi Uchida, Tina Voulgaris,

Sally White, and Dr. Kaspar Zimmermann. I would like to thank Dian Buchness and Maureen Renta for their generous and extremely able assistance. I would like to thank my parents, Phyllis and Seymour, and my sister, Susan, for the caring help that they have always given me.

ABSTRACT

Substitutionally inert transition metal complexes have been constructed which bind to DNA and deliver additional labile metal ions to promote cleavage of the phosphodiester backbone. Both oxidative and hydrolytic DNA cleavage have been explored through the use of different chelates and reactive metal ions.

To explore oxidative chemistry, two complexes, $Ru(DIP)_2DSTM$ and $Ru(DIP)_2DSTE$, have been synthesized by tethering two bis(2-picolyl)amine or bis(2-ethylpyridyl)amine chelates to the $Ru(DIP)_3^{2+}$ moiety. Both complexes promote site-selective oxidative DNA cleavage in the presence of $CuSO_4$ and a thiol, with the site-selectivity being governed by the $Ru(DIP)_3^{2+}$ core. Copper-ligand binding affinity, complex-DNA binding mode, and the Cu^{2+}/Cu^{+} redox potential all appear to sensitively influence the cleavage efficiency. Product analysis of the DNA cleavage reaction is consistent with hydrogen abstraction from C1', C3', and C4' of the deoxyribose ring. The $Ru(DIP)_3^{2+}$ core therefore serves as a vehicle to deliver oxidative reactions to DNA. These complexes may be valuable for the design of drugs that cleave DNA *in vivo*.

The complexes $Ru(phen)_2DSTM$, $Ru(phen)_2$(DSTM-AE), $Ru(phen)_2$(DSTM-AP), and $Rh(phi)_2$(DSTM-AP) have also been prepared so as to explore the delivery of secondary metal ions and functionalities to promote DNA hydrolysis. The complexes each have two tethered bis(2-picolyl)amine chelating groups; the latter three complexes also have two 2-dimethylaminoethyl or 3-dimethylaminopropyl groups designed for general acid assistance. DNA hydrolysis has not been established, but $Ru(phen)_2$(DSTM-AP) promotes efficient DNA cleavage in the presence of Zn^{2+}. Product analysis of DNA oligonucleotide cleavage by $Ru(phen)_2$(DSTM-AP) is consistent with a $^1O_2$ mediated reaction which is remarkably enhanced compared to those of ruthenium complexes lacking the tethered chelates; this reactivity may indicate that $Ru(phen)_2$(DSTM-AP) promotes abasic site cleavage. $Rh(phi)_2$(DSTM-AP), which does not sensitize $^1O_2$ formation, promotes still more efficient DNA cleavage. The mechanism is yet to be established.

TABLE OF CONTENTS

LIST OF FIGURES

LIST OF TABLES

Chapter 1:
Basic Pathways of DNA Cleavage

Deoxyribonucleic acid (DNA) is the basic genetic blueprint of all living things. The basic unit of DNA is the nucleotide, which contains a purine or pyrimidine base, a 2'-deoxyribose sugar, and a phosphate group (Figure 1.1). The base of a nucleotide can be adenine, thymine, cytosine, or guanine. The DNA nucleotides are linked together through highly stable phosphodiester bonds to form a strand. The strand thus consists of a sugar-phosphate backbone, and a sequence of DNA bases. Two DNA strands will anneal to form a double helix, which is the most common DNA structure in living organisms. DNA structure is in fact highly heteromorphic, and is affected by local variations in the DNA sequence, DNA-binding proteins, and other factors. The most common double helical form of DNA is B-DNA (Figure 1.2).

Figure 1.1. Illustration of a single DNA nucleotide, shown here with a guanine base.

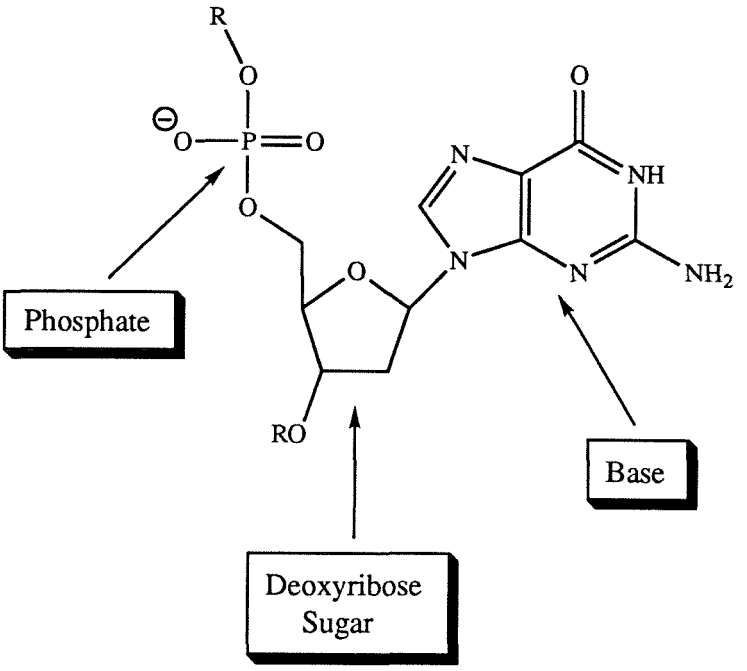

Figure 1.2. B-DNA

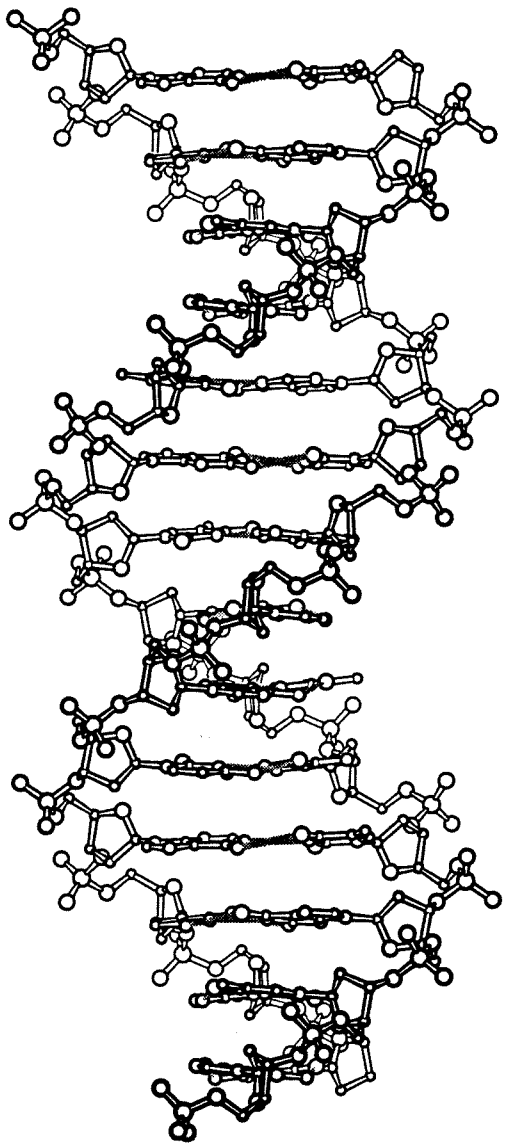

From W. Saenger (1984) "Principles of Nucleic Acid Structure"
Springer-Verlag, New York, 262.

The sequence of the DNA bases is a code that is transcribed into RNA, and then translated into proteins. Proteins play an important structural role in all organisms, and the enzymes, which are a subset of the proteins, are the major source of catalytic function. DNA is therefore a master set of instructions that defines the differences between species, and much of the differences between individuals within a species. Different DNA sequences can result in organisms as diverse as a human being and a single-celled bacterium.

There are several important reasons to study the cleavage of DNA by synthetic molecules. One of them is gene suppression. If a gene is doing damage to a patient, such as an activated oncogene that is contributing to cancer, then the suppression of that gene by DNA cleavage would be an important goal. Similarly, a gene important to the life cycle of a harmful virus could be suppressed by DNA cleavage as an anti-viral therapy. Another important objective is gene mapping and genome sequencing. Cleavage of a large genome or chromosome by restriction enzymes will result in an unmanageably large number of small fragments, but the use of synthetic molecules that promote DNA cleavage at fewer sites could produce larger fragments that could be used for gene mapping. Finally, DNA cleavage with restriction enzymes has been used for gene cloning and manipulation. DNA cleavage by synthetic molecules can be used to supplement restriction enzymes provided that the synthetic molecules produce DNA termini that can be religated enzymatically.

The DNA base, the deoxyribose sugar, and the phosphodiester bond itself are all targets of the various DNA-cleaving molecules. The structure and reactivity of the cleaving molecule will determine the target moiety on DNA. Various DNA-cleaving molecules and their target moieties are summarized in Table 1.1.[1] The nature of the target DNA moiety and of the DNA cleavage chemistry will affect the product DNA

termini. A hydrolytic attack on the DNA phosphate will produce either 5'-phosphate and 3'-hydroxyl termini, or 3'-phosphate and 5'-hydroxyl termini. Most, but not all, natural nucleases utilize this pathway, and produce 5'-phosphate and 3'-hydroxyl termini. Attacks on the DNA sugar frequently involve abstraction of a C1', C3', C4', or C5' hydrogen as the initial step. A series of chemical steps follow the initial hydrogen abstraction that result in DNA strand scission. Some pathways of oxidative attack on the DNA sugar, for instance the oxygen-independent C4' hydrogen abstraction pathway, require treatment with alkali for strand scission. The products of an attack on the DNA sugar will usually be a 5'-phosphate terminus; a 3'-phosphate, phosphoglycolate, or phosphoglycaldehyde terminus; and either a free nucleic acid base or a nucleic acid base attached to a small sugar fragment. Mechanisms subsequent to an attack on the DNA sugar are discussed in chapter 3, and discussed more extensively in Stubbe and Kozarich.[2] An attack on the DNA base will result in either an aldehydic abasic site, or a site containing a damaged base. Generally, efficient strand scission subsequent to the attack on the DNA base requires alkali treatment. The final result will usually be 5'-phosphate and 3'-phosphate termini.

Table 1.1. Molecules that Promote DNA Cleavage and their Target DNA Moieties

DNA-Cleaving Molecule	Target DNA Moiety
Formic acid	Base (G, A)
Dimethylsulfate	Base (G)
$Ru(phen)_3^{2+}$	Base (G > T > C ≈ A)
Neocarzinostatin	Sugar
Fe·bleomycin	Sugar
$Fe(EDTA)^{2-}$	Sugar
$Cu(phen)_2^{+}$	Sugar
$Rh(DIP)_3^{3+}$	Sugar
$Rh(phen)_2phi^{3+}$	Sugar
Restriction enzymes	Phosphate
DNase I	Phosphate
Staphylococcal nuclease	Phosphate

It is useful to divide DNA cleavage into two broad classes: hydrolytic and oxidative. Hydrolytic cleavage involves attack on the DNA phosphate by water or hydroxide. Strong acid will cause DNA hydrolysis, but under mild (physiological) conditions, hydrolysis is strongly impeded by the negative charge and resonance stabilization of the phosphate, and by the poor alkoxide leaving group. The 5'-phosphate and 3'-hydroxyl termini which are the result of DNA hydrolysis by most natural nucleases can be religated enzymatically. Oxidative cleavage involves attack on the DNA sugar or base, and is easily achieved under mild conditions by redox-active metals and reagents. The result of oxidative cleavage is usually a 5'-phosphate terminus, a 3'-phosphate, phosphoglycolate, or phosphoglycaldehyde terminus, and a one nucleotide gap in between. The one nucleotide gap and the absence of the proper (5'-phosphate and 3'-hydroxyl) termini will prevent the DNA from being religated enzymatically. The results of typical hydrolytic and oxidative cleavage are illustrated in Figure 1.3.

For the purpose of developing DNA-cleaving drugs for gene suppression, hydrolytic cleavage may be superior because the functionalities that promote hydrolytic cleavage would tend to be less likely to cause random damage to nearby biomolecules than oxidatively active functionalities. On the other hand, an oxidative DNA-cleaving drug would have the advantage of creating damage to the target gene that might be more difficult to repair enzymatically. But for the purpose of developing new tools for biotechnology, hydrolytic cleavage is clearly superior to oxidative because if the termini are one 5'-phosphate and one 3'-hydroxyl, then the DNA can be religated enzymatically. This would allow for the splicing of interesting genes into plasmids, which could be transformed into bacteria.

Another aspect involved in the design of molecules that promote DNA cleavage is recognition. Molecules that promote sequence neutral DNA cleavage are useful for

Figure 1.3. Illustration of typical termini produced by hydrolytic and oxidative DNA cleavage. Other termini are possible from either pathway.

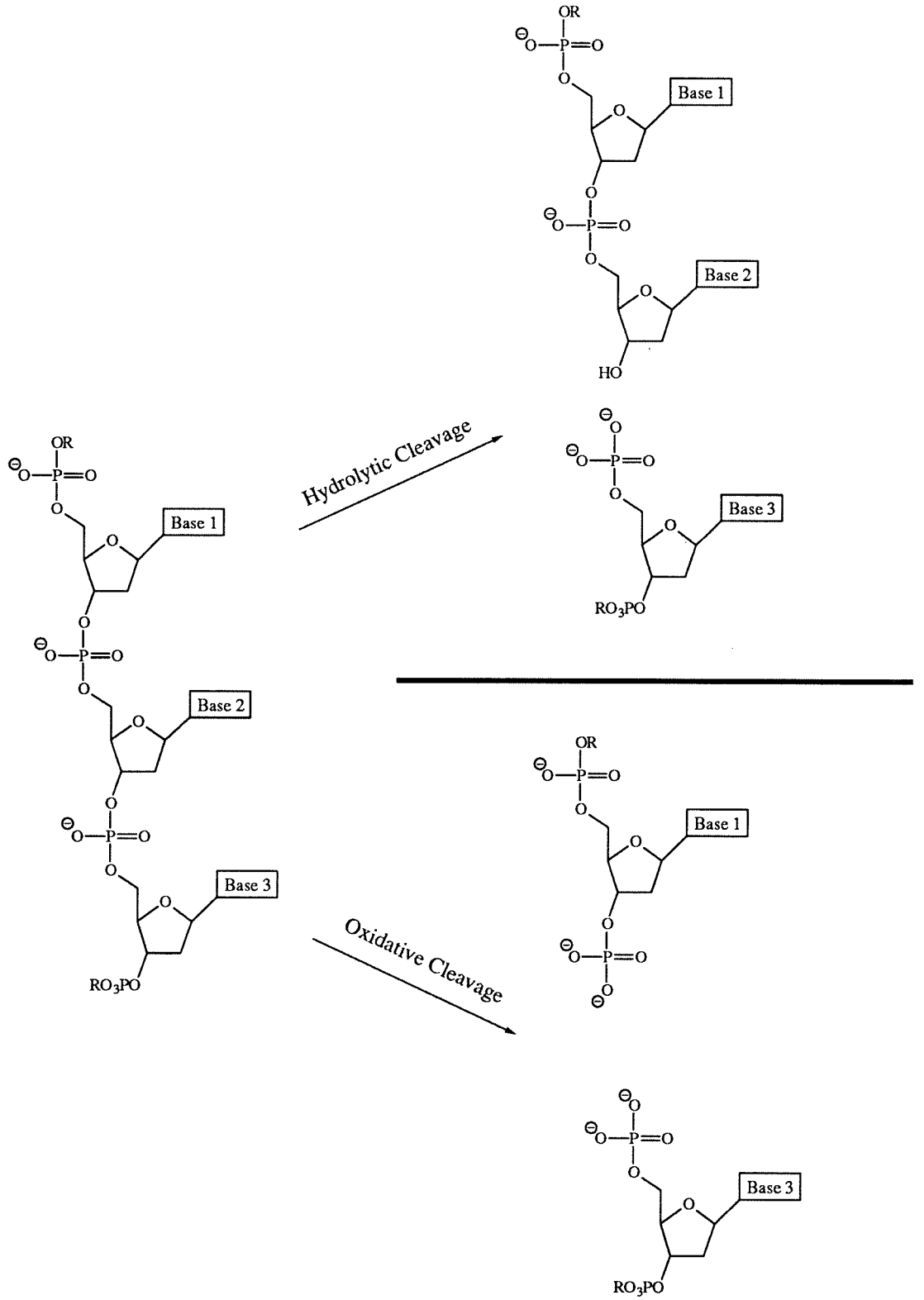

both the footprinting of DNA-binding proteins,[3] and for affinity cleavage.[4] Molecules that promote sequence-selective or structure-selective DNA cleavage would be useful for gene mapping and DNA-cleaving drugs. DNA is structurally heterogeneous, and aspects of both DNA secondary and tertiary structure can be recognized by both proteins and synthetic molecules. Coordinatively saturated metal complexes have been successfully used to explore the recognition of DNA structure. Such metal complexes with rigid, well-defined structures can recognize sites on DNA on the basis of shape or hydrogen bonding interactions. For example, $Rh(DIP)_3^{3+}$ recognizes DNA with tertiary structure (such as a cruciform),[5] while $Rh(phen)_2phi^{3+}$ recognizes sites on B-DNA with an open major groove (such as CCAG sequences).[6]

However, studied here is DNA cleavage chemistry rather than DNA recognition. Coordinatively saturated ruthenium and rhodium complexes, with tethered metal chelates and other functionalities, have been designed. The positive charge, hydrophobicity, and intercalative potential of the complexes provide the driving force for binding to DNA. The tethered chelates, in the presence of additional labile metal ions, could then promote DNA cleavage. Redox-active additional metal ions (such as copper or iron) could be used to study oxidative DNA cleavage, while less redox-active metal ions (such as zinc), in conjunction with other functionalities, could potentially be used to study hydrolytic DNA cleavage. The coordinatively saturated ruthenium or rhodium core complex serves as the delivery system for the cleavage chemistry of the labile metal ions and other functionalities. The ideal is that the structure of the core complex could be varied to affect site-selective DNA recognition, while the tethered chelates, the labile metal ions, and the other functionalities could be varied to affect the efficiency and the oxidative or hydrolytic nature of the DNA cleavage. The result would be cleavage of the desired nature at the DNA site recognized by the core complex.

In chapter 2, the synthesis and the characterization of the metal complexes are described. In chapter 3, the efficient oxidative DNA cleavage reaction of the complexes in the presence of added copper is described. In chapter 4, the possible utilization of the complexes for hydrolytic DNA cleavage in the presence of less redox-active metals is described.

References

1. J. K. Barton & A. M. Pyle (1990) *Prog. Inorg. Chem.* **38:** 413-475.
2. J. Stubbe & J. W. Kozarich (1987) *Chem. Rev.* **87:** 1107-1136.
3. K. Uchida, A. M. Pyle, T. Morii, & J. K. Barton (1989) *Nucl. Acids Res.* **27:** 259-279.
4. J. S. Taylor, P. G. Schultz, & P. B. Dervan (1984) *Tetrahedron* **40:** 457-465.
5. M. R. Kirshenbaum, R. Tribolet, & J. K. Barton (1988) *Nucl. Acids Res.* **16:** 7943-7960.
6. A. M. Pyle, E. C. Long, & J. K. Barton (1989) *J. Am. Chem. Soc.* **111:** 4520-4522.

Chapter 2:
Synthesis and Characterization of Metal-Activated DNA Nucleases

2.1. Introduction

In the design of synthetic molecules that promote DNA cleavage for the purpose of drug design, structural probing, genetic mapping, or the development of new tools for biotechnology, it is useful to divide the proposed molecule into two functional "domains," a binding "domain," and a cleavage "domain." The binding domain of the molecule recognizes specific DNA sequences or structures ("sites") using motifs such as hydrogen bonding contacts, Van der Waal's contacts, and/or steric repulsion. The binding domain serves to deliver the entire molecule to specific DNA sites whereupon the cleavage domain promotes DNA strand scission. Ideally, candidate molecules in the binding and cleavage domains can be developed independently of each other. Variations in the binding domain would allow specific DNA sites to be selected, while variations in the cleavage domain would affect both the efficiency and the nature (e.g., oxidative or hydrolytic) of the DNA cleavage.[1-3]

The approach that was used in the construction of synthetic DNA nucleases utilizes a single ruthenium or rhodium atom at the center of a coordinatively saturated octahedral metal complex. The central metal provides the complex with structural rigidity and with positive charge that increases the binding affinity of the complex towards negatively charged DNA. Each complex contains three phenanthroline-like ligands. Two of the ligands are unfunctionalized and form the binding domain of the complex. The third ligand is functionalized to contain a pair of tethered metal chelates; this is the cleavage domain of the complex. In the presence of additional labile redox-active metals such as copper, the complex can promote efficient oxidative DNA

cleavage. In the presence of less redox-active metals such as zinc, hydrolytic DNA cleavage has been attempted.

This chapter describes the synthesis and characterization of the five complexes $Ru(DIP)_2DSTM$, $Ru(phen)_2DSTM$, $Ru(phen)_2$(DSTM-AE), $Ru(phen)_2$(DSTM-AP), and $Rh(phi)_2$(DSTM-AP); the full names and structures are shown in Figure 2.1. The binding domains of these complexes consist of pairs of 4,7-diphenyl-1,10-phenanthroline (DIP), 1,10-phenanthroline (phen), and 9,10-phenanthrenequinonediimine (phi) ligands. The basis of the cleavage domain is the bis(2-picolyl)amine chelating group. DSTM-AE and DSTM-AP also contain tethered 2-dimethylaminoethyl or 3-dimethylaminopropyl groups, respectively; the intent is that these groups, when protonated, could provide general acid assistance to the leaving group in DNA hydrolysis.

2.2. Experimental

Instrumentation and Materials. NMR spectra were recorded on Varian or JEOL 300 or 400 MHz spectrophotometers. ^1H NMR spectra were referenced to 7.24 for $CDCl_3$, 5.30 for CD_2Cl_2, 4.65 for D_2O, and 2.49 for DMSO-d_6. Chemical shift peak assignments were based on electronegativity, nearest-neighbor coupling, and comparisons to similar compounds. Absorption spectra were recorded on Varian CARY 2200 or DMS 300 UV-Visible spectrophotometers. Extinction coefficients were determined with a Varian Atomic Absorption Spectrophotometer equipped with a GTA-95 Graphite Tube Atomizer. 50% DMF in water was used as the solvent for atomic absorption studies of the extinction coefficient of $Ru(DIP)_2DSTM$. 100% water was used for atomic absorption studies of $Ru(phen)_2DSTM$, $Ru(phen)_2$(DSTM-AE), and $Ru(phen)_2$(DSTM-AP). Since the extinction coefficients of the above three $Ru(phen)_2L$

Figure 2.1. Ruthenium and Rhodium Complexes with Tethered Metal Chelating Groups

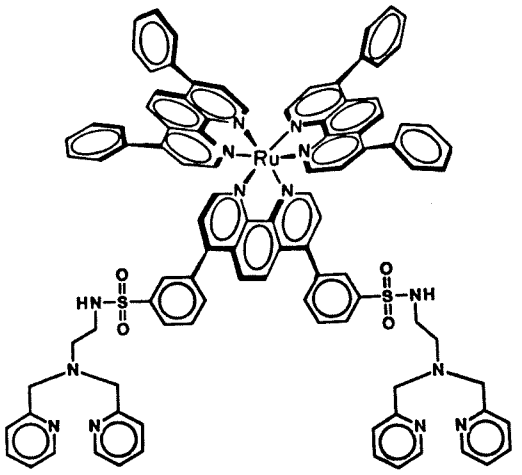

$Ru(DIP)_2DSTM$

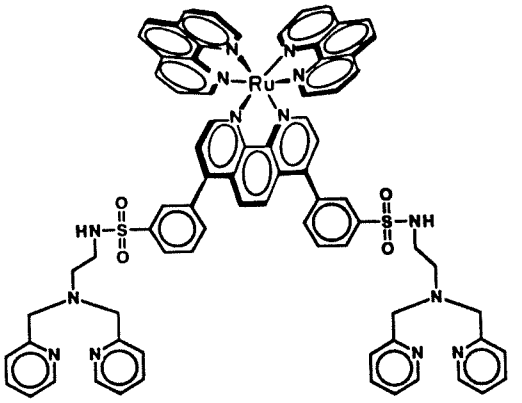

$Ru(phen)_2DSTM$

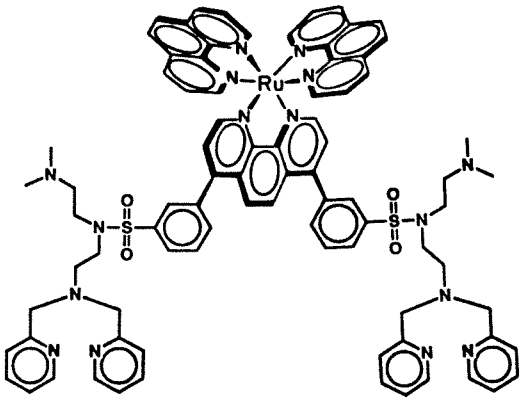

$Ru(phen)_2(DSTM\text{-}AE)$

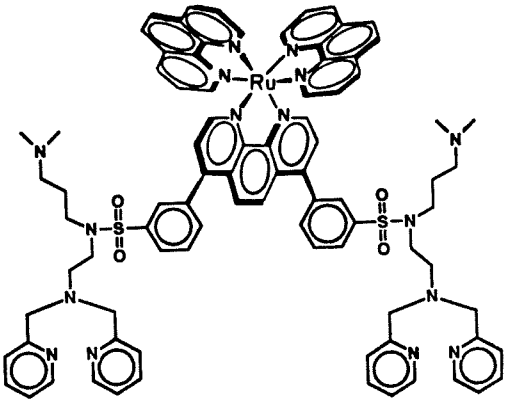

$Ru(phen)_2(DSTM\text{-}AP)$

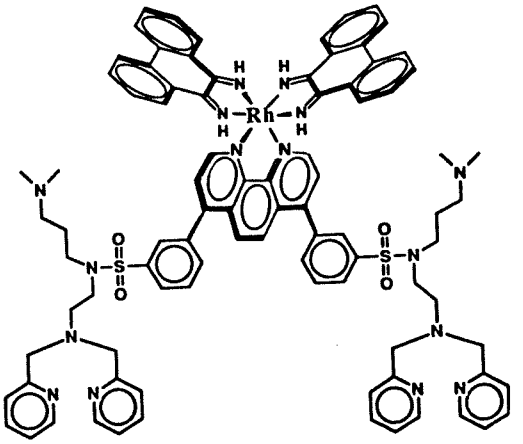

$Rh(phi)_2(DSTM\text{-}AP)$

Figure 2.1. (cont.) Ruthenium and Rhodium Complexes with Tethered Metal Chelating Groups

$Ru(DIP)_2DSTM$	Ru(4,7-diphenyl-1,10-phenanthroline)$_2$[4,7-diphenyl-1,10-phenanthroline disulfonic acid, tetra(pyridylmethyl)--di(ethylenediamine)disulfonamide]
$Ru(phen)_2DSTM$	Ru(1,10-phenanthroline)$_2$[4,7-diphenyl-1,10-phenanthroline disulfonic acid, tetra(pyridylmethyl)-di(ethylenediamine)-disulfonamide]
$Ru(phen)_2$(DSTM-AE)	Ru(1,10-phenanthroline)$_2$[4,7-diphenyl-1,10-phenanthroline disulfonic acid, tetra(pyridylmethyl)-di(2-dimethylamino-ethyl)-di(ethylenediamine)disulfonamide]
$Ru(phen)_2$(DSTM-AP)	Ru(1,10-phenanthroline)$_2$[4,7-diphenyl-1,10-phenanthroline disulfonic acid, tetra(pyridylmethyl)-di(3-dimethylamino-propyl)-di(ethylenediamine)disulfonamide]
$Rh(phi)_2$(DSTM-AP)	Rh(9,10-phenanthrenequinonediimine)$_2$[4,7-diphenyl-1,10-phenanthroline disulfonic acid, tetra(pyridylmethyl)-di(3-dimethylaminopropyl)-di(ethylenediamine)disulfonamide]

complexes agreed within uncertainty, the data for the three complexes were averaged to determine the value to be used for all three complexes.

The ultrapure Milli-Q water was used for the synthetic reactions. "NH_4OH" refers to the usual 30% solution by weight of NH_3 in water. J. T. Baker 'Baker-flex' alumina and silica TLC plates with fluorescent indicator were used. Ninhydrin staining of silica TLC plates was done by dipping the plate with tweezers into a solution of 300 mg. ninhydrin dissolved in 97 ml 1-butanol and 3 ml acetic acid. The plate was dried briefly on a paper towel, and then heated in an oven set at 100-120 °C. 60-200 mesh (140 Å) silica from Aldrich Chemicals and 80-200 mesh (Brockman Activity I) alumina from Fisher Scientific were used for column chromatography.

Precautions Taken During Synthesis and Purification. It is known that amines are easily oxidized.[4] This slow but inevitable reaction was observed when amines were exposed to the atmosphere for long periods of time (days) as progressive color changes. Initially the oxidizing amines would turn yellow (occasionally, green), followed by orange, brown, and finally, black. Oxidation reactions were greatly minimized by storing the amines as dry solids or oils, under vacuum or argon, and at -60 °C or below. These precautions were taken whenever possible when an amine needed to be stored for 12 hours or longer. These precautions were also taken after the amines were coupled to $DIP(SO_3Na)_2$, and in all ruthenium and rhodium metal complexes that contain amines. Since the amine DPNED in crystalline form appears to resist oxidation far more than the other amines (which are oils), DPNED was not deprotected to DEN until DEN was needed for the next synthetic step.

Since ruthenium complexes are known to react with visible light, all intermediates and products containing ruthenium were protected with aluminum foil as much as was practical. Rhodium complex intermediates and products were similarly

protected as a precaution. Extreme pH was avoided during ligand and complex purification in order to minimize the possibility of acid-catalyzed sulfonamide hydrolysis, and the possibility of hydroxide attack on the ruthenium and rhodium metal centers.

2.3. Synthesis of Metal Chelating Groups and Tethered Dimethyl Amines

The basic synthetic method used in this section is the alkylation of an amine with an alkyl chloride. Although product yields were sometimes low, high product purities were generally obtained, except in the case of DPDEN. The NMR spectra of all four amines are shown in Appendix I.

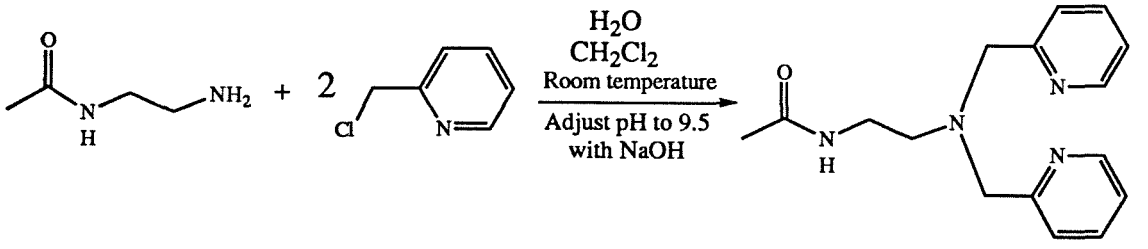

N-Acetyl-N',N'-Di(2-Picolyl)ethylenediamine [DPNED]. The N-acetylethylenediamine starting material (Aldrich Chemicals) was purified by vacuum distillation to eliminate the more volatile ethylenediamine and the less volatile N,N'-diacetylethylenediamine impurities. 18.5 g. (0.181 moles) N-acetylethylenediamine and 60.8 g. 2-picolyl chloride hydrochloride (0.371 moles, Aldrich Chemicals) were dissolved in about 250 ml water. The pH was adjusted to 9.5 with a fairly concentrated NaOH solution, and 250 ml CH_2Cl_2 were added. The reaction was stirred at room temperature in the dark under nitrogen for 4-8 days, periodically adding NaOH to neutralize the HCl generated by the reaction and maintain the pH in the 8.5-9.5 range.

To minimize the reaction of hydroxide with 2-picolyl chloride, pH's over 9.5 were avoided. When no further significant pH decrease was observed, then the solvents were removed by rotary evaporation to yield a dark red viscous solid. The red solid was poured into a 1000 ml beaker, a 100 ml portion of ethyl acetate was poured directly over the red mixture, and the product was extracted into the solvent by vigorous manual stirring with a hard, stainless steel butter knife (for smaller scale reactions, a spatula was sufficient). The ethyl acetate was decanted from the red solid, and fresh solvent was poured on top of the solid. This procedure was repeated 20 to 40 times with 30-70 ml portions of ethyl acetate. All ethyl acetate fractions were combined, and the solvent was removed by rotary evaporation to yield crude product (an off-white solid). An alumina column was prepared, using 5 g. neutral alumina per gram of crude product. The column was washed with methanol, and then ethyl acetate. The crude product was redissolved in hot ethyl acetate, and flashed through the column with additional ethyl acetate. The final product was allowed to crystallize by slow evaporation. Yield: 20.3 g. (39%) large, diamond-shaped crystals of DPNED. ^{1}H NMR (Figure 2.6, 400 MHz, $CDCl_3$); δ(ppm) 8.54 (d, 2 H), 7.63 (broad s, 1 H), 7.60 (td, 2 H), 7.31 (d, 2 H), 7.16 (dd, 2 H), 3.85 (s, 4 H), 3.30 (q, 2 H), 2.71 (t, 2 H), 2.00 (s, 3 H).

The reaction scale affects the time required for complete reaction, with larger scale reactions requiring longer times. Product formation can be qualitatively monitored by ethanol/silica TLC, visualized with a UV lamp or stained with iodine. The product has an R_f of 0.44; monoalkylated and trialkylated impurities stay near the baseline, and picolyl chloride and picolyl alcohol appear to have R_f's near 0.7. Product yields tend to vary substantially; a double scale reaction resulted in a disappointing 20% yield.

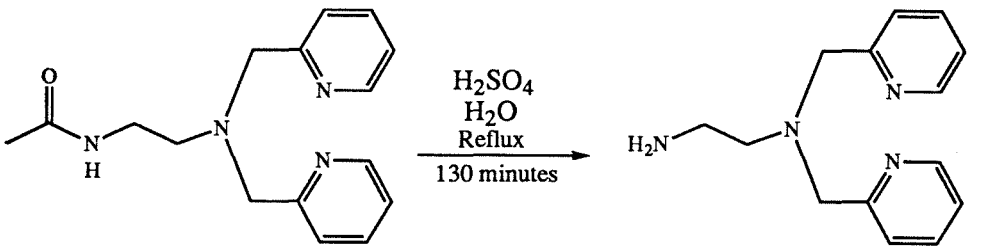

N,N-Di(2-Picolyl)ethylenediamine [DEN]. 4.54 g. DPNED were dissolved in a mixture of 18.5 ml concentrated H_2SO_4 and 46.4 ml water, refluxed for 130 minutes, and then cooled in an ice bath. Concentrated NaOH was added until the product was forced out of solution as a light yellow oil. The product was then extracted into CH_2Cl_2, and the CH_2Cl_2 was removed by rotary evaporation. Yield: 3.34 g. (86%) DEN . The reaction conditions are similar to those for the hydrolysis of 2-phenylbutanamide.[5] ^1H NMR (400 MHz, $CDCl_3$); δ(ppm) 8.48 (d, 2 H), 7.60 (t, 2 H), 7.44 (d, 2 H), 7.10 (dd, 2 H), 3.79 (s, 4 H), 2.72 (t, 2 H), 2.59 (t, 2 H). ^1H NMR (Figure 2.7, 400 MHz, D_2O); δ(ppm) 8.14 (d, 2H), 7.51 (td, 2H), 7.15 (d, 2H), 7.05 (dd, 2H), 3.41 (s, 4H), 2.42 (t, 2H), 2.32 (t, 2H).

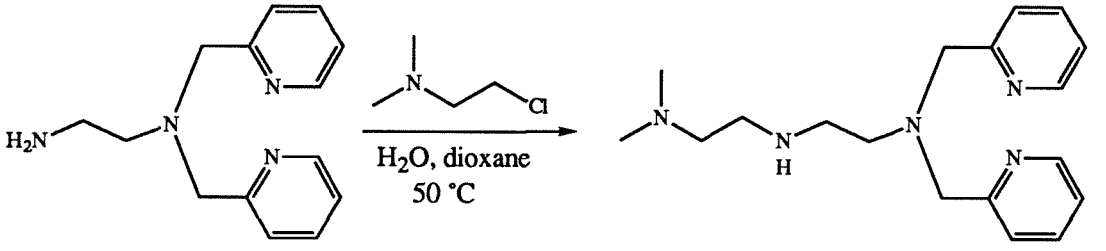

N-(2-Dimethylaminoethyl)-N',N'-Di(2-Picolyl)ethylenediamine [DEDEN]. 4.41 g. (0.018 moles) of DEN were reacted with 3.7 g. (1.4 equivalents, 0.026 moles) of 2-dimethylaminoethyl chloride hydrochloride (Aldrich Chemicals). The reactants were dissolved in 5 ml 5 M aqueous NaOH (to neutralize the HCl) and 25 ml 1,4-dioxane, and heated at 50 °C for 5 days. Over the course of the reaction, the solution changed

from yellow to orange. The reaction was monitored by silica TLC (stained with ninhydrin) with 10% NH_4OH in methanol as the eluent; the DEDEN migrates faster than the starting material DEN. The solvents were removed by rotary evaporation, and ethyl acetate was poured on top of the dry residue. Crude product was extracted with a spatula into the ethyl acetate using a procedure similar to that for the synthesis of DPNED, except that less ethyl acetate was used due to the smaller scale of the reaction. The ethyl acetate extract contained a mixture of starting material DEN and the monoalkylated product DEDEN, and a small amount of dialkylated impurity. Charged tetraalkylammonium salts did not dissolve in the ethyl acetate. The ethyl acetate extracts were combined, and the solvent was removed by rotary evaporation to yield 1.632 g. of a yellow oil.

The oil was purified by silica column chromatography, using 9% NH_4OH in methanol as the eluent. The eluent was collected in fractions, and the location and purity of the fractions that contained product were determined by TLC (stained with ninhydrin). Colored impurity that did not stain with ninhydrin eluted first, followed by product DEDEN, and finally by DEN. A 40% NH_4OH in methanol wash was used to clean the column, and fractions that contained mostly DEDEN with some DEN impurity were recolumned using 9% NH_4OH in methanol, and the eluent was again collected in fractions. All fractions that contained DEDEN but no DEN were combined, and the NH_4OH and methanol solvents were removed by rotary evaporation to yield 434 mg. yellow oil.

The DEDEN coeluted with bis(2-picolyl)amine impurity. To remove this impurity, the silica column was recleaned with 40% NH_4OH in methanol, followed by an extensive methanol wash. The product was loaded onto the column in methanol (no NH_4OH). The column was washed with over one liter of methanol to eliminate the bis(2-picolyl)amine impurity, which eluted as a faint yellow band. Methanol/silica (no

NH_4OH) can be used as a TLC system to distinguish DEDEN from bis(2-picolyl)amine; without the NH_4OH, the bis(2-picolyl)amine moves while the DEDEN remains at the baseline. The product DEDEN was collected by elution with 9% NH_4OH in methanol, and it was determined by TLC which fractions contained the product. These fractions were combined, and the solvents were removed by rotary evaporation. In order to eliminate trace NH_3 (which would also react with $DIP(SO_2Cl)_2$ in the next step) the product was redissolved in methanol, the methanol was removed by rotary evaporation, and the product was thoroughly pumped dry. This procedure was repeated.

Yield: 406 mg. (7.1%) DEDEN. ^1H NMR (Figure 2.8, 400 MHz, $CDCl_3$); δ(ppm) 8.47 (d, 2 H), 7.60 (t, 2 H), 7.47 (d, 2 H), 7.08 (dd, 2 H), 3.79 (s, 4 H), 2.70 (s, 4 H), 2.55 (t, 2 H), 2.32 (t, 2H), 2.15 (s, 6H). If bis(2-picolyl)amine impurity were present, the ^1H NMR would show a singlet at 3.93 ppm.

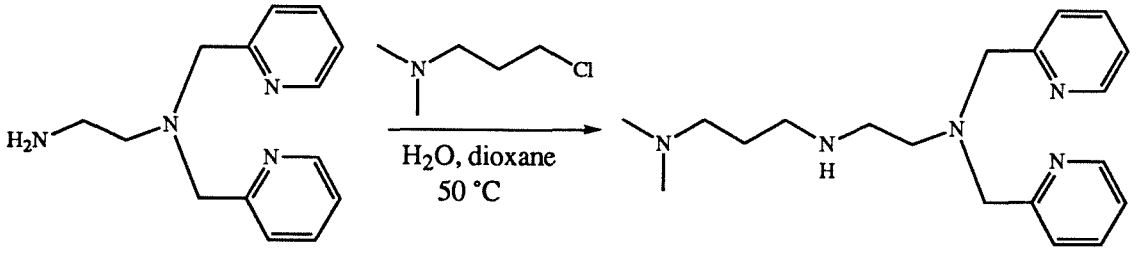

N-(3-Dimethylaminopropyl)-N',N'-Di(2-Picolyl)ethylenediamine [DPDEN]. 4.40 g. (0.018 moles) of DEN were reacted with 4.3 g. (1.5 equivalents, 0.027 moles) of 2-dimethylaminopropyl chloride hydrochloride (TCI America Organic Chemicals). The reactants were dissolved in 5.46 ml 5 M aqueous NaOH (to neutralize the HCl) and 27.3 ml 1,4-dioxane, and heated at 50 °C for 7 days. This reaction was worked up in a similar manner as was done for DEDEN (above), with the following exceptions:

1. The reaction (at 50 °C in 87% dioxane) was monitored by silica TLC using 7% NH_4OH in isopropanol as the eluent. Chromatographic purification was also conducted using 7% NH_4OH in isopropanol as the eluent.

2. Since chromatographic separation between the starting material DEN and the product DPDEN was poorer, more extensive chromatography needed to be conducted.

3. Unlike DEDEN, DPDEN is less mobile than the starting material DEN.

4. Bis(2-picolyl)amine impurity does not appear to be produced by this reaction. The DPDEN was nevertheless washed with methanol on silica, and collected with 10% NH_4OH in methanol, in a similar manner to the procedure for the purification of DEDEN.

Yield: 281 mg. (4.7%) DPDEN. ^1H NMR (Figure 2.9, 400 MHz, $CDCl_3$); δ(ppm) 8.48 (d, 2 H), 7.60 (t, 2 H), 7.44 (d, 2 H), 7.11 (dd, 2 H), 3.79 (s, 4 H), 2.68 (m, 4H), 2.45 (t, 2H), 2.22 (t, 2H), 2.16 (s, 6H), 1.57 (quin, 2H). Unlike in the case of DEDEN, peaks suggesting the presence of a 5-15% impurity remained in the final NMR of DPDEN. ^1H NMR (400 MHz, $CDCl_3$) of putative impurity: δ(ppm) 7.50 (d), 2.60 (m), 2.33 (t), 2.12 (s), 1.5 (quin).

Discussion of the Synthesis and Characterization of the Amines. The primary reaction of the above synthetic scheme is the alkylation of an amine with an alkyl halide. Although the reaction is simple and safe, the level of alkylation is difficult to control since primary, secondary, and tertiary amines are all nucleophilic. The result is the significant formation of side products due to underalkylation and overalkylation. The elimination of these side products requires several purification steps and results in lower product yields.[6,7] Since all of the above alkylation products (DPNED, DEDEN, and DPDEN) contain tertiary amines, overalkylation to quarternary ammonium salts is a major side reaction of all three alkylations. In the above purification procedures, the

products are separated from the bulk of the quarternary ammonium salts by extraction of the products into the relatively nonpolar solvent ethyl acetate. Remaining quarternary ammonium salts (if any) would be removed from the product by the alumina or silica adsorbents during the column chromatography.

The synthesis and purification of DPNED are greatly simplified since only one nucleophilic amine group is present. The major product is the desired tertiary amine, but both the secondary amine and the quarternary ammonium salt are also formed in considerable quantity. Of the three products, only the desired DPNED is extracted into ethyl acetate to a significant extent. The alumina column then appears to remove much of the remaining secondary amine and quarternary ammonium salt, as well as colored oxidized impurities. Highly pure DPNED is then obtained by crystallization in ethyl acetate. Since DPNED provides the basic bis(2-picolyl)amine building block of all five metal complexes, it is fortunate that pure DPNED can be synthesized in fairly good yield.

The next synthetic step is the acid hydrolysis of DPNED to DEN, where the acetyl protecting group is removed. Pure DEN is produced in high yield by this simple and quantitative reaction, despite the harsh conditions of the acid hydrolysis. The product DEN can be either directly coupled to $DIP(SO_2Cl)_2$ to form DSTM, or can be alkylated to DEDEN or DPDEN, which are the precursors to DSTM-AE and DSTM-AP, respectively.

The alkylation of DEN to DEDEN or DPDEN are low yield reactions. The syntheses require that the primary amine of the starting material DEN be alkylated precisely once to a secondary amine. Unlike in the case of the synthesis of DPNED, both the starting material and the product DEDEN or DPDEN are extracted into ethyl acetate, so more extensive chromatography is required to separate starting material from product. An additional problem is that the primary halides 2-dimethylaminoethyl

chloride and 3-dimethylaminopropyl chloride are less reactive towards nucleophilic substitution than the benzylic halide 2-picolyl chloride.[8] The lower reactivity of the primary alkyl chlorides requires higher temperatures for the alkylation reactions. The higher temperatures appear to increase the formation of quarternary ammonium salts by overcoming steric kinetic barriers. The formation of quarternary ammonium salts is further increased since both DEDEN and DPDEN have two tertiary amines each that can be alkylated, in contrast to DPNED, which has one tertiary amine.

The ratio of alkyl chloride to starting amine strongly affects the syntheses of DEDEN and DPDEN. A ratio of about 1.5 equivalents of alkyl chloride per equivalent of starting amine appears optimal. A greater amount of alkyl chloride results in the overproduction of quarternary ammonium salts, which reduces the yield of the reaction. A lesser amount results in too little product formation relative to the starting amine, which complicates the chromatographic separation. A ratio of one equivalent of alkyl chloride per equivalent of starting amine is insufficient since the dimethylaminoalkyl chloride can react with itself both intra- and intermolecularly, which does not leave enough available to alkylate the starting amine DEN.

The chromatographic separation of DEN from the products DEDEN and DPDEN is greatly improved by the presence of ammonium hydroxide in the eluent. The ammonium hydroxide maintains an alkaline chromatographic environment and thus reduces the proton transfer reactions among amine functional groups that would complicate the chromatography and lead to streaking and low mobilities. With ammonium hydroxide in an alcohol as the eluent, DEDEN is the most mobile, followed by DEN, and then by DPDEN. This order of elution is surprising considering the structural similarity between DEDEN and DPDEN. A possible explanation for this is that DEDEN forms an intramolecular hydrogen bond between the secondary amine proton and the dimethylamine group lone pair involving an entropically favored 5-

membered ring. This intramolecular hydrogen bonding reduces the interaction between the amine groups and the silica and as a result, DEDEN is more mobile than DEN. Since a similar intramolecular hydrogen bond in DPDEN would involve a less entropically favored 6-membered ring, there is a greater degree of interaction between DPDEN and the silica, which results in a lower mobility than DEN. This is illustrated in Figure 2.2. The unique mobility of DEDEN may be responsible for its more successful chromatography and higher final purity. In contrast, it is difficult to completely purify DPDEN due to an unknown impurity that appears to comigrate with DPDEN during the chromatography. This impurity appears to gradually increase over time, indicating that it might be a slow oxidation product.

The impurity bis(2-picolyl)amine is formed as a side product of the DEDEN synthesis. Unlike DEDEN and DPDEN, which each have three amine functional groups, bis(2-picolyl)amine has only one amine group; thus bis(2-picolyl)amine is mobile on silica in methanol in the absence of ammonium hydroxide, while DEDEN and DPDEN remain largely immobile. This property enables the removal of bis(2-picolyl)amine from the product DEDEN despite their similar mobilities on silica in the presence of ammonium hydroxide. A possible mechanism for the formation of bis(2-picolyl)amine is shown in Figure 2.3. The dimethylamine group conducts an intramolecular nucleophilic attack involving a six-membered ring. The leaving group is bis(2-picolyl)amine. Although amines are normally poor leaving groups, bis(2-picolyl)amine is a better leaving group due to the electron withdrawing effect of the pyridine rings. The corresponding intramolecular nucleophilic attack is more difficult in the case of DPDEN because it would involve an entropically less favored seven-membered ring.

The synthesis of DPNED and its deprotection to DEN result in high purities and good yields. The synthesis of DEDEN results in high purity, but a barely acceptable

Figure 2.2. Illustration of possible intramolecular hydrogen bonding in DEDEN involving a 5-membered ring. This hydrogen bonding reduces the interaction between DEDEN and silica relative to the interaction between DPDEN and silica.

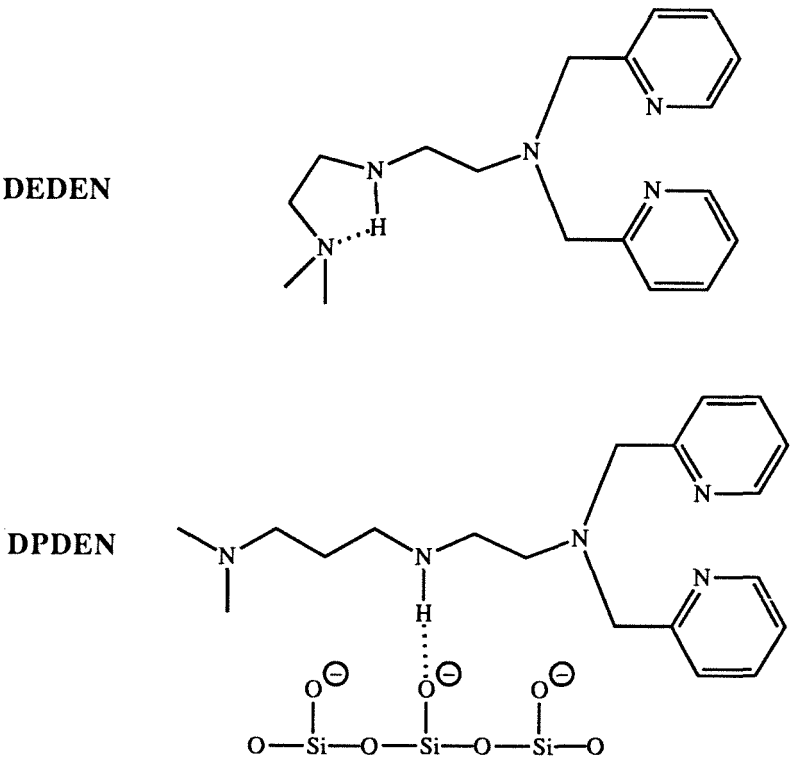

Figure 2.3. Possible mechanism for the formation of bis(2-picolyl)amine from DEDEN by an intramolecular nucleophilic attack involving a six-membered ring.

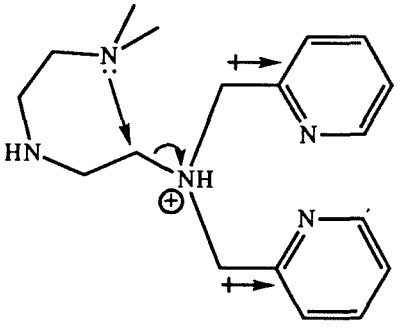

7% yield. The synthesis of DPDEN results in lower purity, and a less acceptable 4.7% yield. As will be seen in Chapter 4, metal complexes to which DPDEN is a precursor appear to have the most potential to promote DNA phosphodiester hydrolysis. Therefore, the development of improved methods for the synthesis of DPDEN would be desirable.

The use of finer silica (more suitable for flash chromatography) is likely to result in a cleaner chromatographic separation and therefore higher reaction yields. The use of iodide anion as a nucleophilic catalyst should be explored.[6] 83% 1,4-dioxane and 17% water as the reaction solvent appear to result in cleaner reactions than 100% water, but the optimum percentages of dioxane and water should be investigated further. The best reaction temperature and the best ratio of alkyl chloride to the starting amine DEN should also be determined. The identification and characterization of the impurity that is produced during the synthesis of DPDEN is important, and would assist rational efforts to develop a method for the removal of this impurity from the DPDEN product. In the absence of such a method, the production of the impurity can be minimized (although not eliminated entirely) by the development of faster and less harsh alkylation reaction conditions as described above.

Synthetic routes to DEDEN and DPDEN not involving alkylation should also be considered. The reductive amination of DEN with 2-dimethylaminoacetaldehyde or 3-dimethylaminopropanal may be possible provided that the aldehydes would react with DEN faster than they self-react. An initial unsuccessful scheme for the synthesis of DEDEN is shown in Figure 2.4. DEN was successfully reacted with chloroacetyl chloride at -78 °C, followed by excess dimethylamine. Attempts were then made to reduce the resultant product to DEDEN with either BH_3 in THF or with $LiAlH_4$. The reduction reactions appeared to fail due to the instability of the bis(2-picolyl)amine group to the reducing agents.

Figure 2.4. Early unsuccessful attempts to synthesize DEDEN.

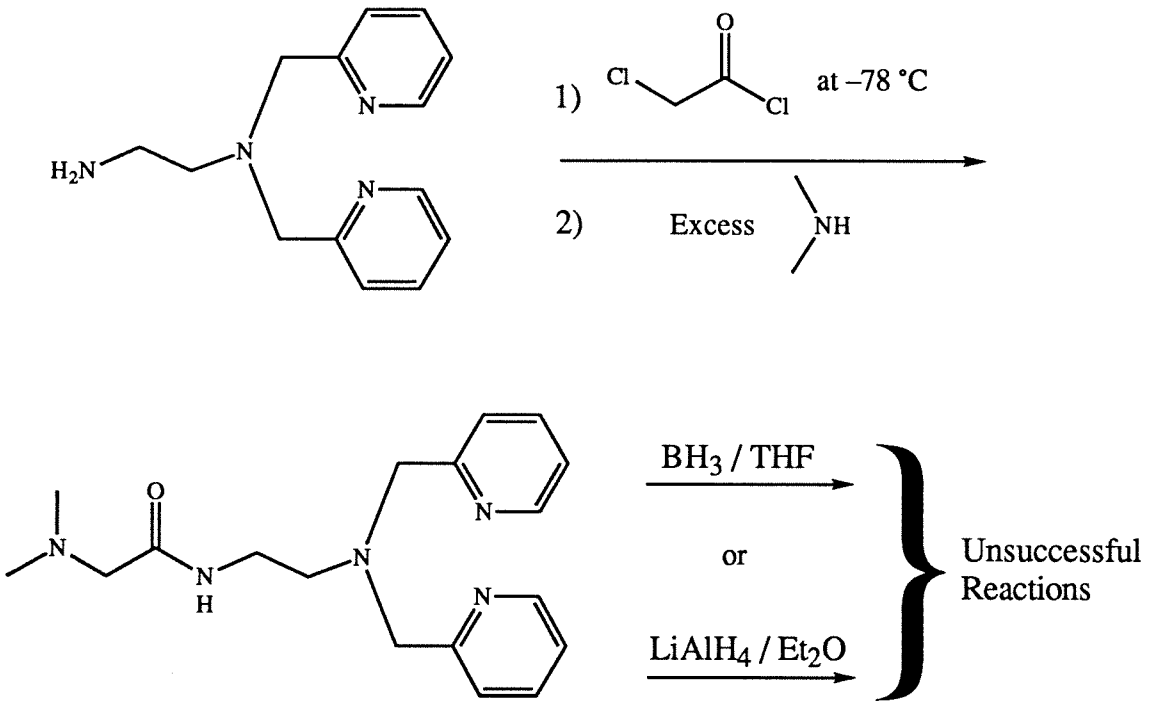

2.4. Synthesis of Diphenylphenanthroline Disulfonamide Ligands with Tethered Metal Chelates

The meta-meta isomer of $DIP(SO_3Na)_2$ was isolated and characterized. Two equivalents of each of the amines DEN, DEDEN, and DPDEN were then tethered to meta,meta-$DIP(SO_3Na)_2$ through sulfonamide linkages. The product ligands DSTM, DSTM-AE, and DSTM-AP form the cleavage domains of the five DNA-cleaving complexes shown in Figure 2.1.

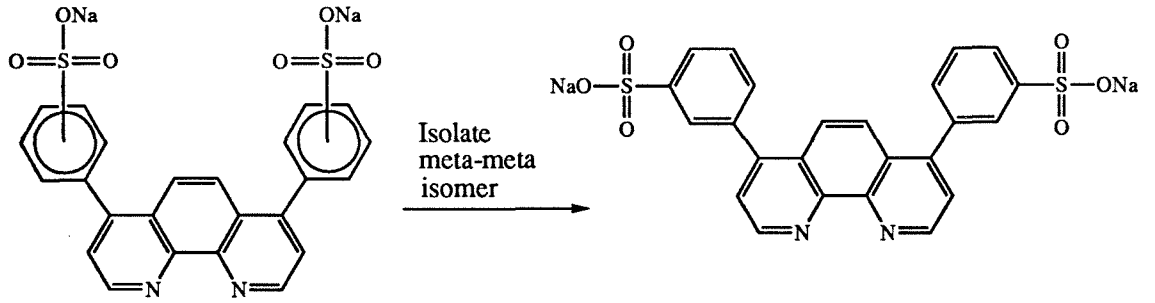

Isolation of Meta,Meta-4,7-Diphenyl-1,10-Phenanthroline Disulfonate. 4,7-diphenyl-1,10-phenanthroline disulfonate [$DIP(SO_3Na)_2$] was purchased from GFS Chemicals as a mixture of isomers. 25 g. $DIP(SO_3Na)_2$ were refluxed in 200 ml methanol for 10-20 minutes and filtered hot. The solid which was filtered off was dissolved in minimum hot deionized (Milli-Q) water, which was then removed by rotary evaporation. The solid was again refluxed in methanol (8 ml methanol per gram of solid) for 10-20 minutes and filtered hot. The solid that was filtered off was dissolved in minimum hot deionized water, which was filtered until clear. Methanol was added to the solution, precipitating out the meta-meta isomer. The meta-meta isomer was collected by vacuum filtration and washed with methanol, for a yield of 5.1 g. (20%).[9] ^1H NMR (Figure 2.10, 400 MHz, D_2O); δ(ppm) 8.46 (d, 2 H), 7.66 (d, 2 H), 7.46 (s, 2 H), 7.21 (t, 2 H), 7.03 (d, 2 H), 6.81 (s, 2 H), 6.76 (d, 2 H). Since glass fritted

filters contain some iron, a porcelain Buchner funnel with Whatman filter paper was used for the filtrations in the above procedure in order to minimize the formation of red iron complex impurities. Prior to coupling to an amine, the purified m,m-DIP($SO_3Na)_2$ was stored at room temperature as a dry powder.

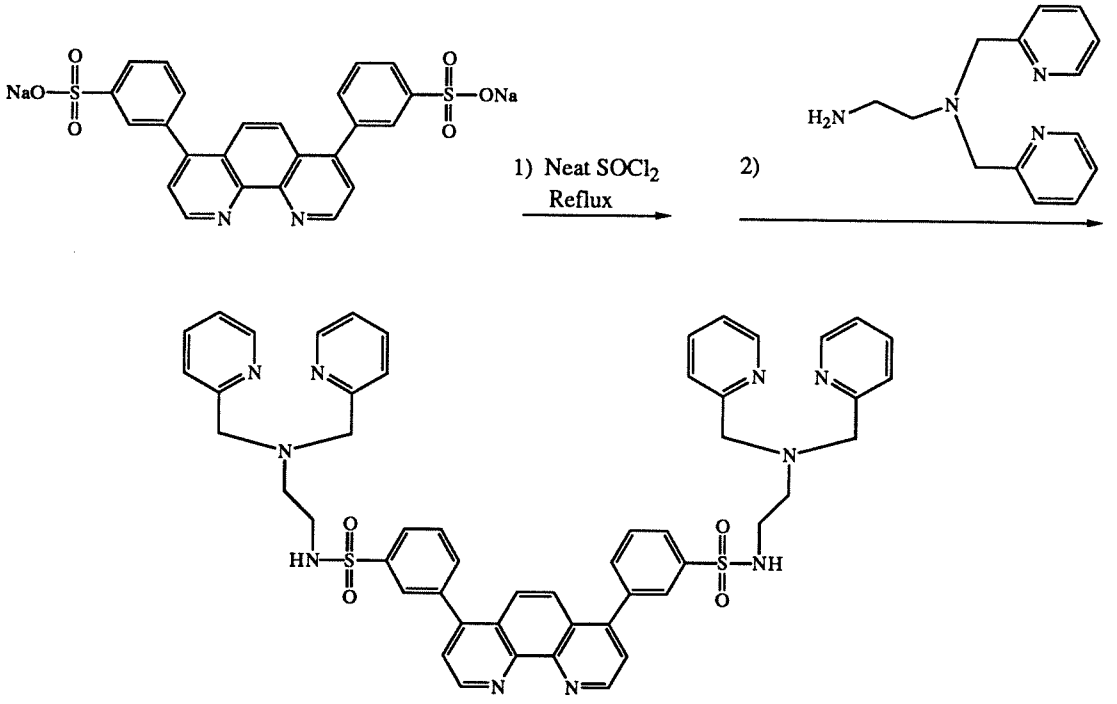

4,7-Diphenyl-1,10-Phenanthroline Disulfonic Acid, Tetra(pyridylmethyl)-Di(ethylenediamine)disulfonamide [DSTM]. 0.5 g. meta,meta-DIP($SO_3Na)_2$ were refluxed in 3.0 ml 99+% $SOCl_2$ (Aldrich Chemicals) under nitrogen or a calcium chloride drying tube for 2-4 days. The $SOCl_2$ was removed by rotary evaporation, and the yellowish DIP($SO_2Cl)_2$ residue was dissolved in CH_2Cl_2. 0.5-0.7 g. DEN were dissolved in CH_2Cl_2. The DIP($SO_2Cl)_2$ solution was added to the DEN solution at -78 °C with stirring. The reaction was allowed to warm up to room temperature. Undissolved solid was removed by vacuum filtration using a fine porosity (4 to 5.5 micron) frit. The solution was run through a column (diameter = 1 cm) containing a 1

cm layer of silica over a 5 cm layer of basic alumina. The CH_2Cl_2 was then removed by rotary evaporation, yielding a yellow oil. Water was added to the oil to dissolve the DEN and precipitate the DSTM as a tan solid. The flask was swirled, and was allowed to stand overnight. The water was decanted from the DSTM, and the DSTM was immediately rinsed with water. The DSTM was columned through basic alumina with ethanol, through silica-basic alumina with CH_2Cl_2 (as above), and again through basic alumina with ethanol; the DSTM was dried by rotary evaporation after each column. Yield: 5-20%. ^1H NMR (Figure 2.11, 300 M Hz, $CDCl_3$); δ(ppm) 9.15 (d, 2 H), 8.50 (broad s, 2 H), 8.43 (ddd, 4 H), 7.99 (dt, 2 H), 7.97 (s, 2 H), 7.59 (d, 2 H), 7.57 (m, 2 H), 7.50 (s, 2 H), 7.39 (d, 2 H), 7.38 (td, 4 H), 7.06 (d, 4 H), 6.97 (dd, 4 H), 3.70 (s, 8 H), 3.08 (t, 4 H), 2.77 (t, 4 H).

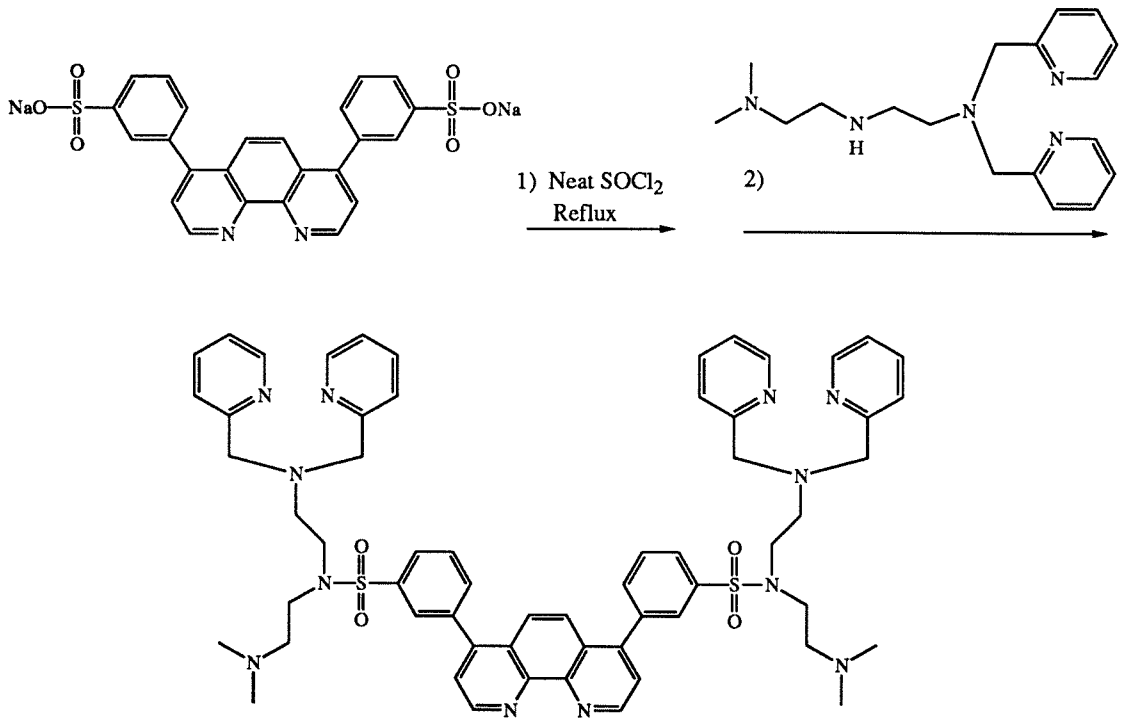

4,7-Diphenyl-1,10-Phenanthroline Disulfonic Acid, Tetra(pyridylmethyl)-Di(2-Dimethylaminoethyl)-Di(ethylenediamine)disulfonamide [DSTM-AE]. 0.252 g. (470 moles) m,m-DIP(SO $_3$Na)$_2$ were refluxed in 3.4 ml $SOCl_2$ for 4 days, and then the $SOCl_2$ was removed by rotary evaporation. 0.406 g. (1.3 mmoles) DEDEN were dissolved in CH_2Cl_2. The $DIP(SO_2Cl)_2$ was dissolved in CH_2Cl_2 and added to the DEDEN solution at -78 °C with stirring. The reaction was allowed to warm to room temperature, was filtered through a 4 to 5.5 micron frit, and the solvent was then removed by rotary evaporation. The residue was chromatographed on silica using 10% NH_4OH in 1,4-dioxane. The chromatography was monitored by silica TLC with 10% NH_4OH in dioxane eluent, stained with iodine; the starting material DEDEN has an R_f of 0.28 and the product DSTM-AE has an R_f of .41. The chromatography was only partially successful in removing the DEDEN from the DSTM-AE; fractions containing mixtures of DSTM-AE and DEDEN were combined, and the solvents were removed by

rotary evaporation. Water was added to the residue to dissolve the DEDEN and precipitate the DSTM-AE. The flask was swirled, and was allowed to stand overnight. The water was decanted from the DSTM-AE, and the DSTM-AE was immediately rinsed with water. Yield: 57 mg. (11%). ^{1}H NMR (Figure 2.12, 400 M Hz, $CDCl_3$); δ(ppm) 9.26 (d, 2 H), 8.44 (ddd, 4 H), 7.94 (s, 2 H), 7.89 (dt, 2 H), 7.73 (s, 2 H), 7.69 (d, 2 H), 7.62 (t, 2 H), 7.57 (td, 4 H), 7.56 (d, 2 H), 7.45 (d, 4 H), 7.07 (dd, 4 H), 3.81 (s, 8 H), 3.35 (t, 4 H), 3.15 (t, 4 H), 2.78 (t, 4 H), 2.28 (broad t, 4 H), 2.02 (s, 12 H).

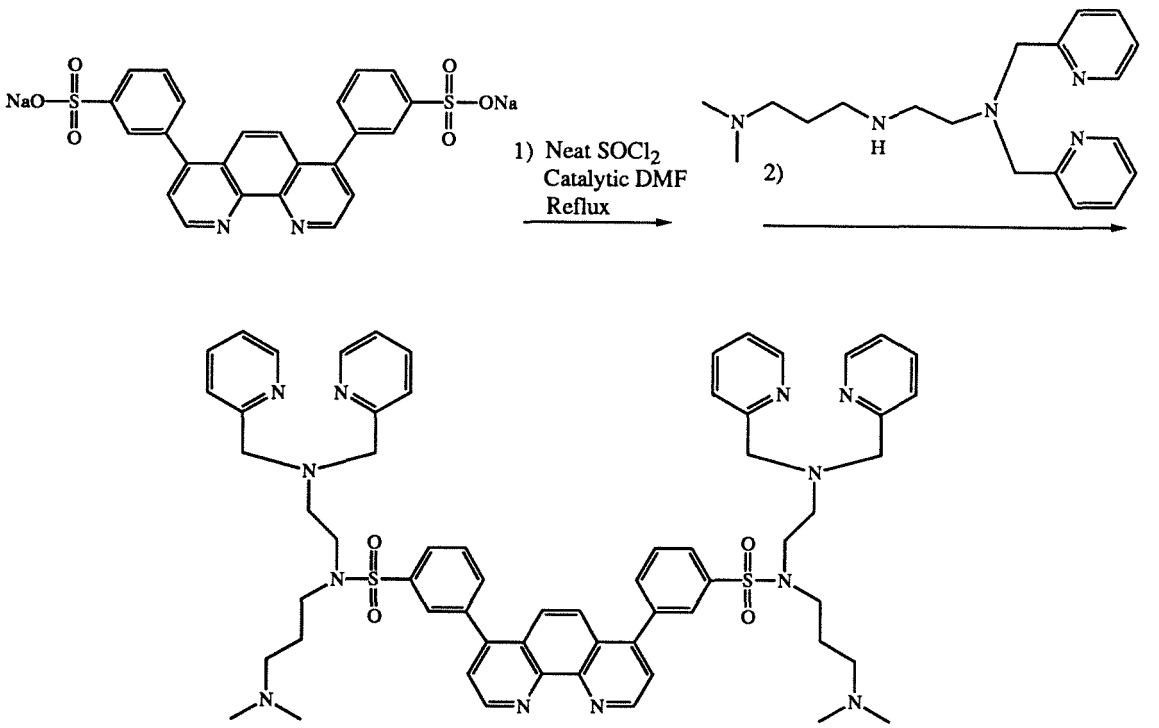

4,7-Diphenyl-1,10-Phenanthroline Disulfonic Acid, Tetra(pyridylmethyl)-Di(3-Dimethylaminopropyl)-Di(ethylenediamine)disulfonamide [DSTM-AP]. 60 mg. (112 moles) m,m-DIP(SO_3Na) $_2$ and 2 1 N,N-dimethylformamide catalyst were refluxed in approximately 6 ml $SOCl_2$ for 4.5 days. The $SOCl_2$ was then removed by rotary evaporation to give a dark yellow solid. 188 mg. (575 moles) DPDEN were dissolved in CH_2Cl_2. The DIP(SO_2Cl)$_2$ was dissolved in CH_2Cl_2 and added to the

DPDEN at -78 °C with stirring. 200 l triethylamine were added to the reaction, and the reaction was then allowed to warm to room temperature. The solution was filtered through a 4 to 5.5 micron frit, and the solvent was removed by rotary evaporation. Water was added to the residue to dissolve the DPDEN and precipitate the DSTM-AP. The flask was swirled, and allowed to stand at +4 °C for 90 minutes. The water was decanted from the precipitate, and the precipitate was immediately rinsed with water. The precipitate appeared to be a mixture of a white solid (presumably DSTM-AP), and a pink solid (presumably iron complex). The pink solid was more soluble in methanol, while the white solid was more soluble in CH_2Cl_2. The solid mixture was eluted through a column containing a thin layer of silica on top of basic alumina (as was done during the purification of DSTM) with an approximately 50/50 v/v mixture of CH_2Cl_2 and methanol. Much of the pink impurity was retained by the silica. The solvents were removed by rotary evaporation. Since a small amount of pink impurity remained, the product was redissolved in CH_2Cl_2, and eluted through a fresh silica-basic alumina column with methanol. The solvents were removed by rotary evaporation to yield 36 mg. (29%) DSTM-AP. ^1H NMR (Figure 2.13, 400 M Hz, CD_2Cl_2); δ(ppm) 9.23 (d, 2 H), 8.43 (d, 4 H), 7.92 (s, 2 H), 7.87 (dt, 2 H), 7.76 (s, 2 H), 7.73 (d, 2 H), 7.66 (t, 2 H), 7.60 (d, 2 H), 7.59 (td, 4 H), 7.45 (d, 4 H), 7.09 (dd, 4 H), 3.79 (s, 8 H), 3.31 (t, 4 H), 3.12 (t, 4 H), 2.75 (t, 4 H), 2.07 (t, 4 H), 2.02 (s, 12 H), 1.52 (quin, 4 H).

Discussion of the Synthesis and Characterization of m,m-DIP($SO_3Na)_2$, DSTM, DSTM-AE, and DSTM-AP. DIP($SO_3Na)_2$ is commercially available as a mixture of isomers, with the sulfonate groups on either the meta or the para positions of the phenyl rings. The mixture appears to consist of approximately 1/9 para-para, 4/9 meta-para, and 4/9 meta-meta. This is consistent with a random distribution of isomers between one para and two meta positions on each phenyl ring, with the phenanthroline

moiety playing no directing role other than the steric exclusion of the ortho isomers. The meta-meta isomer proved to be the simplest to isolate and purify; therefore it was exclusively used in the subsequent synthetic steps in order to facilitate the ^1H NMR characterization of the final complexes. The separation procedure is based on the differential solubility of the various isomers in methanol. The para-para isomer is soluble in both hot and cold methanol, the meta-para isomer is soluble in hot but not in cold methanol, and the meta-meta isomer is not soluble in either hot or cold methanol. Therefore, the hot methanol filtrations isolate largely the meta-meta isomer, while leaving the meta-para and para-para isomers in solution.[9,10]

The m,m-DIP($SO_3Na)_2$ was refluxed in $SOCl_2$ to form m,m-DIP($SO_2Cl)_2$, which was then coupled to DEN, DEDEN, or DPDEN to produce DSTM, DSTM-AE, or DSTM-AP, respectively. N,N-dimethylformamide (DMF) was used as a catalyst[11] only in the case of DSTM-AP; the result was a significantly increased final yield. DMF catalyst was not used in the synthesis of DSTM or DSTM-AE to avoid the possible production of impurities; however, it is not clear that small amounts of DMF produce impurities. Although the final DSTM-AP product was less pure than the final DSTM and DSTM-AE products, this could be due to the lower purity of the DPDEN starting material.

Although slightly different procedures were used for the purification of DSTM, DSTM-AE, and DSTM-AP, the basic concepts behind each purification step are similar, and it is likely that the procedures can be used interchangeably. Throughout the purification procedures, the production of pink and/or red impurities was observed; this was attributed to the formation of iron(DSTM)$_3$ and related complexes. In order to minimize iron contamination, fritted glassware used for filtration was first soaked in aqueous solutions of spare DIP($SO_3Na)_2$ (left over from the isolation of the meta-meta isomer), and then thoroughly rinsed with Milli-Q water. The filtration of the DSTM,

DSTM-AE, and DSTM-AP reaction mixtures removes charged species that are insoluble in CH_2Cl_2. Such charged species include unreacted $DIP(SO_3Na)_2$ starting material, NaCl, and perhaps $DIP(SO_3Na)_2$ coupled to only a single amine as well. The ligands DSTM, DSTM-AE, and DSTM-AP, and the starting amines DEN, DEDEN, and DPDEN are all highly soluble in CH_2Cl_2.

After the removal of the CH_2Cl_2 solvent by rotary evaporation, the key step in the purification procedures is the addition of water to remove the starting amine. This step is effective even if the starting amine is present in considerably greater quantity than the product ligand. The attempt to instead separate DSTM-AE from DEDEN by silica gel chromatography using 10% NH_4OH in dioxane was not very successful. Finally, silica was used to remove the red iron complex impurities from the product ligands. The product ligands are mobile in methanol on silica, while the iron complex impurities are retained. It was observed that if DSTM was eluted through a column only containing silica and then dried, then it would no longer be soluble in CH_2Cl_2 after ten and a half weeks of storage. This was attributed to sulfonamide hydrolysis or alcoholysis catalyzed by the somewhat acidic silica. To avoid this, longer columns of basic alumina were used below the silica columns, and the ligands were quickly flashed through the silica/basic alumina columns. Column of 1 cm diameter containing 0.5-1.0 cm silica over 5-10 cm basic alumina were typically used for the purification of DSTM and DSTM-AP. Longer or thicker columns were not used so as to minimize the loss of product.

2.5. Assembly of DNA-Cleaving Complexes

The *bis* chelate complexes $Ru(DIP)_2Cl_2$, $Ru(phen)_2Cl_2$, and $Rh(phi)_2Cl_3$ have been synthesized by modifications of established procedures. The five complexes $Ru(DIP)_2$DSTM, $Ru(phen)_2$DSTM, $Ru(phen)_2$(DSTM-AE), $Ru(phen)_2$(DSTM-AP),

and Rh(phi)$_2$(DSTM-AP) were then assembled from the above three *bis* chelate complexes and the ligands DSTM, DSTM-AE, and DSTM-AP.

An unsuccessful attempt was made to synthesize Ru(phi)$_2$Cl$_2$ as a possible precursor to Ru(phi)$_2$(DSTM-AP).

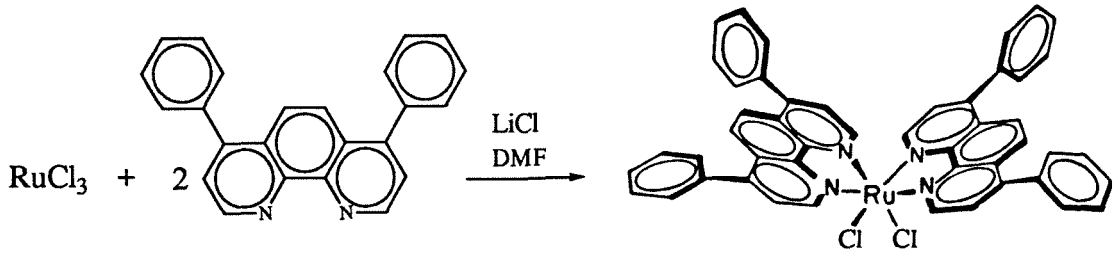

Ru(DIP)$_2$Cl$_2$. 16 g. DIP (4,7-diphenyl-1,10-phenanthroline, Aldrich or GFS chemicals), 5.8 g. RuCl$_3$·3 H$_2$O (42% Ru by weight, a gift from Engelhard) and 11.4 g. LiCl were heated at 100-120 °C in 1 liter DMF for 2 hours. The DMF was removed by rotary evaporation. The solid was dissolved in 700 ml hot ethanol, and crude Ru(DIP)$_2$Cl$_2$ was precipitated by the addition of 1 liter cold water, and was immediately collected by vacuum filtration. A column was prepared in CH$_2$Cl$_2$, using 210 g. acidic alumina per gram of crude Ru(DIP)$_2$Cl$_2$. The crude Ru(DIP)$_2$Cl$_2$ was loaded onto the column with CH$_2$Cl$_2$. Acetone was eluted, the mobile green-brown fraction was discarded, and the purple Ru(DIP)$_2$Cl$_2$ fraction was collected. Orange Ru(DIP)$_3$Cl$_2$ impurity remains on the column. The acetone was removed by rotary evaporation.[12] ^{1}H NMR (400 MHz, CDCl$_3$); δ(ppm) 10.73 (d, 2 H), 8.10 (d, 2 H), 8.00 (d, 2 H), 7.96 (d, 2 H), 7.94 (d, 2 H), 7.54-7.71 (m, 10 H), 7.42-7.50 (m, 6 H), 7.38 (dd, 4 H), 7.16 (d, 2H).

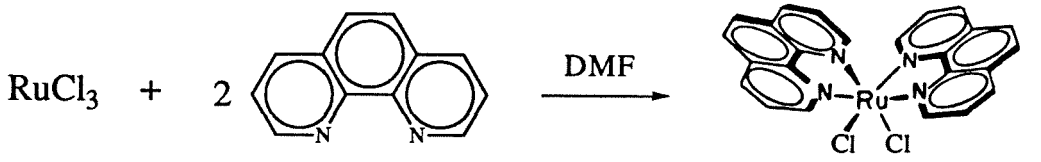

Ru(phen)$_2$Cl$_2$. 0.313 g. 1,10-phenanthroline (Aldrich Chemicals) and 0.186 g. $RuCl_3 \cdot H_20$ (42% Ru by weight, a gift from Engelhard) were stirred in 5 ml anhydrous DMF at 100 °C to refluxing temperature. Small amounts of the reaction mixture were observed in a Pasteur pipette in order to monitor the reaction. When orange solution [$Ru(phen)_3^{2+}$] was observed in the pipette, the heating was discontinued. The DMF was removed by rotary evaporation, and the residue was dissolved in hot ethanol. Water was added to precipitate the $Ru(phen)_2Cl_2$, leaving most of the $Ru(phen)_3^{2+}$ in solution. The flask was cooled in an ice bath, and the $Ru(phen)_2Cl_2$ was immediately collected by vacuum filtration. The $Ru(phen)_2Cl_2$ was washed with water to remove the rest of the $Ru(phen)_3^{2+}$. Since $Ru(phen)_2(H_2O)_2^{2+}$ is also orange, the water wash was stopped before too much product was bled into the water. The $Ru(phen)_2Cl_2$ was washed with diethyl ether to yield 88.6 mg. (22% if anhydrous) purple solid. ^{1}H NMR (400 MHz, DMSO-d_6); δ(ppm) 10.27 (d, 2 H), 8.70 (d, 2 H), 8.28 (d, 2 H), 8.24-8.18 (m, 4 H), 8.13 (d, 2 H), 7.74 (d, 2 H), 7.32 (dd, 2 H). $Ru(phen)_2Cl_2$ is soluble in DMSO, DMF, and somewhat soluble in hot alcohols.

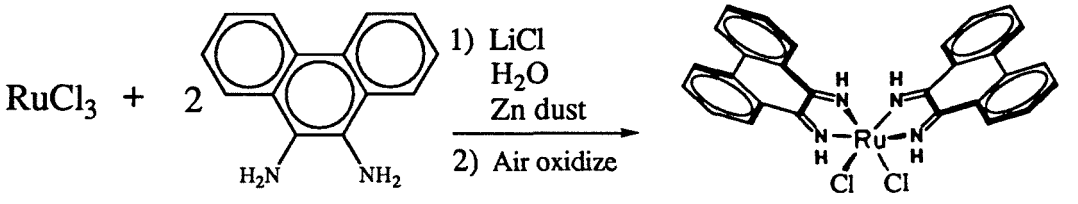

Ru(phi)$_2$Cl$_2$. The synthesis of $Ru(phi)_2Cl_2$, a possible precursor to $Ru(phi)_2$(DSTM-AP), was attempted. A procedure similar to the synthesis of

Ru(bpy)(*o*-benzoquinonediimine)$_2^{2+}$ was used,[13] except LiCl was added to increase the yield of Ru(phi)$_2$Cl$_2$ relative to that of Ru(phi)$_3^{2+}$. 199 mg. RuCl$_3$·3H$_2$O (Johnson Matthey), 363 mg. 9,10-diaminophenanthrene (DAP, Aldrich Chemicals), 46 mg. zinc dust, and 485 mg. LiCl were refluxed in water under nitrogen for two hours. The reaction mixture was then exposed to air, poured into an open beaker, and 529 µl NH_4OH were added. The reaction mixture was stirred in the open beaker for two days. The solid product was then collected by vacuum filtration, and washed extensively with water, diethyl ether, and ethanol. The product was a black solid, and contained Ru(phi)$_3^{2+}$ impurity, and a mixture of *cis*- and *trans*-Ru(phi)$_2$Cl$_2$. In the ^{1}H NMR in DMSO-d$_6$ of the phi imine protons, Ru(phi)$_3^{2+}$ is observed as a singlet at 13.49 ppm, *trans*-Ru(phi)$_2$Cl$_2$ as a singlet at 11.78 ppm, and *cis*-Ru(phi)$_2$Cl$_2$ as singlets at 12.07 and 11.62 ppm (Figure 2.14). The synthesis of Ru(phi)$_2$(DSTM-AP) was abandoned in favor of Rh(phi)$_2$(DSTM-AP) because of the low purity and instability in DMF solution of Ru(phi)$_2$Cl$_2$.

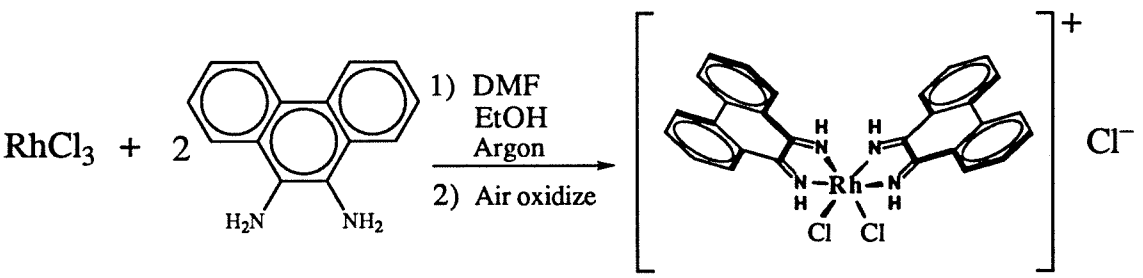

Rh(phi)$_2$Cl$_3$. 101.5 mg. (0.48 mmoles) RhCl$_3$ hydrate (Aldrich Chemicals) were dissolved in 100% ethanol with a heat gun. 221.4 mg. 9,10-diaminophenanthrene (DAP, Aldrich Chemicals) and 6.6 mg. hydrazine hydrochloride were dissolved in 15 ml DMF. The solutions were mixed, purged with argon, and heated to 78 °C under argon overnight. The solution was then stirred in an open beaker for two days. The suspension gradually turned orange during this period. The solid product was collected

by vacuum filtration, and thoroughly washed with water, ethanol, and chloroform. Green oxidation products of DAP were eliminated by these washings.[14] Yield: 175 mg. (59%) orange solid.

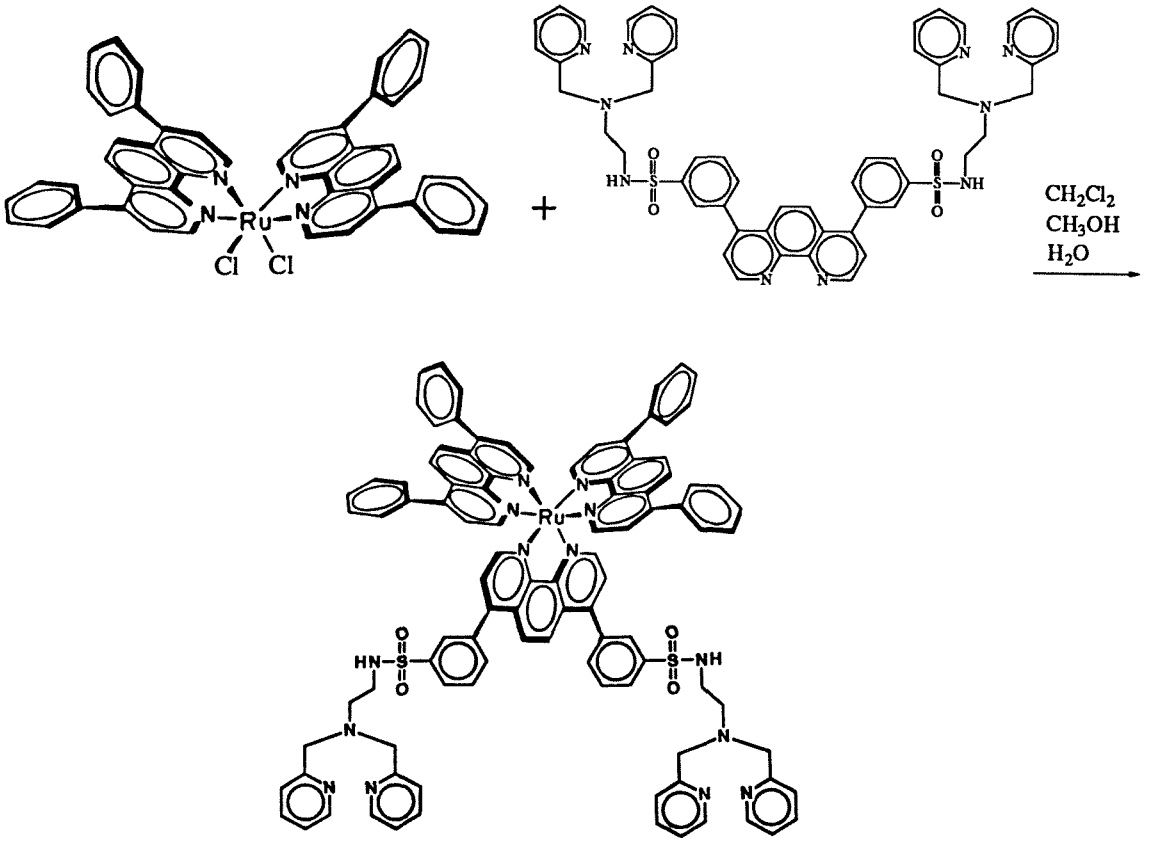

Ru(DIP)$_2$DSTM. 50 mg. Ru(DIP)$_2$Cl$_2$ were dissolved in minimum CH_2Cl_2. A 2/1 v/v methanol water mixture was added to give a homogeneous solution. The solution was stirred to preaquate the Ru(DIP)$_2$Cl$_2$; the preaquation reaction was monitored by alumina TLC with methanol as the eluent. A methanol solution of 1.2-1.5 equivalents of DSTM was added, and the mixture was stirred at 25-50 ^oC overnight to form Ru(DIP)$_2$DSTM. This reaction was also monitored by alumina/methanol TLC; Ru(DIP)$_2$Cl$_2$ is purple and the most mobile, Ru(DIP)$_2$(H_2O)Cl$^+$ and/or Ru(DIP)$_2$(H_2O)$_2^{2+}$ is reddish-purple and less mobile, and Ru(DIP)$_2$DSTM is less

mobile still and luminescent orange. When little $Ru(DIP)_2(Cl \text{ or } H_2O)_2$ remained, the solvents were removed by rotary evaporation. A column was prepared in CH_2Cl_2 using 70 mg. neutral alumina per mg. of solid. The complex was loaded onto the column in CH_2Cl_2, purple $Ru(DIP)_2Cl_2$ impurity was eluted off with acetone, the column was washed with CH_2Cl_2, and the orange product $Ru(DIP)_2$DSTM was eluted with methanol. The methanol was removed by rotary evaporation. To get rid of excess DSTM and other impurities, the complex was dissolved in minimum CH_2Cl_2, and excess benzene was added which precipitated complex of higher purity. The solution was allowed to stand at room temperature in the dark for 7-9 days, then the complex was collected by vacuum filtration on a medium porosity (10-15 micron) frit and washed with benzene. This CH_2Cl_2-benzene precipitation was repeated. Yield: 60 mg. (56% assuming two chloride counterions are present) orange solid.

$Ru(DIP)_2$DSTM is soluble in CH_2Cl_2, $CHCl_3$, methanol, and ethanol. Solid $Ru(DIP)_2$DSTM is not directly soluble in water. An aqueous solution of $Ru(DIP)_2$DSTM can be obtained by dissolving the solid in a small amount of methanol, transferring the methanol solution to a greater volume of water, and then removing the methanol by high vacuum. However, aqueous solutions of greater than 15 M $Ru(DIP)_2$DSTM tend to be unstable, and develop precipitates over the course of several days. ^1H NMR (Figure 2.15, 400 MHz, $CDCl_3$); δ(ppm) 8.75 (d, 2 H), 8.73 (d, 2 H), 8.64 (d, 2 H), 8.53 (broad s, 2 H), 8.46 (d, 4 H), 8.16 (s, 4 H), 8.10 (s, 2 H), 7.97 (d, 2 H), 7.91 (d, 2 H), 7.82-7.87 (m, 6 H), 7.45-7.63 (m, 28 H), 7.17 (d, 4 H), 7.02 (dd, 4 H), 3.73 (s, 8 H), 3.04 (broad s, 4 H), 2.76 (t, 4 H). The extinction coefficient (determined by atomic absorption spectroscopy) of $Ru(DIP)_2$DSTM at the visible maximum is consistent within uncertainty to the value of 2.95×10^4 $M^{-1}cm^{-1}$ for $Ru(DIP)_3Cl_2$.[15] UV/vis (Figure 2.20) {nm(ε[$M^{-1}cm^{-1}$])}: 220 (sh, 101 000), 278 (125 000), 317 (sh, 32

000), 446 (29 500). MW excluding counterions = 1707.0 g/mol. FAB/MS(+) (Figure 2.25) (*m/z*, [assignment]): 1705 $[M - 2H]^+$, 766 $[M - DSTM]^+$.

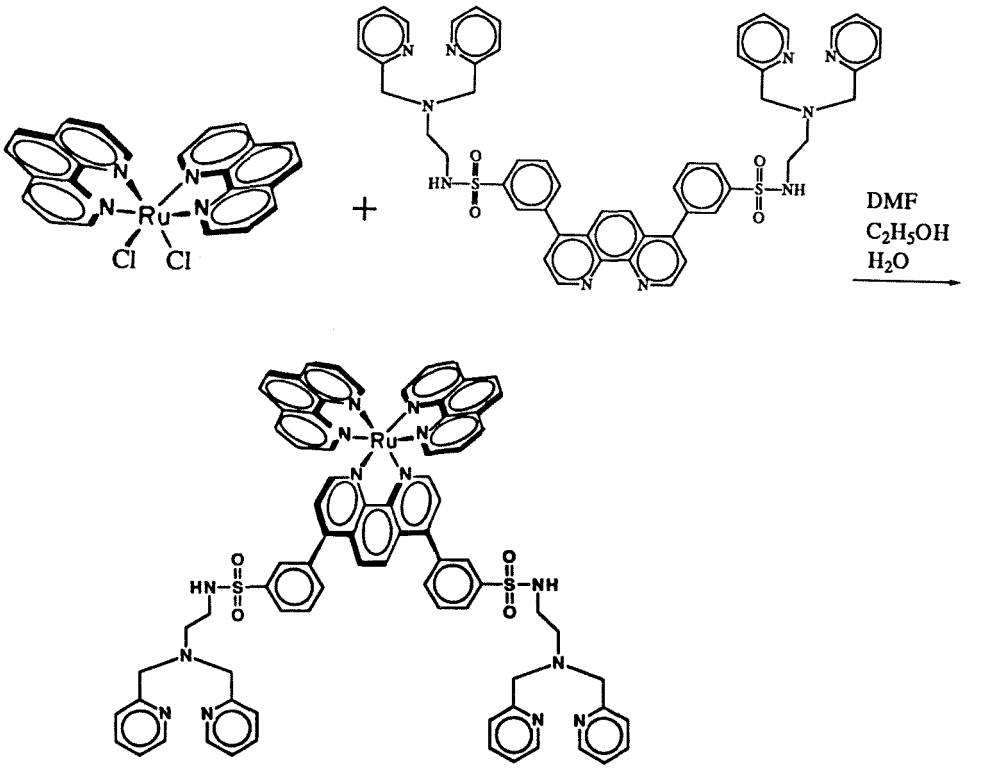

Ru(phen)$_2$DSTM. 25.2 mg. (47 moles) Ru(phen)$_2$Cl$_2$ were dissolved in 4 ml DMF. 57 mg. (61 moles) DSTM were dissolved in 10 ml ethanol and 4 ml DMF. The solutions were mixed, and 3 ml water were added. The reaction was stirred in the dark at room temperature for three hours, and then at 67 °C for three and a half hours to give an orange solution. The reaction was stirred at room temperature overnight, and then the solvents were removed by rotary evaporation. The residue was dissolved in water and the insoluble brown-purple solid was removed by vacuum filtration through a medium porosity (10 to 15 micron) frit. The orange aqueous solution was dried by rotary evaporation. The residue was dissolved in minimum CH_2Cl_2, approximately 80 ml benzene were added to precipitate the product, and the flask was swirled. The flask

was allowed to stand for a period of time from several hours to several days to permit the product to collect on the bottom of the flask. The benzene was decanted from the product, the product was washed with benzene, and then dried by high vacuum. If solid product is decanted along with the benzene, then it can be recovered by vacuum filtration using a medium porosity frit, dissolved in water, and then dried by rotary evaporation. This CH_2Cl_2/benzene precipitation was repeated four more times. A neutral alumina column was prepared in CH_2Cl_2, using 100 mg. alumina per mg. of remaining product. The product was loaded onto the alumina with CH_2Cl_2, and the column was washed with acetone, and then with CH_2Cl_2. The product was eluted with methanol, which was removed by rotary evaporation for a yield of 30 mg. (43% assuming two chloride counterions) orange solid. Ru(phen)$_2$DSTM is soluble in CH_2Cl_2, $CHCl_3$, methanol, and water. ^{1}H NMR (Figure 2.16, 400 MHz, $CDCl_3$). The extinction coefficient at the visible maximum equals (2.3 ± 0.2) x 10^4 $M^{-1}cm^{-1}$. UV/vis (Figure 2.21) {nm(ε[$M^{-1}cm^{-1}$])}: 222 (109 000), 263 (121 000), 310 (sh, 17 000), 437 (23 000). MW excluding counterions = 1402.6 g/mol. FAB/MS(+) (Figure 2.26) (*m/z*, [assignment]): 1402 $[M - H]^+$, 702 $[M + H]^{2+}$.

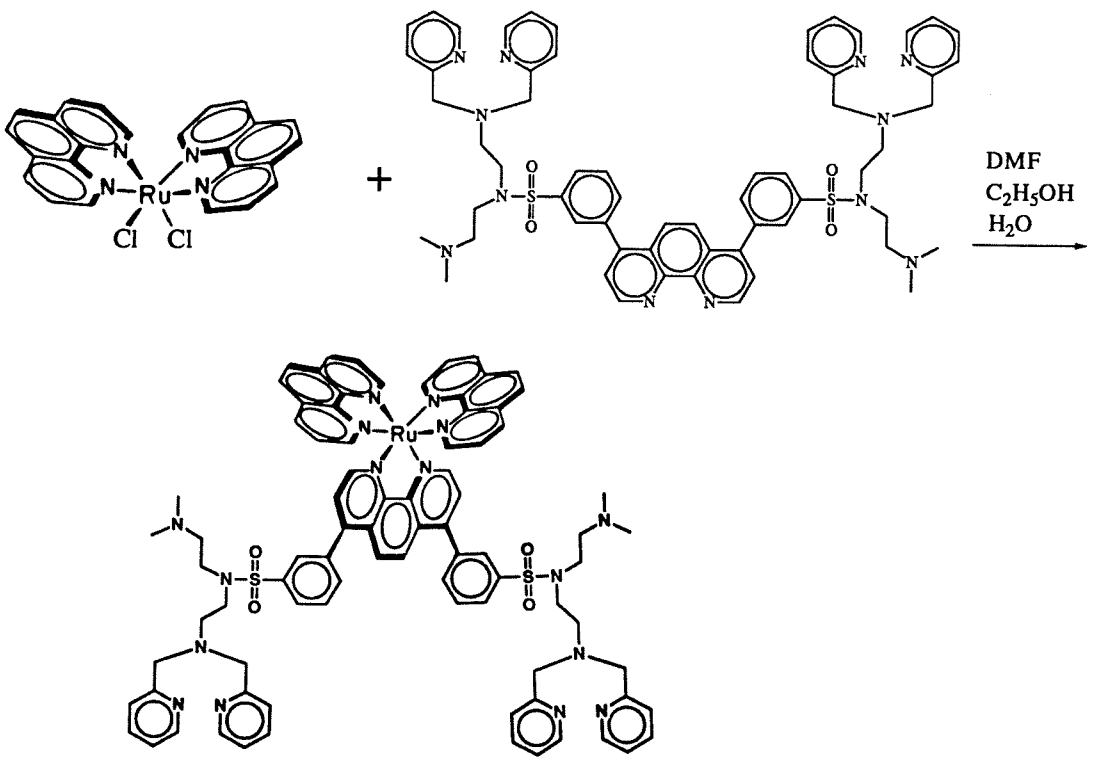

Ru(phen)$_2$(DSTM-AE). 24.2 mg. (45 moles) Ru(phen) $_2$Cl$_2$were dissolved in 5 ml DMF. 57 mg. DSTM-AE (53 moles) were dissolved in 6 ml ethanol. The solutions were mixed, and 3 ml water were added. The reaction was stirred in the dark at room temperature overnight, and then at 64 °C for three hours. The solvents were removed by rotary evaporation, and the residue was dissolved in water. The insoluble material was removed by vacuum filtration through a 10-15 micron frit. The aqueous solution was decanted to another flask to remove some precipitate that developed later. The aqueous solution was dried by rotary evaporation. Five CH_2Cl_2-benzene precipitations were done in a similar manner to the procedure for Ru(phen)$_2$DSTM. There were 56 mg. product after the fifth CH_2Cl_2-benzene precipitation. A neutral alumina column was prepared in CH_2Cl_2, using 5 g. alumina. The product was loaded onto the column in CH_2Cl_2, washed extensively with CH_2Cl_2, and eluted with methanol. The product was dried by rotary evaporation.

Since NMR indicated that about 7 1/2% $Ru(phen)_2Cl_2$ impurity was present in the product, further purification was conducted. The product was dissolved in minimum CH_2Cl_2, excess anhydrous diethyl ether was added, and the flask was swirled. The flask was allowed to stand for four days, and the product was collected by vacuum filtration and washed with anhydrous diethyl ether. The product was dissolved in about 60 ml water. 15 ml 2.5 M NaCl were then added in an attempt to precipitate $Ru(phen)_2Cl_2$ impurity. The flask was allowed to stand for one week, then the NaCl solution was filtered through a 10-15 micron frit. Little solid was removed by the frit. The water was removed by rotary evaporation. To remove most of the NaCl, the dried product was extracted into ethanol, and the undissolved NaCl was removed by vacuum filtration. The ethanol was removed by rotary evaporation. To remove the remaining NaCl, this desalting procedure was repeated with CH_2Cl_2. A neutral alumina column was prepared in CH_2Cl_2, using 6.2 g. alumina. The product was loaded onto the column in CH_2Cl_2, washed extensively with CH_2Cl_2, and eluted with methanol. The product was dried by rotary evaporation. Another CH_2Cl_2-benzene precipitation was conducted. To eliminate hydrophobic impurities, the product was dissolved in water. The aqueous solution was washed once with cyclohexane and three times with HPLC grade CH_2Cl_2 in a separatory funnel. The water was removed by rotary evaporation for a yield of 28 mg. (38% assuming two chloride counterions) orange solid. Only 8 mg. were lost to the CH_2Cl_2 washes. $Ru(phen)_2$(DSTM-AE) is soluble in CH_2Cl_2, $CHCl_3$, methanol, and water. ^1H NMR (Figure 2.17, 400 MHz, $CDCl_3$). The extinction coefficient at the visible maximum equals (2.3 0.2) x 10^{4} $M^{-1}cm^{-1}$. UV/vis (Figure 2.22) {nm(ε[$M^{-1}cm^{-1}$])}: 222 (109 000), 263 (124 000), 312 (sh, 16 000), 438 (23 000). MW excluding counterions = 1544.9 g/mol. FAB/MS(+) (Figure 2.27) (*m/z*, [assignment]): 1547 $[M + 2H]^+$, 1233 [M + 2H - DEDEN]$^+$, 774 $[M + 3H]^{2+}$.

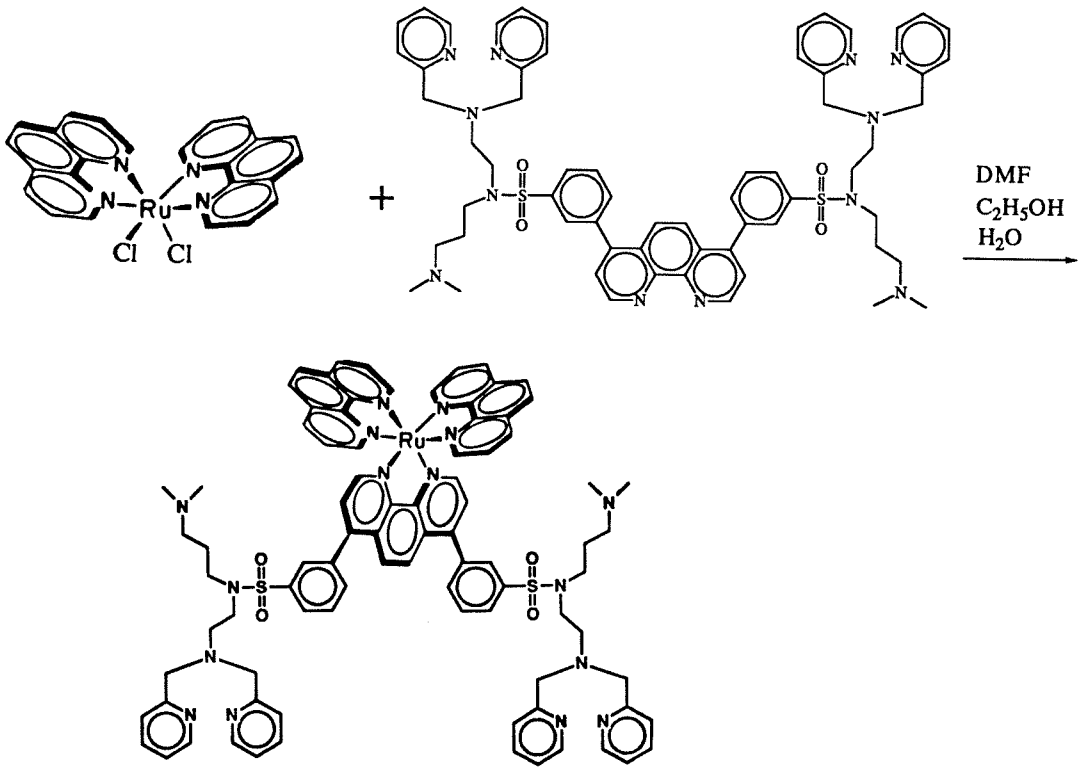

Ru(phen)$_2$(DSTM-AP). 32 mg. (60 moles) Ru(phen)$_2$Cl$_2$ were dissolved in 5.5 ml DMF by stirring at room temperature. 103 mg. DSTM-AP (93 moles) were dissolved in 5.5 ml ethanol. The solutions were mixed, and 3.5 ml water were added. The reaction was stirred at 60 °C for five hours to give a clear orange solution. The solvents were removed by rotary evaporation. The residue was dissolved in water and filtered through a medium porosity (10-15 micron) frit. Three CH_2Cl_2/benzene precipitations were done in a similar manner to the procedure for Ru(phen)$_2$DSTM. A neutral alumina column was prepared in CH_2Cl_2 using 7.8 g. neutral alumina. The product was loaded onto the column with CH_2Cl_2, and extensively washed with CH_2Cl_2. To remove Ru(phen)$_2$Cl$_2$ impurity, the column was washed with 100 ml 15% isopropanol in CH_2Cl_2. The first 40 ml of the isopropanol-CH_2Cl_2 wash were medium orange, and the next 60 ml were light orange. The product was collected by elution with methanol. The methanol was removed by rotary evaporation for a yield of 40 mg.

(40% assuming two chloride counterions) orange solid. Ru(phen)$_2$(DSTM-AP) is soluble in CH_2Cl_2, $CHCl_3$, methanol, and water. ^{1}H NMR (Figure 2.18, 400 MHz, $CDCl_3$). The extinction coefficient at the visible maximum equals (2.3 0.2) x 10^4 M $^{-1}$cm^{-1}. UV/vis (Figure 2.23) {nm(ε[M^{-1}cm^{-1}])}: 221 (108 000), 263 (120 000), 312 (sh, 17 000), 438 (23 000). MW excluding counterions = 1572.9 g/mol. FAB/MS(+) (Figure 2.28) (*m/z*, [assignment]): 1573 $[M]^+$, 1263 $[M + H_2O - DPDEN]^+$, 786 $[M]^{2+}$.

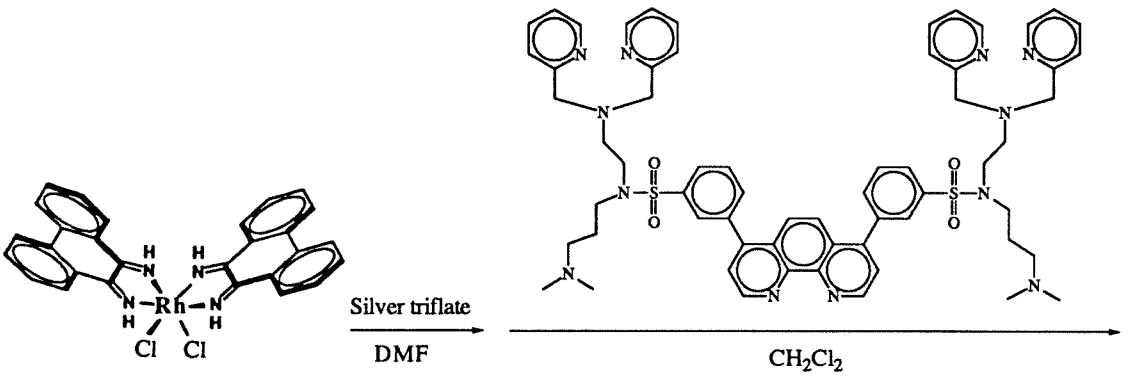

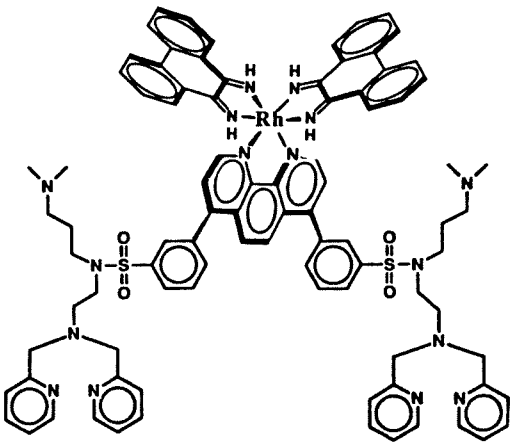

Rh(phi)$_2$(DSTM-AP). 10.5 mg. (17 moles) Rh(phi)$_2$Cl$_3$ and 13.4 mg. (51 moles) silver triflate were stirred in the dark at 82 °C in DMF for one day. To remove the AgCl precipitate, the DMF solution was then centrifuged for 13 minutes at 14 krpm. The DMF supernatant was added to a solution of 19 mg. (17 moles) DSTM-AP in HPLC grade CH_2Cl_2. The reaction was stirred for 12 hours at 85 °C, and then the

solvents were removed by rotary evaporation. In order to replace any triflate counterions with chlorides, a Sephadex QAE-25 anion exchange column was prepared. The column was washed with water, 100 mM NaCl, and then extensively washed with additional water. The water was then gradually replaced with 50% HPLC grade methanol. The product was eluted through the column with 50% methanol. The solvents were removed by rotary evaporation, and the residue was redissolved in water. The solution was washed in a separatory funnel with two portions of $CHCl_3$. The aqueous layer was dried by rotary evaporation, for a yield of 20 mg. (68% assuming three chloride counterions) orange solid. ^1H NMR (Figure 2.19, 400 MHz, CD_3OD), UV/vis (Figure 2.24). MW excluding counterions = 1626.8 g/mol. Time of flight MS(+) (Figure 2.29) (*m/z*, [assignment]): 1541 [M - $(CH_2)_3N(CH_3)_2]^+$, 1455 [M - $2(CH_2)_3N(CH_3)_2]^+$, 1161 [M - 2H - $N(CH_2C_5H_4N)_2$ - DPDEN]$^+$, 1099 [M + 2H - $C_6H_4SO_2$ - DPDEN]$^+$.

Discussion of the Synthesis and Characterization of the *Bis* Chelate Complexes of Ruthenium and Rhodium. The syntheses of the ruthenium *bis* chelate complexes were based on the synthesis of $Ru(bpy)_2Cl_2$.[16] The purifications require the removal of *tris* chelate complex impurities from the product *bis* chelate complexes. In the case of $Ru(DIP)_2Cl_2$, LiCl is used to favor the formation of the *bis* chelate complex over the *tris* chelate complex, $Ru(DIP)_3^{2+}$. The purification method is based on the greater polarity and water solubility of the charged $Ru(DIP)_3^{2+}$ relative to the neutral $Ru(DIP)_2Cl_2$. When the crude product is dissolved in ethanol and water is added, the product $Ru(DIP)_2Cl_2$ precipitates, leaving much of the $Ru(DIP)_3^{2+}$ in solution. The remaining $Ru(DIP)_3^{2+}$ is eliminated by chromatography. The less polar $Ru(DIP)_2Cl_2$ elutes in acetone, while the more polar $Ru(DIP)_3^{2+}$ remains on the alumina until the column is washed with methanol. The impurity 4-hydroxy-4-methyl-2-pentanone was

present in the final $Ru(DIP)_2Cl_2$ product, and was observed in the ^1H NMR: δ(ppm) 3.8 (s, 1 H), 2.61 (s, 2 H), 2.16 (s, 3 H), 1.23 (s, 6 H). This impurity was produced by an aldol condensation of acetone during the chromatography, or was present to begin with in the acetone eluent. This impurity was removed during the CH_2Cl_2 wash of the alumina chromatography during the synthesis of $Ru(DIP)_2DSTM$.

Somewhat different methods were used for the synthesis and purification of $Ru(phen)_2Cl_2$. Although LiCl had been used in a previous synthesis of $Ru(phen)_2Cl_2$,[17] it was not used in this case to avoid the possibility of underreaction. It was found that if underreaction occurred, then no orange $Ru(phen)_3^{2+}$ would be formed, and the product would be purple but not pure, with purple ruthenium *mono*-phenanthroline and colorless free phenanthroline present in the final product. It is therefore important to check the purity by ^1H NMR. The purification method was similar to that of $Ru(DIP)_2Cl_2$, where the addition of water to an ethanol solution precipitates the product *bis* chelate complex, leaving the *tris* chelate impurity in solution. Alumina chromatography proved to be unnecessary in the case of $Ru(phen)_2Cl_2$ because $Ru(phen)_3^{2+}$ is very water soluble and was completely removed by washing the $Ru(phen)_2Cl_2$ product in a glass frit. The less water soluble $Ru(DIP)_3^{2+}$ could not be completely removed from the product $Ru(DIP)_2Cl_2$ without chromatography.

The syntheses of $Ru(phi)_2Cl_2$ and $Rh(phi)_2Cl_3$ are one-pot, two step processes. The first step is the coordination of the 9,10-diaminophenanthrene ligands, and the second step is the air oxidation of the ligands to 9,10-phenanthrenequinonediimine [phi]. $Rh(phi)_2Cl_3$ is easily formed, and most $Rh(phi)_2Cl_3$ syntheses lead to a mixture of *cis* and *trans* isomers. The relative amounts of *cis* and *trans* vary from synthesis to synthesis, but do not affect the coordination of a third ligand to rhodium in the next step.[14] The particular synthesis described above resulted in 89% *cis*- and 11% *trans*-

$Rh(phi)_2Cl_3$. The ratio of *cis* to *trans* $Rh(phi)_2Cl_2$ can be determined by integration of the imine protons of the ^1H NMR in DMSO-d_6. The synthesis of $Ru(phi)_2Cl_2$ proved to be more problematical, and required the addition of LiCl. In the absence of LiCl, $Ru(phi)_3^{2+}$ was the sole product of the reaction. Even in the presence excess LiCl, it was not possible to produce $Ru(phi)_2Cl_2$ without producing $Ru(phi)_3^{2+}$. In contrast to $Ru(DIP)_2Cl_2$ and $Ru(phen)_2Cl_2$, it proved difficult to separate $Ru(phi)_2Cl_2$ from *tris* chelate complex impurity. The $Ru(phi)_2Cl_2$ complex proved to be unstable in DMF solution in the absence of excess chloride ion, and tended to disproportionate to $Ru(phi)_3^{2+}$. Therefore, $Ru(phi)_2Cl_2$ proved to be an unsuitable synthetic precursor, and the synthesis of $Ru(phi)_2$(DSTM-AP) was discontinued; $Rh(phi)_2$(DSTM-AP) was instead synthesized.

Unlike $Rh(phi)_2Cl_3$, where the ratio of *cis* to *trans* varies from synthesis to synthesis, the ratio of *cis*-$Ru(phi)_2Cl_2$ to *trans*-$Ru(phi)_2Cl_2$ remains constant at about 71% *cis* to 29% *trans*. In three different syntheses, the amount of $Ru(phi)_2Cl_2$ that was *cis* (determined by integration of the phi imine protons of the ^1H NMR in DMSO-d_6) was 71%, 70%, and 72%. This indicates that in DMSO-d_6 the *cis* and *trans* isomers are in a thermodynamic equilibrium that is slow on the NMR time scale but may be fast chemically. The DMSO-d_6 may facilitate this equilibrium by exchanging with the chloride ligands.

Discussion of the Synthesis and Characterization of *Tris* Chelate Complexes of Ruthenium. Water substitution was used to facilitate the addition of a third ligand to $Ru(DIP)_2Cl_2$ and $Ru(phen)_2Cl_2$. The water replaces one or both chloride ligands. The water then leaves, allowing DSTM, DSTM-AE, or DSTM-AP to coordinate to the ruthenium metal center. A mixture of CH_2Cl_2, methanol, and water was used as a solvent for the synthesis of $Ru(DIP)_2$DSTM. CH_2Cl_2 was used because $Ru(DIP)_2Cl_2$ is

highly soluble in that solvent, and the methanol was used to dissolve the DSTM and to create a homogeneous solvent system despite the presence of both CH_2Cl_2 and water. A mixture of DMF, ethanol, and water was used as a solvent for the addition of a third ligand to $Ru(phen)_2Cl_2$. The DMF was used to dissolve the $Ru(phen)_2Cl_2$, and the ethanol was used to dissolve the DSTM, DSTM-AE, and DSTM-AP. Excess third ligand was used in the synthesis of all four ruthenium complexes in order to minimize the possibility of one ligand coordinating to two ruthenium atoms through both its phenanthroline moiety and its bis(2-picolyl)amine moiety. As the coordination reactions of the third ligands progressed, it was observed that the reactions went from purple to orange, an indication of the formation of the *tris* chelate complexes. The reactions were also followed by TLC.

Purification of $Ru(DIP)_2DSTM$. The first step in the purification of $Ru(DIP)_2DSTM$ is alumina chromatography. The crude complex is loaded onto alumina in the nonpolar solvent CH_2Cl_2. Elution with acetone then efficiently removes the $Ru(DIP)_2Cl_2$ starting material. The subsequent elution of CH_2Cl_2 then removes any 4-hydroxy-4-methyl-2-pentanone ("diacetone") impurity that was produced by the acetone elution, or was present to begin with in the $Ru(DIP)_2Cl_2$ starting material. The more highly charged $Ru(DIP)_2DSTM$ product is then collected by elution with methanol. When the $Ru(DIP)_2DSTM$ was allowed to remain on the column overnight, the ^1H NMR of the final product showed evidence of sulfonamide hydrolysis. Air pressure was therefore used to increase the solvent flow rate and reduce the length of time that the complex remained on the column. A significant amount of DSTM ligand starting material elutes with the product. This DSTM is eliminated by CH_2Cl_2-benzene precipitation. Both the $Ru(DIP)_2DSTM$ and the DSTM dissolve in the CH_2Cl_2, and the benzene causes the $Ru(DIP)_2DSTM$ to precipitate while leaving the DSTM in solution.

Characterization of Ru(DIP)$_2$DSTM. The ^{1}H NMR of Ru(DIP)$_2$DSTM in $CDCl_3$ has been putatively assigned utilizing electronegativity, nearest-neighbor coupling, and comparisons to analogous compounds. Ru(DIP)$_2$Cl$_2$ or DSTM impurity, if present, could be detected by ^{1}H NMR. The downfield 2,9 phenanthroline protons of the above two impurities are well separated from all Ru(DIP)$_2$DSTM resonances, and can be detected at approximately 10.5 for Ru(DIP)$_2$Cl$_2$ and 9.2 ppm for DSTM. The absence of a peak near 9.2 ppm in the NMR of the purified Ru(DIP)$_2$DSTM also indicates that even if some of the DSTM wrongly coordinated to ruthenium through the bis(2-picolyl)amine moiety, (leaving the phenanthroline moiety free) then it was not present in the final product. The mass spectrum is also consistent with pure product. The visible spectrum of Ru(DIP)$_2$DSTM has a maximum at 445 2 nm produced by metal to ligand charge transfer. This can be compared to the maximum of its analogue Ru(DIP)$_3$Cl$_2$ at 460 nm. The extinction coefficient of Ru(DIP)$_2$DSTM at the visible maximum is consistent within uncertainty to the value of 2.95 x 10^4 $M^{-1}cm^{-1}$ for Ru(DIP)$_3$Cl$_2$.[15] Ru(DIP)$_2$DSTM also shows the characteristic luminescence of *tris*-phenanthroline complexes of ruthenium, although this was not explored in much detail. The poor aqueous solubility of Ru(DIP)$_2$DSTM is consistent with the highly hydrophobic nature of the three diphenylphenanthroline ligands. To minimize precipitation, aqueous stock solutions of Ru(DIP)$_2$DSTM at concentrations higher than 15 M were avoided. Extensive contact of a purely aqueous solution of the complex with plastic or dust also resulted in precipitation. To prevent this, the atomic absorption spectroscopy was conducted using solutions of Ru(DIP)$_2$DSTM in 50% DMF and 50% water by volume. The net charge of the complex (and therefore the number of associated chloride ions) in aqueous solutions has not been studied. If both tertiary amines are protonated, then the net charge would be +4.

Purification of Ru(phen)$_2$DSTM, Ru(phen)$_2$(DSTM-AE), and Ru(phen)$_2$(DSTM-AP). Ru(phen)$_2$DSTM, Ru(phen)$_2$(DSTM-AE), and Ru(phen)$_2$(DSTM-AP) could not be purified in the same manner as Ru(DIP)$_2$DSTM, primarily due to differences between the properties of the starting materials Ru(DIP)$_2$Cl$_2$ and Ru(phen)$_2$Cl$_2$. It was observed that all three Ru(phen)$_2$L complexes had similar properties. Although different methods were used in the purification of the three Ru(phen)$_2$L complexes, the method used for the purification of Ru(phen)$_2$(DSTM-AP) appeared to be the best. It is likely that the method used for the purification of Ru(phen)$_2$(DSTM-AP) could be successfully used for all three complexes. The first step in the purification was dissolving the dried product in water, followed by vacuum filtration. The insoluble material that was filtered from the aqueous solution was presumably Ru(phen)$_2$Cl$_2$ and DSTM-AP starting material. In order to remove the remainder of the DSTM-AP, CH_2Cl_2-benzene precipitations were conducted in the same manner as was done for the purification of Ru(DIP)$_2$DSTM. The remainder of the Ru(phen)$_2$Cl$_2$ was then removed by alumina chromatography. Unlike Ru(DIP)$_2$Cl$_2$, Ru(phen)$_2$Cl$_2$ does not elute in acetone, so 15% isopropanol in CH_2Cl_2 was used instead. Some of the product was lost to this eluent. The Ru(phen)$_2$(DSTM-AP) was collected with methanol and dried by rotary evaporation to complete the purification. In the case of Ru(phen)$_2$(DSTM-AE), the less efficient purification methods resulted in the presence of hydrophobic impurities detectable in the ^{1}H NMR in $CDCl_3$ at around 1.2 and 0.8 ppm. Most of these impurities were removed from the product by the washing of an aqueous solution of the product with CH_2Cl_2 in a separatory funnel.

Characterization of Ru(phen)$_2$DSTM, Ru(phen)$_2$(DSTM-AE), and Ru(phen)$_2$(DSTM-AP). Due to the lower symmetry of the Ru(phen)$_2$L complexes, peak assignment of the ^{1}H NMR was more difficult. The aliphatic resonances, three of the pyridine resonances, and one of the phenyl resonances could be assigned based on the

spectra of DSTM, DSTM-AE, and DSTM-AP, but the other resonances formed part of a $Ru(phen)_2DIP$ system that was not easy to assign. As in the case of $Ru(DIP)_2DSTM$, the NMR spectra of all three $Ru(phen)_2L$ complexes showed little resonance near 10.5 or 9.2 ppm, which indicates that $Ru(phen)_2Cl_2$ and free phenanthroline moiety were not present in the final products. The overall purity of $Ru(phen)_2DSTM$ and $Ru(phen)_2(DSTM\text{-}AE)$ appeared to be high based on the lack of baseline peaks in the aromatic region. The actual ratio of aliphatic to aromatic proton resonances was close to the calculated ratio in the case of $Ru(phen)_2DSTM$ (0.333 calculated, 0.308 found). The aliphatic region of the spectrum of $Ru(phen)_2(DSTM\text{-}AE)$ was inexplicably broadened, leading to disagreement between the actual and calculated aliphatic/aromatic ratios (0.783 calculated, 0.637 found). $Ru(phen)_2(DSTM\text{-}AP)$ appeared to be somewhat less pure due to the presence of baseline peaks in the aromatic region. This could indicate that partial sulfonamide hydrolysis has taken place, or that other impurities were carried over from the DSTM-AP ligand used in the synthesis. The actual aliphatic/aromatic ratio for $Ru(phen)_2(DSTM\text{-}AP)$ was also somewhat lower than the calculated ratio (0.870 calculated, 0.713 found), which could also be due to partial sulfonamide hydrolysis. The mass spectra of the three $Ru(phen)_2L$ complexes were consistent with the above interpretations of the NMR spectra. The mass spectra of $Ru(phen)_2DSTM$ and $Ru(phen)_2(DSTM\text{-}AE)$ showed both singly and double charged molecular ions as the strongest peaks. The mass spectrum of $Ru(phen)_2(DSTM\text{-}AE)$ also showed a weaker peak at 1233 m/z produced by a single S-N fragmentation. The mass spectrum of $Ru(phen)_2(DSTM\text{-}AP)$ showed singly and double charged molecular ions, but also showed a peak at 1263 that arises from sulfonamide hydrolysis. This supports the NMR interpretation that the $Ru(phen)_2(DSTM\text{-}AP)$ may contain partially hydrolyzed material as an impurity.

The UV-visible spectra of the three $Ru(phen)_2L$ complexes are virtually identical. All three complexes have a visible maximum at 437-438 nm due to metal to ligand charge transfer. The extinction coefficient of the $Ru(phen)_2L$ complexes at the visible maximum is $2.3 \times 10^4\ M^{-1}cm^{-1}$. This value is between that of $Ru(phen)_3Cl_2$ (1.96×10^4) and $Ru(DIP)_3Cl_2$ (2.95×10^4), which is reasonable for a $Ru(phen)_2DIP$ system.[18] In contrast to $Ru(DIP)_2DSTM$, the $Ru(phen)_2L$ complexes are all directly soluble in water, and more concentrated aqueous solutions could be made. This is consistent with the lower hydrophobicity of the two phenanthroline (phen) ligands relative to the diphenylphenanthroline (DIP) ligands. Due to their hydrophobic third ligands (DSTM, DSTM-AE, and DSTM-AP), the $Ru(phen)_2L$ complexes are also soluble in nonpolar solvents such as CH_2Cl_2 and $CHCl_3$. As described in the experimental section for $Ru(phen)_2$(DSTM-AE), the complex remained mostly in the aqueous layer when partitioned between water and CH_2Cl_2. The net charge of the $Ru(phen)_2L$ complexes (and therefore the number of associated chloride ions) in aqueous solutions has not been studied. If all tertiary amines are protonated, then the net charge of $Ru(phen)_2DSTM$ would be +4, and the net charge of $Ru(phen)_2$(DSTM-AE) or $Ru(phen)_2$(DSTM-AP) would be +6.

Discussion of the Synthesis and Characterization of $Rh(phi)_2$(DSTM-AP). The complex $Rh(phi)_2Cl_2^+$ is highly inert to further substitution at the rhodium metal due to the strength of the Rh-Cl bonds; this is in contrast to $Ru(DIP)_2Cl_2$ and $Ru(phen)_2Cl_2$, where the chloride ligands are easily replaced by water.[19] The method used for the synthesis or $Rh(phi)_2$(DSTM-AP) utilizes silver triflate to remove the chloride ligands from the $Rh(phi)_2Cl_2^+$.[20] Three equivalents of silver triflate were used per equivalent of $[Rh(phi)_2Cl_2]^+Cl^-$ in order to precipitate all the chloride as AgCl. Excess silver was not used so as to minimize the possibility of amine oxidation of

DSTM-AP by Ag^+. The chloride ligands were presumably replaced by DMF ligands from the solvent, and the AgCl precipitate was then removed by centrifugation. The labile DMF ligands were then replaced by DSTM-AP to form $Rh(phi)_2$(DSTM-AP). In order to produce a more water soluble complex, anion exchange chromatography was used to replace the triflate counterions with chlorides. An aqueous solution of the complex was then washed with $CHCl_3$ in a separatory funnel to remove hydrophobic impurities. Attempts were made to purify the product further using reversed-phase HPLC, but the attempts were unsuccessful due to poor resolution and the low mobility of the complex on the column. The poor resolution may have been due to hydrogen bonding interactions between the silica backbone of the stationary phase and protonated amine and/or pyridine groups of $Rh(phi)_2$(DSTM-AP). Preliminary attempts at HPLC purification using a POROS 10 R2 reversed-phase column from PerSeptive Biosystems (which does not have a silica backbone) appeared to be more promising.[21]

The ^1H NMR of the product had poor resolution in the aromatic region. The aliphatic region had more peaks than the DSTM-AP ligand starting material. This indicates that the product is likely to be a mixture of isomers, with DSTM-AP coordinating to the rhodium either through the phenanthroline moiety or through the bis(2-picolyl)amine moiety. The presence of additional impurities cannot be ruled out by the NMR. The mass spectrum showed no molecular ion, but showed fragments of $Rh(phi)_2$(DSTM-AP) at 1541 and 1455 m/z due to the loss of one or two 3-dimethylaminopropyl groups, respectively. The assignments of the mass spectrum peaks at 1161 and 1099 m/z (Figure 2.29) are more speculative, and alternate assignments are possible.

The UV-visible spectrum of the complex is consistent with a $Rh(phi)_2L$ complex, with the characteristic rhodium-phi peak at 372 nm (Figure 2.24). The effect of pH on the visible spectrum of the complex was not studied, nor was atomic

absorption used to determine an extinction coefficient of the complex. It is likely that the visible spectrum of the complex is pH-dependent due to acid-base equilibria at the phi imine protons in a similar manner as $Rh(phi)_2bpy$.[22] Although the complex $Rh(phi)_2$(DSTM-AP) requires further purification and characterization, the efficient oxidative cleavage promoted by the complex (described in Chapter 4) and the mass spectrum indicate that the complex is at least partially the desired product. Further work on the complex is in progress.

2.6. Conclusions

The same basic scheme has been used to synthesize all five of the complexes. This scheme is illustrated for $Ru(DIP)_2$DSTM in Figure 2.5. The starting material N-acetylethylenediamine is alkylated twice with 2-picolyl chloride to form the bis(2-picolyl)amine chelating group. The acetyl protecting group is removed by acid hydrolysis to form the key intermediate N,N-di(2-picolyl)ethylenediamine (DEN). DEN can be monoalkylated with 2-dimethylaminoethyl chloride or 3-dimethylaminopropyl chloride to form DEDEN or DPDEN, respectively. The next step is the coupling of the amines DEN, DEDEN, or DPDEN to the meta-meta isomer of 4,7-diphenyl-1,10-phenanthrolinedisulfonate [$DIP(SO_3Na)_2$] to form the ligands DSTM, DSTM-AE, or DSTM-AP, respectively. The final step is the coordination of the ligands DSTM, DSTM-AE, or DSTM-AP to the *bis* chelate complexes $Ru(DIP)_2Cl_2$, $Ru(phen)_2Cl_2$, or $Rh(phi)_2Cl_3$. For the ruthenium complexes, water was sufficient to labilize the chlorides for the final coordination step, but for the coordination of DSTM-AP to $Rh(phi)_2Cl_3$, silver triflate was used to labilize the chlorides.

The advantage of the above scheme is that the side products of the alkylation reactions can (for the most part) be removed while the intermediates are still of

Figure 2.5. Synthetic Scheme for $Ru(DIP)_2DSTM$

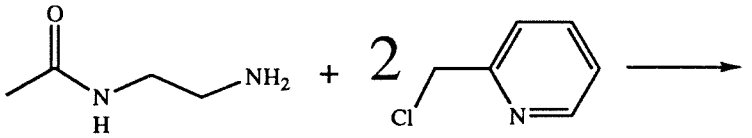

N-Acetylethylenediamine

2-Picolyl chloride

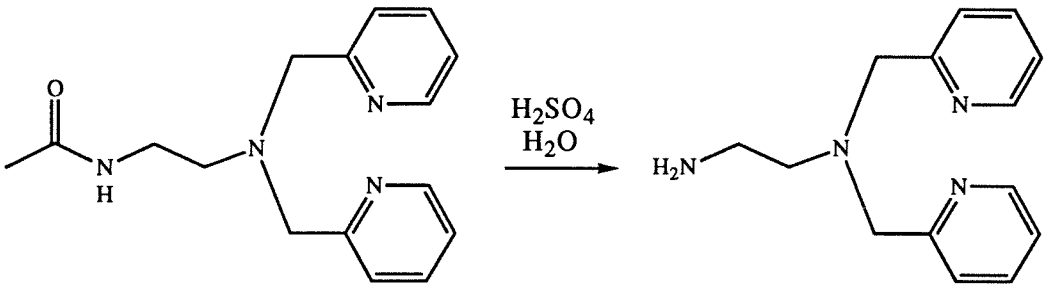

N-Acetyl-N',N'-di(2-picolyl)ethylenediamine

DPNED

N,N-Di(2-picolyl)ethylenediamine

DEN

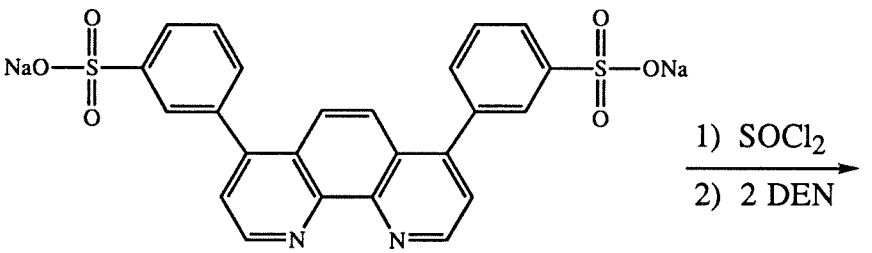

meta,meta-4,7-Diphenyl-1,10-phenanthroline disulfonate

$DIP(SO_3Na)_2$

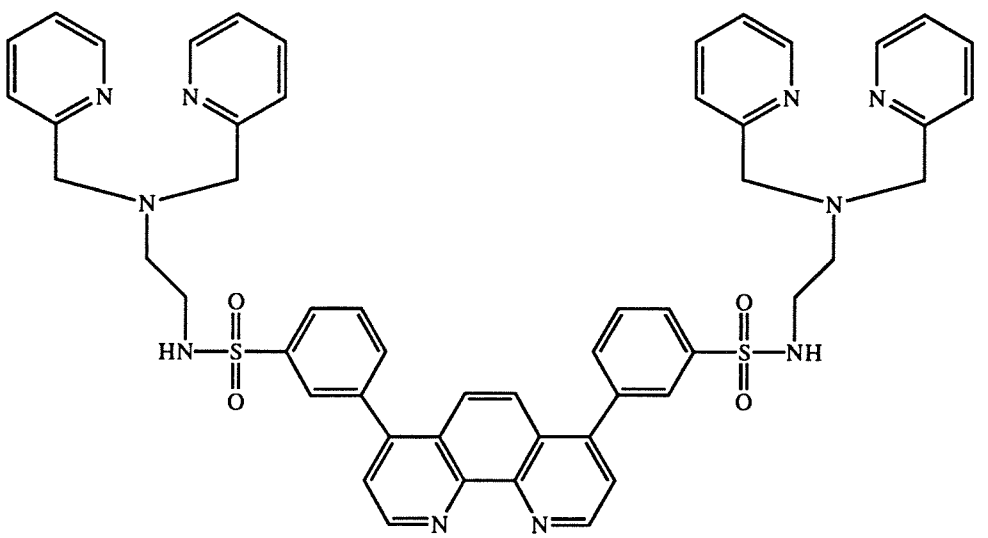

DSTM

Figure 2.5. (cont.) Synthetic Scheme for $Ru(DIP)_2DSTM$

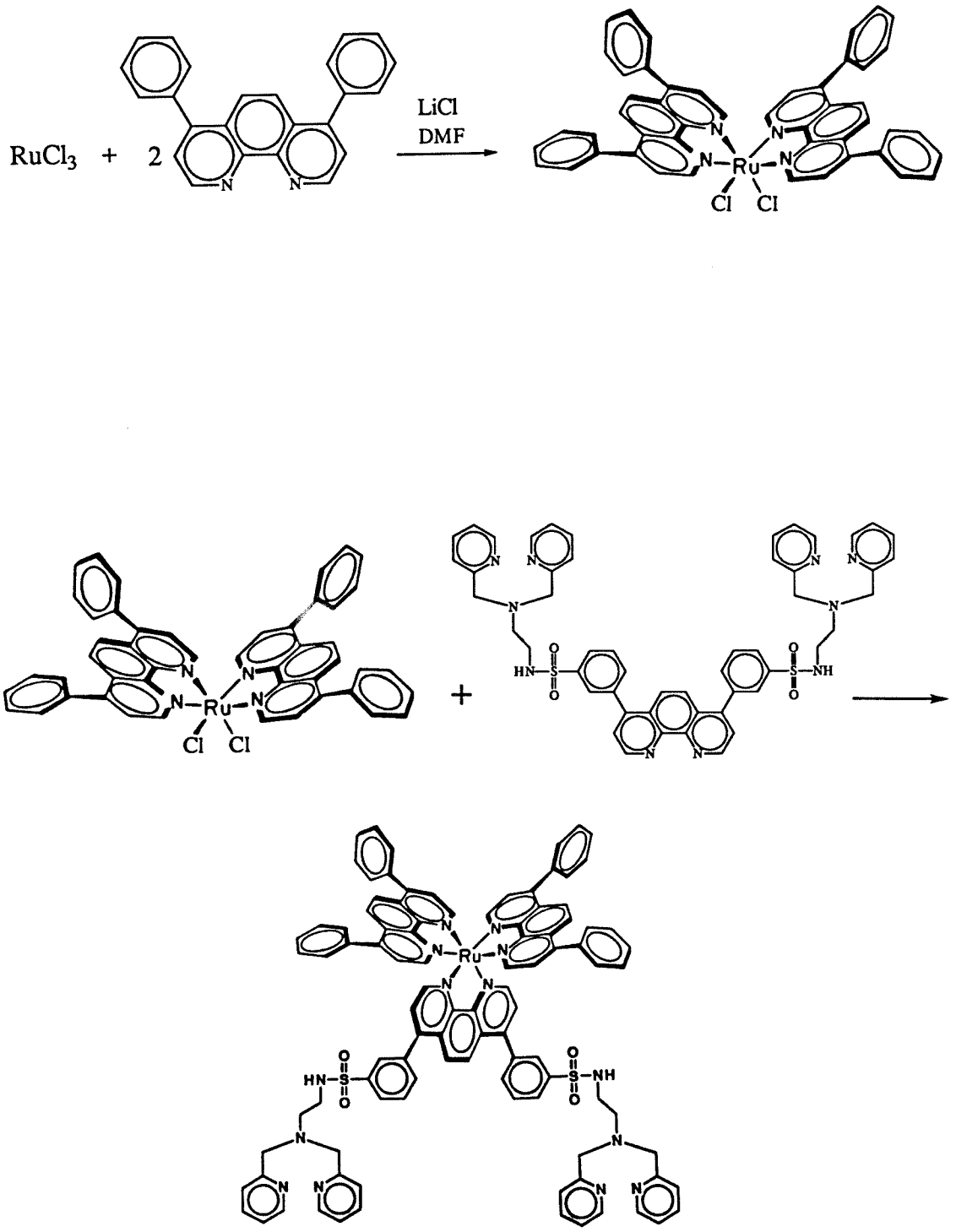

relatively low molecular weights. An alternative synthetic scheme, where ethylenediamine was coupled to $DIP(SO_3Na)_2$ and then alkylated, was less successful due to purification difficulties and possible sulfonamide alkylation.[23] A drawback of the illustrated scheme is the possibility that the ligands DSTM, DSTM-AE, and DSTM-AP might coordinate to the ruthenium or rhodium metal through the bis(2-picolyl)amine moiety rather than through the phenanthroline moiety. For the ruthenium complexes, this did not appear to be a problem, but in the case of $Rh(phi)_2$(DSTM-AP), the final reaction appeared to produce a mixture of coordination isomers. An alternative scheme involves the synthesis of $Rh(phi)_2[DIP(SO_3)_2]$, to be followed by coupling to DPDEN to form $Rh(phi)_2$(DSTM-AP). This scheme avoids the possibility of rhodium coordination to bis(2-picolyl)amine, and is currently under investigation in our laboratory.

The five complexes $Ru(DIP)_2$DSTM, $Ru(phen)_2$DSTM, $Ru(phen)_2$(DSTM-AE), $Ru(phen)_2$(DSTM-AP), and $Rh(phi)_2$(DSTM-AP) have been synthesized as possible DNA nucleases. The intent is that the $Ru(DIP)_2^{2+}$, $Ru(phen)_2^{2+}$, or $Rh(phi)_2^{3+}$ moiety deliver the complex in a site-selective manner to DNA so that the third ligand (DSTM, DSTM-AE, or DSTM-AP) could promote DNA cleavage through an additional labile chelated metal and/or an attached protonated dimethylaminoalkyl group. The complexes $Ru(DIP)_2$DSTM, $Ru(phen)_2$DSTM, and $Ru(phen)_2$(DSTM-AE) were successfully synthesized in fairly high (92-98%) purity. Due to difficulties in the purification of the amine DPDEN, and partial sulfonamide hydrolysis of DSTM-AP, the final purity of $Ru(phen)_2$(DSTM-AP) and $Rh(phi)_2$(DSTM-AP) were lower. The synthesis of $Rh(phi)_2$(DSTM-AP) appeared to be further complicated by partial coordination of DSTM-AP to rhodium through the bis(2-picolyl)amine moiety.

References

1. P. G. Schultz & P. B. Dervan (1983) *Proc. Natl. Acad. Sci. USA* **80:** 6834.
2. R. S. Youngquist & P. B. Dervan (1987) *J. Am. Chem. Soc.* **109:** 7564.
3 J. H. Griffen & P. B. Dervan (1987) *J. Am. Chem. Soc.* **109:** 6840.
4. A. Streitwieser, Jr. & C. H. Heathcock (1981) "Introduction to Organic Chemistry, 2nd Edition" Macmillan Publishing Co., New York, 758-759.
5. Ibid., 543.
6. D. H. R. Barton & W. D. Ollis (1979) "Comprehensive Organic Chemistry, vol. 2" Pergamon Press, Oxford, 4-5.
7. S. Patai (1968) "The Chemistry of the Amino Group" Interscience Publishers, John Wiley & Sons, London, 45-52.
8. F. A. Carey & R. J. Sundberg (1990) "Advanced Organic Chemistry, 3rd Edition, Part A: Structure and Mechanisms" Plenum Press, New York, 296.
9. The procedure for the separation of the isomers of $DIP(SO_3Na)_2$ was developed R. W. Cruse, M. Pustilnik, & L. A. Basile.
10. L. A. Basile (1989) Ph.D. Thesis, Columbia University, 118-119.
11. H. M. Bosshard, R. Moray, M. Schmid, & H. Zollinger (1959) *Helv. Chim. Acta.* **62:** 1633.
12. L. A. Basile (1989) Ph.D. Thesis, Columbia University, 92-93. The chromatographic procedure for $Ru(DIP)_2Cl_2$ was developed by R. W. Cruse.
13. P. Belser, A. v. Zelewsky, & M. Zehnder (1981) *Inorg. Chem.* **20:** 3098-3103.
14. A. M. Pyle (1989) Ph.D. Thesis, Columbia University, 94-95.
15. C. T. Lin, W. Bottcher, M. Chou, C. Creutz, & N. J. Sutin (1976) *J. Am. Chem. Soc.* **98:** 6536.
16. B. P. Sullivan, D. J. Salmon, & T. J. Meyer (1978) *Inorg. Chem.* **17:** 3334-3341.
17. A. T. Danishevsky (1987) Ph.D. Thesis, The City University of New York,

Hunter College, 59-60.

18. J. P. Rehmann (1988) Ph.D. Thesis, Columbia University, 13.

19. A. M. Pyle (1989) Ph.D. Thesis, Columbia University, 128-129.

20. A. Sitlani (1993) Ph.D. Thesis, California Institute of Technology, 107-109.

21. R. H. Terbrueggen, unpublished results.

22. A. M. Pyle (1989) Ph.D. Thesis, Columbia University, 118-123.

23. R. W. Cruse, unpublished results.

Appendix I. NMR Spectra

Figure 2.6. ^{1}H NMR of DPNED in $CDCl_3$

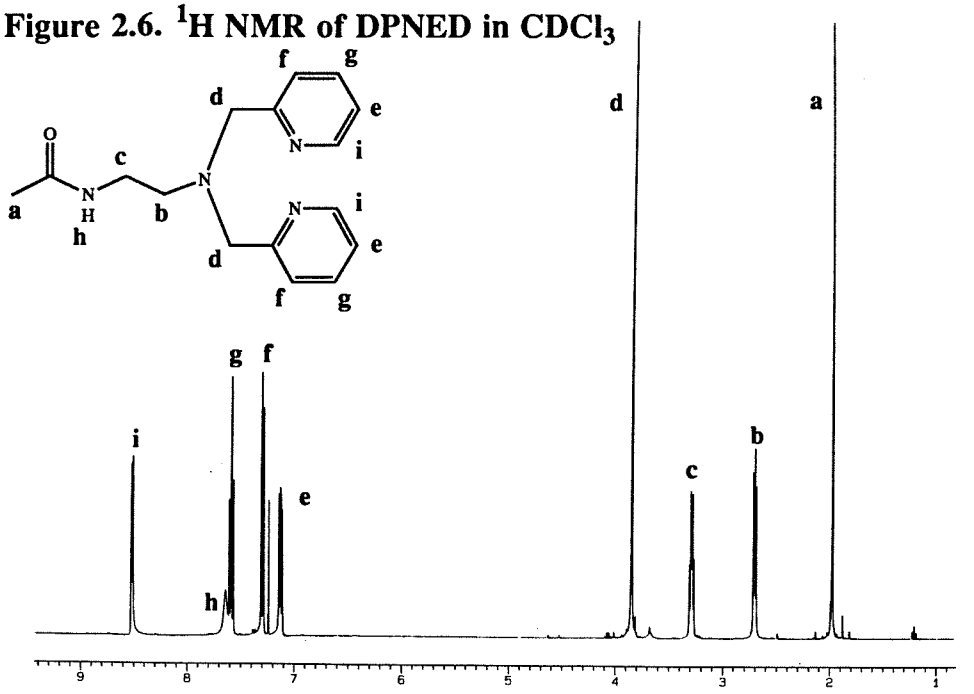

Figure 2.7. ^{1}H NMR of DEN in D_2O

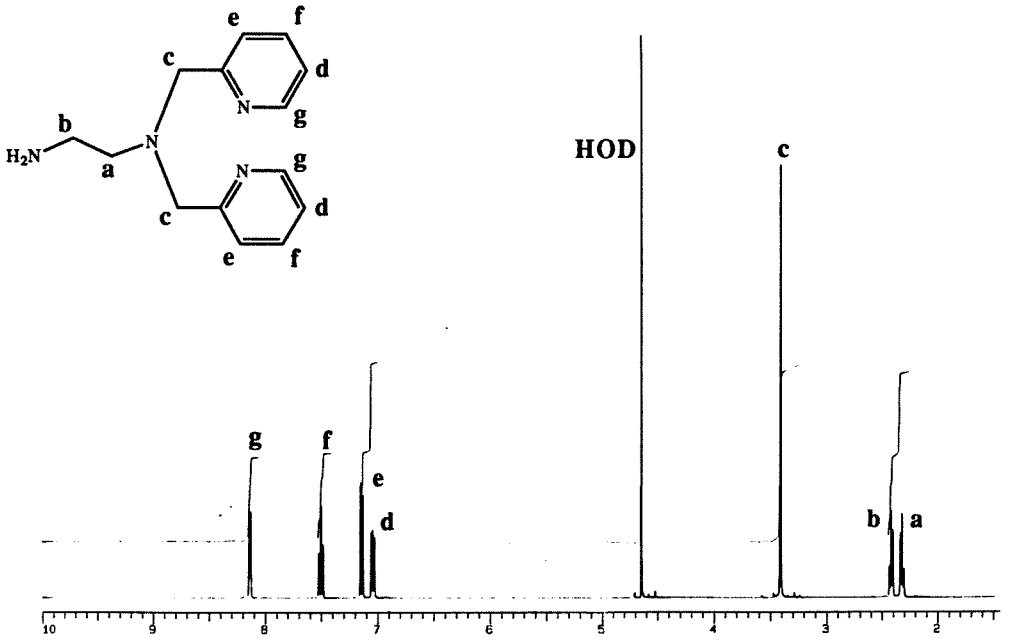

Figure 2.8. ^{1}H NMR of DEDEN in $CDCl_3$

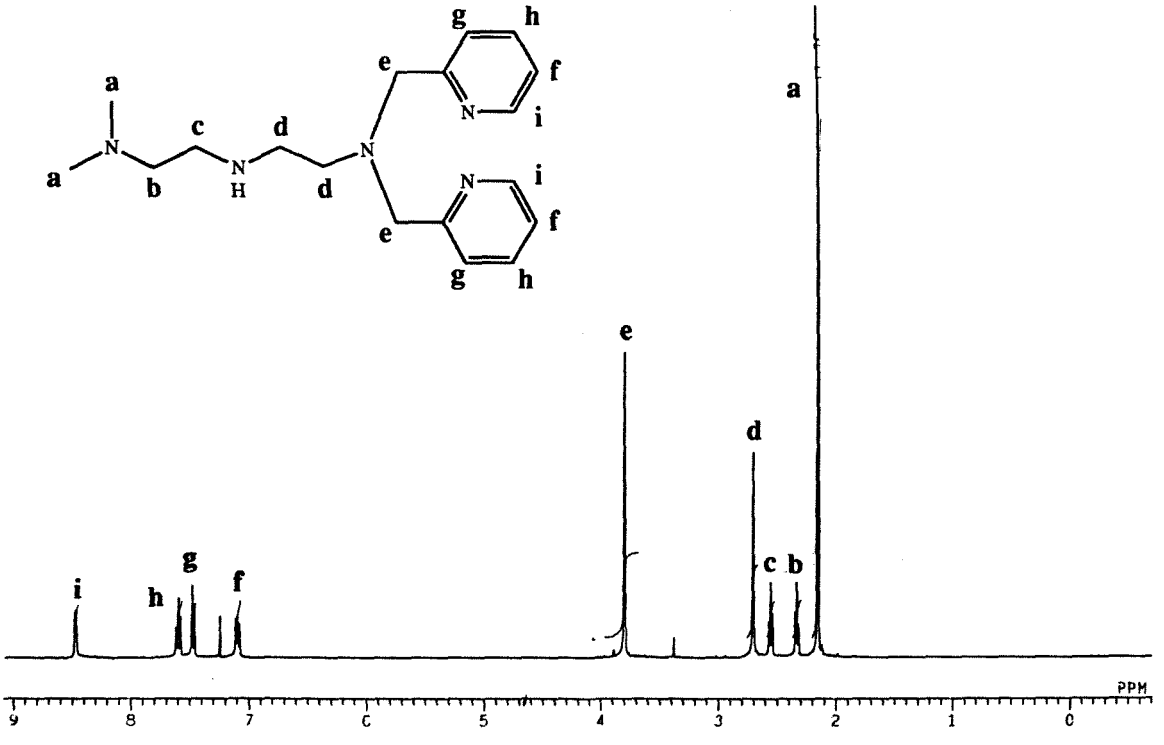

Figure 2.9. ^{1}H NMR of DPDEN in $CDCl_3$

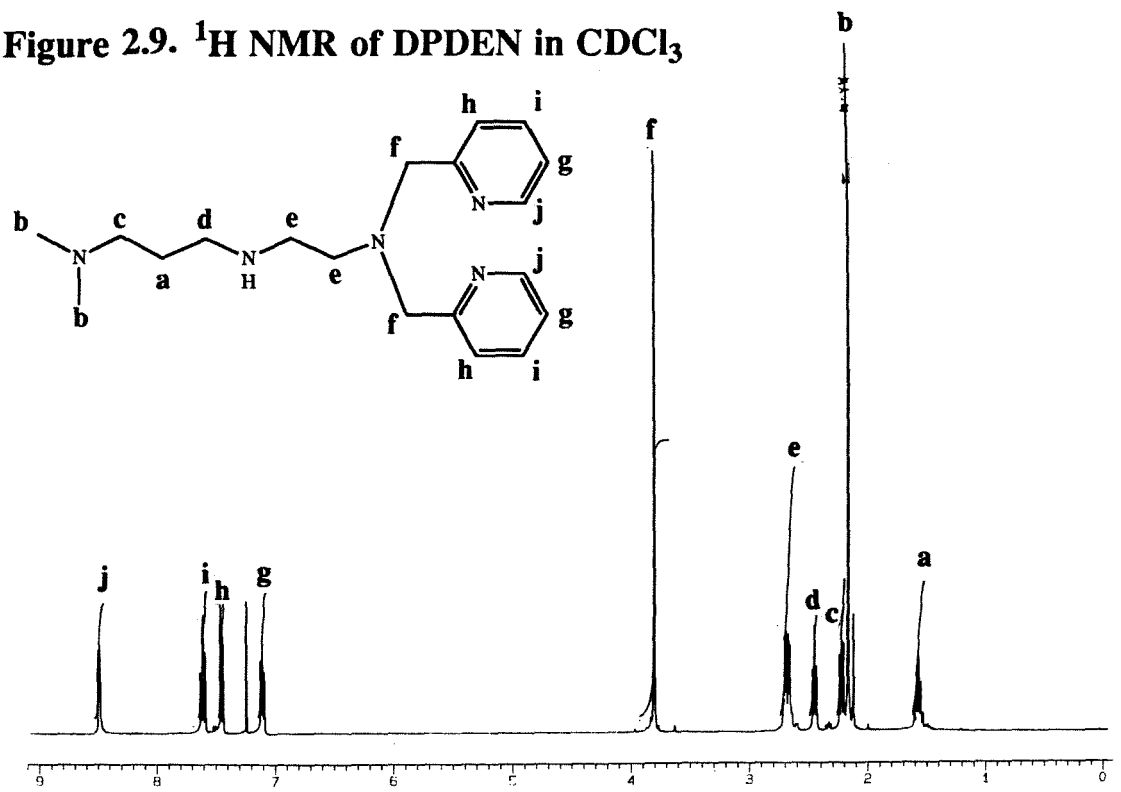

Figure 2.10. ^{1}H NMR of meta,meta-DIP($SO_3Na)_2$ in D_2O

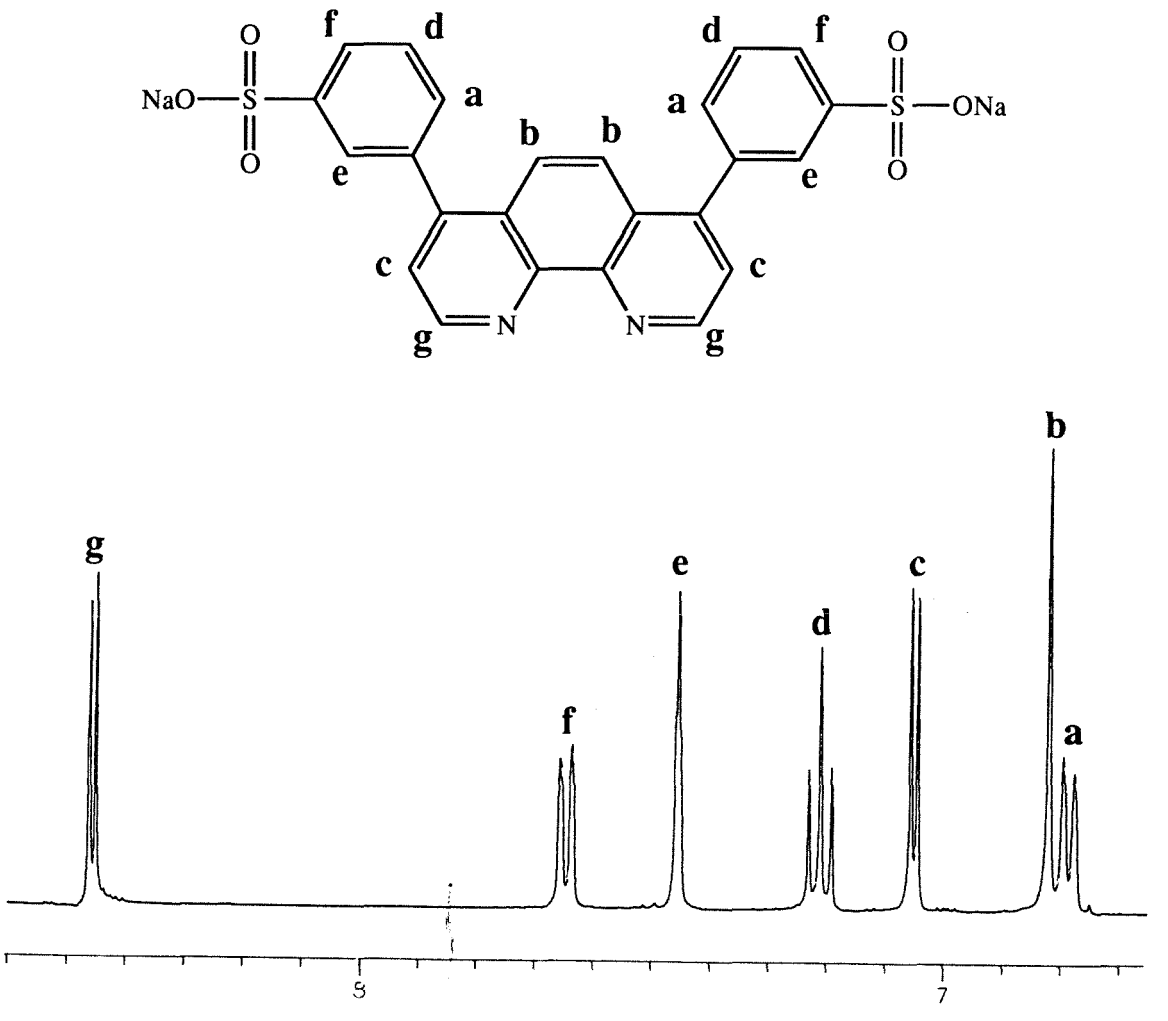

Figure 2.11. ^{1}H NMR of DSTM in $CDCl_3$*

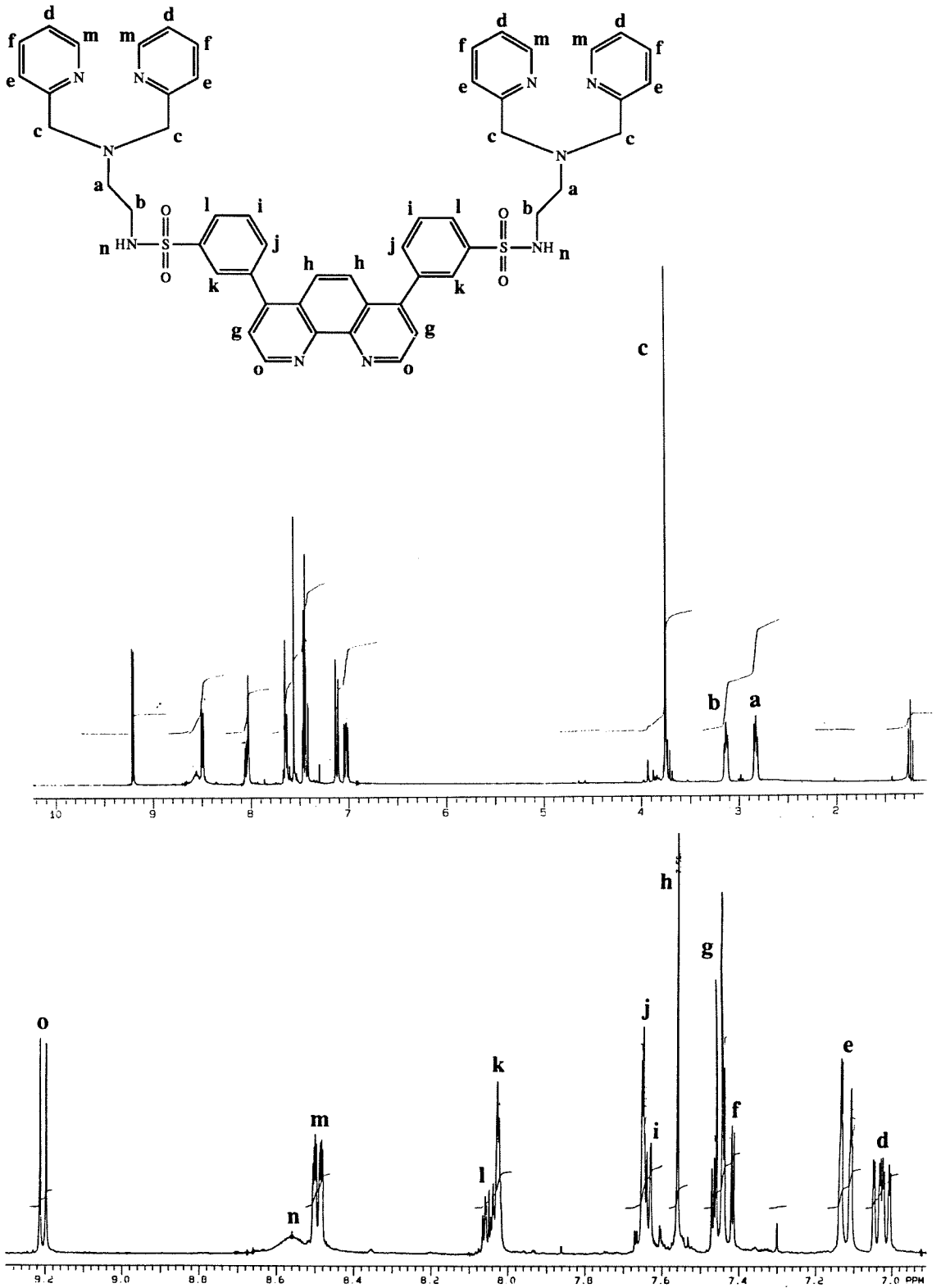

* $CHCl_3$ not referenced to 7.24 ppm; corrected chemical shifts listed in section 2.4.

Figure 2.12. ^{1}H NMR of DSTM-AE in $CDCl_3$

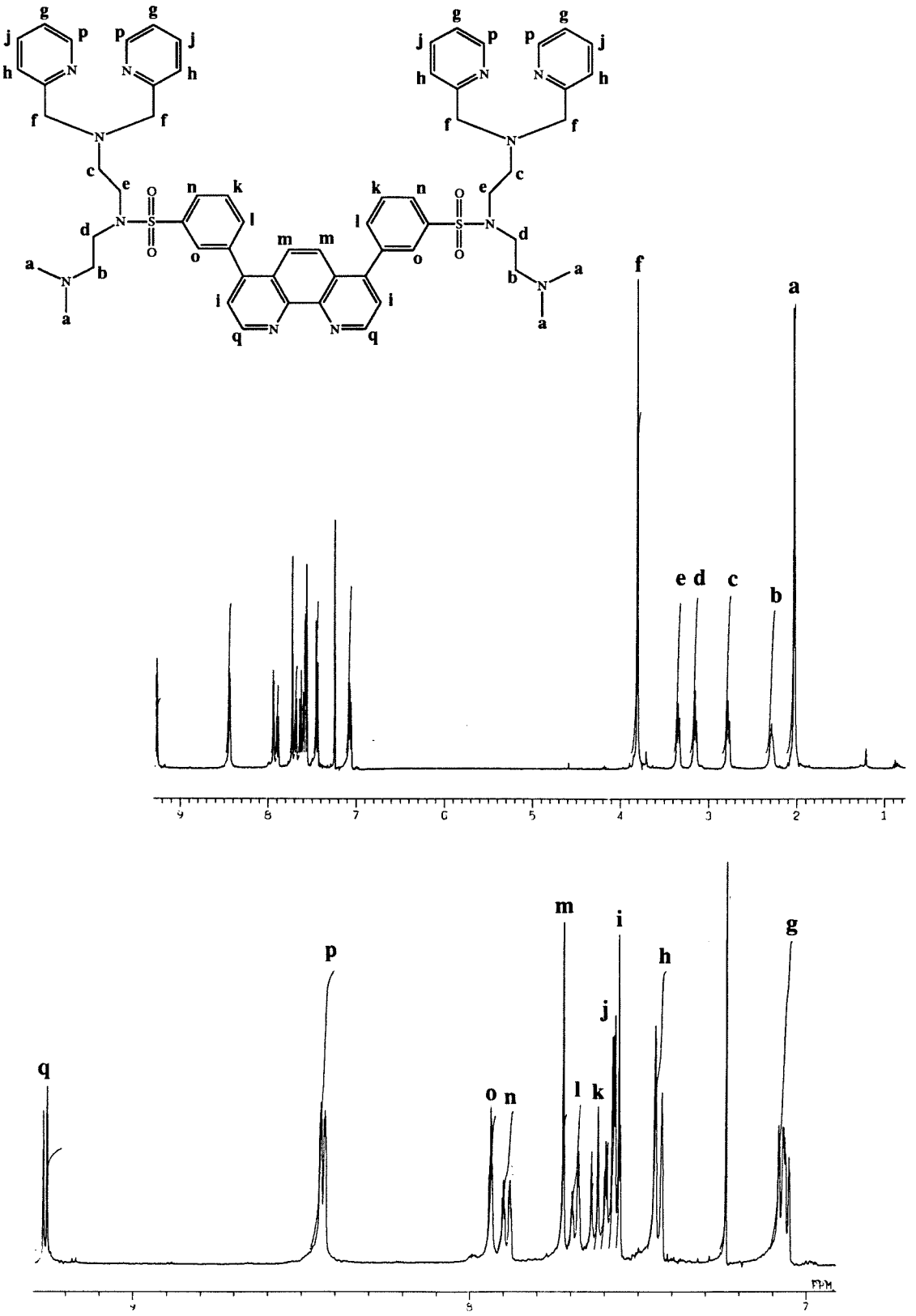

Figure 2.13. ^{1}H NMR of DSTM-AP in CD_2Cl_2

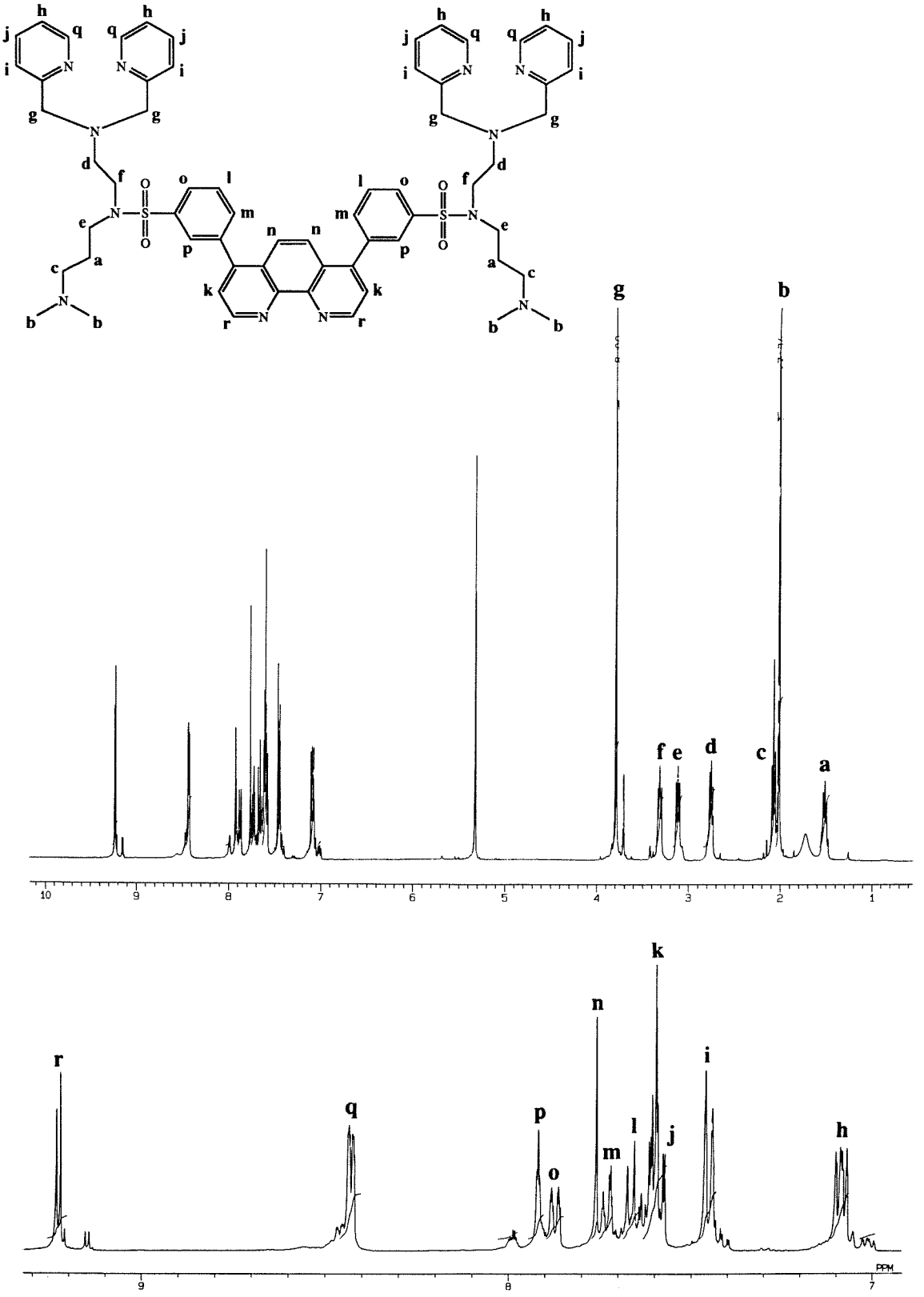

Figure 2.14. ^{1}H NMR of *cis*- and *trans*-$Ru(phi)_2Cl_2$, and $Ru(phi)_3^{2+}$ in DMSO-d_6

a: *cis*-$Ru(phi)_2Cl_2$ imine protons

b: *trans*-$Ru(phi)_2Cl_2$ imine protons

c: $Ru(phi)_3^{2+}$ imine protons

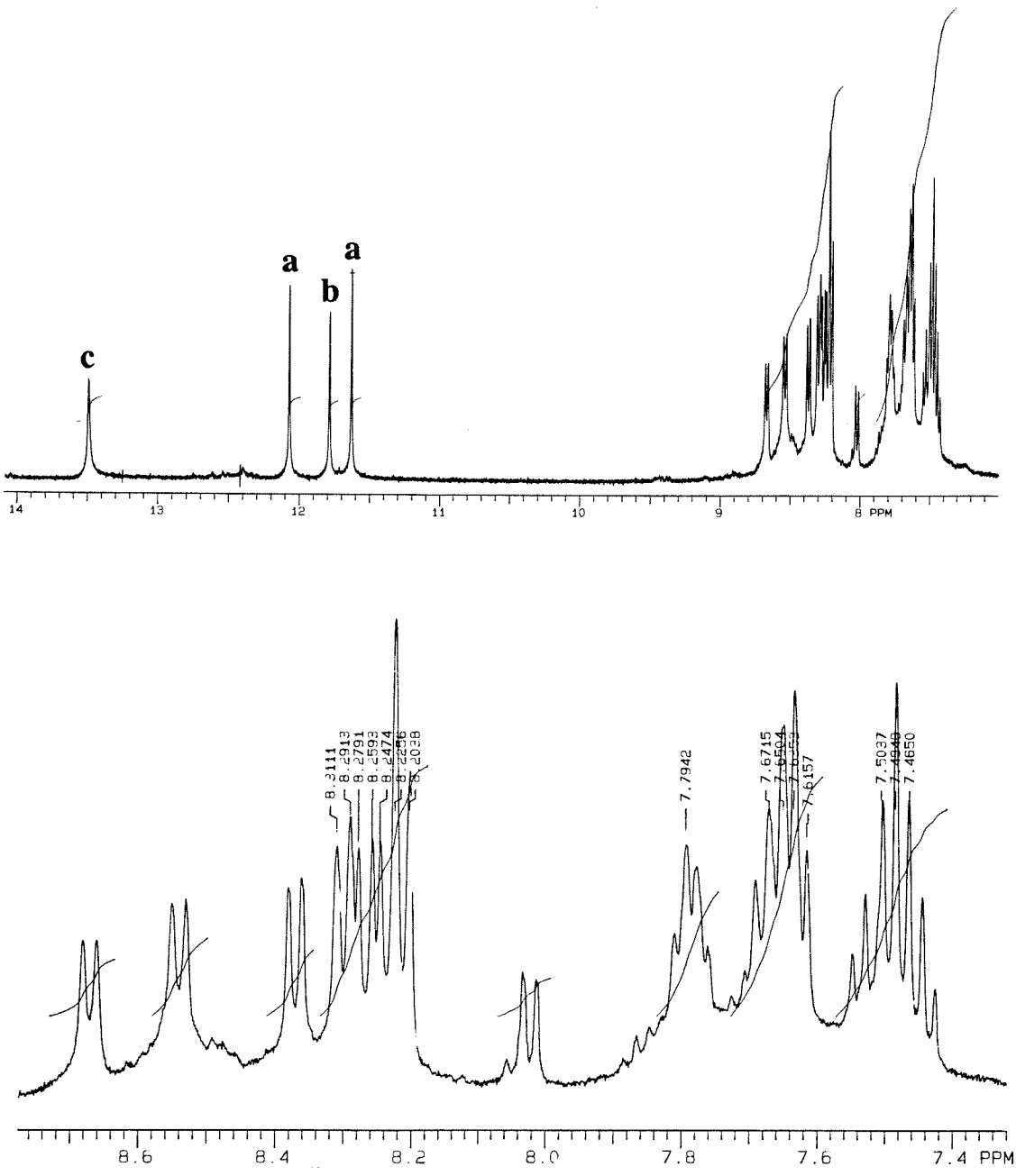

Figure 2.15. ^{1}H NMR of Ru(DIP)$_2$DSTM in CDCl$_3$*

Complex shown next page

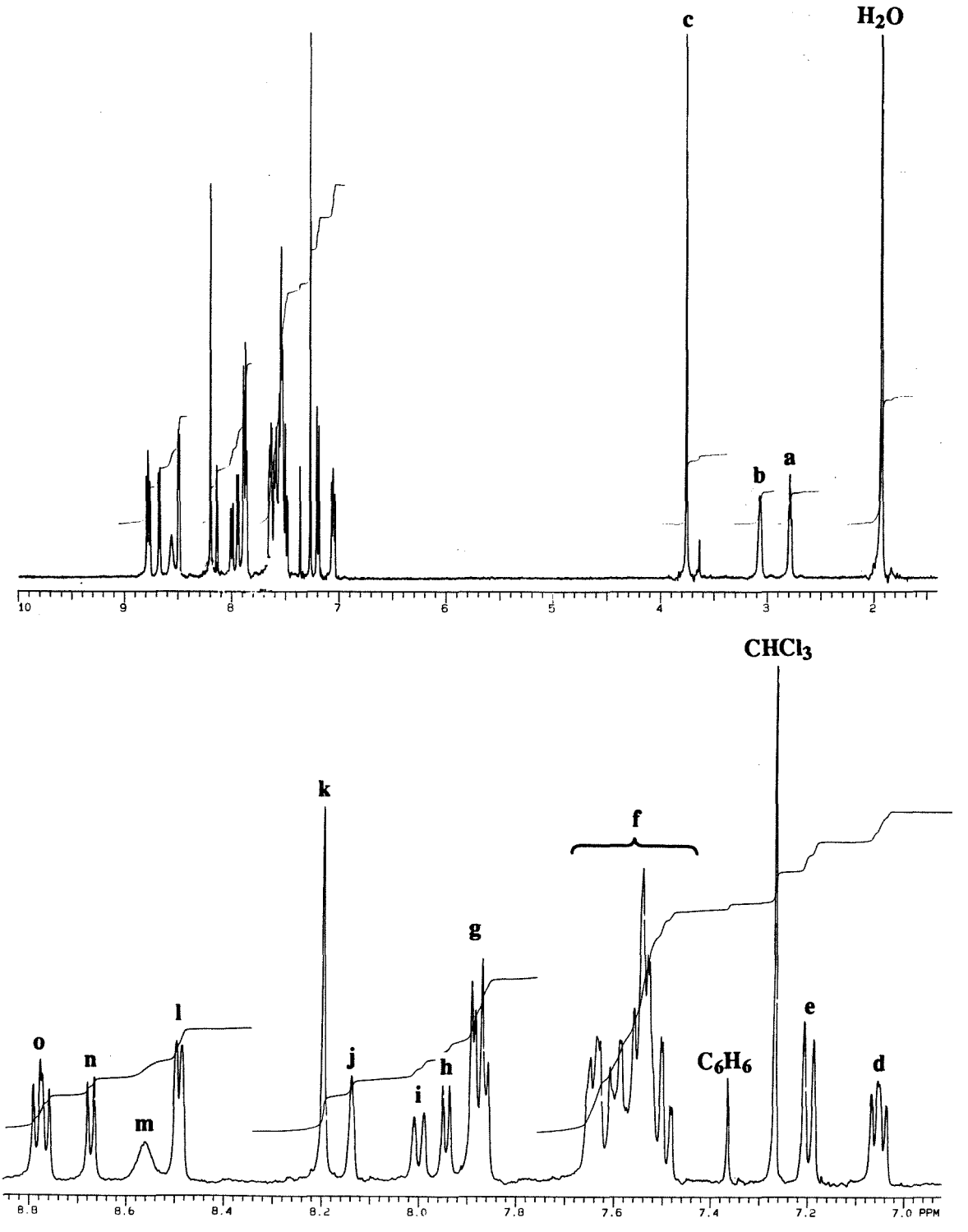

*$CHCl_3$ not referenced to 7.24 ppm; corrected chemical shifts listed in section 2.5.

Figure 2.15. (cont.) ^{1}H NMR of Ru(DIP)$_2$DSTM in $CDCl_3$

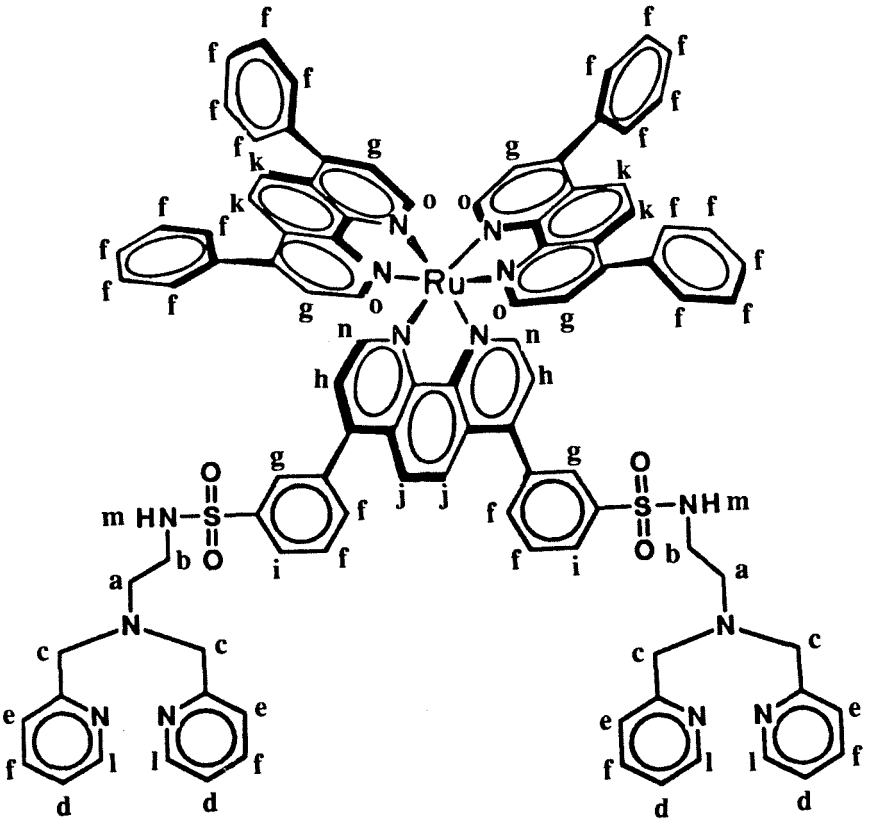

Figure 2.16. ^{1}H NMR of Ru(phen)$_2$DSTM in $CDCl_3$

Complex shown next page

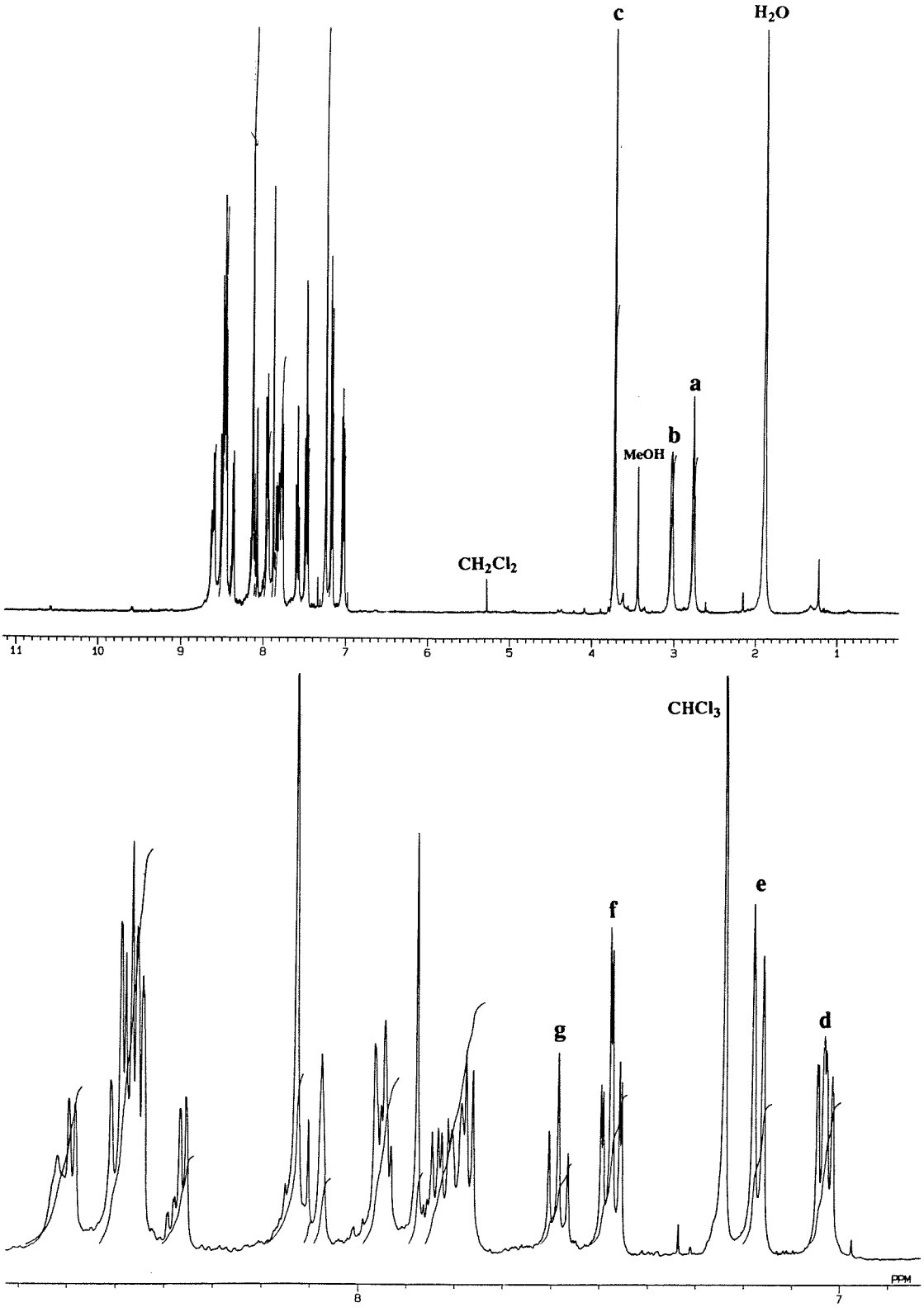

Figure 2.16. (cont.) ^{1}H NMR of Ru(phen)$_2$DSTM in $CDCl_3$

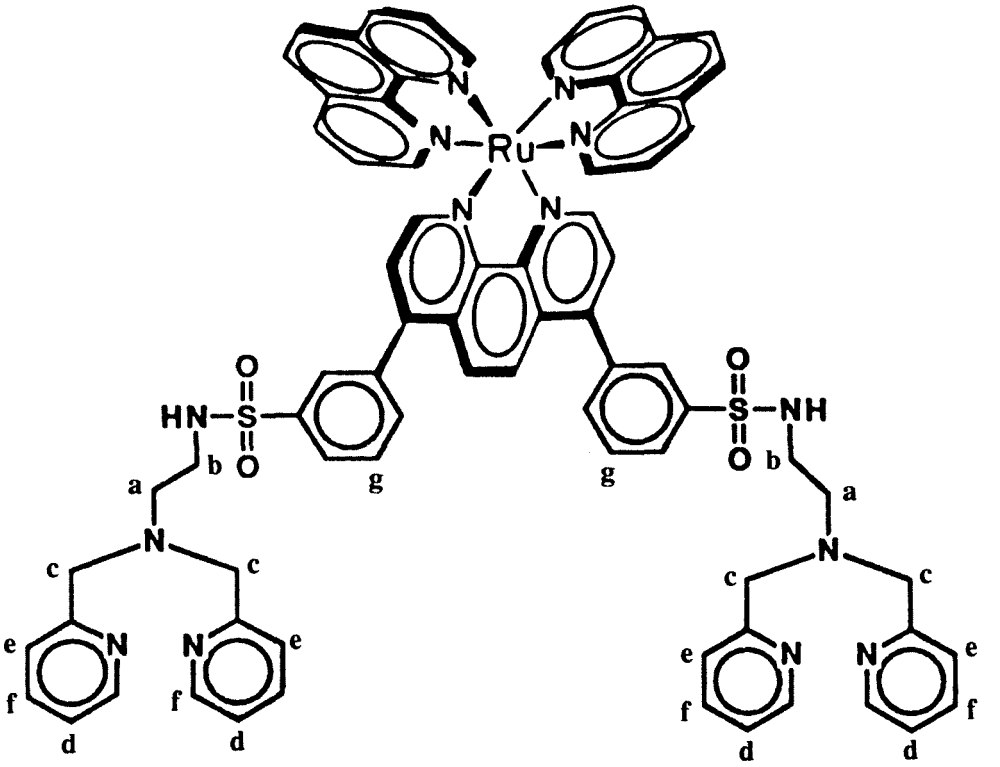

Figure 2.17. ^{1}H NMR of $Ru(phen)_2(DSTM\text{-}AE)$ in $CDCl_3$

Complex shown next page

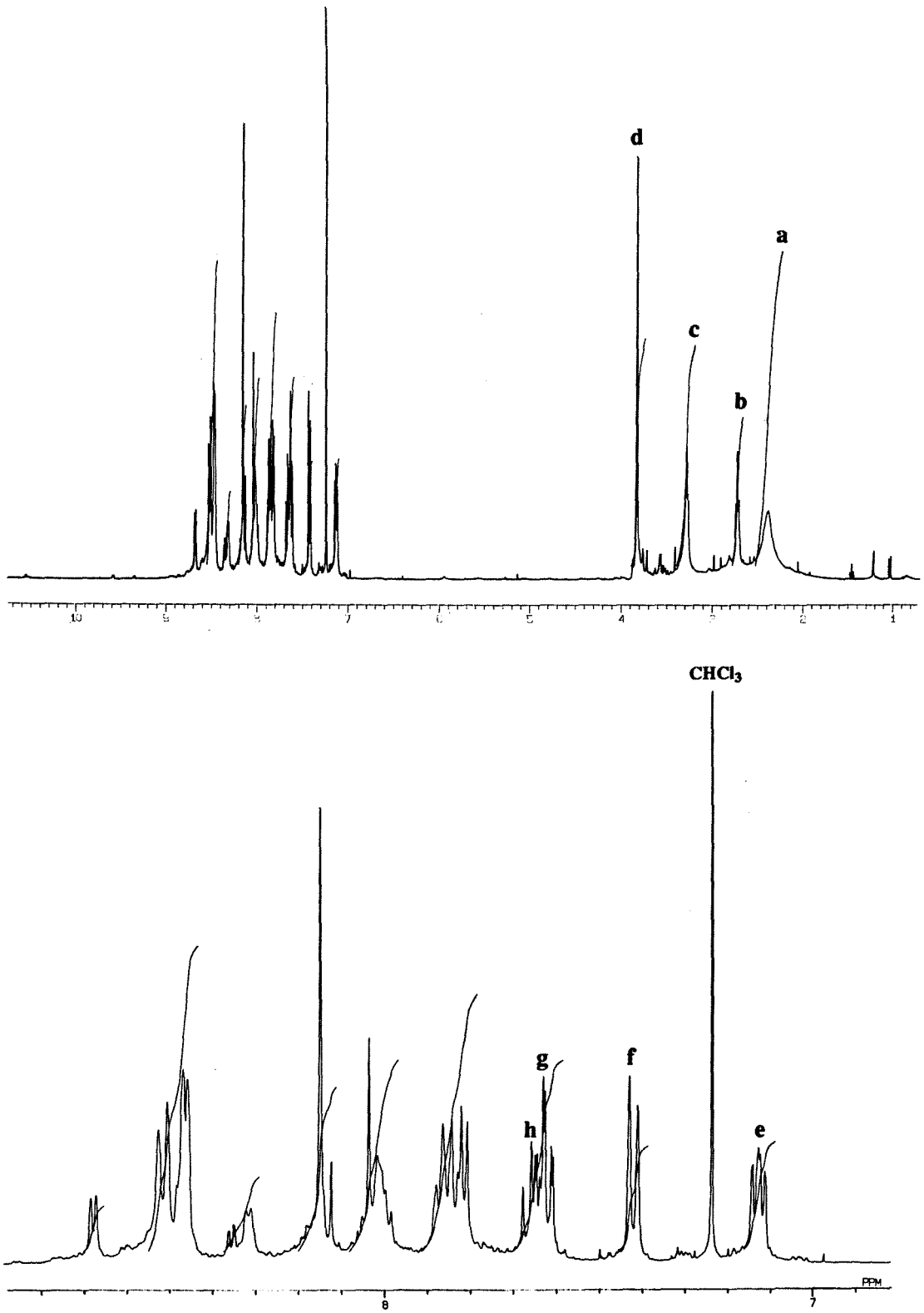

Figure 2.17. (cont.) ^{1}H NMR of Ru(phen)$_2$(DSTM-AE) in $CDCl_3$

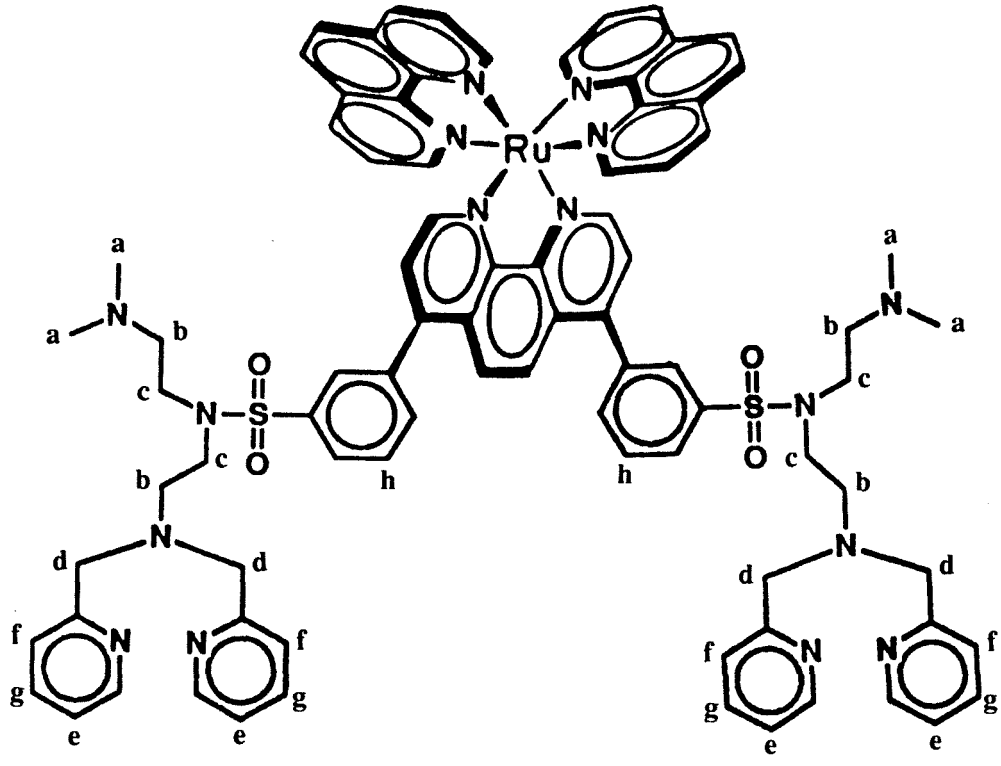

Figure 2.18. ^{1}H NMR of Ru(phen)$_2$(DSTM-AP) in $CDCl_3$

Complex and aliphatic region of spectrum shown next page

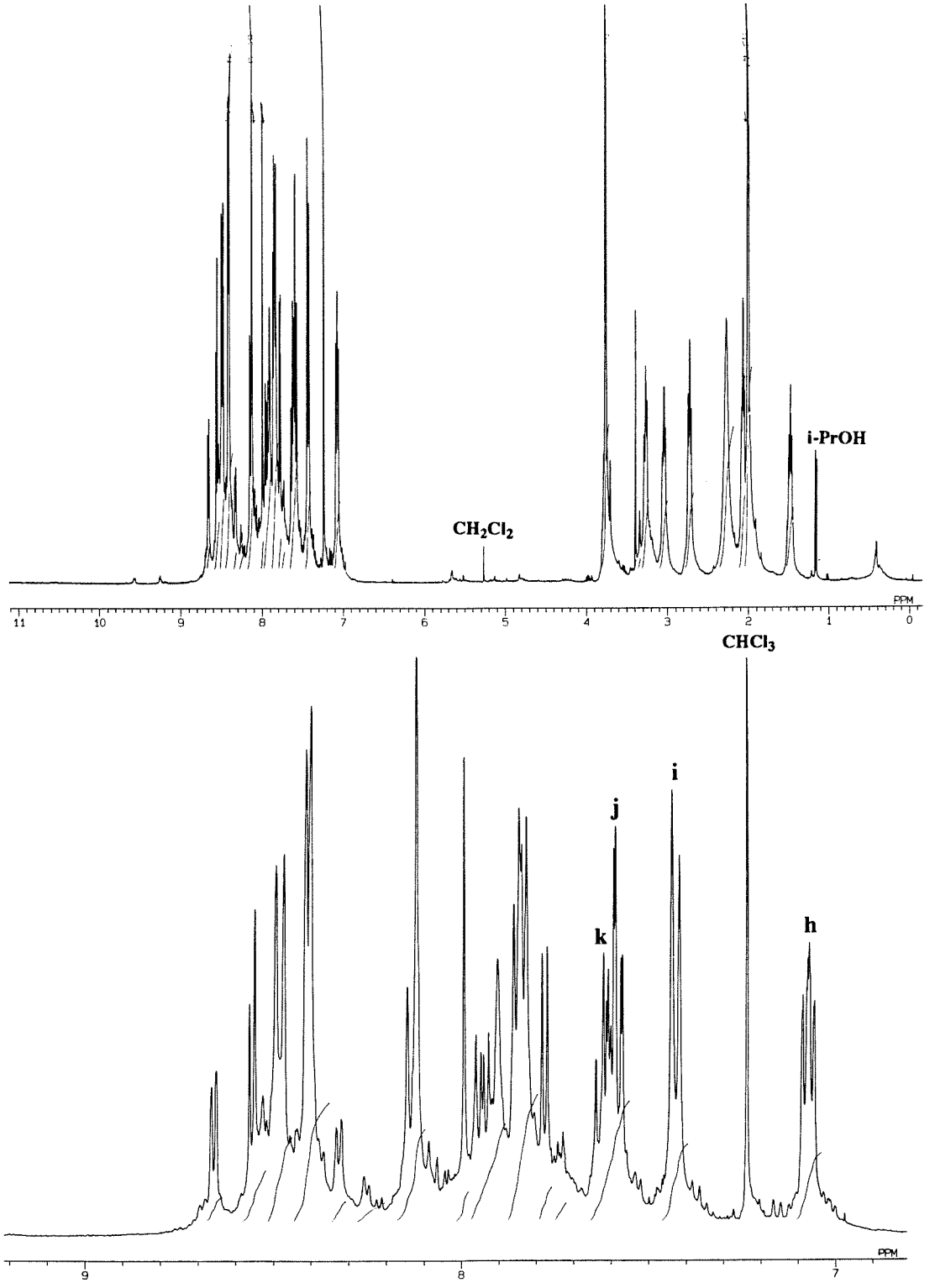

Figure 2.18. (cont.) ^{1}H NMR of Ru(phen)$_2$(DSTM-AP) in $CDCl_3$

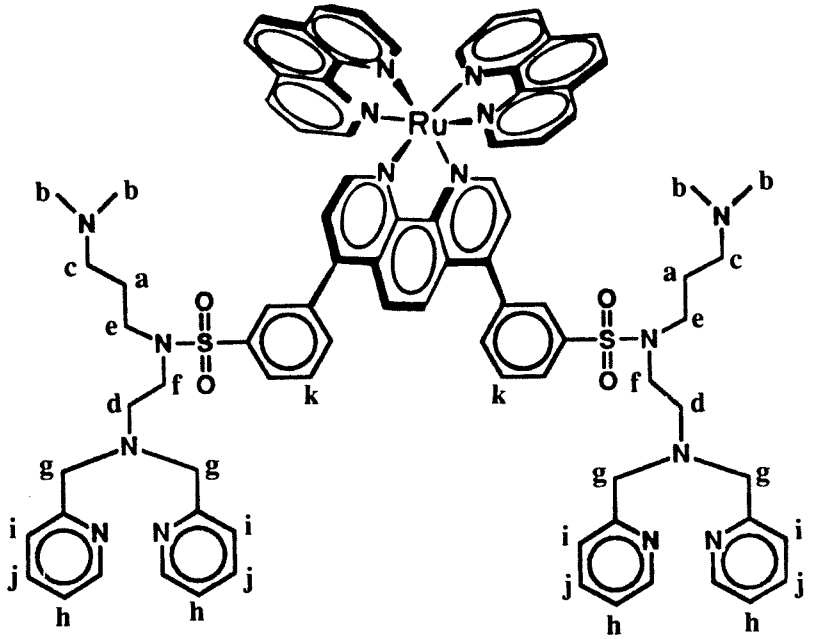

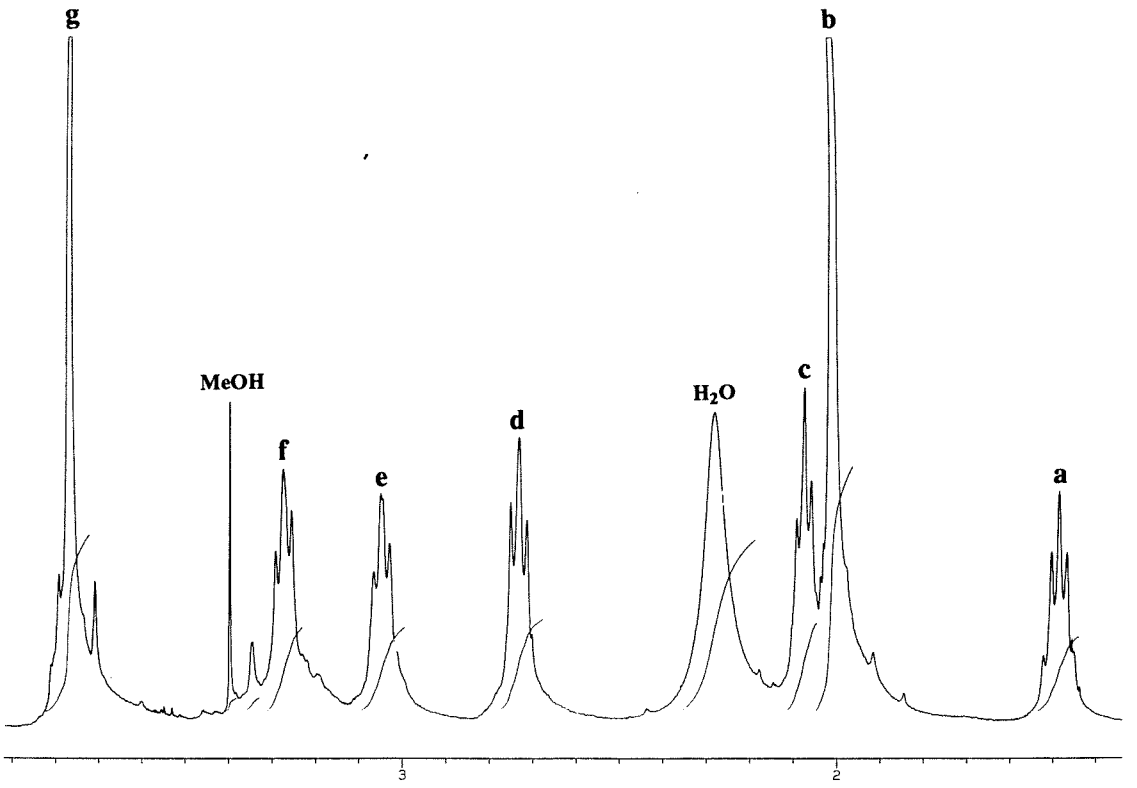

Figure 2.19. ^{1}H NMR of $Rh(phi)_2(DSTM\text{-}AP)$ in CD_3OD

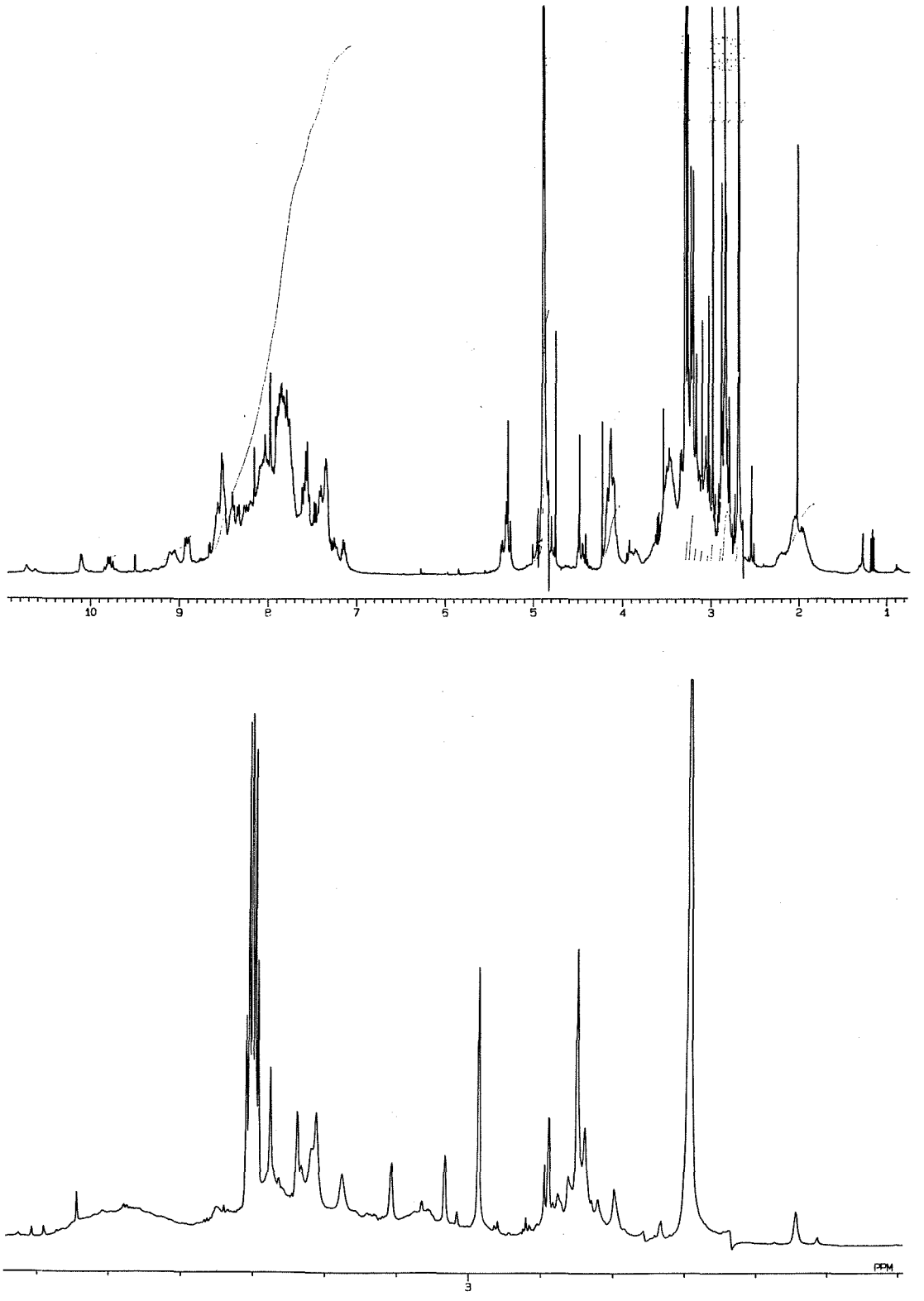

Appendix II. UV-Visible Spectra

Figure 2.20. UV-Visible Spectrum of $Ru(DIP)_2DSTM$

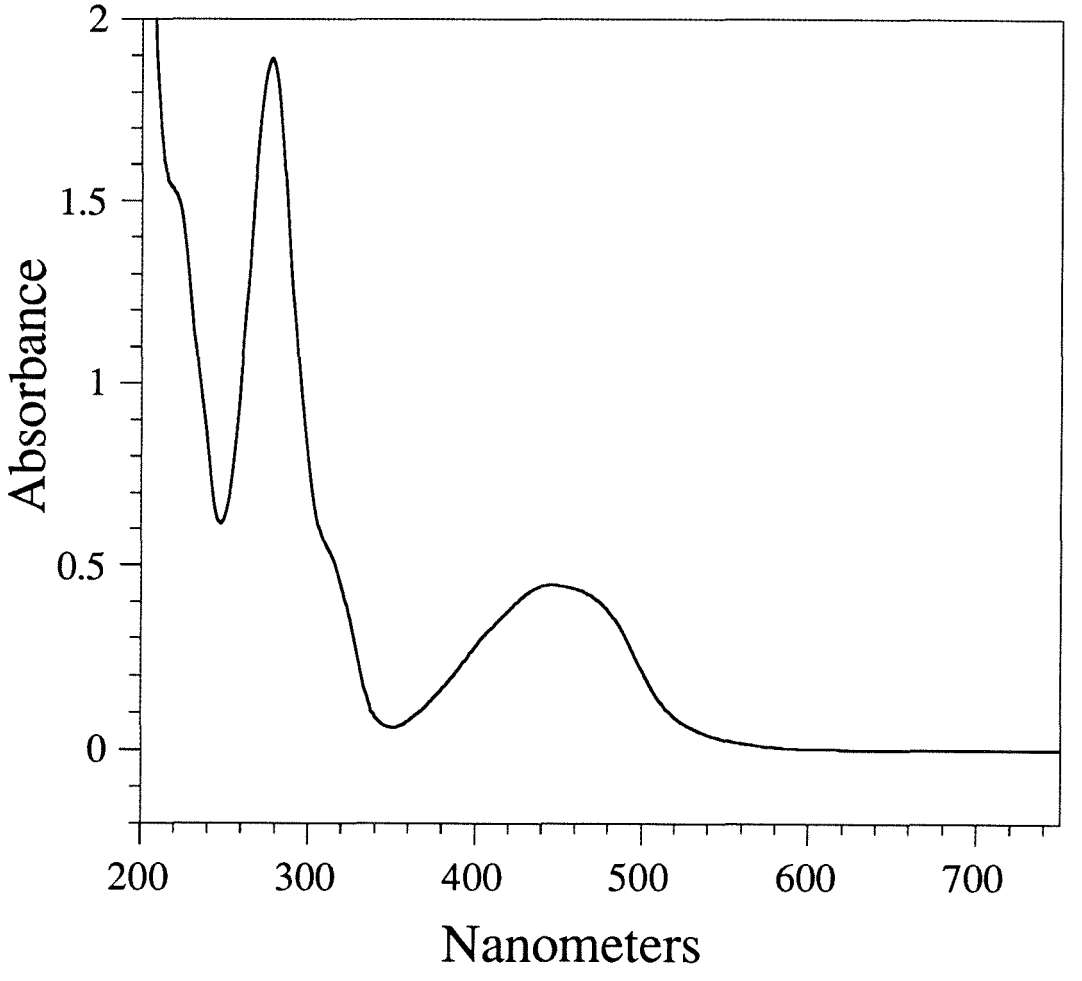

Figure 2.21. UV-Visible Spectrum of $Ru(phen)_2DSTM$

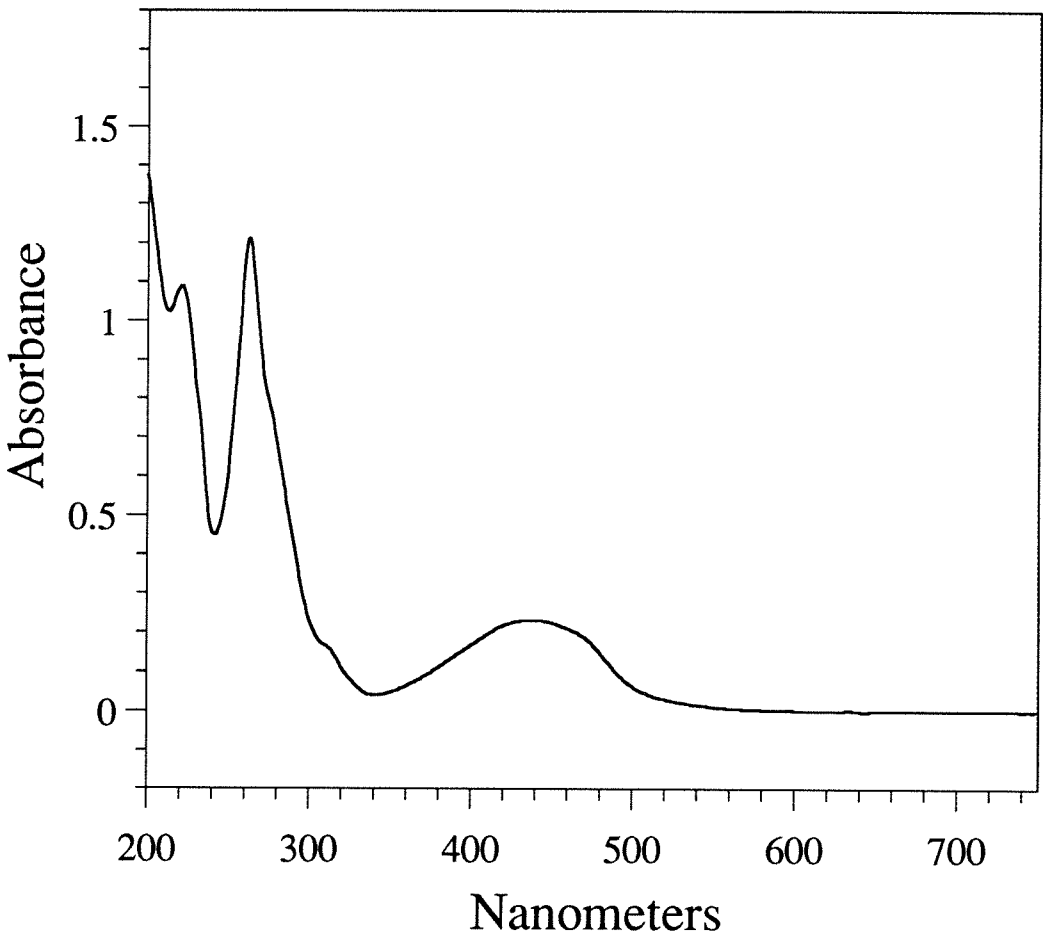

Figure 2.22. UV-Visible Spectrum of $Ru(phen)_2(DSTM\text{-}AE)$

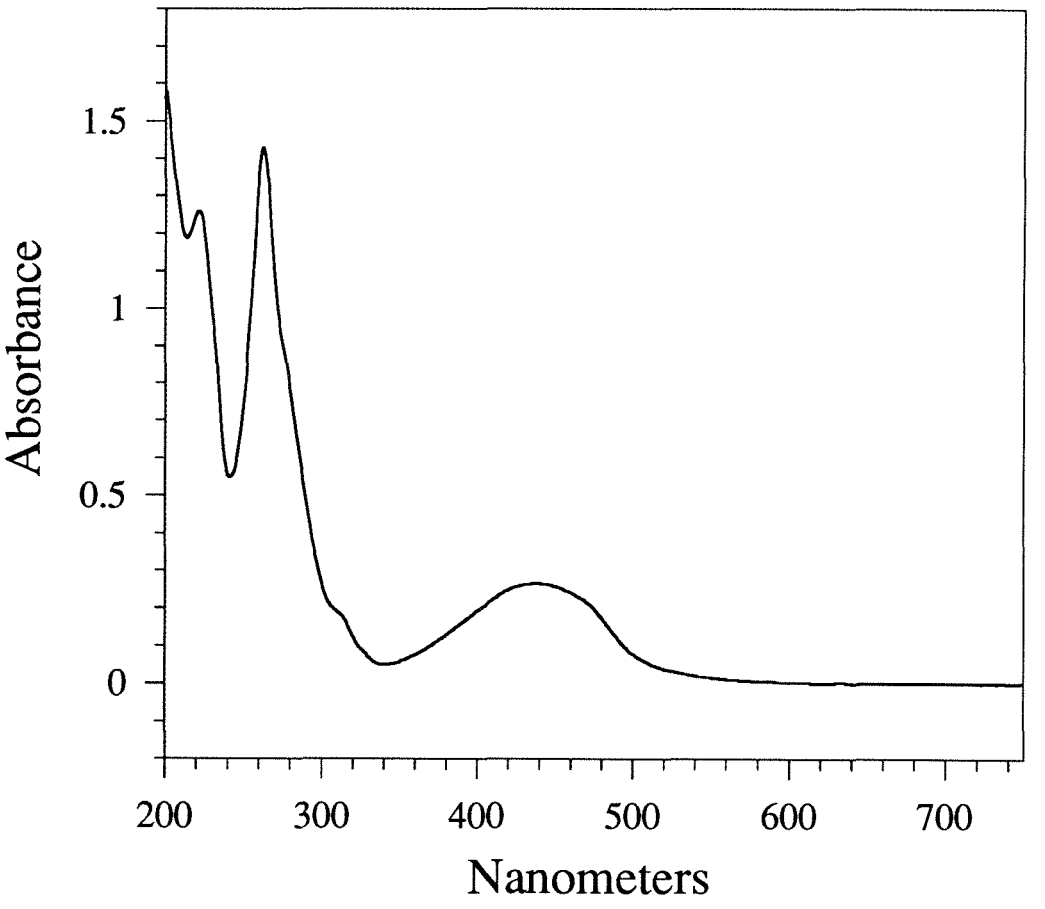

Figure 2.23. UV-Visible Spectrum of $Ru(phen)_2(DSTM\text{-}AP)$

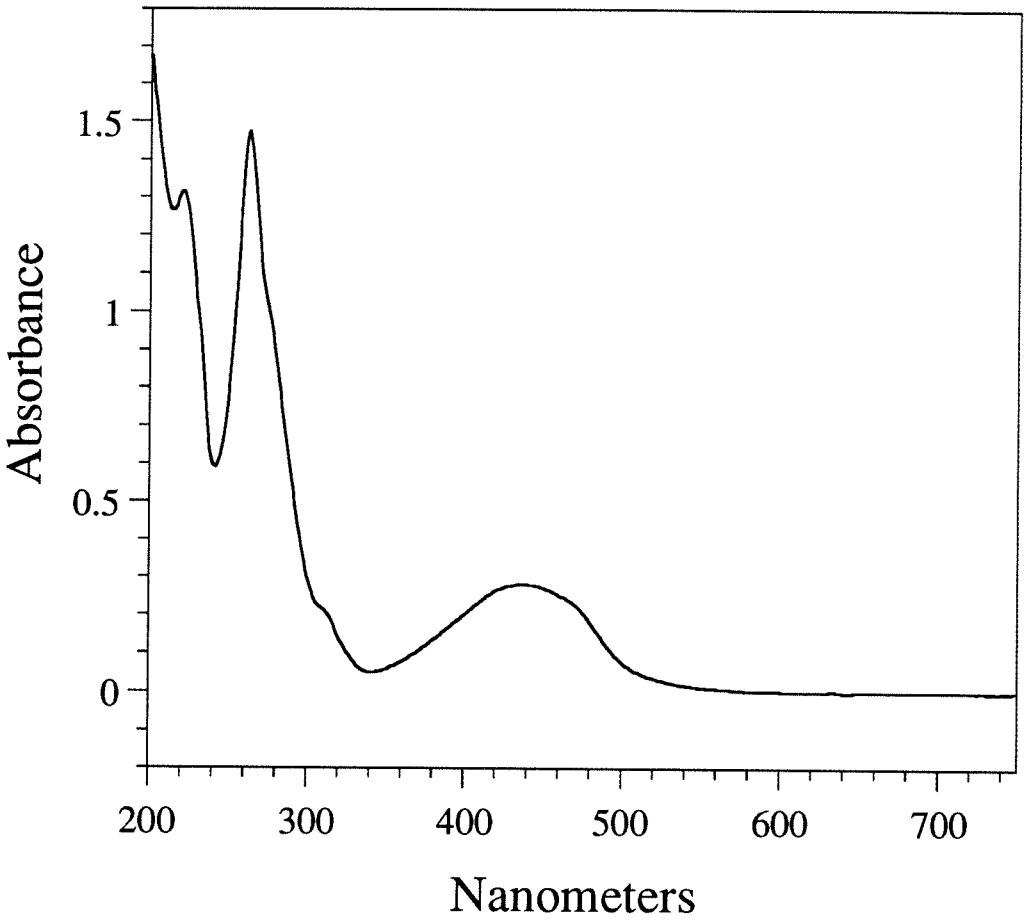

Figure 2.24. UV-Visible Spectrum of $Rh(phi)_2(DSTM\text{-}AP)$

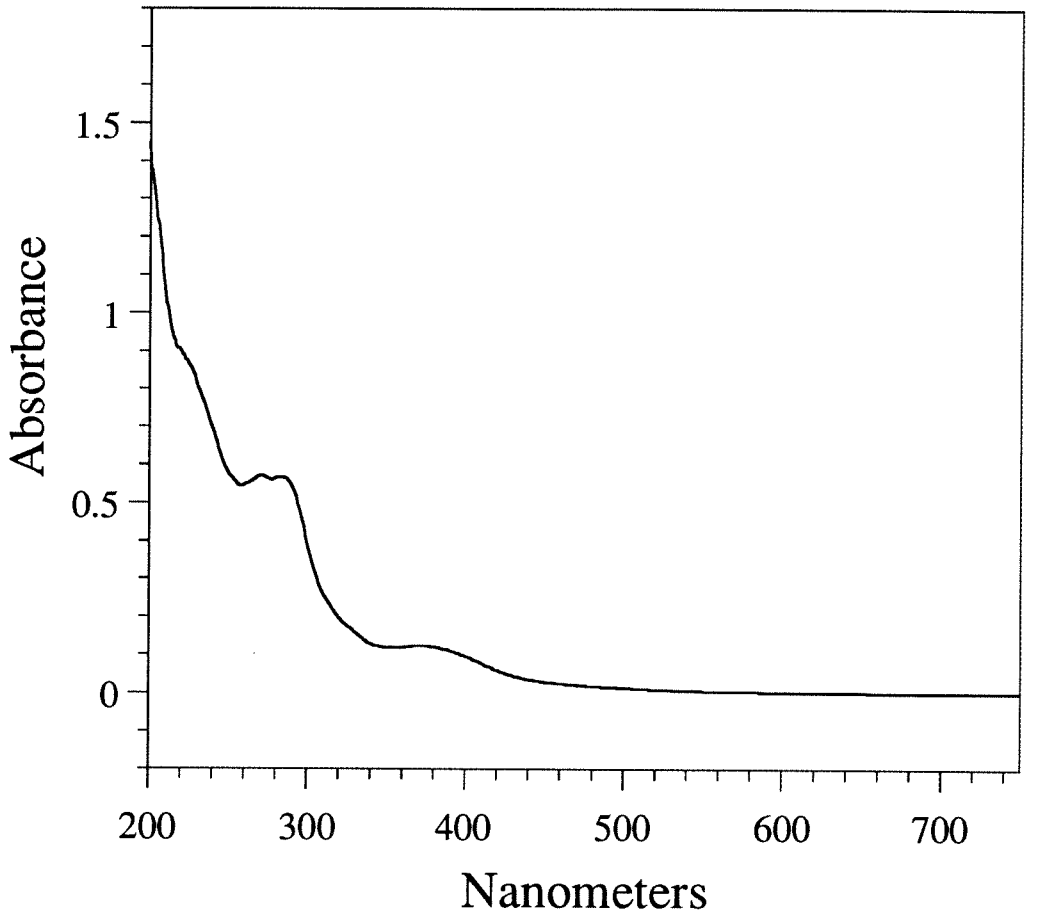

Appendix III. Mass Spectra

Figure 2.25. Mass Spectrum of $Ru(DIP)_2DSTM$

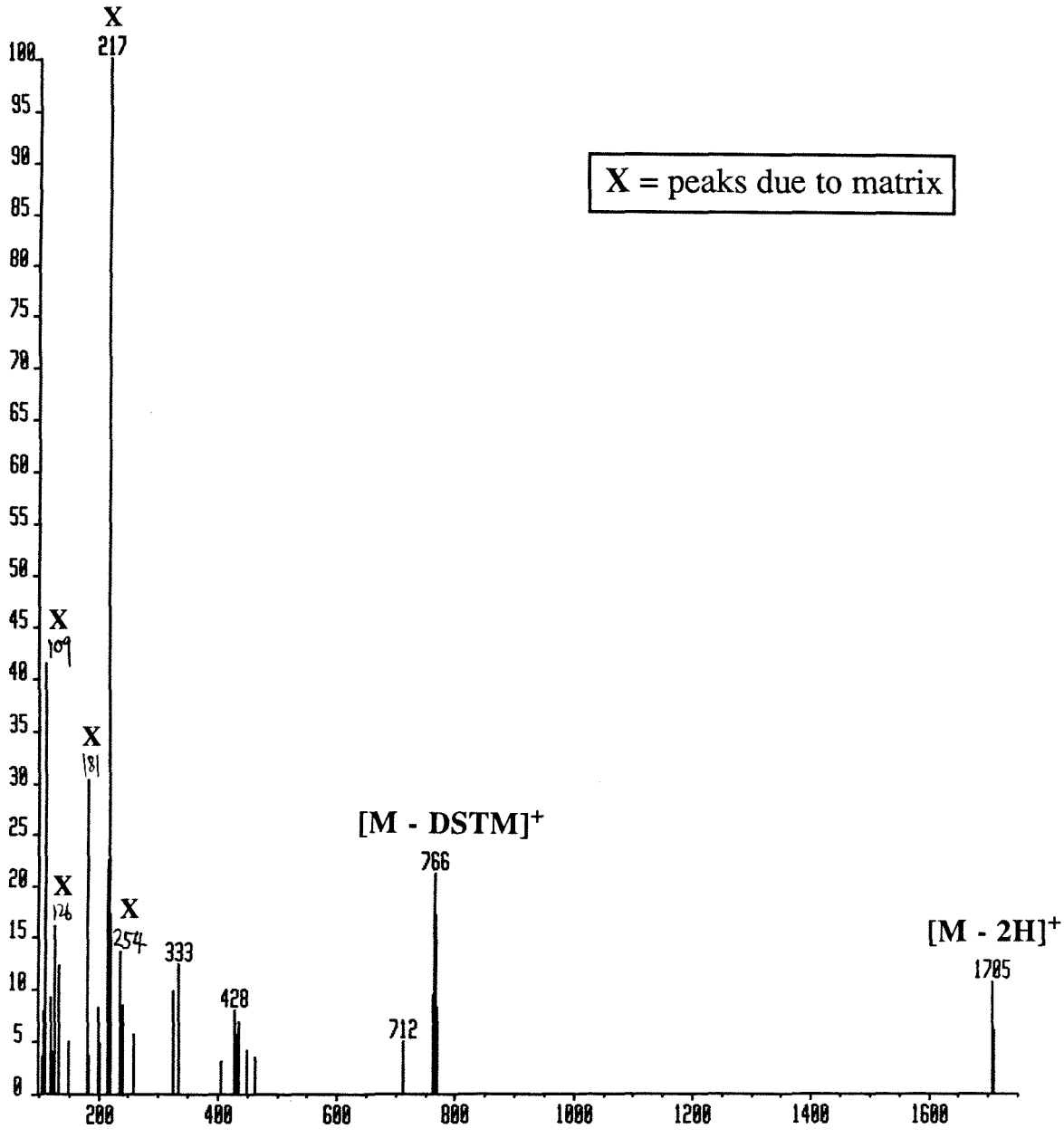

Figure 2.26. Mass Spectrum of $Ru(phen)_2DSTM$

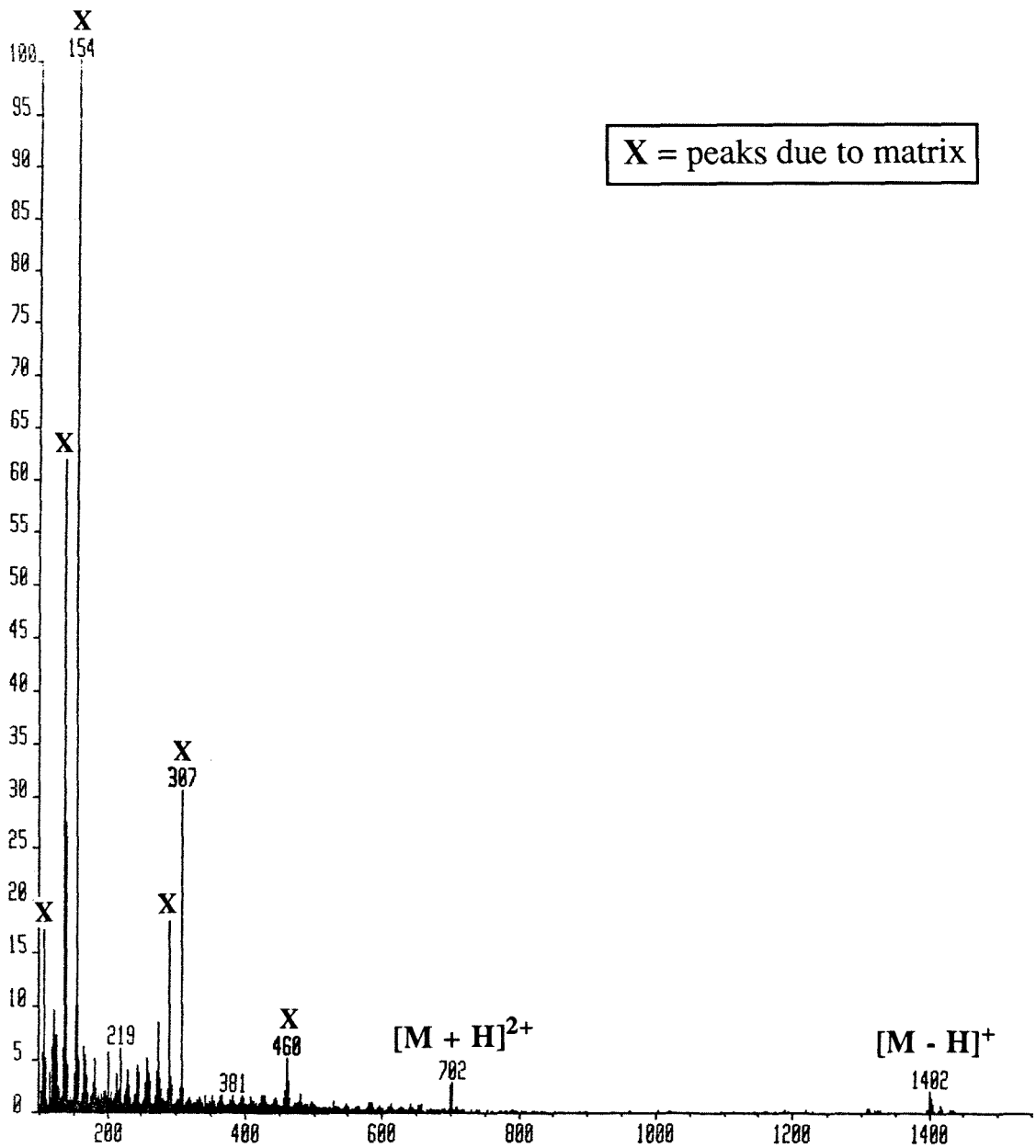

Figure 2.27. Mass Spectrum of $Ru(phen)_2(DSTM\text{-}AE)$

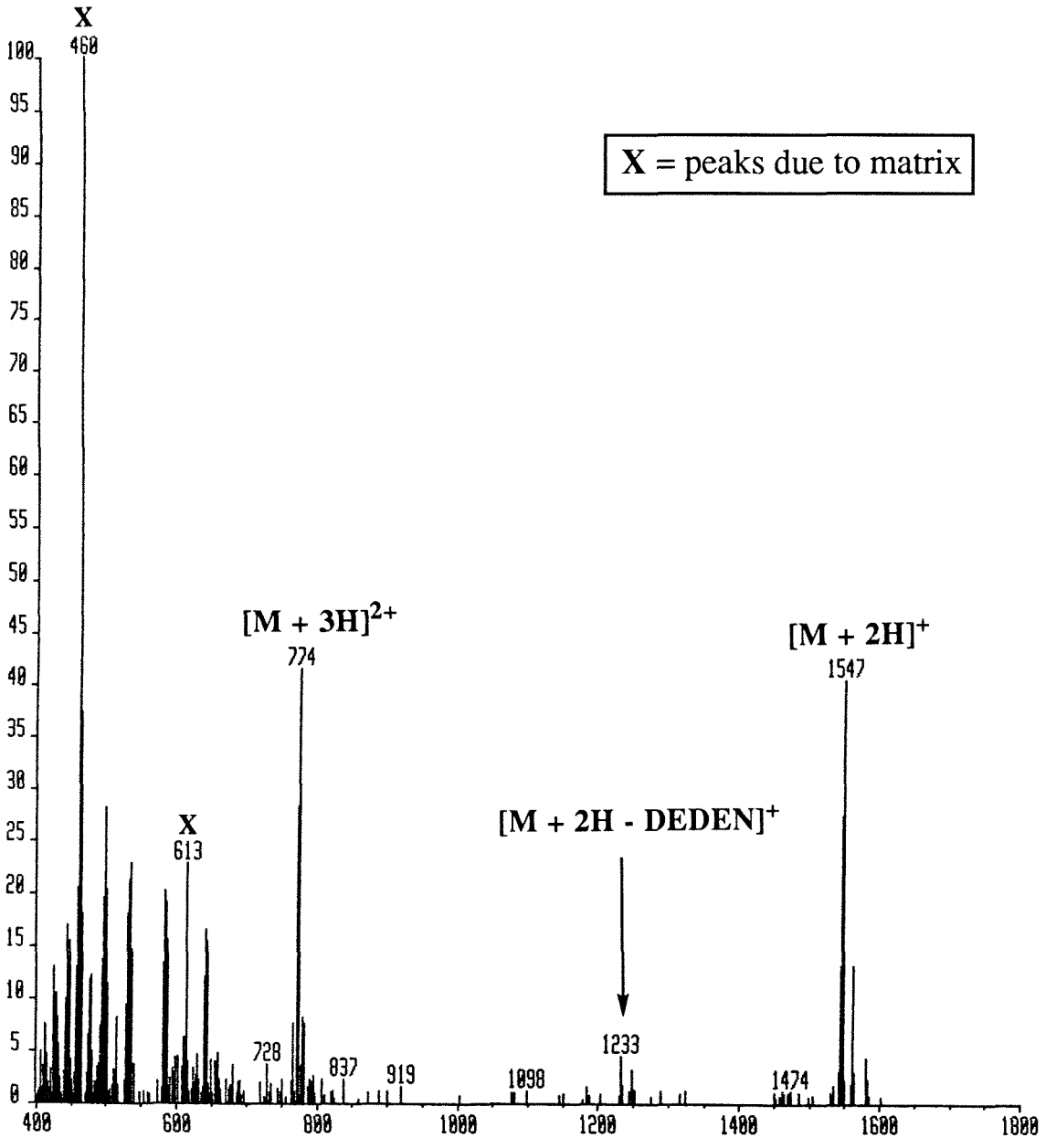

Figure 2.28. Mass Spectrum of $Ru(phen)_2(DSTM\text{-}AP)$

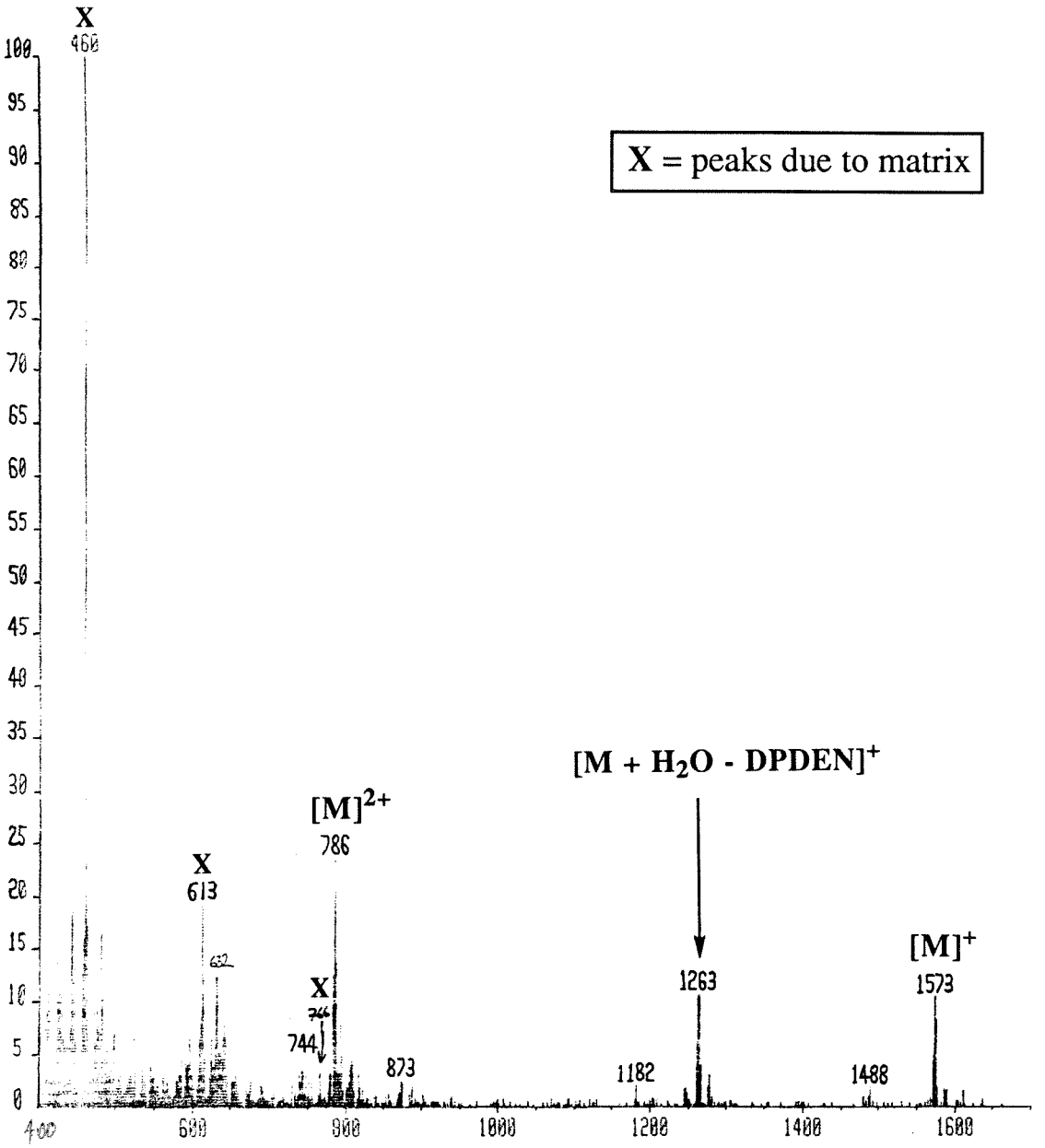

Figure 2.29. Mass Spectrum of $Rh(phi)_2(DSTM\text{-}AP)$

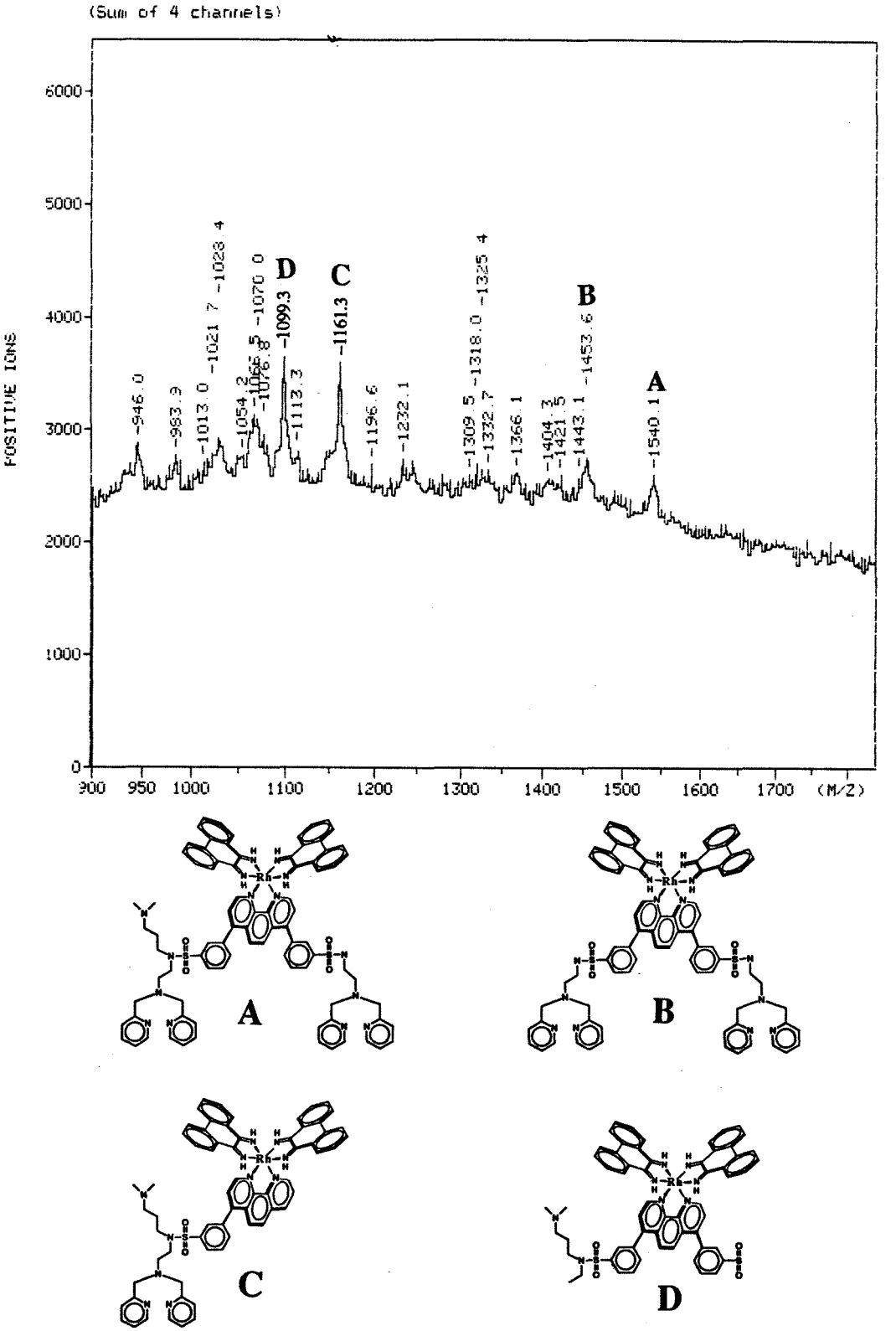

Chapter 3:
Copper-Activated Oxidative DNA Cleavage by $Ru(DIP)_2DSTM$ and $Ru(DIP)_2DSTE$

3.1 Introduction

The ability to suppress genes at will would be valuable for the treatment of cancer and the control of viruses. There is therefore a great deal of interest in the development of small molecules that promote DNA cleavage.[1-4] Oxidative DNA cleavage has been especially well studied due to the ease by which reactive oxygen species can be generated near the DNA double helix. The most success in oxidative DNA cleavage has been achieved through the use of iron and copper redox chemistry. The Fe(II)·EDTA oxidative DNA cleavage moiety has been used in both affinity cleavage and in DNA footprinting.[5] The identity of the reactive oxygen species produced by Fe(II)·EDTA is controversial, with both diffusible free hydroxyl radical and a ferryl iron-oxo species having been proposed.[6] The oxidative DNA cleavage promoted by Cu(1,10-phenanthroline)$_2^+$ [Cu(phen)$_2^+$] and a reducing agent has also been well studied.[6,7] The exact nature of the reactive copper-oxo species which attacks DNA is not known either, but it appears unlikely that the copper serves to bring diffusible free hydroxyl radicals to the vicinity of the DNA.[8] The lack of involvement of diffusible radicals in copper redox DNA cleavage is an advantage for the purpose of the design of DNA cleaving drugs, since diffusible radicals might attack biomolecules that were not intended to be the target of the drugs.

The accepted chemical pathway of copper redox-mediated DNA cleavage is shown in Figure 3.1. Copper (II) is first converted to copper (I) by an added reducing agent, usually ascorbate or a thiol. The copper (I) then reacts with H_2O_2 to form a reactive copper-oxo species that is not yet fully understood. This reactive oxidant may

be a hydroxyl radical that remains coordinated to the copper until the moment that the oxidant attacks DNA, or it may be a copper-bound hydroperoxy radical. The copper-oxo species then is thought to attack the DNA sugar to promote strand scission, regenerating copper (II) that is available for another redox cycle. The H_2O_2 reactant is produced from O_2 by copper and the reducing agent, or additional H_2O_2 can be introduced into the reaction mixture to accelerate the reaction.[7]

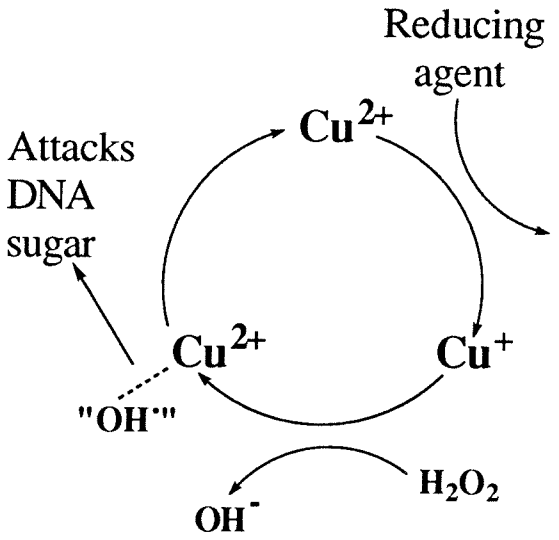

Figure 3.1. Chemical Pathway of DNA Cleavage by Copper

For the purpose of the design of DNA cleaving drugs, it is important to consider the conditions under which the drugs must operate *in vivo*. The intracellular concentration of the thiol glutathione is 5 mM in animal cells.[9] It is known that high concentrations of thiols inhibit DNA cleavage by $Cu(phen)_2^+$. It has been proposed by Veal et al. that this inhibition is due to the formation of Cu(phen)(thiolate) complexes which have little or no nuclease activity.[10] Since $Cu(phen)_2^+$ promotes little DNA cleavage at physiological thiol concentrations, it would be worthwhile to investigate the effect of varying the ligands bound to copper on cleavage efficiency. In the design of such ligands, factors such as the copper-ligand binding affinity and the redox potential

of the Cu^{2+}/Cu^{+} couple should be considered. The overall affinity of a potential nuclease for DNA, its DNA site-selectivity, and the nature of its binding interaction with DNA are also important factors.

The mechanism of DNA cleavage by chemical nucleases should also be investigated. Oxidative attack on a DNA base is not likely to lead to strand scission unless the DNA is further treated with alkali. Oxidative attack on the DNA sugar frequently leads to strand scission. Product analyses and other studies can establish which DNA sugar protons are the target of oxidative attack of a particular chemical nuclease, and thus indicate whether the nuclease is bound in the DNA major or minor groove. It has been shown that $Cu(phen)_2^{+}$ promotes DNA cleavage by C1' hydrogen abstraction as the major pathway, and C4' hydrogen abstraction as the minor pathway. This result indicates that oxidative attack by $Cu(phen)_2^{+}$ occurs in the DNA minor groove.[7,11,12] In contrast, the photoactivated DNA nuclease $Rh(phi)_2bpy^{3+}$ (Figure 3.2) intercalates in the DNA major groove, and promotes cleavage by abstraction of the DNA major groove C3' hydrogen.[13]

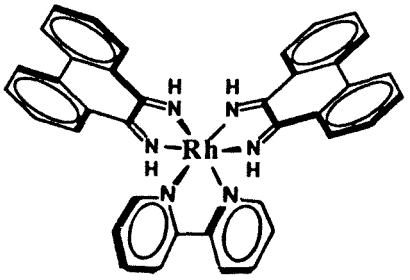

Figure 3.2. $Rh(phi)_2bpy$

The two complexes $Ru(DIP)_2DSTM$ and $Ru(DIP)_2DSTE$ (Figure 3.3) have been designed as artificial nucleases. Described here is their redox-mediated DNA cleavage chemistry with copper. Both complexes have three hydrophobic 4,7-diphenylphenanthroline (DIP) ligands. These hydrophobic DIP ligands give these

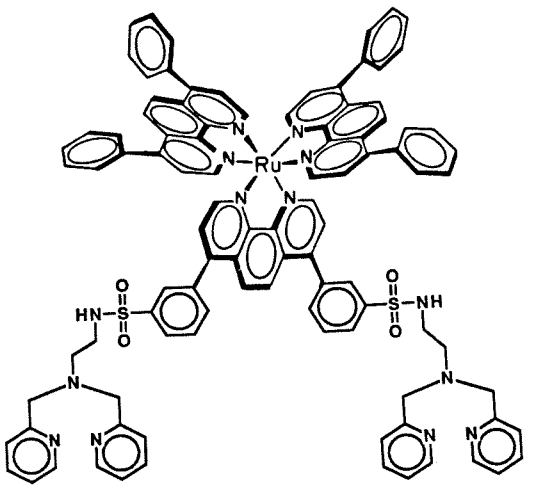

Ru(DIP)$_2$DSTM

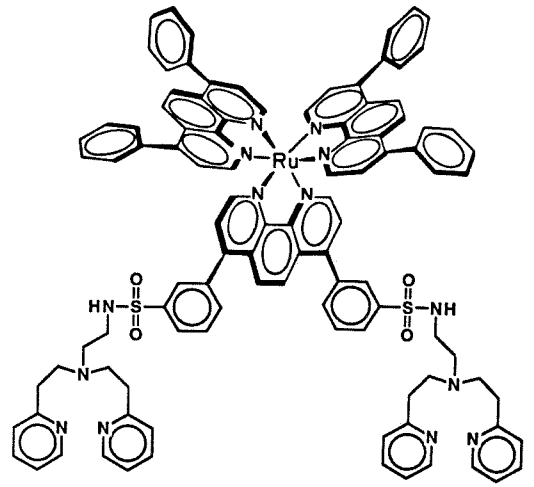

Ru(DIP)$_2$DSTE

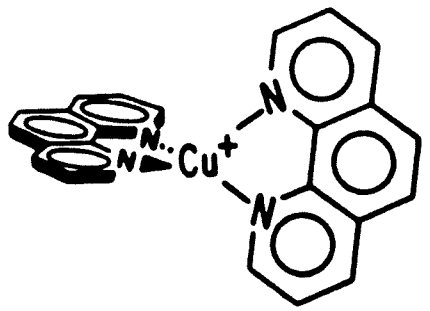

Cu(phen)$_2^+$

Figure 3.3. The two complexes Ru(DIP)$_2$DSTM and Ru(DIP)$_2$DSTE each contain a pair of metal chelates tethered to a Ru(DIP)$_3^{2+}$ core. Ru(DIP)$_2$DSTM will bind Cu^{2+} with five-membered chelate rings, and Ru(DIP)$_2$DSTE will bind Cu^{2+} with six-membered chelate rings. The DNA cleavage reaction promoted by Ru(DIP)$_2$DSTM and Ru(DIP)$_2$DSTE in the presence of Cu^{2+} and a reducing agent has been compared to that of the well studied DNA nuclease Cu(phen)$_2^+$.

complexes a remarkable selectivity for DNA conformations with tertiary structure that can better protect the DIP ligands from solvent. Linked to one of the DIP ligands on each complex is a pair of additional metal chelating groups. $Ru(DIP)_2DSTM$ was designed to bind additional labile metal ions with five-membered chelate rings, while $Ru(DIP)_2DSTE$ binds additional labile metal ions with six-membered chelate rings. The positively charged ruthenium metal center and the hydrophobic DIP ligands provide the driving force for the binding of the complex to DNA, while the tethered metal chelates can promote efficient DNA cleavage in the presence of copper (II) and a reducing agent. The potential of the Cu^{2+}/Cu^{+} redox couple of copper bound to $Ru(DIP)_2DSTM$ and $Ru(DIP)_2DSTE$ has been investigated by cyclic voltammetry on water soluble analogues. The DNA cleavage efficiency of copper bound to $Ru(DIP)_2DSTM$ and $Ru(DIP)_2DSTE$ has been compared the cleavage efficiency of the well-studied $Cu(phen)_2^{+}$, and the effect of the coordination environment around the copper on cleavage efficiency is discussed. The DNA site-selectivity of the cleavage reaction of $Ru(DIP)_2DSTM$ and $Ru(DIP)_2DSTE$ has been studied by low-resolution mapping. Finally, the mechanism of the cleavage reaction of $Ru(DIP)_2DSTM$ and $Ru(DIP)_2DSTE$ has been investigated by analysis of the DNA cleavage products.

3.2 Experimental

Cyclic Voltammetry. DPNED was synthesized as described in section 2.3, and DENED was synthesized by Dr. Richard Cruse as will be described in a manuscript for publication. A CV-27 cyclic voltammograph from Bioanalytical Systems was used, equipped with an RXY recorder and a C-1 A/B cell stand. Typically, 5 ml solutions were used, containing 2 mM $CuSO_4$, 3 mM ligand, 25 mM trizma·H_2SO_4 buffer (the 20 X buffer stock was adjusted to pH 7.8), and 5 mM Na_2SO_4. The solutions were purged with argon for at least 12 minutes, and were then scanned from –300 mV to +700 mV

(relative to SHE) at 20 mV/s until the voltammogram was constant. A glassy carbon working electrode was used, along with a Ag/AgCl reference electrode (+200 ± 2 mV relative to SHE), and a platinum auxiliary electrode. Alternate conditions were explored, including different $CuSO_4$ and ligand concentrations, additional NaCl or Na_2SO_4, and scan rates up to 500 mV/s. The use of a platinum rather than a glassy carbon working electrode was also investigated. As a control, cyclic voltammetry was done on ferrocene, $Cu(phen)_2^+$, and Cu(2,9-dimethyl-1,10-phenanthroline)$^+$ [$Cu(DMP)_2^+$]. Ferrocene was dissolved in DMF, and the concentrated DMF solution was added to water. This resulted in precipitation, but sufficient ferrocene remained in solution to obtain a good voltammogram. Stock solutions of 20 mM phen and 20 mM DMP were made in 30 mM H_2SO_4, and stock solutions of DPNED and DENED were made in water. Milli-Q deionized water was used in all solutions.

Quantitative Comparisons of DNA Cleavage Efficiency by Agarose Gel Electrophoresis. The DNA plasmid pBR322 was used as the substrate. Prior to the DNA cleavage reactions, the plasmid pBR322 contained approximately 80% supercoiled plasmid (form I) and 20 % nicked or open circular plasmid (form II). The cleavage reactions transform supercoiled plasmid to nicked plasmid. Two nicks on the same plasmid no more than several nucleotide base pairs apart transform the plasmid to linear (form III). The three plasmid forms were separated by agarose gel electrophoresis, with supercoiled having the highest mobility, followed by linear and then by nicked. This is illustrated in Figure 3.6.

The pBR322 was purchased from Boehringer Mannheim, and purified by Centricon™ to remove the EDTA. The plasmid was stored in either 5 mM Na_2SO_4 and 25 mM trizma·H_2SO_4, or in 2.5 mM Na_2SO_4 and 12.5 mM trizma·H_2SO_4. Immediately after purification by Centricon, the plasmid was divided into aliquots. One

aliquot was stored at +4 °C and used as the DNA stock solution for a period of time from several weeks to several months, and the remaining aliquots were stored at -20 °C until needed. $Ru(DIP)_2DSTM$ was synthesized as described in chapter 2, and $Ru(DIP)_2DSTE$ was synthesized by Dr. Richard Cruse as will be described in a manuscript for publication. Solid $Ru(DIP)_2DSTM$ and $Ru(DIP)_2DSTE$ were stored at -60 °C or below, in the dark, and under argon. Stock solutions of $Ru(DIP)_2DSTM$ and $Ru(DIP)_2DSTE$ were made by dissolving a small amount of solid complex in approximately 50 µl methanol, and transferring the solution to 5-40 ml water. The methanol was then removed using a high vacuum pump without heating. The concentration of the solutions were determined by visible spectroscopy, using an extinction coefficient of 29,500 $M^{-1}cm^{-1}$ at the visible maximum (445 nm). Solutions were stored in the dark at room temperature. Solutions were generally between 7 µM and 12 µM $Ru(DIP)_2DSTM$ or $Ru(DIP)_2DSTE$, since in a more concentrated solution the complex might precipitate out of solution. Ruthenium complex solutions were discarded after two months. The stock solution of 20 mM 1,10-phenanthroline (phen) was made in 30 mM H_2SO_4. The buffer stock solution contained 100 mM Na_2SO_4 and 500 mM trizma, adjusted to pH 7.8 with H_2SO_4. The solution was autoclaved and stored at +4 °C. The copper stock solution was 5 mM, made from 99.999% $CuSO_4 \cdot 5H_2O$ (Aldrich Chemicals), and then autoclaved. The ultrapure Milli-Q (from Millipore) deionized distilled water was used for all stock solutions, and for all DNA cleavage reactions. Solutions of 2-mercaptoethanol and H_2O_2 were made fresh for each experiment from neat 2-mercaptoethanol or 3.4% H_2O_2 (by weight), respectively.

The DNA cleavage conditions varied from experiment to experiment; the exact conditions are shown in the figure caption for each experiment. Typical cleavage reaction conditions were 13 mM trizma·H_2SO_4, 2.6 mM Na_2SO_4, 20 µM DNA base pairs pBR322, 4 or 8 µM $CuSO_4$, and either 4 µM $Ru(DIP)_2DSTM$, 4 µM

$Ru(DIP)_2DSTE$, 16 μM phen, or nothing (as a control). The total reaction volumes were 30 μl. The ruthenium complex or phenanthroline solutions were mixed with the $CuSO_4$ solution, vortexed, and added to solutions of DNA in buffer. The resultant solutions were not vortexed so as to minimize the DNA precipitation from solution caused by the positively charged, hydrophobic, ruthenium complexes. The solutions were preincubated at 37 °C for approximately 15 minutes, then the cleavage reactions were initiated by the addition of a mixture of 2-mercaptoethanol and H_2O_2. The reactions were then further incubated at 37 °C. Exposure of the reaction mixtures to room light was reduced by covering the reactions with aluminum foil during the incubations; this minimized the possibility of the ruthenium complexes promoting DNA cleavage through the light-activated singlet oxygen mechanism. The reactions were then quenched by the addition of 10 μl of a solution containing 29% sucrose, 0.29% bromophenol blue, 58 mM EDTA, and 2.5% SDS. In some experiments, the reactions were quenched by the addition of 2 μl 25 mM EDTA, with dye and SDS being added later. The quenched reactions were vortexed thoroughly. A 1% agarose gel was prepared in 100 mM trizma-borate and 2 mM EDTA. 33 μl of the quenched reactions were loaded onto the gel. The gel was run at 75 V for approximately 140 minutes. The gel was stained in ethidium bromide for 5-15 minutes, destained overnight at +4 °C in approximately 1 mM $MgSO_4$, and illuminated from below with 302 nm UV light from a Spectroline™ Transilluminator Model TR-302. The gel was then photographed with a Polaroid 600 camera equipped with a red filter and Polaroid 655 Positive/Negative Instant Pack Film.

The data on the negative of the gel photograph were quantitated with an LKB Ultroscan XL Enhanced Laser Densitometer. For each cleavage reaction sample, the percentage of supercoiled, nicked, and linearized plasmid was determined. Except in Figure 3.7, the percentage nicked in the copper control sample which contained the least

percentage nicked was subtracted from the percentage nicked of all samples. The "% Cleavage" of Figures 3.8 through 3.10 and Table 3.2 is defined as the percentage nicked in each reaction sample (adjusted by the subtraction described above) plus twice the percentage linearized plasmid.

Low-Resolution Mapping. The oxidative DNA cleavage reactions were done in a total volume of 24 µl. The reaction conditions were 13 mM trizma·H_2SO_4, 2.6 mM Na_2SO_4, 50 µM DNA base pairs pBR322, 10 µM $CuSO_4$, 500 µM 2-mercaptoethanol, 200 µM H_2O_2, and either 5 µM Ru(DIP)$_2$DSTM, 5 µM Ru(DIP)$_2$DSTE, or no ruthenium complex. Samples with Ru(DIP)$_2$DSTM were incubated for 10 minutes at 37 °C; other samples were incubated for 60 minutes at 37 °C. The copper reactions were then quenched by the addition of 2 µl 25 mM EDTA, and then vortexed for 5 seconds. 3 µl 10X REact® 2 buffer (Bethesda Research Laboratories) were added to each sample, followed by 10 units (1 or 2 µl) of the restriction enzyme *Hind* III, *Ava* I, *Nde* I, or no enzyme. The samples were vortexed for 8 seconds, and then were incubated at 37 °C for 90 minutes. 10 µl of a dye solution (29% sucrose, 0.29% bromophenol blue, 58 mM EDTA, and 2.5% SDS) were added to each sample, and the samples were again vortexed. 33 µl of each sample were loaded onto a 1% agarose gel, along with two lanes containing 0.5 µg of 1 Kb DNA Ladder (Bethesda Research Laboratories). The gel was run for 260 minutes at 75 V, and stained and photographed as described in the previous section.

The distance traveled by the DNA was determined by scanning the data on the negative of the gel photograph with an LKB Ultroscan XL Enhanced Laser Densitometer. The distance traveled by the molecular weight markers was plotted against the logarithm of the size of the markers to obtain a standard curve. The final location of the cleavage sites of Ru(DIP)$_2$DSTM and Ru(DIP)$_2$DSTE were determined

from the smaller fragments produced by each restriction enzyme, using the average of two or three enzymes from each of two different experiments.

HPLC Product Analysis. Phenol-extracted calf thymus DNA was purchased from Pharmacia, and purified by Centricon™ to remove traces of EDTA. 120 μl of a solution of ruthenium complex and $CuSO_4$ were added to a 40 μl solution of DNA in buffer. The samples were preincubated at 37 °C for at least 23 minutes, and then the reaction was initiated by the addition of 40 μl of a solution of 1 mM 2-mercaptoethanol and 1 mM H_2O_2. The final reaction mixtures had total volumes of 200 μl, and contained 13 mM trizma·H_2SO_4, 2.6 mM Na_2SO_4, 58 μM DNA base pairs, 3 μM $Ru(DIP)_2DSTM$ or $Ru(DIP)_2DSTE$, 6 μM $CuSO_4$, 200 μM 2-mercaptoethanol, and 200 μM H_2O_2. Reactions were incubated at 37 °C for 30 minutes and then quenched by the addition of 10 μl 20 mM 2,9-dimethyl-1,10-phenanthroline. EDTA was not used to quench the reaction because it produces a peak at 260 nm with a retention time similar to the products of the DNA cleavage reaction. Samples were centrifuged for 10 minutes at 14 krpm, and 100 μl aliquots were injected onto a Cosmosil 5 μ, 15-cm C-18 HPLC column, washed with 500 mM ammonium formate at 1.5 ml/minute. Products were detected by UV absorbance at 260 nm.

Cleavage and Product Analysis of the Radiolabeled DNA Oligonucleotide 5'-CTGGCATACCGGTATGCCAG-3'. The above oligonucleotide was synthesized on a Pharmacia Gene Assembler using phosphoramidite chemistry and purified by reverse-phase HPLC. 2 picomoles of the oligonucleotide were then ^{32}P 5'-radiolabeled using T4 polynucleotide kinase and purified by Nensorb™ (Du Pont). 100% labeling efficiency was assumed for the purposes of oligonucleotide quantitation. The copper redox cleavage reaction of $Ru(DIP)_2DSTM$ was compared with the DNA cleavage

reactions of $Cu(phen)_2^+$, $Rh(phi)_2bpy^{3+}$, and iron-bleomycin. The final DNA concentration in all samples was 18 μM base pairs in a buffer containing 2.5 mM Na_2SO_4 and 12.5 mM trizma·H_2SO_4, with a total reaction volume of 20 μl. The conditions for each sample are described in the caption to Figure 3.13. For the copper-activated reactions, an 8 μl solution of $CuSO_4$ and either $Ru(DIP)_2DSTM$, 1,10-phenanthroline, or no ligand, was added to a 8 μl solution of oligonucleotide in buffer. The reaction was preincubated for at least 12 minutes at 37 °C, and the reaction was then initiated by the addition of 4 μl of a solution containing 1 mM 2-mercaptoethanol and 1 mM H_2O_2. For the $Cu(phen)_2^+$ reaction, final concentrations of 3 μM $CuSO_4$ and 12 μM phen were used. For the $Ru(DIP)_2DSTM$ reaction, final concentrations of 9 μM $CuSO_4$ and 3 μM $Ru(DIP)_2DSTM$ were used. After 20 minutes at 37 °C (2 1/2 minutes in the case of the $Cu(phen)_2^+$ reaction), the reaction was quenched by the addition of 2 μl 25 mM EDTA. The $Rh(phi)_2bpy^{3+}$ sample contained 4.5 μM $Rh(phi)_2bpy^{3+}$, and the 20 μl solution was irradiated with a 1000 W Hg/Xe lamp at 310 nm for 6 minutes, and then 2 μl of a 25 mM solution of EDTA were added. For the iron-bleomycin reaction, 6 μl water, 2 μl freshly prepared 80 μM $FeSO_4$ (99.999%, Aldrich Chemicals), and then 4 μl 20 μM bleomycin were added to an 8 μl solution of DNA. After 7 minutes at room temperature, 2 μl 25 mM EDTA were added to the sample, which was cooled to -78 °C and immediately dried *in vacuo*.

7 μl aliquots were removed from some samples (as stated in the caption to Figure 3.13) for treatment with NaOH or with $NaBH_4$, and the remainder were dried *in vacuo*. Samples were treated with NaOH as follows: 3.5 μl 300 mM NaOH were added to the 7 μl aliquot, and the sample was heated at 60 °C for 2 minutes. The reaction was cooled on dry ice for 5 seconds, and 3.5 μl 300 mM HCl were added. The reaction was cooled to -78 °C, and dried *in vacuo*. Samples were treated with $NaBH_4$ as follows: 3.5 μl of 900 mM $NaBH_4$ (freshly dissolved in 900 μM NaOH) were added to a 7 μl aliquot.

After 90 minutes at room temperature, the samples were cooled on dry ice for 5 seconds, 3.5 µl 900 mM acetic acid were added, and the reaction was cooled to -78 °C and dried *in vacuo*.

The dried samples were resuspended in 98% formamide loading dye (10 ml formamide, 200 µl 0.5 M EDTA, 10 mg. bromophenol blue, and 10 mg. xylene cyanol), heated at 90 °C for 3 minutes, chilled on wet ice for 3 minutes, and loaded onto a 20% denaturing polyacrylamide sequencing gel which was run at 1700 V for four hours. Except as noted in the caption to Figure 3.13, 20 kcpm were loaded per lane. The gel was exposed to x-ray film with an intensifying screen for 4 days at approximately -70 °C, and then developed.

3.3. Results

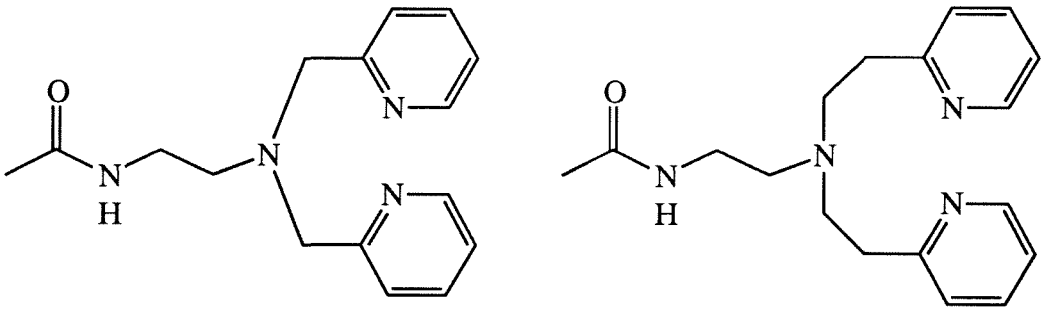

DPNED
Analogue of $Ru(DIP)_2DSTM$

DENED
Analogue of $Ru(DIP)_2DSTE$

Figure 3.4. Water-Soluble Analogues for Cyclic Voltammetry

Determination of the Cu^{2+}/Cu^{+} Redox Couple of DPNED and DENED by Cyclic Voltammetry. Since $Ru(DIP)_2DSTM$ and $Ru(DIP)_2DSTE$ are not very water soluble, the potential of the Cu^{2+}/Cu^{+} redox couples of copper bound to the ruthenium complexes has been investigated through the use of cyclic voltammetry on water soluble analogues (Figure 3.4). N-acetyl-N',N'-di(2-picolyl)ethylenediamine [DPNED]

is an analogue for $Ru(DIP)_2DSTM$, and N-acetyl-N',N'-di(2-ethylpyridyl)ethylenediamine [DENED] is an analogue for $Ru(DIP)_2DSTE$. The results are summarized in Table 3.1. All potentials are reduction potentials relative to SHE. To obtain a value for the redox potential of the Cu^{2+}/Cu^{+} transition of copper bound to DPNED and DENED, the conditions of 2 mM $CuSO_4$ and 3 mM ligand were used. Typical voltammograms under these conditions are shown in Figure 3.5. The mean peak potential (E_{av}) was obtained by averaging the oxidation and reduction peak potentials. The three boldface values for DPNED and DENED were averaged to obtain a value for the redox potential of DPNED of **-23 ± 20 mV**, and a value for DENED of **$+203 \pm 20$ mV**. The separation between oxidation and reduction peak potentials was approximately 75 mV in the case of DPNED and 165 mV in the case of DENED. Since these values are greater than 60 mV, both systems are quasi-reversible. E_{av} for DPNED does not vary significantly with scan rate or the ratio of ligand to copper; E_{av} for DENED varies by $\pm$ 10 mV. The addition of 455 mM NaCl adds approximately 30 mV to the measured mean peak potential of both analogues; the addition of 250 mM Na_2SO_4 subtracts approximately 30 mV from both analogues. To verify the accuracy of the measurements, three known redox potentials were measured. Values of +395 mV, +188 mV, and +590 mV were obtained for ferrocinium/ferrocene, $Cu(phen)_2^{2+}/Cu(phen)_2^{+}$, and $Cu(DMP)_2^{2+}/Cu(DMP)_2^{+}$, respectively. The corresponding literature values are +400 mV, +174 mV, and +594 mV, respectively.[14,15]

Earlier experiments were done using a platinum working electrode rather than a glassy carbon working electrode. In the case of DPNED, the results were essentially the same, except there was an unexplainable drift in E_{av} measurements over several months from approximately 0 mV to –27 mV. In the case of DENED, E_{av} measurements from experiments conducted with a platinum working electrode were less reproducible, and

Table 3.1. Summary of Cyclic Voltammetry Results

Ligand	mM $CuSO_4$	mM Ligand	Work. Electr.	mM Trizma	mM Na_2SO_4	mM NaCl	Scan Rate (mV/s)	ΔE_p (mV)	E_{av} (mV)
DPNED	2	3	GC	25	5	0	20	75	**–27**
DPNED	2	3	GC	25	5	0	20	80	**–20**
DPNED	2	3	GC	25	5	0	20	75	**–22**
DPNED	2	2	GC	25	5	0	100	95	–22
DPNED	2	2	GC	25	5	0	500	130	–25
DPNED	2	4	GC	25	5	0	20	75	–22
DPNED	1.8	2.7	GC	22.7	4.5	455	20	55	+8
DPNED	1	1.5	GC	25	250	0	20	60	–50
DENED	2	3	GC	25	5	0	20	170	**+205**
DENED	2	3	GC	25	5	0	20	165	**+198**
DENED	2	3	GC	25	5	0	20	160	**+205**
DENED	2	2	GC	25	5	0	100	245	+198
DENED	2	4	GC	25	5	0	20	155	+213
DENED	1.8	2.7	GC	22.7	4.5	455	20	115	+233
DENED	1	1.5	GC	25	250	0	20	145	+178
$Fe(Cp)_2$	0	0	GC	25	5	0	100	40	+395
phen	2	6	Pt	25	5	0	20	135	+188
DMP	2	6	Pt	25	5	0	200	120	+590

Key

DPNED:	N-acetyl-N',N'-di(2-picolyl)ethylenediamine
DENED:	N-acetyl-N',N'-di(2-ethylpyridyl)ethylenediamine
$Fe(Cp)_2$:	Ferrocene
phen:	1,10-phenanthroline
DMP:	2,9-dimethyl-1,10-phenanthroline
GC:	Glassy carbon working electrode
Pt	Platinum working electrode
Trizma:	Trizma·H_2SO_4 (pH of 500 mM stock adjusted to 7.8)
ΔE_p:	Separation between oxidation and reduction peaks
E_{av}:	Mean peak potential, (average of oxidation and reduction peak potentials), reduction potential relative to SHE

Boldface E_{av} values were averaged to determine the Cu^{2+}/Cu^{+} redox potential for DPDEN and DENED. Potential(DPNED) = **–23 ± 20 mV**, potential(DENED) = **+203 ± 20 mV**. Both potentials are reduction potentials relative to SHE.

A great deal of precipitation occurred when a DMF solution of ferrocene was added to water. The final concentration of ferrocene was therefore unknown, but was probably submillimolar.

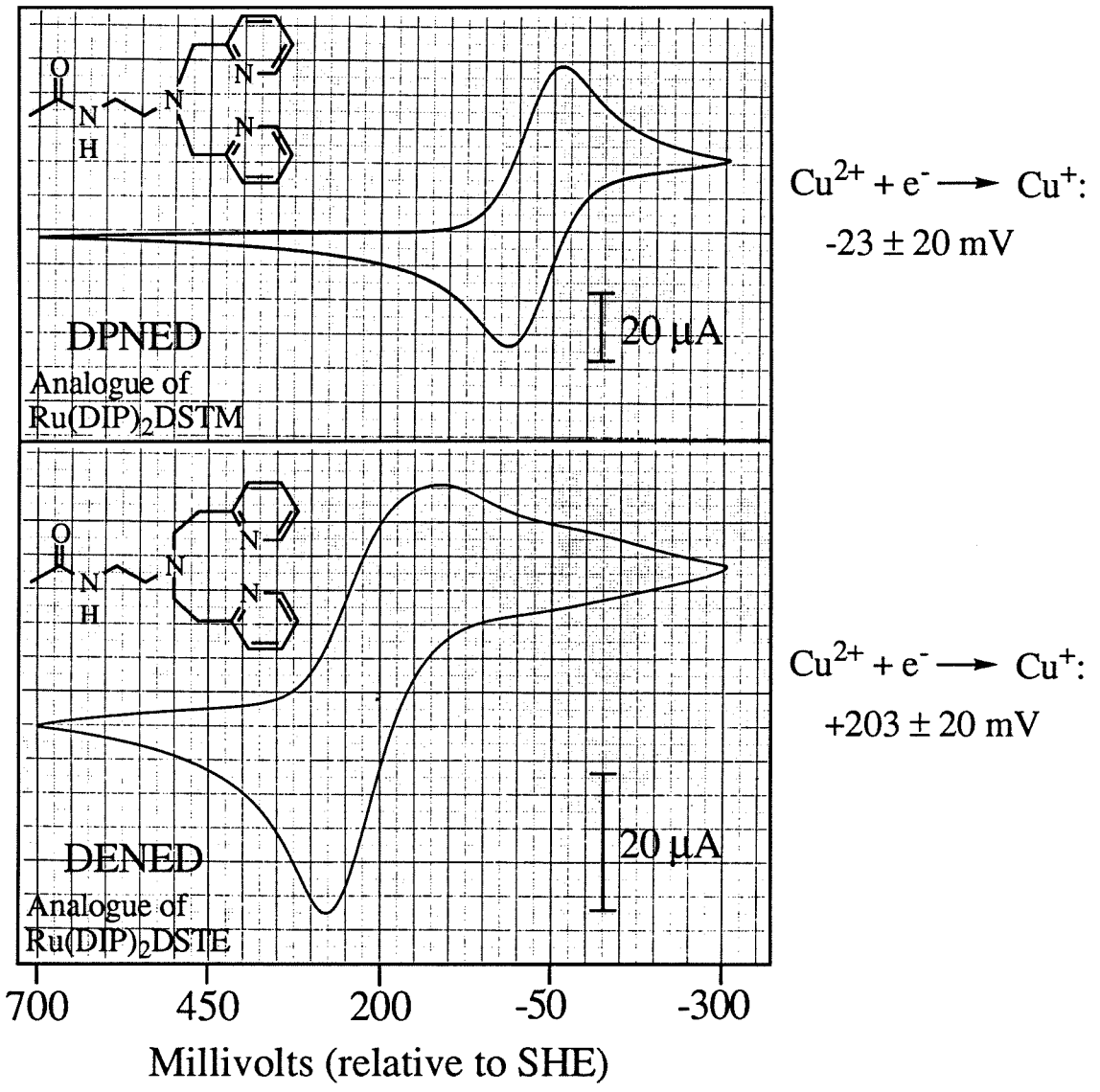

Figure 3.5. Cyclic voltammograms of DPNED and DENED. Conditions: 2 mM $CuSO_4$, 3 mM DPNED or DENED, 25 mM trizma·H_2SO_4, 5 mM Na_2SO_4, scan rate = 20 mV/s.

an additional oxidation peak at +50 ± 30 mV was observed, coupled to a reduction peak below –300 mV.

The quasi-reversibility (i.e., $\Delta E_p > 60$ mV) of the copper/DPNED and copper/DENED systems does introduce some uncertainty into the results.[16] This uncertainty was estimated to be ± 20 mV, but may be far less in the case of DPNED. It is possible, in the case of DENED, that the uncertainty is somewhat higher. The relatively slow scan rate of 20 mV/s was used in order to minimize ΔE_p. The addition of high concentrations of NaCl or Na_2SO_4 resulted in smaller ΔE_p values, but changed the E_{av} measurements. This is reasonable, since DPNED and DENED are likely to be tridentate copper chelators (although amide deprotonation and tetradentate coordination cannot be absolutely ruled out). There is therefore likely to be at least one open coordination site remaining on copper bound to DPNED or DENED. Whether that site were occupied by chloride, water, or sulfate would reasonably be expected to affect the Cu^{2+}/Cu^{+} redox potential. The redox potential values of –23 ± 20 mV for copper/DPNED and +203 ± 20 mV for copper/DENED are therefore not accurate under all conditions, but rather values that are accurate under approximately the conditions of the DNA cleavage experiments. On the other hand, the measured E_{av} appears to be insensitive to the ratio of DPNED or DENED to copper. Even experiments with a 3:1 ligand to copper ratio gave similar measurements for E_{av} (data not shown). It therefore appears that under the conditions of the cyclic voltammetry experiments, copper is binding to one DPNED or DENED ligand only. If copper does bind to two DPNED or DENED ligands, the second ligand is bound too weakly to significantly affect the redox potential.

The reduction potential of $(Cu{\cdot}DPNED)^{2+}$ to $(Cu{\cdot}DPNED)^{+}$ is about 225 mV less favorable than the reduction potential of $(Cu{\cdot}DENED)^{2+}$ to $(Cu{\cdot}DENED)^{+}$. This is reasonable, since it is to be expected that copper bound to DPNED, with its constrained

pair of five-membered chelate rings, would have difficulty making the transition from the distorted square planar (or octahedral) copper (II) state to the tetrahedral copper (I) state. Copper bound to DENED could more easily reach a tetrahedral copper (I) state because there is more leeway in its six-membered chelate rings.[17] $Cu(phen)_2^+$ (although it has five-membered chelate rings) has a Cu^{2+}/Cu^+ redox potential closer to that of copper/DENED because the two phenanthroline ligands are not directly bound to each other, so transition to the tetrahedral copper (I) state is not constrained. $Cu(DMP)_2^+$ has an extremely unstable copper (II) state because of steric clashes of the 2,9-methyl groups.

The Cu^{2+}/Cu^+ redox potential of copper bound to $Ru(DIP)_2DSTM$ or $Ru(DIP)_2DSTE$ will not be absolutely identical to that of copper bound to their respective analogues DPNED or DENED. It is likely that the +2 charge on the ruthenium metal would favor copper (I) over copper (II) due to electrostatic repulsion, which would cause an increase in the reduction potential. The hydrophobicity and the steric bulk of the ruthenium complexes might also have some effect, but it is not clear whether this would tend to increase or decrease the Cu^{2+}/Cu^+ redox potentials. The redox potentials of copper bound to the ruthenium complexes could not be measured directly due to the low aqueous solubility of the ruthenium complexes.

Quantitative Comparisons of DNA Cleavage Efficiency. The copper-activated DNA cleavage efficiency of $Ru(DIP)_2DSTM$ and $Ru(DIP)_2DSTE$ has been compared to that of the well-studied DNA nuclease $Cu(phen)_2^+$. The relative cleavage efficiency has been studied as a function of time, as a function of copper, thiol, and H_2O_2 concentration, and as a function of the thiol/H_2O_2 ratio. These experiments investigate the effect of the structure of the artificial nuclease and the coordination environment around the copper on DNA cleavage efficiency.

Figure 3.6. Cleavage Assay for Plasmid DNA

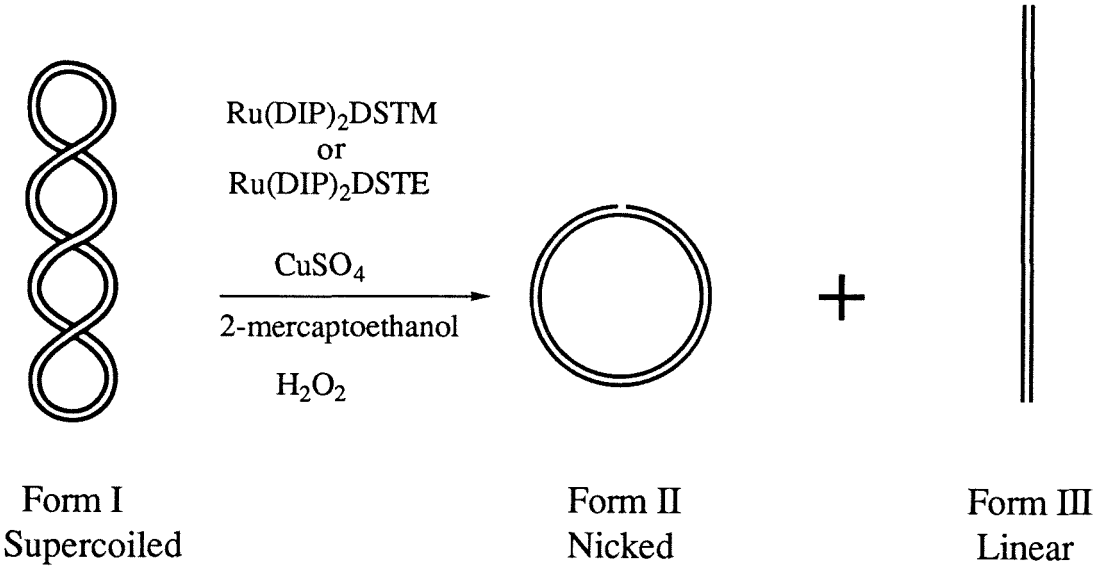

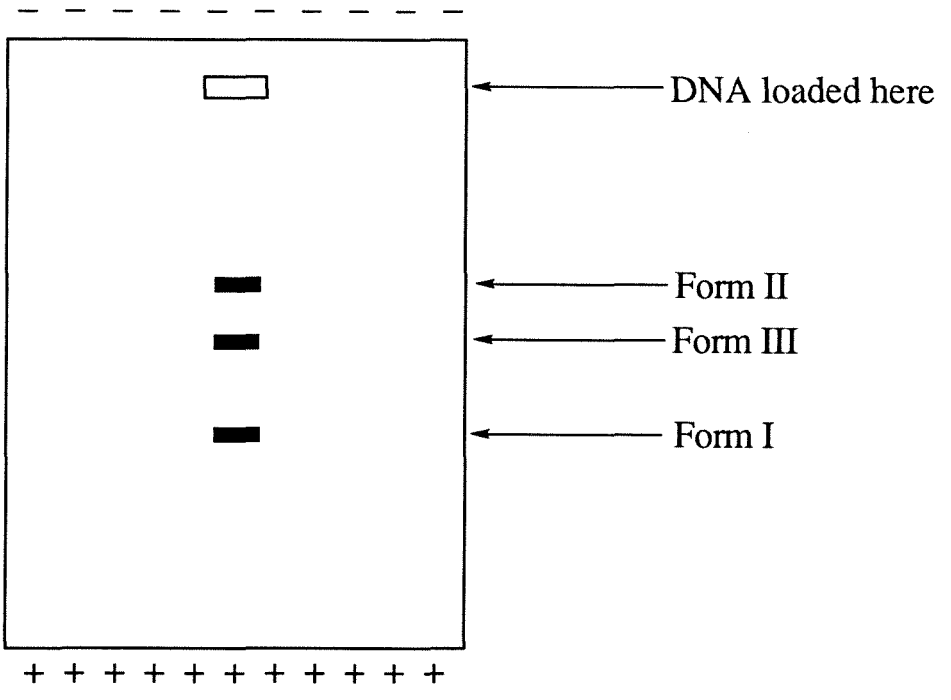

Agarose gel electrophoresis

Limitations of the agarose assay for DNA cleavage. The conversion of supercoiled plasmid DNA to the nicked and linear forms by $Ru(DIP)_2DSTM$, $Ru(DIP)_2DSTE$, and $Cu(phen)_2^+$ has been investigated by agarose gel electrophoresis (Figure 3.6). This technique provides a good picture of the relative cleavage efficiencies of the three complexes, but the data should not be used for the precise determination of reaction rates. The luminescence of ethidium bromide intercalated into plasmid DNA is different for the supercoiled and nicked forms. Also, the assay does not distinguish between plasmid DNA nicked only once and plasmid DNA nicked several times. The definition of "% cleavage" as the percentage of nicked plasmid plus twice the percentage of linearized plasmid is somewhat arbitrary, since two nicks on the same plasmid result in linearization only if the two nicks are close together and on opposite strands. Complexes that promote DNA cleavage in a site-selective manner would thus be more likely to produce linearized plasmid than an equally reactive, sequence neutral, complex.

Time course of the DNA cleavage reaction (Figure 3.7). The complexes $Cu(phen)_2^+$, $Ru(DIP)_2DSTM$, and $Ru(DIP)_2DSTE$ were permitted to react with DNA for increasing amounts of time. The reaction was initiated by the addition of 500 μM 2-mercaptoethanol and 200 μM H_2O_2, and was quenched by the addition of EDTA. Noting that the three graphs have different time scales, under these reaction conditions the order of DNA cleavage efficiency is $Cu(phen)_2^+$ > $Ru(DIP)_2DSTM$ > $Ru(DIP)_2DSTE$, despite the fourfold lower copper concentration in the case of $Cu(phen)_2^+$. All three complexes first produce increasing amounts of nicked plasmid, followed by increasing amounts of linearized plasmid. However, the nature of the time course differs; the complex $Cu(phen)_2^+$ nicks the plasmid almost entirely before much linearized plasmid is produced, while $Ru(DIP)_2DSTM$ and $Ru(DIP)_2DSTE$ start

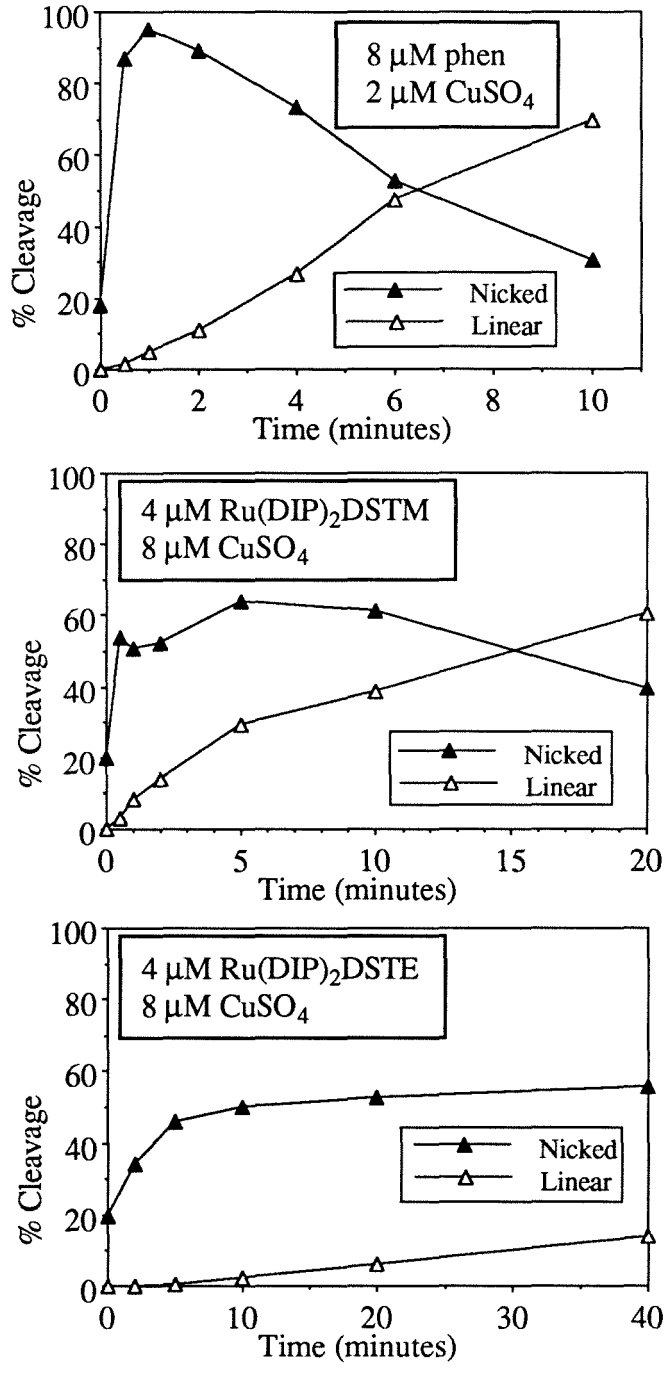

Figure 3.7. Comparison of DNA cleavage promoted by $Cu(phen)_2^+$, $Ru(DIP)_2DSTM$, and $Ru(DIP)_2DSTE$ as a function of reaction time. Note that the three graphs have different time scales. Conditions: 13 mM trizma·H_2SO_4, 2.6 mM Na_2SO_4, 20 μM base pairs pBR322, 500 μM 2-mercaptoethanol, 200 μM H_2O_2, 37 °C.

producing significant amounts of linearized plasmid when the plasmid is approximately 50% nicked.

The studies of DNA cleavage as a function of increasing reaction time illustrate the basic reactivity differences between the three complexes. It is noteworthy that although $Cu(phen)_2^+$ is more efficient, $Ru(DIP)_2DSTM$ and $Ru(DIP)_2DSTE$ yield higher concentrations of linearized plasmid directly than does $Cu(phen)_2^+$. This may be due to the greater site-selectivity of the ruthenium complexes on pBR322 (discussed in the next section), which increases the chance that two cleavage events on the same DNA plasmid would be close enough to produce linearized plasmid. Alternatively, direct plasmid linearization could be caused by a single ruthenium complex molecule with a reactive copper bound to each tethered chelate cleaving twice on the same plasmid. $Ru(DIP)_2DSTM$ and $Ru(DIP)_2DSTE$ could thus be acting as true double-stranded DNA nucleases.

DNA cleavage promoted by $Ru(DIP)_2DSTM$ and $Ru(DIP)_2DSTE$ as a function of copper concentration (Figure 3.8). The complexes $Ru(DIP)_2DSTM$ and $Ru(DIP)_2DSTE$ were reacted with DNA using increasing concentrations of $CuSO_4$. Both complexes promote increasing DNA cleavage with increasing copper concentration. The greatest increase in reactivity occurs when the copper concentration is increased from 0 to 4 μM. Further increases in copper concentration result in lesser increases in DNA cleavage. Overall, $Ru(DIP)_2DSTM$ promotes DNA cleavage more efficiently than $Ru(DIP)_2DSTE$, as was observed in the time course experiment. The complexes do promote some DNA cleavage even in the absence of added $CuSO_4$.

It is to be expected that $Ru(DIP)_2DSTM$, with approximately two and a half orders of magnitude higher affinity for copper (Figure 3.14),[18] would promote DNA cleavage more efficiently than $Ru(DIP)_2DSTE$, and this is confirmed by the results of

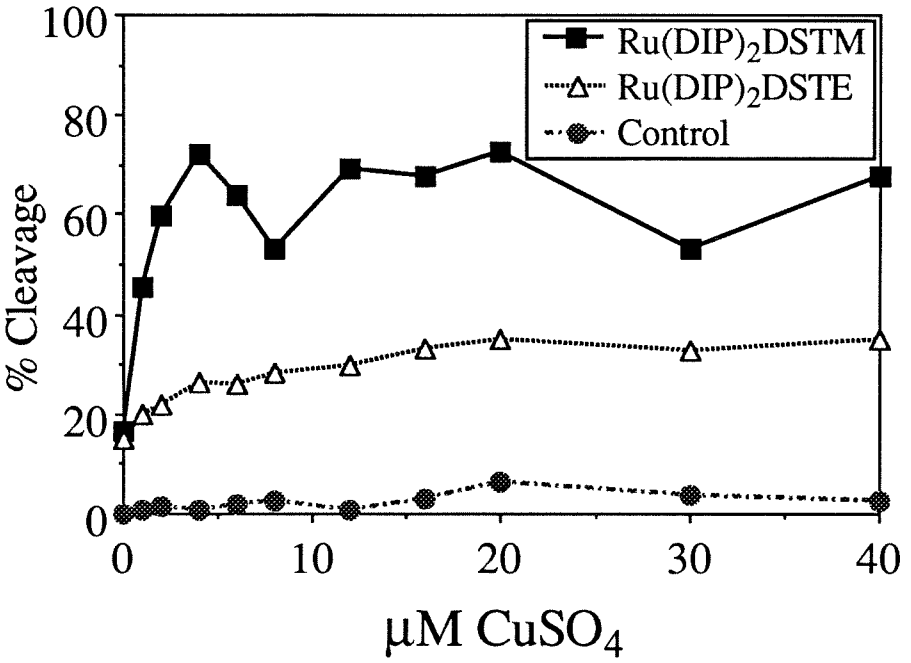

Figure 3.8. Comparison of DNA cleavage promoted by $Ru(DIP)_2DSTM$ and $Ru(DIP)_2DSTE$ as a function of $CuSO_4$ concentration. Conditions: 4 μM $Ru(DIP)_2DSTM$, $Ru(DIP)_2DSTE$, or no Ru complex; 13 mM trizma·H_2SO_4, 2.6 mM Na_2SO_4, 20 μM base pairs pBR322, 200 μM 2-mercaptoethanol, 200 μM H_2O_2, 2 minutes reaction time at 37 °C.

the cleavage assay. The reduced effectiveness of copper concentrations beyond 4 μM at promoting increased DNA cleavage is consistent with the metal binding sites of $Ru(DIP)_2DSTM$ and $Ru(DIP)_2DSTE$ becoming saturated with copper. Furthermore, the leveling off of cleavage by $Ru(DIP)_2DSTE$ at high copper concentrations implies that differences in copper binding affinity are not likely to be the only cause of the far greater DNA cleavage efficiency of $Ru(DIP)_2DSTM$ relative to $Ru(DIP)_2DSTE$. Copper bound to $Ru(DIP)_2DSTM$ appears to be inherently more reactive than copper bound to $Ru(DIP)_2DSTE$.

One would expect that with 4 μM ruthenium complex present, then cleavage efficiency would saturate at 8 μM $CuSO_4$ rather than at 4 μM since there are two copper binding sites per ruthenium complex. A possible explanation for this is that the poor aqueous solubility of the ruthenium complexes results in precipitation, which would lower the copper concentration at which cleavage efficiency would reach a maximum.

It is noteworthy that $Ru(DIP)_2DSTM$ and $Ru(DIP)_2DSTE$ promote some DNA cleavage even in the absence of added copper. This could be due to trace copper in solution, or perhaps to traces of other redox-active metals such as iron. Iron-mediated cleavage by a molecule with the bis(2-picolyl)amine moiety of $Ru(DIP)_2DSTM$ has recently been reported.[19]

DNA cleavage as a function of thiol concentration (Figure 3.9). The complexes $Cu(phen)_2^+$, $Ru(DIP)_2DSTM$ and $Ru(DIP)_2DSTE$ were reacted with DNA using increasing concentrations of the thiol 2-mercaptoethanol. In graph A, $Ru(DIP)_2DSTM$ and $Ru(DIP)_2DSTE$ are compared using thiol concentrations from 0 to 1000 μM in the presence of 200 μM H_2O_2. In graph B, $Ru(DIP)_2DSTM$ and $Cu(phen)_2^+$ are compared using thiol concentrations from 0 to 40 mM in the absence of H_2O_2. All three complexes promote little DNA cleavage at zero thiol. The reactivity (promotion of

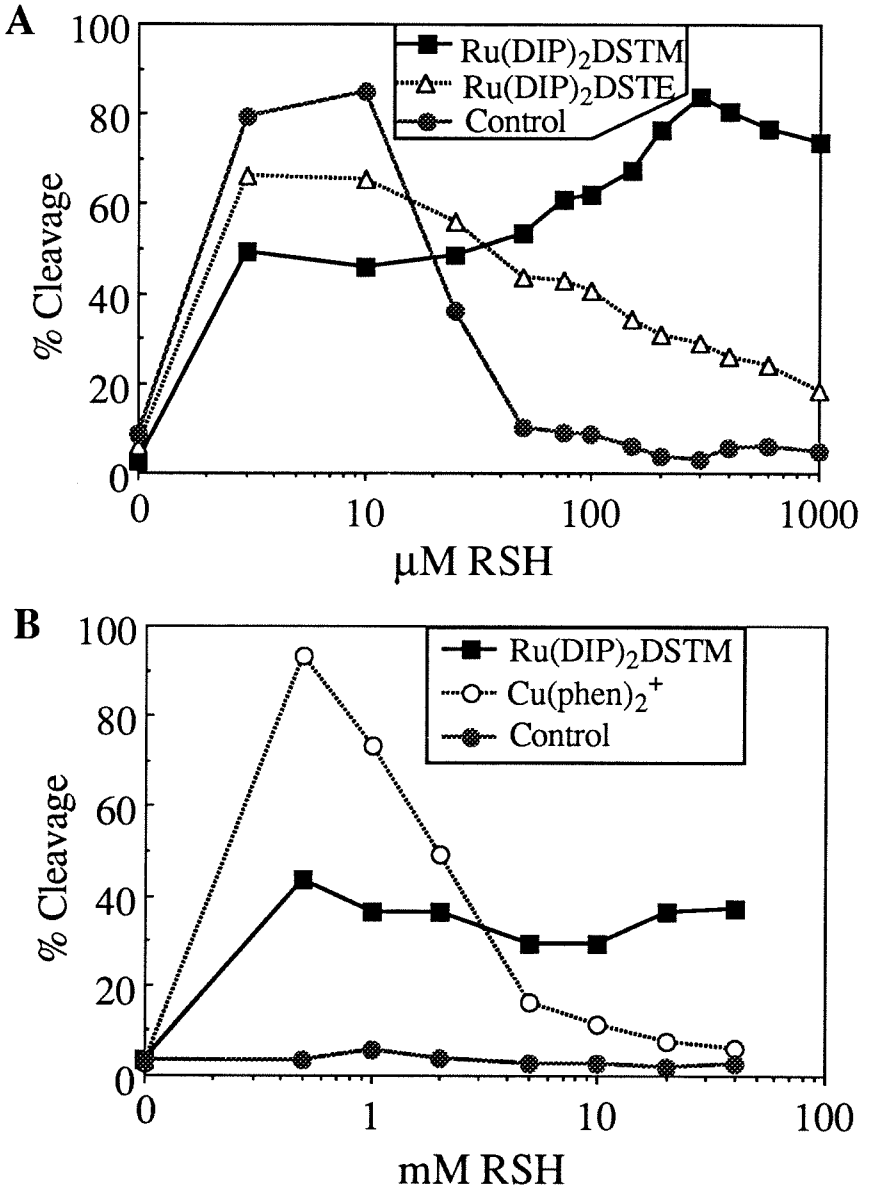

Figure 3.9. Comparison of DNA cleavage promoted by $Ru(DIP)_2DSTM$, $Ru(DIP)_2DSTE$, and $Cu(phen)_2^+$ as a function of 2-mercaptoethanol concentration. Conditions [**both**]: 13 mM trizma·H_2SO_4, 2.6 mM Na_2SO_4, 20 μM base pairs pBR322. [**A**]: 4μM $Ru(DIP)_2DSTM$ or 4 μM $Ru(DIP)_2DSTE$, 8 μM $CuSO_4$, 200 μM H_2O_2, 2 minutes at 37 °C. [**B**]: 4 μM $Ru(DIP)_2DSTM$ or 16 μM phen, 4 μM $CuSO_4$, no H_2O_2, 5 minutes at 37 °C.

DNA cleavage) of all three complexes increases with increasing thiol, reaches a maximum, and then decreases as the excess thiol quenches the reaction. However, the reactivity curve for each complex differs: $Cu(phen)_2^+$ and $Ru(DIP)_2DSTE$ are very sensitive to thiol concentration, and show higher reactivity at low thiol concentrations and lower reactivity at high thiol concentrations, while $Ru(DIP)_2DSTM$ is less sensitive to thiol concentration and shows significant reactivity even at very high thiol concentrations. Other than at high thiol concentrations, the reactivity order is $Cu(phen)_2^+$ > $Ru(DIP)_2DSTM$ > $Ru(DIP)_2DSTE$. It should be noted that in graph A, $CuSO_4$ promotes DNA cleavage at very low thiol concentrations (3, 10, and 25 μM 2-mercaptoethanol) in the absence of $Ru(DIP)_2DSTM$ or $Ru(DIP)_2DSTE$. Therefore, the DNA cleavage in the presence of $Ru(DIP)_2DSTM$ or $Ru(DIP)_2DSTE$ at those thiol concentrations may be largely due to copper not bound to a ruthenium complex. The DNA cleavage of $CuSO_4$ alone is quenched at thiol concentrations greater than or equal to 50 μM.

DNA cleavage as a function of H_2O_2 concentration (Figure 3.10). The complexes $Cu(phen)_2^+$, $Ru(DIP)_2DSTM$, and $Ru(DIP)_2DSTE$ were reacted with DNA using increasing concentrations of H_2O_2. All three complexes show increasing reactivity with increasing H_2O_2. However, under the conditions of high thiol concentration (graph B), the increase in reactivity with increasing H_2O_2 concentration is far greater for $Cu(phen)_2^+$ than it is for $Ru(DIP)_2DSTM$. With no added H_2O_2, $Ru(DIP)_2DSTM$ is more reactive than $Cu(phen)_2^+$, while with 0.2-2.0 mM added H_2O_2, $Cu(phen)_2^+$ is more reactive.

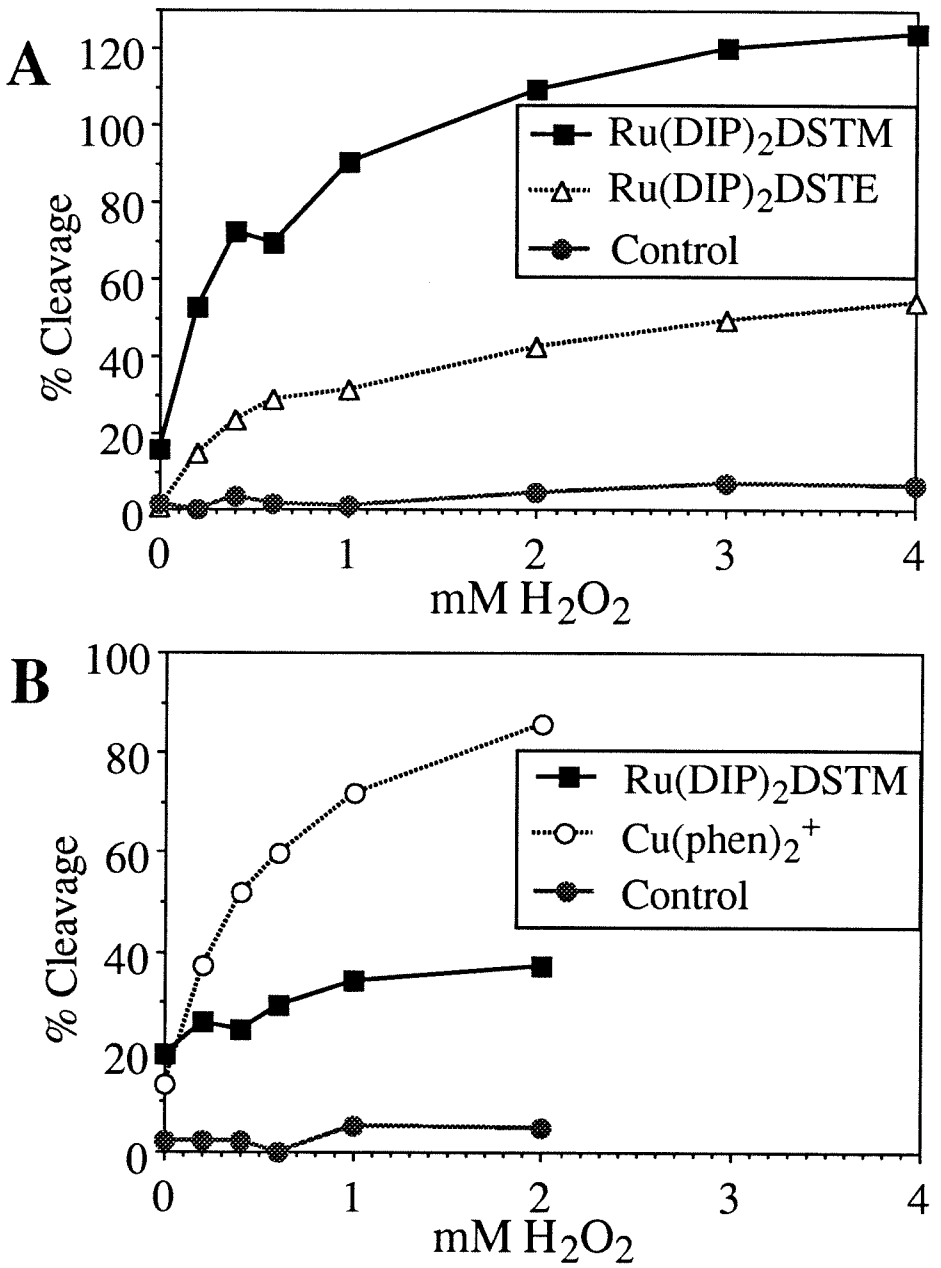

Figure 3.10. Comparison of DNA cleavage promoted by $Ru(DIP)_2DSTM$, $Ru(DIP)_2DSTE$, and $Cu(phen)_2^+$ as a function of H_2O_2 concentration. Conditions [**both**]: 13 mM trizma·H_2SO_4, 2.6 mM Na_2SO_4, 20 μM base pairs pBR322. [**A**]: 4 μM $Ru(DIP)_2DSTM$ or 4 μM $Ru(DIP)_2DSTE$, 8 μM $CuSO_4$, 500 μM 2-mercaptoethanol, 2 minutes at 37 °C. [**B**]: 4 μM $Ru(DIP)_2DSTM$ or 16 μM phen, 4 μM $CuSO_4$, 20 mM 2-mercaptoethanol, 5 minutes at 37 °C.

Table 3.2. Comparison of DNA cleavage efficiency promoted by $Ru(DIP)_2DSTM$, $Ru(DIP)_2DSTE$, and $Cu(phen)_2^+$ as a function of the 2-mercaptoethanol / H_2O_2 ratio.

Experimental Conditions			% DNA Cleavage			
mM RSH	mM H_2O_2	RSH / H_2O_2	DSTM	DSTE	phen	Control
0.1	0.2	0.5	63.5	29.5	82.6	0.7
0.3	0.6	0.5	88.2	31.0	62.6	1.2
1	2	0.5	94.3	30.8	78.4	0.9
0.6	0.2	3	62.4	15.9	32.7	1.0
1.8	0.6	3	62.0	14.5	28.5	0.8
6	2	3	54.7	12.1	26.9	1.2

Conditions: 13 mM trizma·H_2SO_4, 2.6 mM Na_2SO_4, 20 μM base pairs pBR322, 2 minutes at 37 °C. The samples contain either 4 μM $Ru(DIP)_2DSTM$ and 8 μM $CuSO_4$, 4 μM $Ru(DIP)_2DSTE$ and 8 μM $CuSO_4$, or 3 μM phen and 0.75 μM $CuSO_4$. The control contains 8 μM $CuSO_4$.

DNA cleavage as a function of the thiol/H_2O_2 Ratio (Table 3.2). The complexes $Cu(phen)_2^+$, $Ru(DIP)_2DSTM$, and $Ru(DIP)_2DSTE$ were reacted with DNA at two different 2-mercaptoethanol/H_2O_2 ratios, using three different absolute concentrations of thiol and H_2O_2 at each ratio. The reactivity of all three complexes is higher at the 1:2 ratio than at the 3:1 ratio. The reactivity of $Ru(DIP)_2DSTE$ shows a very clear dependence on the thiol/H_2O_2 ratio, even though the absolute concentrations of both thiol and H_2O_2 were varied by a full order of magnitude. The reactivity dependence of $Ru(DIP)_2DSTM$ and $Cu(phen)_2^+$ on the thiol/H_2O_2 ratio is less clear.

The Site-Selectivity of $Ru(DIP)_2DSTM$ and $Ru(DIP)_2DSTE$ on pBR322.

The site-selectivity of the copper cleavage reaction of $Ru(DIP)_2DSTM$ and $Ru(DIP)_2DSTE$ on the DNA plasmid pBR322 has been analyzed by low-resolution mapping. The complexes $Ru(DIP)_2DSTM$ and $Ru(DIP)_2DSTE$ were reacted with the DNA plasmid pBR322 in the presence of copper, 2-mercaptoethanol, and H_2O_2. The samples were reacted long enough to produce linearized plasmid. The samples were

then treated with the restriction endonucleases *Hind* III, *Ava* I, and *Nde* I, and analyzed by agarose gel electrophoresis in order to localize the site or sites at which the complexes cleave pBR322. The gel is shown in Figure 3.11. From the samples to which restriction enzyme was not added, it can be seen that $Ru(DIP)_2DSTM$ promoted more efficient DNA cleavage than $Ru(DIP)_2DSTE$, and produced much more linearized plasmid. When the samples were treated with restriction enzymes, discrete smaller fragments are produced, which indicates that the original linearization promoted by $Ru(DIP)_2DSTM$ and $Ru(DIP)_2DSTE$ was site-selective in nature. The fragments from the $Ru(DIP)_2DSTE$ samples appear identical to the fragments from the $Ru(DIP)_2DSTM$ samples, although lower in intensity.

Using 1 Kb DNA Ladder as a molecular weight marker, the size of the fragments produced by the restriction enzymes was determined. This data is shown in Table 3.3. When a restriction enzyme digests linearized plasmid, a large and a small fragment are produced. Since the size of the smaller fragment can be more accurately determined, the cleavage sites of $Ru(DIP)_2DSTM$ and $Ru(DIP)_2DSTE$ were determined from the smaller fragments. Both complexes linearize pBR322 at approximately the same sites. $Ru(DIP)_2DSTM$ linearizes pBR322 strongly at 3251 ± 50 , and moderately at 4226 ± 50; $Ru(DIP)_2DSTE$ linearizes pBR322 moderately at 3260 ± 50 and weakly at 4215 ± 50.

Figure 3.11. Low resolution mapping of DNA cleavage by $Ru(DIP)_2DSTM$ and $Ru(DIP)_2DSTE$ on pBR322. Conditions: 5 μM $Ru(DIP)_2DSTM$, 5 μM $Ru(DIP)_2DSTE$, or no ruthenium complex; 10 μM $CuSO_4$, 50 μM DNA base pairs pBR322, 500 μM 2-mercaptoethanol, 200 μM H_2O_2. $Ru(DIP)_2DSTM$ samples were incubated for 10 minutes at 37 °C, and others were incubated for 60 minutes at 37 °C. The copper cleavage reaction was quenched, then samples were incubated with 10 units *Hind* III, *Ava* I, or *Nde* I for 90 minutes at 37 °C.

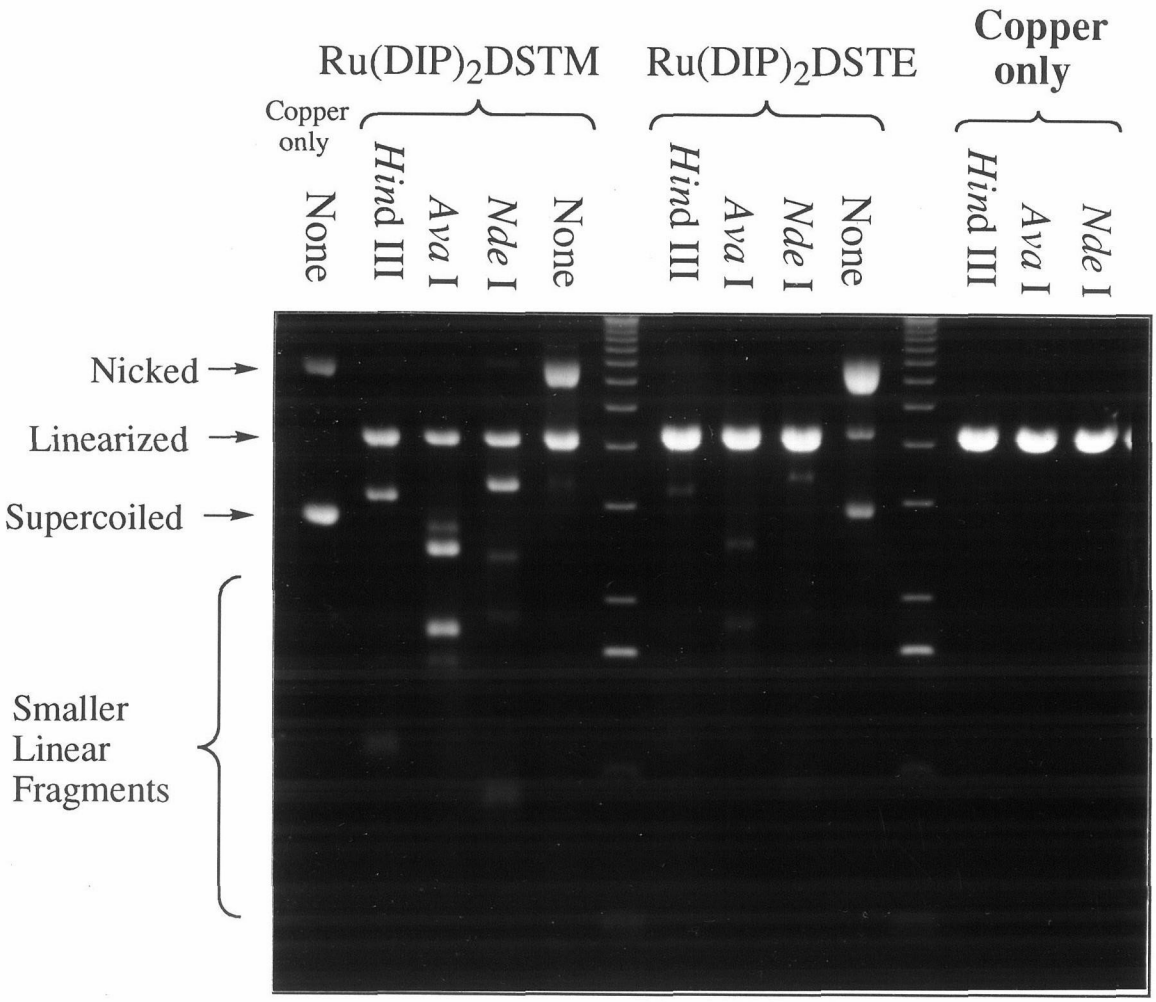
Ru(DIP)2DSTM
Ru(DIP)2DSTE
Copper only
Copper only
None
Hind III
Ava I
Nde I
None
Hind III
Ava I
Nde I
None
Hind III
Ava I
Nde I
Nicked
Linearized
Supercoiled
Smaller Linear Fragments

Table 3.3. Linear DNA Fragments Produced by the Digestion of pBR322 Cleaved by $Ru(DIP)_2DSTM$ or $Ru(DIP)_2DSTE$ with the Restriction Enzymes *Hin*d III, *Ava* I, and *Nde* I.

	$Ru(DIP)_2DSTM$	$Ru(DIP)_2DSTE$
Fragments produced by *Hin*d III digestion	3384, 1112 (s)	3452, 1149 (m)
Fragments produced by *Ava* I digestion	2649, 1853 (s) 2940, 1610 (m)	2712, 1898 (m) 2995, 1670 (w)
Fragments produced by *Nde* I digestion	3533, 883 (s) 2576, 1969 (m)	3656, 914 (m) 2624, 1992 (w)
Cleavage sites, calculated from the smaller fragments	3251 ± 50 (s), 4226 ± 50 (m)	3260 ± 50 (m) 4215 ± 50 (w)

The sizes of all fragments are in DNA base pairs; the locations of the calculated cleavage sites are in base pairs from the *Eco*R I site. Key: (s) = strong site, (m) = moderate site, and (w) = weak site.

Both $Ru(DIP)_2DSTM$ and $Ru(DIP)_2DSTE$ promote site-selective cleavage of the DNA plasmid pBR322, with major cleavage sites at 3250 ± 50 and minor sites at 4220 ± 50. These cleavage sites are identical within experimental uncertainty to those produced by the photochemical cleavage of pBR322 with $Co(DIP)_3^{3+}$ at 3300 ± 100 and 4240 ± 20, and with $Rh(DIP)_3^{3+}$ at 3238/3250 and 4220 ± 80.[20,21] Although the mechanism of the copper-activated oxidative DNA cleavage promoted by $Ru(DIP)_2DSTM$ and $Ru(DIP)_2DSTE$ differs from that of the photochemical cleavage promoted by $Co(DIP)_3^{3+}$ and $Rh(DIP)_3^{3+}$, the site-selectivity of all four complexes is determined by the affinity of their $M(DIP)_3^{n+}$ cores for sites of DNA tertiary structure that could protect the hydrophobic DIP ligands from solvent. The 3250 site is near a known DNA cruciform structure, and the 4220 site is in a highly AT rich area, which increases the likelihood that DNA tertiary structure is present. $Ru(DIP)_2DSTM$ and $Ru(DIP)_2DSTE$ thus appear to be bifunctional molecules, with their $Ru(DIP)_3^{2+}$ cores determining DNA site-selectivity, and their metal-chelating functional groups promoting DNA cleavage in the presence of copper, thiol, and H_2O_2.

Identification of Free Nucleic Acid Bases Produced by the Cleavage of Calf Thymus DNA by $Ru(DIP)_2DSTM$ and $Ru(DIP)_2DSTE$ (Figure 3.12). The complex $Ru(DIP)_2DSTM$, in the presence of copper, 2-mercaptoethanol, and H_2O_2, was reacted with calf thymus DNA for 30 minutes. The reaction was then quenched by the addition of 2,9-dimethyl-1,10-phenanthroline, which chelates copper ions. The free nucleic acid bases cytosine, guanine, and adenine were detected as products of this reaction by HPLC (A). This was confirmed by coinjection of the reaction mixture with a dilute solution of the above three bases (B). The three bases were not produced in significant quantities if 2,9-dimethyl-1,10-phenanthroline was added prior to the addition of 2-mercaptoethanol and H_2O_2 (C). The three bases were also not produced in the absence of copper (D), in the absence of 2-mercaptoethanol and H_2O_2 (E), or in the absence of $Ru(DIP)_2DSTM$ (F). If $Ru(DIP)_2DSTM$ is replaced by $Ru(DIP)_2DSTE$, significantly less free bases are produced due to the lower reactivity of the latter complex (G).

The free nucleic acid bases detected by HPLC as a major product of the DNA cleavage reaction of $Ru(DIP)_2DSTM$ are consistent with the DNA sugar as the site of oxidative attack rather than the DNA bases. The production of free bases is consistent with either C1' hydrogen abstraction or oxygen-independent C3' hydrogen abstraction mechanisms. Due to the poor aqueous solubility of the complexes, no attempt was made to quantitate the free nucleic acid bases, or to identify possible minor products of the DNA cleavage reaction.

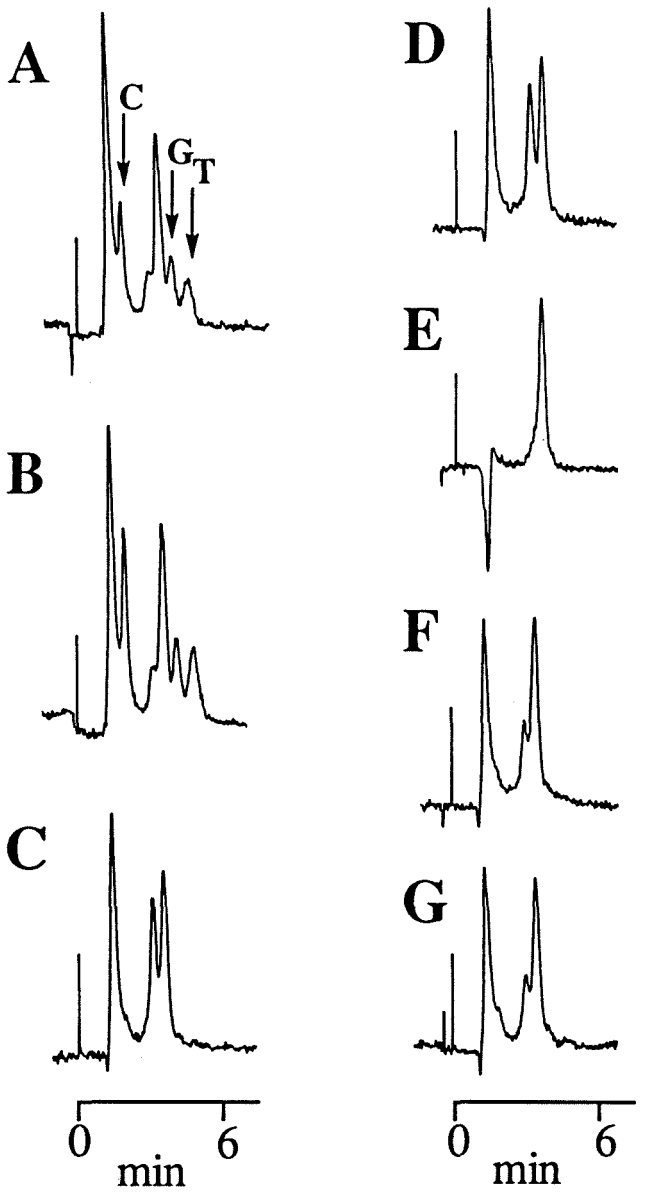

Figure 3.12. HPLC product analysis of the DNA cleavage reactions of $Ru(DIP)_2DSTM$ and $Ru(DIP)_2DSTE$. **A:** 58 μM base pairs calf thymus DNA, 3 μM $Ru(DIP)_2DSTM$, 6 μM $CuSO_4$, 200 μM 2-mercaptoethanol, and 200 μM H_2O_2, were reacted 30 minutes at 37 °C, then quenched with 10 μl 20 mM 2,9-dimethylphen. The free nucleic acid bases cytosine, guanine, and thymine produced by the reaction are labeled. **B:** Trace "A" coinjected with authentic cytosine, guanine, and thymine. **C:** As in trace "A," except the 2,9-dimethylphen was added before the mercaptoethanol and the H_2O_2. **D:** As in trace "A," except no $CuSO_4$. **E:** As in trace "A," except no mercaptoethanol or H_2O_2. **F:** As in trace "A," except no $Ru(DIP)_2DSTM$. **G:** As in trace "A," with 3 μM $Ru(DIP)_2DSTE$ substituted for the $Ru(DIP)_2DSTM$.

Identification of Termini Produced by the Cleavage of a DNA Oligonucleotide by Ru(DIP)$_2$DSTM (Figure 3.13). The complex Ru(DIP)$_2$DSTM, in the presence of $CuSO_4$, the reducing agent 2-mercaptoethanol, and H_2O_2, promotes cleavage of the DNA oligonucleotide CTGGCATACCGGTATGCCAG (lanes O, P, and Q). No significant cleavage is observed in the absence of 2-mercaptoethanol or H_2O_2 (lane B), or in the absence of Ru(DIP)$_2$DSTM (lanes D, E, F and G). The DNA cleavage promoted by Ru(DIP)$_2$DSTM is compared with that promoted by Cu(phen)$_2^+$ (lanes J and K), iron-bleomycin (lanes L, M, and N), and Rh(phi)$_2$bpy^{3+} (lanes R, S, and T). Unlike Cu(phen)$_2^+$ and iron-bleomycin, Ru(DIP)$_2$DSTM shows little sequence selectivity on this short oligonucleotide. Under the conditions of this experiment, Cu(phen)$_2^+$ shows more efficient DNA cleavage than Ru(DIP)$_2$DSTM, even though Ru(DIP)$_2$DSTM was permitted to react with the oligonucleotide for 20 minutes before EDTA was added to quench the reaction, and Cu(phen)$_2^+$ was permitted to react for only 2 1/2 minutes. Both Ru(DIP)$_2$DSTM and Cu(phen)$_2^+$ produce primarily 3'-phosphate termini, which comigrate with the products of the Maxam-Gilbert sequencing reactions (lanes H and I).[22] Both Ru(DIP)$_2$DSTM and Cu(phen)$_2^+$ also produce faster-migrating 3'-phosphoglycolate termini, which comigrate with the primary products of the iron-bleomycin reaction.[6,7] Rh(phi)$_2$bpy^{3+} also produces 3'-phosphoglycaldehyde termini from its oxygen-dependent pathway.[13] These 3'-phosphoglycaldehyde termini migrate slower than their corresponding 3'-phosphate termini, and can be distinguished from the phosphate and phosphoglycolate termini especially well at bases G-4, T-7, C-10, and G-11. At these bases, not much phosphoglycaldehyde is evident in the Ru(DIP)$_2$DSTM and Cu(phen)$_2^+$ reactions.

Upon NaOH treatment, no enhanced cleavage was observed by Ru(DIP)$_2$DSTM (lane P versus lane O). Treatment with $NaBH_4$, which reduces 3'-phosphoglycaldehydes to their corresponding alcohols, produced mobility changes in

Figure 3.13. Cleavage and product analysis of the ^{32}P 5'-radiolabeled DNA oligonucleotide 5'-CTGGCATACCGGTATGCCAG-3'. 20 kcpm loaded in lanes A-G, J-L, O-Q. **A:** 3μM $Ru(DIP)_2DSTM$, no $CuSO_4$, 200 μM 2-mercaptoethanol, 200 μM H_2O_2. **B:** 3 μM $Ru(DIP)_2DSTM$, 9 μM $CuSO_4$, no 2-mercaptoethanol nor H_2O_2. **C:** DNA in buffer only. **D & E:** 9 μM $CuSO_4$, 200 μM 2-mercaptoethanol, 200 μM H_2O_2. **F & G:** 9 μM $CuSO_4$, 2 mM 2-mercaptoethanol, 2 mM H_2O_2. **H & I:** Maxam-Gilbert A+G and C+T reactions, respectively. **J & K:** 12 μM 1,10-phenanthroline, 3 μM $CuSO_4$, 200 μM 2-mercaptoethanol, 200 μM H_2O_2. **L, M, & N:** 8 μM $FeSO_4$, 4 μM bleomycin, with 20, 6.7, and 2.2 kcpm loaded, respectively. **O, P, & Q:** 3 μM $Ru(DIP)_2DSTM$, 9 μM $CuSO_4$, 200 μM 2-mercaptoethanol, 200 μM H_2O_2. **R, S, & T:** 4.5 μM $Rh(phi)_2bpy^{3+}$, irradiated 6 minutes at 310 nm; 30, 15, and 30 kcpm loaded, respectively. **U:** DNA in buffer only, irradiated 6 minutes at 310 nm, 30 kcpm loaded.

P was treated with NaOH. **E, G, K, Q, & T** were treated with $NaBH_4$.

a: 3'-phosphoglycaldehyde fragment at G-4.

b: 3'-phosphoglycaldehyde fragment at G-3 reduced by $NaBH_4$.

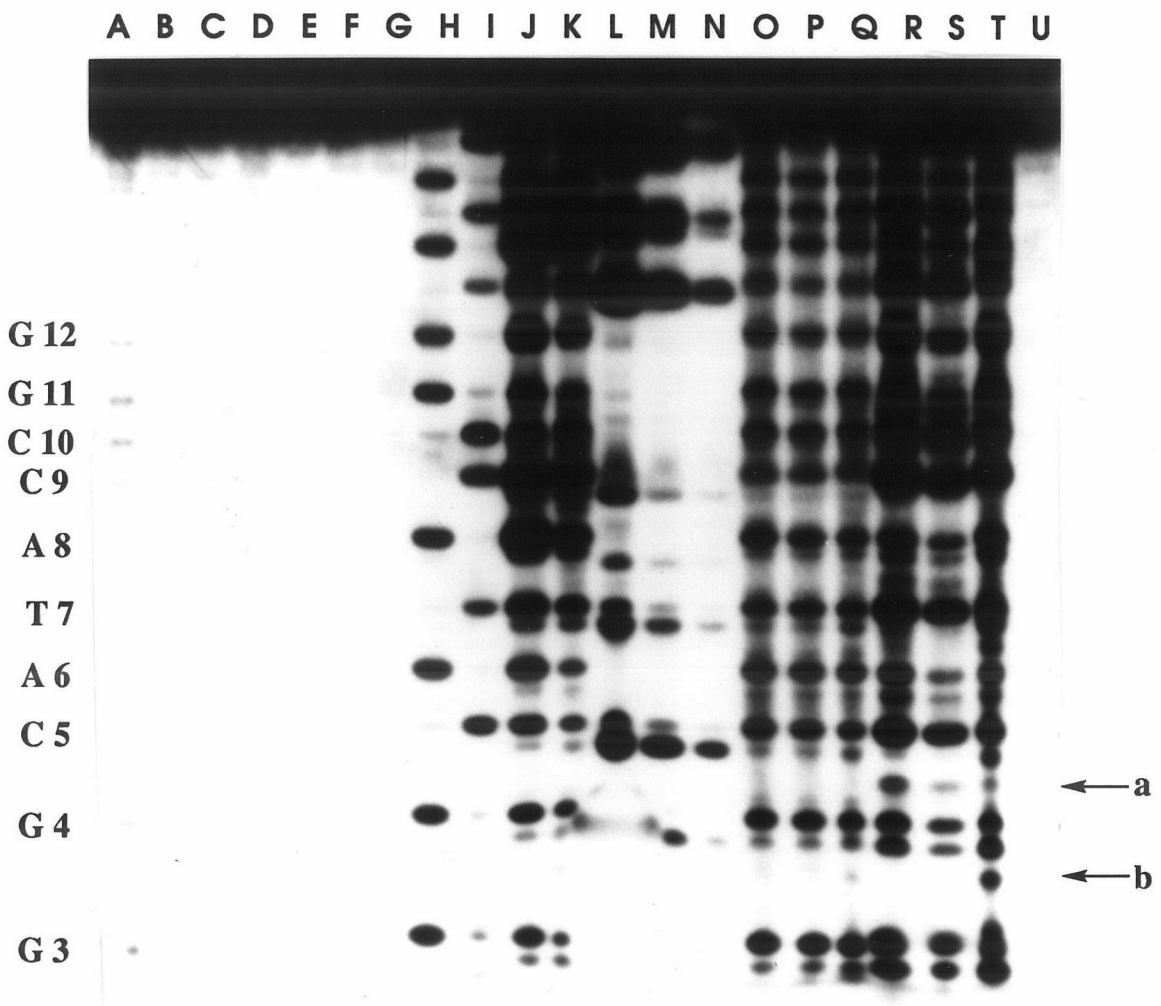
A B C D E F G H I J K L M N O P Q R S T U
G 12
G 11
C 10
C 9
A 8
T 7
A 6
C 5
G 4
G 3
a
b

the DNA cleavage products of $Rh(phi)_2bpy^{3+}$ which are especially evident at base G-3 (band "b"; lane T versus lane R).[13] A small amount of reduced phosphoglycaldehyde can also be observed in the DNA cleavage products of $Ru(DIP)_2DSTM$ (lane Q versus lane O) and $Cu(phen)_2^+$ (lane K versus lane J) at base G-3.

The DNA cleavage by $Ru(DIP)_2DSTM$ on the oligonucleotide 5'-CTGGCATACCGGTATGCCAG-3' is remarkably sequence neutral, in contrast to $Cu(phen)_2^+$, which promotes moderately site-selective DNA cleavage, consistent with local sequence-dependent variations in minor-groove structure.[7] This also contrasts with the site-selective DNA cleavage of $Ru(DIP)_2DSTM$ on the DNA plasmid pBR322. It therefore appears that $Ru(DIP)_2DSTM$ has a high affinity for DNA sites with tertiary structure (such as the cruciform on pBR322), and a lower, nonselective affinity for short, linear DNA (no tertiary structure is likely to form on a 20-mer oligonucleotide where supercoiled stress is absent). The tethered copper chelates appear to promote sequence neutral cleavage, with the site-selectivity (or lack thereof) being determined by the $Ru(DIP)_3^{2+}$ core. Both the lower selectivity and the lower cleavage efficiency of $Ru(DIP)_2DSTM$ relative to $Cu(phen)_2^+$ in the oligonucleotide experiment are consistent with the greater flexibility and entropy inherent in the tethered copper chelates in the case of the ruthenium complex.

The production of 3'-phosphate termini as the major product of the reaction of $Ru(DIP)_2DSTM$ on a DNA oligonucleotide gives further support for either a C1' or an oxygen-independent C3' hydrogen abstraction mechanism. $Ru(DIP)_2DSTM$ also produces as a minor product 3'-phosphoglycolate termini, which results from oxygen-dependent C4' hydrogen abstraction. The mobility change at base G-3 upon $NaBH_4$ treatment is consistent with 3'-phosphoglycaldehyde being present, which is a product of oxygen-dependent C3' hydrogen abstraction.

Overall, the pattern of product 3'-termini produced by $Ru(DIP)_2DSTM$ appears similar to that of $Cu(phen)_2^+$ (which does C1' and C4' hydrogen abstraction). However, since 3'-phosphate termini and free nucleic acid bases can also be produced by an oxygen-independent C3' hydrogen abstraction mechanism, and since a mobility change upon $NaBH_4$ treatment was observed, $Ru(DIP)_2DSTM$ may also promote DNA cleavage by a C3 ' hydrogen abstraction mechanism. Since the C1' hydrogens and the C4' hydrogens are accessible through the DNA minor groove, and the C3' hydrogens are accessible through the DNA major groove, there is therefore evidence that $Ru(DIP)_2DSTM$ promotes DNA cleavage through *both* the minor and the major grooves. The relative amounts of minor groove and major groove DNA cleavage mechanisms cannot be determined without further experiments. It should also be noted that in contrast to $Cu(phen)_2^+$, a $Ru(DIP)_2DSTM$ molecule has the potential to bind in one DNA groove while copper bound to the same molecule approaches DNA from the opposite groove and promotes DNA cleavage. This possibility has been shown to be feasible through molecular modeling.

$Ru(DIP)_2DSTE$ produces the same general pattern of 3'-termini that $Ru(DIP)_2DSTM$ produces (data not shown), but the lower cleavage efficiency of $Ru(DIP)_2DSTE$ makes the detection and identification of termini other than 3'-phosphates difficult. The products of the DNA cleavage reaction of $Ru(DIP)_2DSTM$ and $Ru(DIP)_2DSTE$ on a 3'-radiolabeled oligonucleotide were almost exclusively 5'-phosphate termini (data not shown), which is also consistent with C1', C3', and C4' hydrogen abstraction.

3.4. Discussion.

$Ru(DIP)_2DSTM$ and $Ru(DIP)_2DSTE$ Promote Copper-Activated DNA Cleavage. The above results show that copper can promote DNA cleavage when bound

to ligands other than 1,10-phenanthroline. $Ru(DIP)_2DSTM$ and $Ru(DIP)_2DSTE$ promote DNA cleavage upon the addition of copper, the reducing agent 2-mercaptoethanol, and H_2O_2. Under the conditions used, there is little or no DNA cleavage in the absence of either the ruthenium complexes, copper, or the redox reagents (2-mercaptoethanol and H_2O_2). $Ru(DIP)_2DSTM$ and $Ru(DIP)_2DSTE$ therefore serve as vehicles for the delivery of the copper to conduct the oxidative attack on DNA. The DNA cleavage efficiency of the two complexes relative to each other and to $Cu(phen)_2^+$ depends on the reaction conditions, the coordination environment around the copper, and the structure of the complex as a whole.

Factors Affecting the Efficiency of Copper-Activated DNA Cleavage. As the results show, the order of DNA cleavage efficiency is $Cu(phen)_2^+$ > $Ru(DIP)_2DSTM$ > $Ru(DIP)_2DSTE$ under most of the explored conditions. Under the conditions of high thiol concentrations in the absence of added H_2O_2, $Ru(DIP)_2DSTM$ promotes the most efficient DNA cleavage. Although many factors might be responsible for the differences in cleavage efficiency among the three complexes, they can be classified into the following four categories: (1) The binding affinity of the complexes for DNA. (2) The binding affinity of $Ru(DIP)_2DSTM$, $Ru(DIP)_2DSTE$, and phenanthroline for copper. (3) The ability of the copper bound to the complexes to approach the DNA phosphate-sugar backbone in a manner that allows effective DNA cleavage. (4) The effect of the coordination environment around the copper on inherent reactivity towards promoting DNA cleavage.

1. The binding affinity of the complexes for DNA. Binding constants of $Ru(DIP)_2DSTM$ and $Ru(DIP)_2DSTE$ to DNA have proven to be difficult to determine due to the propensity of the two complexes to precipitate upon the addition of DNA. It

can be assumed, however, that when copper is bound to the tethered chelates, that the ruthenium complexes will have a somewhat higher binding affinity for DNA than $Cu(phen)_2^+$ due to their greater net charge and their hydrophobicity.

2. The binding affinity of Ru(DIP)$_2$DSTM, Ru(DIP)$_2$DSTE, and phenanthroline for copper. Based on analogues of the tridentate copper binding sites in Ru(DIP)$_2$DSTM and Ru(DIP)$_2$DSTE, the binding constants of Cu^{2+} to the ruthenium complexes have been estimated (Figure 3.14). The binding constant of Cu^{2+} to Ru(DIP)$_2$DSTM is estimated to be $10^{14.4}$, based on the analogue bis(2-picolyl)amine. The binding constant of Cu^{2+} to bis(2-ethylpyridyl)amine, the corresponding analogue of Ru(DIP)$_2$DSTE, could not be found. However, based on the binding constants of Cu^{2+} to other ligands, the increase in chelate ring size from five to six appears to reduce the binding constant by about $10^{2.4}$. The binding constant of Cu^{2+} to Ru(DIP)$_2$DSTE is therefore estimated to be 10^{12}. These binding constants compare favorably to that of phenanthroline, which has a binding constant of $10^{7.4} = [Cu(phen)^{2+}]/[Cu^{2+}][phen]$.[18]

It is possible that the sulfonamides of Ru(DIP)$_2$DSTM and Ru(DIP)$_2$DSTE deprotonate and coordinate to copper, making the binding tetradentate rather than tridentate. It is also expected that the positively charged ruthenium centers would affect the copper binding constants as well. The former effect would be expected to raise the binding affinity of the complexes for copper, while the latter effect would be expected to lower it.

Figure 3.14. Analysis of the Binding Affinity of $Ru(DIP)_2DSTM$ and $Ru(DIP)_2DSTE$ for Cu^{2+} Based on Analogues from Martell's Stability Constants[18]

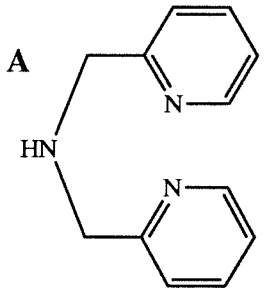

$$\frac{[L{\cdot}Cu^{2+}]}{[Cu^{2+}][L]} = 10^{14.4}$$

B

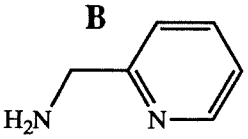

$$\frac{[L{\cdot}Cu^{2+}]}{[Cu^{2+}][L]} = 10^{9.5}$$

C

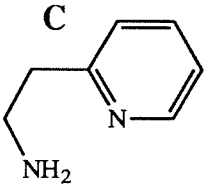

$$\frac{[L{\cdot}Cu^{2+}]}{[Cu^{2+}][L]} = 10^{7.3}$$

D

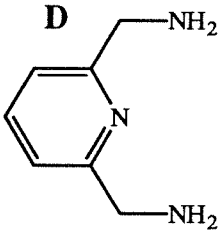

$$\frac{[L{\cdot}Cu^{2+}]}{[Cu^{2+}][L]} = 10^{15.7}$$

E

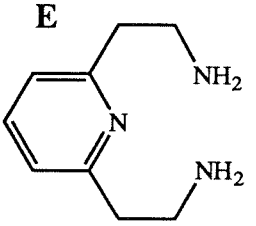

$$\frac{[L{\cdot}Cu^{2+}]}{[Cu^{2+}][L]} = 10^{13.2}$$

F

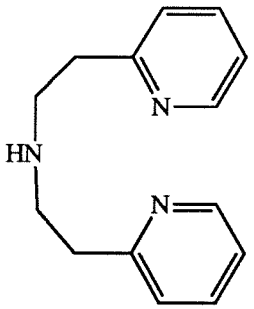

$$\frac{[L{\cdot}Cu^{2+}]}{[Cu^{2+}][L]} \text{ is estimated to be } 10^{12}$$

The binding constant of Cu^{2+} to bis(2-picolyl)amine [**A**], an analogue of $Ru(DIP)_2DSTM$, is $10^{14.4}$. The binding constant of Cu^{2+} to bis(2-ethylpyridyl)amine [**F**], the corresponding analogue of $Ru(DIP)_2DSTE$, could not be found in the literature. Based on the four ligands **B**, **C**, **D**, and **E**, the increase in chelate ring size from five to six decreases the binding constant by approximately $10^{2.4}$. The binding constant of Cu^{2+} to the $Ru(DIP)_2DSTE$ analogue is therefore estimated to be 10^{12}. In comparison, the binding constant of Cu^{2+} to a single 1,10-phenanthroline ligand is $10^{7.4}$.

3. The ability of the copper bound to the complexes to approach the DNA backbone. It is to be expected that copper bound to the large, bulky $Ru(DIP)_2DSTM$ and $Ru(DIP)_2DSTE$ complexes would have much more difficulty approaching the DNA backbone than $Cu(phen)_2^+$. As discussed above, $Ru(DIP)_2DSTM$ and $Ru(DIP)_2DSTE$ probably have a higher affinity for DNA than $Cu(phen)_2^+$, and definitely have a higher affinity for copper than phenanthroline (factors 1 and 2). It is therefore likely that the greater accessibility of the copper of $Cu(phen)_2^+$ to the DNA backbone is a major factor in the greater DNA cleavage efficiency of $Cu(phen)_2^+$.

4. The effect of the coordination environment around the copper on inherent reactivity towards promoting DNA cleavage. Copper-activated redox cleavage of DNA involves the reduction of Cu(II) to Cu(I), which then binds to H_2O_2, and promotes DNA cleavage, returning to the Cu(II) state. Since both the Cu(I) state and the Cu(II) state need to be accessible for facile DNA cleavage, ligands which modulate the Cu^{2+}/Cu^+ redox potential might be expected to have a substantial effect on DNA cleavage efficiency. The complex Cu(2,9-dimethylphenanthroline)$_2^+$ provides an illustration of this. This complex has a Cu^{2+}/Cu^+ potential of +594 mV due the steric effect of the 2,9-methyl groups in making the square planar Cu(II) state less accessible.[14] Cu(II) is in fact so inaccessible that the complex remains in the Cu(I) state and does not promote any DNA cleavage whatsoever.[12] When the potential of the Cu^{2+}/Cu^+ transition is less extreme, the effect of the potential on DNA cleavage efficiency is less clear. The cyclic voltammetry results show that the analogue of $Ru(DIP)_2DSTM$ has a Cu^{2+}/Cu^+ transition at -23 ± 20 mV (relative to SHE), and the $Ru(DIP)_2DSTE$ analogue has a Cu^{2+}/Cu^+ transition at $+203 \pm 20$ mV. The $Cu(phen)_2^{2+}/Cu(phen)_2^+$ transition is known to be +174 mV.[14] Since all three complexes promote DNA cleavage, copper complexes with Cu^{2+}/Cu^+ potentials in the -20 to +200 mV range appear to have both their Cu(II) states and their Cu(I) states

accessible. Since the Cu(I) state of copper bound to $Ru(DIP)_2DSTM$ is less stable than that of $Ru(DIP)_2DSTE$ and $Cu(phen)_2^+$, it is therefore inherently more reactive. This may play a role in the greater DNA cleavage efficiency of $Ru(DIP)_2DSTM$ at high thiol concentrations.

The thiol concentration clearly has a dramatic effect on DNA cleavage efficiency. Although thiol is required to initiate the reaction, higher concentrations of thiol quench DNA cleavage. Moreover, thiol clearly quenches the cleavage reactions of the three complexes unequally. The cleavage reactions of $Cu(phen)_2^+$ and $Ru(DIP)_2DSTE$ are strongly quenched by high thiol concentrations, while $Ru(DIP)_2DSTM$ is less sensitive to thiol concentration, and promotes DNA cleavage even at high thiol concentrations. Two possible mechanisms for this are illustrated in Figure 3.15. Mechanism A is that thiol directly competes with $Ru(DIP)_2DSTM$, $Ru(DIP)_2DSTE$, and phenanthroline for copper; and that $Ru(DIP)_2DSTM$, with the highest affinity for copper, can thus promote efficient DNA cleavage even in the presence of high thiol concentrations. Mechanism B is that thiol competes with H_2O_2 for binding sites on Cu (I) bound to $Ru(DIP)_2DSTM$, $Ru(DIP)_2DSTE$, and phenanthroline. Cu (I) with bound H_2O_2 can promote DNA cleavage, while Cu(I) with bound thiol cannot. $Ru(DIP)_2DSTM$, which has the bound copper with the least stable and therefore the most reactive Cu(I) state, might be expected to be best able to resist this mechanism of quenching as well. The ability of additional H_2O_2 to compensate for the DNA cleavage inhibition by thiol (Figure 3.10) supports Mechanism B, since if thiol were preventing copper from binding to $Ru(DIP)_2DSTE$ and phenanthroline at all, then the additional H_2O_2 should not increase DNA cleavage efficiency by much. The mechanism of H_2O_2 compensating for the quenching of DNA cleavage by high thiol concentrations cannot be the direct oxidation of thiols to disulfides by H_2O_2, since in the case of graph B of Figure 3.10 the thiol concentration is two orders of magnitude

Figure 3.15. Possible Mechanisms for the Quenching of DNA Cleavage by High Thiol Concentrations

Mechanism A: Thiol directly competes with the chelating ligands for copper

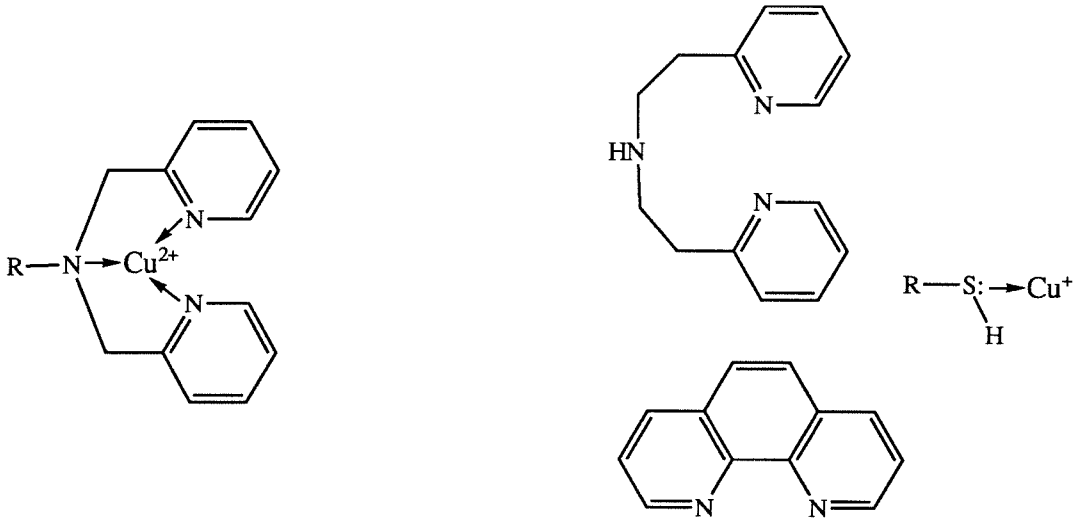

Mechanism B: Thiol competes with H_2O_2 for sites on the copper complexes

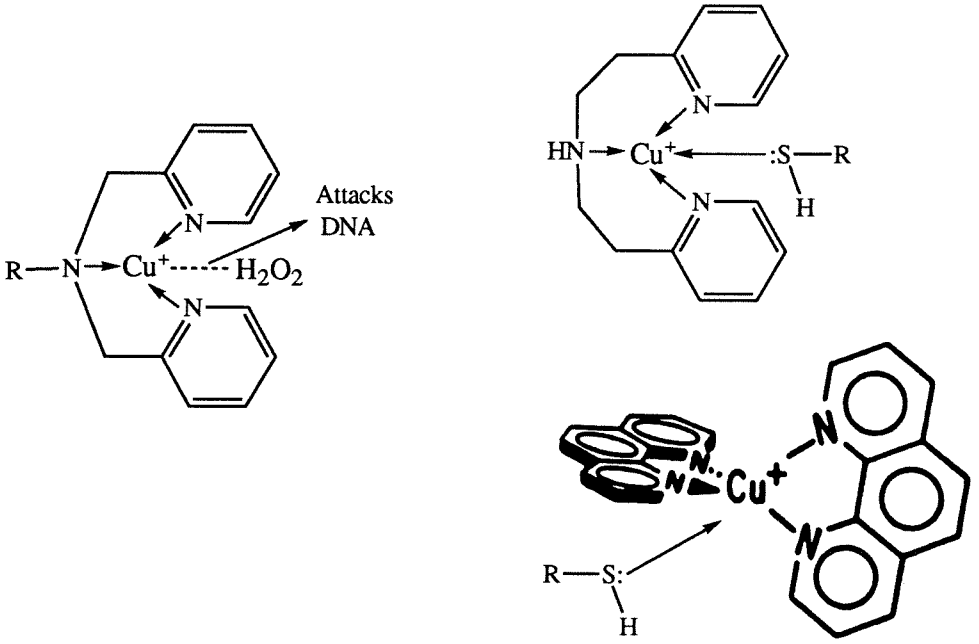

Mechanism A involves direct competition between thiols and phen, $Ru(DIP)_2DSTM$, and $Ru(DIP)_2DSTE$ for copper. Since $Ru(DIP)_2DSTM$ has the highest affinity for copper, high thiol concentrations would reduce DNA cleavage by $Ru(DIP)_2DSTM$ the least. Mechanism B involves competition between thiols and H_2O_2 for binding sites on the Cu(I) complexes. Since Cu(I) bound to $Ru(DIP)_2DSTM$ is the least stable (most reactive), it might resist quenching by this mechanism as well.

higher than the H_2O_2 concentration at which a strong effect can be seen (20 mM compared to 200 μM). Further support for Mechanism B can be seen in Table 3.2, where there is a strong correspondence between the ratio of thiol to H_2O_2 and the DNA cleavage efficiency of Ru(DIP)$_2$DSTE. However, since the correspondence is not as strong in the case of Cu(phen)$_2^+$, Mechanism A may be operating as well.

In summary, the greater DNA cleavage efficiency of Ru(DIP)$_2$DSTM relative to Ru(DIP)$_2$DSTE appears to be caused by the greater affinity for copper of Ru(DIP)$_2$DSTM, and the greater inherent reactivity of copper bound to Ru(DIP)$_2$DSTM due to its less stable Cu(I) state. The greater DNA cleavage efficiency of Cu(phen)$_2^+$ appears to be due to the greater accessibility of the copper atom to the DNA backbone. The highly reactive Cu(I) state of copper bound to Ru(DIP)$_2$DSTM also appears to play a role in the ability of Ru(DIP)$_2$DSTM to promote DNA clevage even at high thiol concentrations.

Relative Roles of the Ru(DIP)$_3^{2+}$ Cores and the Tethered Chelates of Ru(DIP)$_2$DSTM and Ru(DIP)$_2$DSTE. The low resolution mapping study shows that the Ru(DIP)$_3^{2+}$ core of Ru(DIP)$_2$DSTM and Ru(DIP)$_2$DSTE confers a high selectivity for DNA sites with tertiary structure. In contrast, the complexes promote sequence neutral cleavage of short DNA oligonucleotides where tertiary structure is absent. The site-selectivity of the ruthenium complexes on the oligonucleotide is in marked contrast to Cu(phen)$_2^+$, which promotes sequence selective DNA cleavage due to local variations in the DNA minor groove structure (Figure 3.13).[7] It is likely that the flexibility inherent in the tethers between the DNA-binding Ru(DIP)$_3^{2+}$ cores and the DNA-cleaving chelates is responsible for the sequence neutral cleavage of Ru(DIP)$_2$DSTM and Ru(DIP)$_2$DSTE. The ruthenium complexes thus appear to act as

bifunctional DNA nucleases, with the $Ru(DIP)_3^{2+}$ binding to DNA in a site-selective manner, and the tethered chelates promoting sequence neutral DNA cleavage.

Mechanistic Studies. Investigations into the mechanism of DNA cleavage by $Ru(DIP)_2$DSTM and $Ru(DIP)_2$DSTE could assist in understanding the nature of the interactions of the ruthenium complexes and their functional groups with DNA. Mechanistic studies on $Ru(DIP)_2$DSTM have proved more successful than studies on $Ru(DIP)_2$DSTE due to the far greater DNA cleavage efficiency of the former complex. HPLC analysis resulted in the detection of free nucleic acid bases (Figure 3.12) as a major product of the DNA cleavage reaction of $Ru(DIP)_2$DSTM. This indicates that the reaction is occurring on the DNA sugar, rather than on the DNA bases.

Determining the hydrogen on the DNA sugar that is the subject of the oxidative attack would indicate the DNA groove in which the attacking species is present. Oxidative attack on the C3' hydrogen indicates major groove DNA cleavage, while oxidative attack on the C1' or C4' hydrogens indicates minor groove DNA cleavage. Oxidative attack the C5' or C5" hydrogens indicate either major or minor groove cleavage, while oxidative attack on the C2' or C2" hydrogens is less likely to occur, and less likely to lead to DNA strand scission if it did occur. The products resulting from abstraction of the various DNA sugar hydrogens are shown in Figure 3.16. Following C3' or C4' hydrogen abstraction, the chemical pathway leading to DNA strand scission (and therefore the resultant products) depends on whether or not dioxygen was involved. The free nucleic acid bases detected by HPLC from the $Ru(DIP)_2$DSTM cleavage reaction could be produced by C1', C3' oxygen-independent, or C4' oxygen-independent hydrogen abstraction cleavage mechanisms. 5' phosphate termini are produced by all mechanisms except C5' hydrogen abstraction. 3'-phosphate termini are produced by C1', C3' oxygen-independent, and C5' hydrogen abstraction cleavage

Figure 3.16. Products Produced by Hydrogen Abstraction at the DNA Sugar

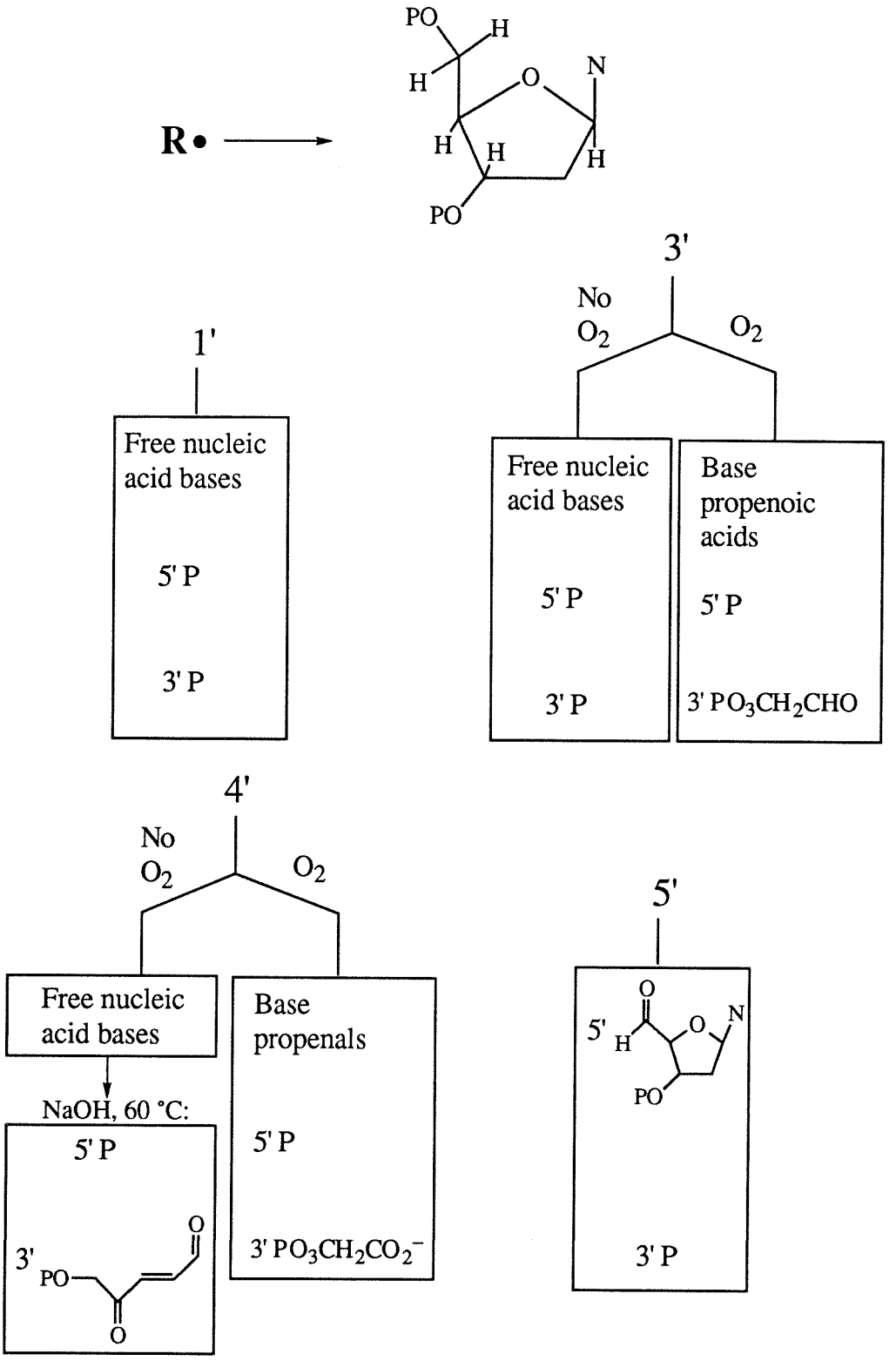

mechanisms. 3'-phosphoglycaldehyde termini are produced by the C3' oxygen-dependent mechanism, and 3'-phosphoglycolate termini are produced by the C4' oxygen-dependent mechanism.[6] The C1', C4' oxygen-dependent, and C3' oxygen-independent and -dependent hydrogen abstraction mechanisms are shown in Figure 3.17. $Cu(phen)_2^+$ binds in the DNA minor groove, and promotes DNA cleavage primarily by C1' hydrogen abstraction, and secondarily by C4' hydrogen abstraction.[7,11,12] $Rh(phi)_2bpy$ binds in the DNA major groove and promotes DNA cleavage primarily by C3' hydrogen abstraction.[13] Neocarzinostatin promotes DNA cleavage by C4' and C5' hydrogen abstraction,[23] and iron-bleomycin promotes DNA cleavage primarily by C4' hydrogen abstraction.[24]

The DNA cleavage mechanism of the ruthenium complexes involves attack on the DNA sugar, with some abstraction of both the minor groove C1' and C4' hydrogens, and the major groove C3' hydrogen. Multiple mechanisms for the DNA cleavage by $Ru(DIP)_2DSTM$ would not be surprising, considering the large size of the complex, and the flexibility inherent in the tethered chelates that might allow the complex to bind in one DNA groove and promote cleavage from the other groove. The relative amounts of each cleavage mechanism have not yet been determined. Footprinting with reagents that promote DNA cleavage from the major and minor groove, more HPLC product analysis, and cleavage of DNA with ^3H-labeled sugar rings should be done in order to better understand the mechanism of the copper-activated cleavage reaction of $Ru(DIP)_2DSTM$. The mechanism of the DNA cleavage reaction of $Ru(DIP)_2DSTM$ on pBR322 should be investigated by high-resolution PAGE, so as to understand the mode of binding of $Ru(DIP)_2DSTM$ to the DNA sites with tertiary structure for which it has a high affinity.

Figure 3.17. Mechanism of DNA Cleavage by C1', C4' Oxygen-Dependent, and C3' Hydrogen Abstraction

C1' H Abstraction

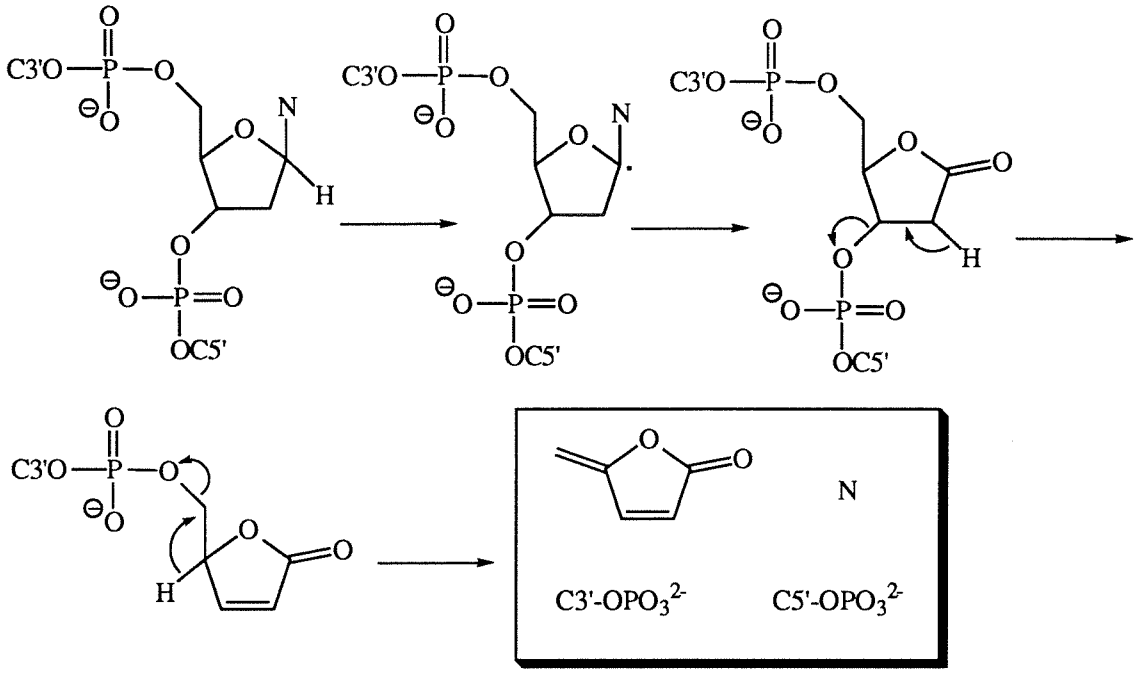

C4' H Abstraction, Oxygen-Dependent

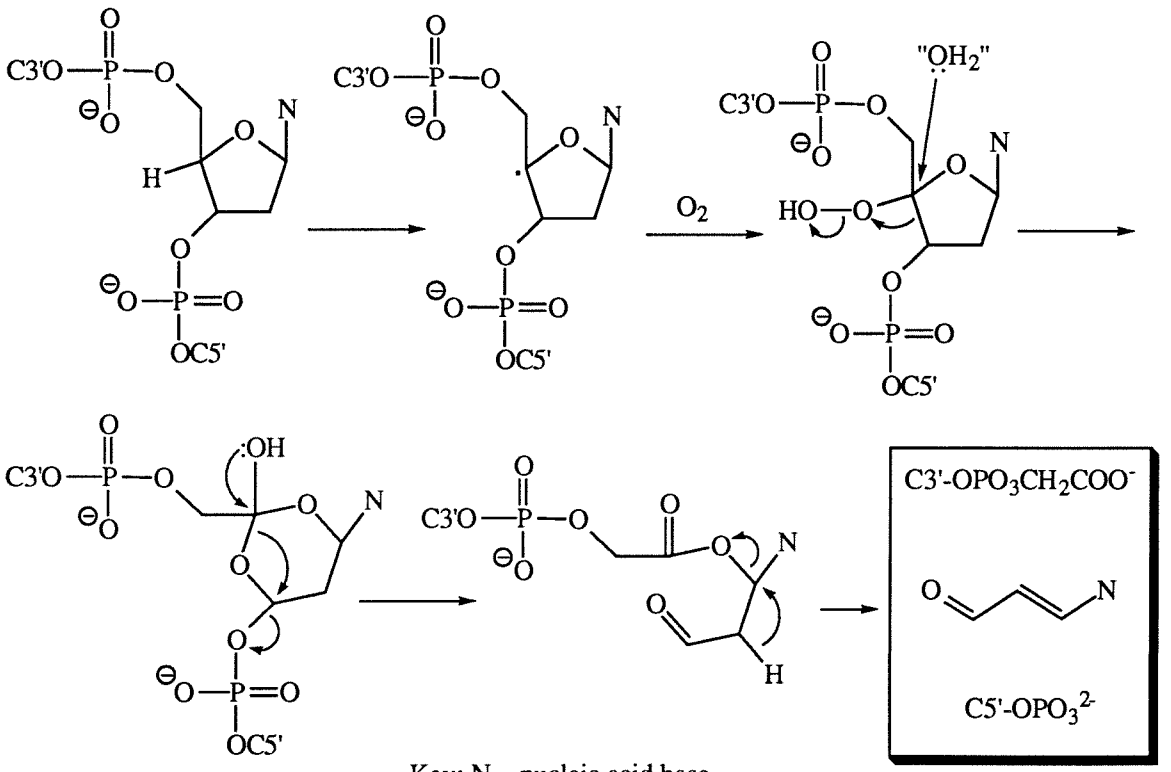

Key: N = nucleic acid base

Adapted from Stubbe & Kozarich (1987) *Chem. Rev.* **87:** 1107

Figure 3.17. (cont.) Mechanism of DNA Cleavage by C1', C4' Oxygen-Dependent, and C3' Hydrogen Abstraction

C3' H Abstraction, Oxygen-Independent

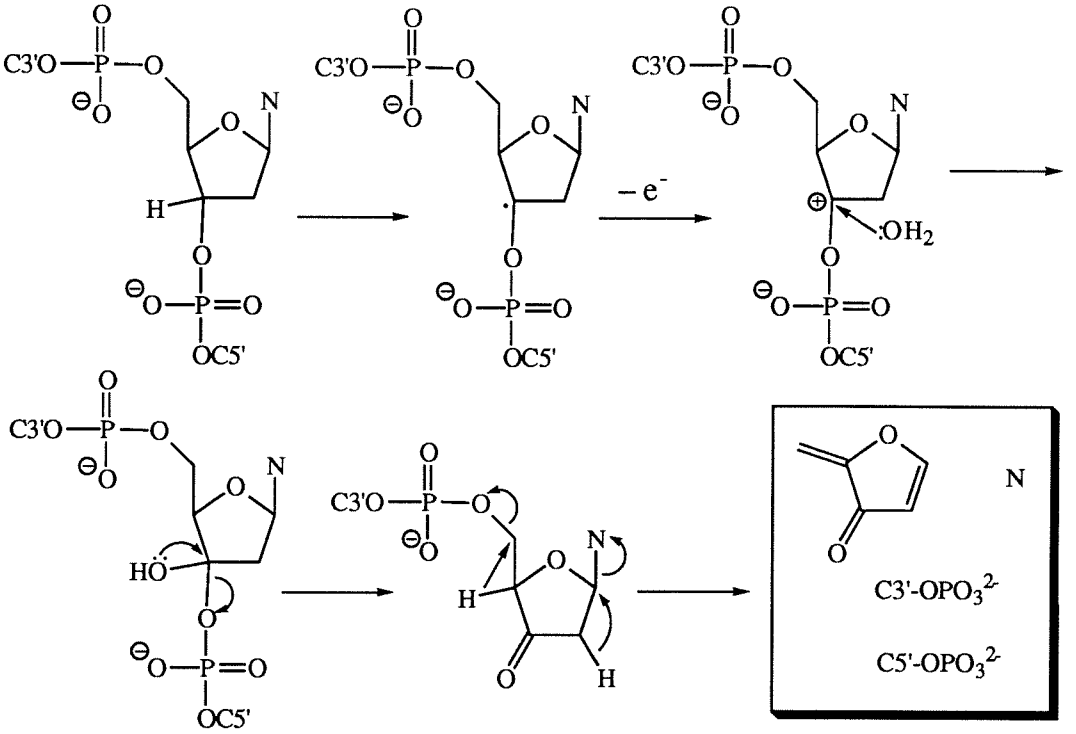

C3' H Abstraction, Oxygen-Dependent

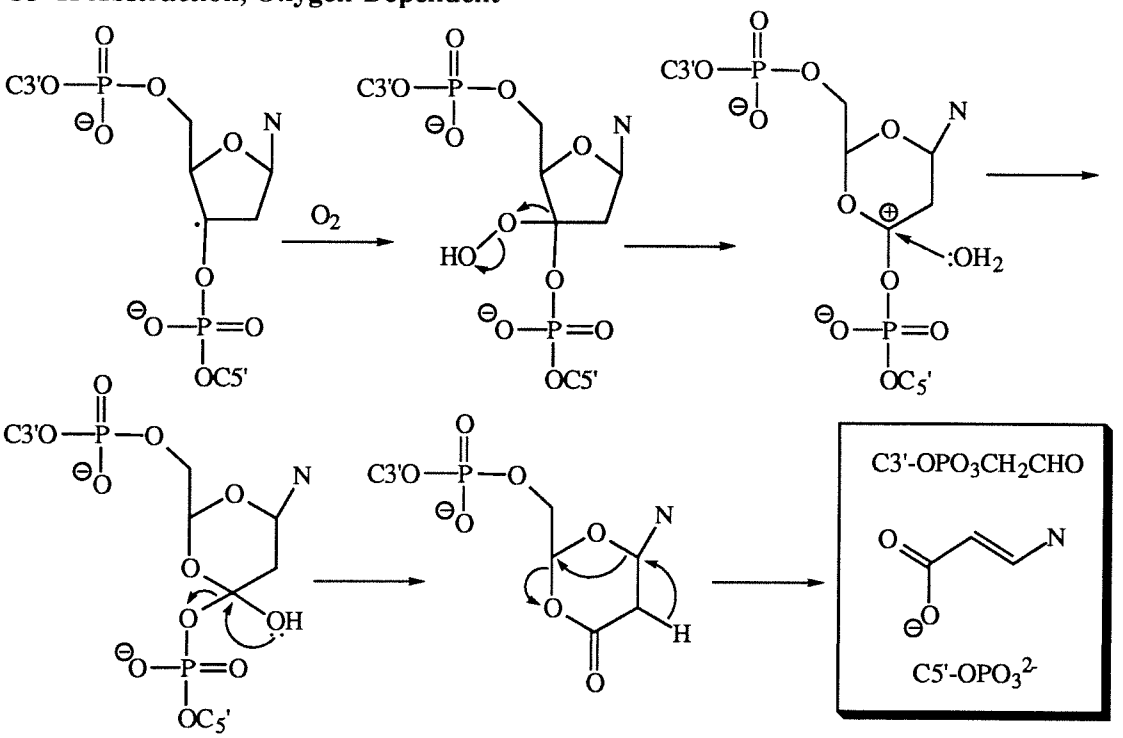

Key: N = nucleic acid base

Adapted from Stubbe & Kozarich (1987) *Chem. Rev.* **87:** 1107

Comparison to Other Studies. Iron-mediated DNA cleavage with the metal-binding site of $Ru(DIP)_2DSTM$ has been reported by Groves et al.[19] Groves tethered the bis(2-picolyl)amine chelating group with an ethylene linker to an oligonucleotide and detected sequence-selective DNA cleavage in the presence of iron and a reducing agent. Groves did not detect DNA cleavage when copper was substituted for iron. However, the conditions used for DNA cleavage by $Ru(DIP)_2DSTM$ were substantially different from those used by Groves. Groves used a DNA cleavage reaction buffer of 50 mM NaCl and 50 mM trizma·HCl, and incubated at 25 °C for 1.5 hours, while the $Ru(DIP)_2DSTM$ reaction buffer was 2.6 mM Na_2SO_4 and 13 mM trizma·H_2SO_4, with incubation at 37 °C for 2 to 5 minutes. Differences in the DNA-binding molecule to which the bis(2-picolyl)amine moiety was tethered [an oligonucleotide or $Ru(DIP)_3^{2+}$] may also have had an effect on DNA cleavage efficiency. Under conditions involving high copper concentrations, $CuSO_4$ promotes DNA cleavage in the absence of $Ru(DIP)_2DSTM$ (data not shown). It is possible that the conditions that Groves used did not fall within the "window" in which copper plus the bis(2-picolyl)amine moiety promotes DNA cleavage, but copper alone does not.

3.5. Conclusions.

The complexes $Ru(DIP)_2DSTM$ and $Ru(DIP)_2DSTE$ promote DNA cleavage in the presence of copper and a reducing agent. The site-selectivity of the DNA cleavage is determined by the $Ru(DIP)_3^{2+}$ cores, with the tethered chelates promoting sequence neutral cleavage. Products of the DNA clevage reaction have been detected that are consistent with a cleavage mechanism involving abstraction of DNA sugar hydrogens from both the minor and major grooves. The coordination environment around the copper affects both the stability of the copper complex and modulates the redox potential, thus affecting the cleavage efficiency under various conditions. Although the

ruthenium complexes promoted less efficient copper-activated DNA cleavage than phenanthroline under many conditions, this may very well be due to interference from the bulky, unfunctionalized, DIP ligands, rather than to an inherent lack of reactivity of the DSTM and DSTE functional groups. $Ru(DIP)_2DSTM$ appears to promote more efficient DNA cleavage than $Ru(DIP)_2DSTE$ due to a combination of the higher affinity of $Ru(DIP)_2DSTM$ for copper, and the greater inherent reactivity of copper bound to $Ru(DIP)_2DSTM$ due to its less stable (more reactive) Cu(I) state. $Ru(DIP)_2DSTM$ is of particular interest due to its high affinity for copper and its ability to promote DNA cleavage at high thiol concentrations. Keeping in mind that the concentration of glutathione in animal cells is around 5 mM,[9] it would be worthwhile to see whether phenanthroline or the bis(2-picolyl)amine functional group of $Ru(DIP)_2DSTM$ would be better at promoting DNA cleavage *in vivo*.

References

1. J. K. Barton & A. M. Pyle (1990) *Prog. Inorg. Chem.* **38:** 413.
2. H. E. Moser & P. B. Dervan (1987) *Science* **238:** 645.
3. (1989) "Metal-DNA Chemistry; ACS Symposium Series 402" T. D. Tullius, Ed., American Chemical Society, Washington, DC.
4. L. S. Kappen, I. H. Goldberg, S. H. Wu, J. Stubbe, L. Worth Jr., & J. W. Kozarich (1990) *J. Am. Chem. Soc.* **112:** 2797.
5. P. B. Dervan (1986) *Science* **232:** 464-470.
6. J. Stubbe & J. W. Kozarich (1987) *Chem. Rev.* **87:** 1107-1136.
7. D. S. Sigman (1986) *Acc. Chem. Res.* **19:** 180-186.
8. (a) S. Goldstein & G. Czapski (1985) *Inorg. Chem.* **24:** 1087. (b) K. Yamamoto & S. Kawanishi (1989) *J. Biol. Chem.* **264:** 15435.
9. L. Stryer (1988) "Biochemistry, 3rd ed." W. H. Freeman and Company, New York, 592.
10. J. M. Veal, K Merchant, & R. L. Rill (1991) *Nucl. Acids. Res.* **19:** 3383-3388.
11. T. E. Goyne & D. S. Sigman (1987) *J. Am. Chem. Soc.* **109:** 2846-2848.
12. T. B. Thederahn, M. D. Kuwabara, T. A. Larsen, & D. S. Sigman (1989) *J. Am. Chem. Soc.* **111:** 4941-4946.
13. A. Sitlani, E. C. Long, A. M. Pyle, & J. K. Barton (1992) *J. Am. Chem. Soc.* **114:** 2303-2312.
14. B. R. James & R. J. P. Williams (1961) *J. Chem. Soc.* 2007-2019.
15. P. Vanysek (1986) "CRC Handbook of Chemistry and Physics, 67th Edition" R. C. Weast, M. J. Astle, & W. H. Beyer, eds., CRC Press, Inc., Boca Raton, Florida, D-152.
16. G. A. Mabbott (1983) *J. Chem. Ed.* **60:** 697-702.
17. D. D. Perrin & C. J. Hawkins (1963) *Proc. Australian Conf. Electrochem., 1st,*

Sydney, Hobart, Australia 115-123 (published 1965).

18. (a) A. E. Martell (1975) "Critical Stability Constants, vol. 2" Plenum Press, New York, 209, 213, 246, 251. (b) Ibid., (1982) vol. 5, 242.

19. J. T. Groves & I. O. Kady (1993) *Inorg. Chem.* **32:** 3868-3872.

20. J. K. Barton & A. L. Raphael (1985) *Proc. Natl. Acad. Sci. USA* **82:** 6460-6464

21. M. R. Kirshenbaum, R. Tribolet, & J. K. Barton (1988) *Nucl. Acids Res.* **16:** 7943-7960.

22. R. P. Hertzberg & P. B. Dervan (1984) *Biochemistry* **23:** 3934-3945.

23. B. L. Frank, L. Worth Jr., D. F. Christner, J. W. Kozarich, J. Stubbe, L. S. Kappen, & I. H. Goldberg (1991) *J. Am. Chem. Soc.* **113:** 2271-2275.

24. N. Hamamichi, A. Natrajan, & S. M. Hecht (1992) *J. Am. Chem. Soc.* **114:** 6278-6291.

Chapter 4: Investigations of Metal Complexes for Hydrolytic DNA Cleavage

4.1. Introduction

Restriction enzymes, which cleave DNA hydrolytically at specific sites, have played a critical role in the development of biotechnology. There has been increasing interest in synthetic molecules that promote phosphodiester hydrolysis, both in order to understand the mechanism of natural restriction enzymes and to construct artificial restriction enzymes with different specifities from the natural ones. Such artificial restriction enzymes could potentially be used in cloning, gene mapping, or in DNA-cleaving drugs. For the purpose of designing new tools for gene cloning, hydrolytic cleavage is superior because the cleaved DNA can be religated enzymatically. For the purpose of drug design, hydrolytic cleavage also may be superior to oxidative cleavage because it would be less likely to cause random damage to nearby biomolecules *in vivo*.

The phosphodiester bonds of DNA are difficult to hydrolyze, because the negative charge inhibits nucleophilic attack on the phosphorus,[1] and because alkoxide is a poor leaving group. Enzymes utilize several mechanisms to catalyze phosphodiester hydrolysis. These include the neutralization of the negative charge on the phosphate, the coordination of nucleophiles to attack the phosphate (so as to gain the advantage of intramolecularity), and the stabilization of the alkoxide leaving group by providing a general acid.[2] An example of this is staphylococcal nuclease (Figure 4.1). An active site Ca^{2+} ion coordinates a hydroxide nucleophile to attack the phosphorus, while two active site arginine residues orient the substrate, and provide both charge neutralization and general acid assistance to the leaving group.[3]

For phosphate electrophiles, there is a strong correlation between the strength of the nucleophile and the pK_a of its conjugate acid. This in contrast to carbon electrophiles,

where the polarizability of the nucleophile is also important.[4] Therefore, in the design of molecules that promote phosphate hydrolysis at physiological pH, the pK_a of the conjugate acid of the nucleophile should also be near 7. Depending on the metal and the coordination environment around it, the pK_a of a metal-coordinated hydroxide can frequently be near 7. Since natural nucleases often utilize metal-coordinated hydroxides as nucleophiles for phosphodiester hydrolysis, a great deal of attention has focused on the development of metal complexes as synthetic nucleases.

The researchers Trogler and Chin have studied the hydrolysis of model phosphodiesters with metal complexes. Trogler found that $Cu(bpy)(H_2O)_2^{2+}$ and $Ni(tren)(H_2O)_2^{2+}$ promote the hydrolysis of bis(4-nitrophenyl)-phosphate with rate enhancements of 2000 and 1200, respectively.[1,5] Studies of the production of 4-nitrophenolate as a function of pH showed a sigmoidal curve with an inflection point at pH 7 for $Cu(bpy)(H_2O)_2^{2+}$. $Ni(tren)(H_2O)_2^{2+}$ showed increasing production of 4-nitrophenolate past pH 10. Since $Cu(bpy)(H_2O)_2^{2+}$ has a pK_a of 7 and $Ni(tren)(H_2O)_2^{2+}$ has a pK_a of 12.1, this is evidence that the active catalysts are the metal hydroxides $Cu(bpy)(H_2O)(OH)^{+}$ and $Ni(tren)(H_2O)(OH)^{+}$. The proposed mechanism was that the water ligand of copper or nickel was replaced by a phosphate oxygen, followed by intramolecular attack on the phosphorus by the metal hydroxide, and finally by dissociation of the phosphate from the metal (Figure 4.2). The metal serves both to neutralize the negative charge on the phosphate, and to deliver the coordinated nucleophile. Consistent with this mechanism, it was found that $Zn(tren)^{2+}$, $Cu(tren)^{2+}$, and $Cu(bpy)_2^{2+}$ were poor at catalyzing phosphodiester cleavage. Zn(II) is tetrahedral, and Cu(II) is square planar, so none of the above three complexes have the necessary two open coordination sites.[1,5] Also consistent with this mechanism, Chin found that $Co(cyclen)^{3+}$, which has two open coordination sites, promoted phosphodiester

Figure 4.1. The Mechanism of Staphylococcal Nuclease
(From Kneeland et al.)[3]

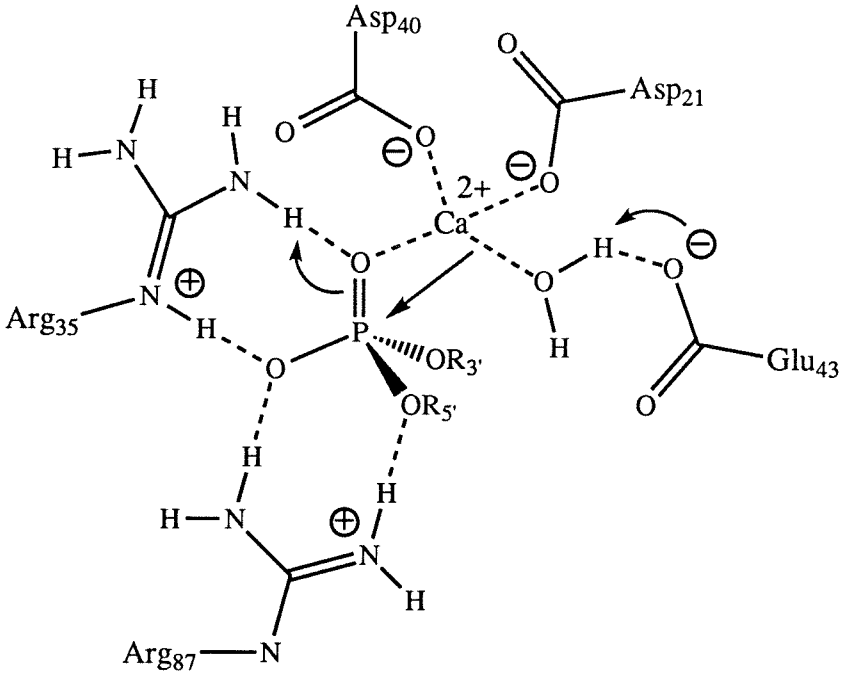

Figure 4.2. Proposed mechanism for the hydrolysis of model phosphodiesters by transition metal complexes with two open coordination sites. The metal provides both charge neutralization and an intramolecular nucleophilic attack.

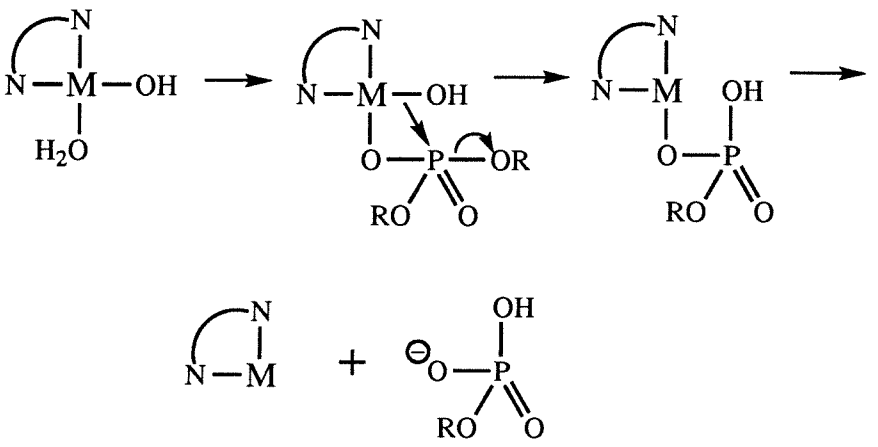

hydrolysis, while $Co(tetren)^{3+}$, which only has one open coordination site, did not [cyclen = $(NHCH_2CH_2)_4$, tetren = $(H_2NCH_2CH_2NHCH_2CH_2)_2NH$].[6]

Most model studies of phosphodiester hydrolysis have used substrates with 4-nitrophenolate leaving groups. 4-nitrophenolate leaving groups are a popular choice because they can be detected spectrophotometrically and because the activated leaving group greatly facilitates phosphodiester hydrolysis (the pk_a of 4-nitrophenol is 7.15).[7] However, studies using 4-nitrophenolate leaving groups do not reflect the true difficulty of hydrolyzing the phosphodiester bonds of DNA. With 4-nitrophenolate leaving groups, the rate limiting step is the attack of the nucleophile on the phosphorus. With the much poorer alkoxide leaving groups that are found on DNA, the trigonal bipyramidal transition state will usually collapse to form starting material rather than product.[8,9] Kim and Chin found that $Co(cyclen)^{3+}$ did promote the hydrolysis of dimethylphosphate (which has poor leaving groups comparable to those of DNA) at neutral pH, but the reaction required several weeks at 60 °C.[6]

None of these transition metal catalysts have achieved the estimated 10^{12} rate enhancement that is required to quickly hydrolyze DNA, with its poorer alkoxide leaving groups.[10] Also, the use of redox active metals such as copper and cobalt may result in oxidative rather than hydrolytic DNA cleavage. Others have studied the metal-activated phosphodiester hydrolysis of RNA, where the reaction is greatly facilitated by the intramolecular attack of the ribose 2' OH on the phosphorus.[11] Morrow et al. have demonstrated efficient RNA cleavage with macrocyclic lanthanide(III) complexes.[12]

Although it is true that natural nucleases almost always require metal ions for their activity, there have been some recent successes in the development of catalysts of phosphodiester hydrolysis that do not require metals. Anslyn showed that a bis-alkylguanidinium compound catalyzed RNA cleavage in imidazole buffer. In the proposed mechanism, free imidazole acts as a general base to assist the intramolecular

attack of the 2'-OH of RNA, while the alkylguanidinium groups orient the substrate and provide both charge neutralization to the phosphate and general acid assistance to the leaving group (Figure 4.3). The catalyst was designed as a mimic of staphylococcal nuclease.[13]

Figure 4.3. Proposed Mechanism of RNA Cleavage by a Bis-Alkylguanidinium Receptor (from Smith et al.)[12]

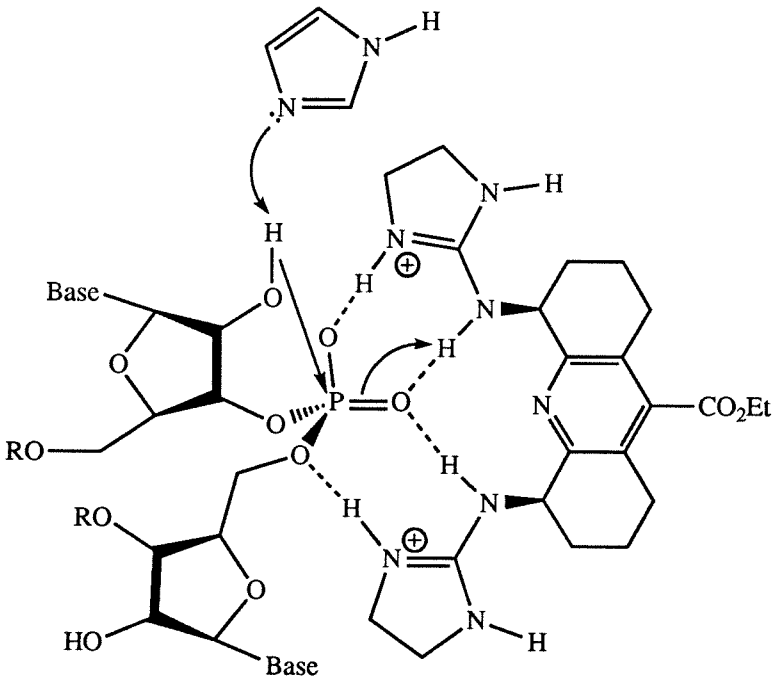

RNA is certainly an easier substrate to hydrolyze, but for the purpose of drug design, DNA cleavage may be more important because of the high turnover rate of mRNA *in vivo*. Also, DNA hydrolysis is clearly more important for genome mapping and for the design of artificial restriction enzymes with applications to biotechnology.

Transition metal complexes have been designed to bind to DNA and deliver additional labile metal ions to the DNA phosphate backbone, in order to promote DNA hydrolysis under mild (physiological) conditions. $Ru(DIP)_2macro^{n+}$, the first example of such a complex, was constructed by tethering two tris(2-aminoethyl)amine metal

chelates to a $Ru(DIP)_3^{2+}$ core.[14] Since it has proven difficult to remove $Ru(DIP)_2macro^{n+}$ from DNA in order to analyze the DNA cleavage products, the five complexes $Ru(DIP)_2$DSTM, $Ru(phen)_2$DSTM, $Ru(phen)_2$(DSTM-AE), $Ru(phen)_2$(DSTM-AP), and $Rh(phi)_2$(DSTM-AP) (Figure 4.4) have been constructed. All five complexes contain two tethered bis(2-picolyl)amine groups which have been designed for the purpose of promoting DNA phosphodiester hydrolysis in the presence of added labile metal ions. The complexes $Ru(phen)_2$(DSTM-AE), $Ru(phen)_2$(DSTM-AP), and $Rh(phi)_2$(DSTM-AP) have additional dimethylaminoalkyl groups which would be protonated at neutral pH, and have been designed for the purpose of providing general acid assistance to the leaving group in DNA hydrolysis. All five complexes have two unfunctionalized 4,7-diphenyl-1,10-phenanthroline (DIP), 1,10-phenanthroline (phen), or 9,10-phenanthrenequinonediimine (phi) ligands which have been designed to provide a binding interaction between the complexes and DNA. The potential of the five complexes to promote DNA cleavage has been investigated by agarose gel electrophoresis. The nature of the DNA cleavage mechanism has been investigated by product analysis using high-resolution polyacrylamide gel electrophoresis. The effect of the structure of the metal complexes on their respective DNA cleavage reactions is discussed.

Figure 4.4. Ruthenium and Rhodium Complexes with Tethered Metal Chelating Groups

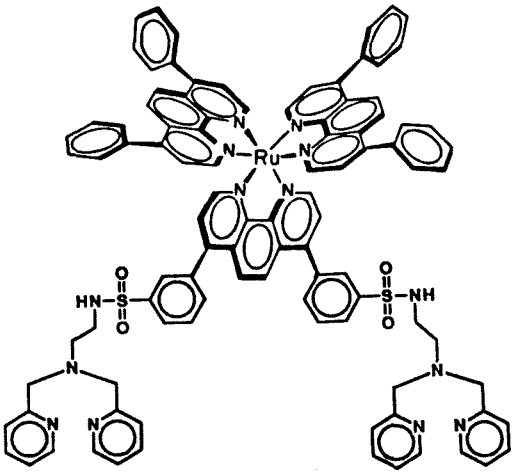

$Ru(DIP)_2DSTM$

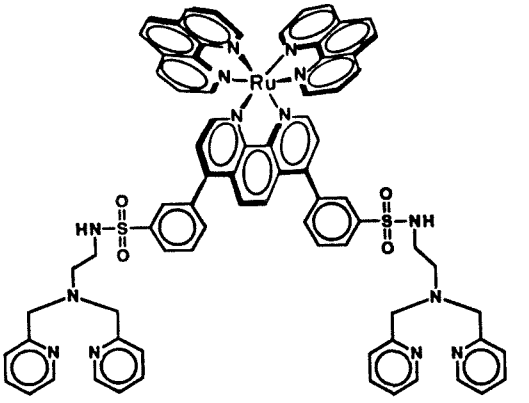

$Ru(phen)_2DSTM$

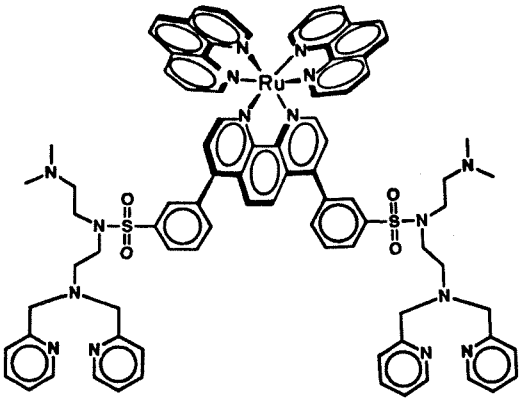

$Ru(phen)_2(DSTM\text{-}AE)$

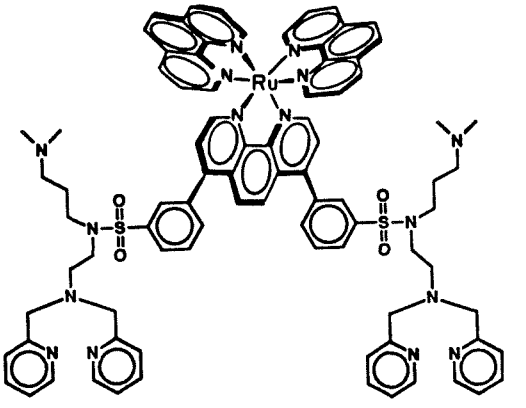

$Ru(phen)_2(DSTM\text{-}AP)$

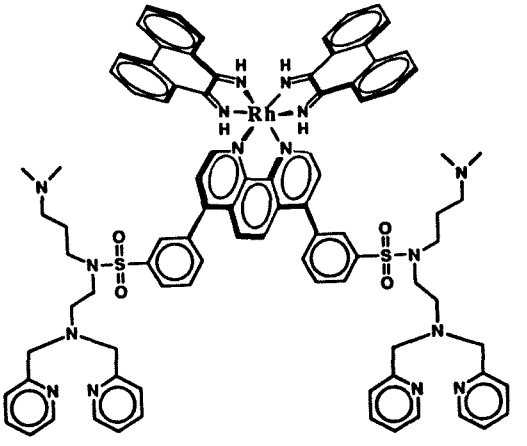

$Rh(phi)_2(DSTM\text{-}AP)$

4.2. Experimental

Quantitative Comparisons of DNA Cleavage Efficiency by Agarose Gel Electrophoresis. The DNA plasmid pBR322 was used as the substrate. Prior to the DNA cleavage reactions, the plasmid pBR322 contained approximately 80% supercoiled plasmid (form I) and 20 % nicked or open circular plasmid (form II). The cleavage reactions transform supercoiled plasmid to nicked plasmid. Two nicks on the same plasmid no more than several nucleotide base pairs apart transform the plasmid to linear (form III). The three plasmid forms were separated by agarose gel electrophoresis, with supercoiled having the highest mobility, followed by linear and then by nicked. This is illustrated in Figure 3.6.

The pBR322 was purchased from either Bethesda Research Laboratories (Figure 4.5 and Figure 4.6 experiments) or Boehringer Mannheim (Figure 4.9 experiment). Due to its higher (1 mM) initial EDTA concentration, the pBR322 purchased from Boehringer Mannheim was purified by Centricon™ and was stored in 5 mM Na_2SO_4 and 25 mM trizma·H_2SO_4. Solid $Ru(DIP)_2DSTM$, $Ru(phen)_2DSTM$, $Ru(phen)_2$(DSTM-AE), $Ru(phen)_2$(DSTM-AP), and $Rh(phi)_2$(DSTM-AP) were stored at -60 °C or below, in the dark, and under argon or vacuum. Stock solutions of $Ru(DIP)_2DSTM$ were made by dissolving a small amount of solid complex in approximately 50 µl methanol, and transferring the solution to 5-40 ml water. The methanol was then removed using a high vacuum pump without heating. Stock solutions of the other four complexes were made by dissolving the solid complexes directly in water. The concentration of the solutions were determined by visible spectroscopy, using extinction coefficients at the visible maximum of 29,500 $M^{-1}cm^{-1}$ for $Ru(DIP)_2DSTM$, and 23,000 $M^{-1}cm^{-1}$ for $Ru(phen)_2DSTM$, $Ru(phen)_2$(DSTM-AE), and $Ru(phen)_2$(DSTM-AP). The concentration of $Rh(phi)_2$(DSTM-AP) solutions

were determined using the extinction coefficient of 23,600 at the isosbestic point 350 nm of its analogue $Rh(phi)_2bpy$.[15] Solutions were stored in the dark at room temperature, and were discarded after one month. The buffer stock solution contained 100 mM Na_2SO_4 and 500 mM trizma, adjusted to pH 7.8 with H_2SO_4. The solution was autoclaved and stored at +4 °C. The zinc stock solution was 20 mM, and was made from 99.999% $ZnSO_4 \cdot 7H_2O$ (Aldrich Chemicals). The ultrapure Milli-Q (from Millipore) deionized distilled water was used for all stock solutions, and for all DNA cleavage reactions. The nonionic detergent TRITON X-100 was purchased from CALBIOCHEM and was used in the Figure 4.5 and 4.6 experiments to reduce DNA precipitation.

The DNA cleavage conditions varied from experiment to experiment; the exact conditions are shown in the figure caption for each experiment. Typical cleavage reaction conditions were 12.5 mM trizma·H_2SO_4, 2.5 mM Na_2SO_4, 0 or 1% TRITON X-100, 20 or 30 μM DNA base pairs pBR322, 0 to 2 mM $ZnSO_4$, and 0 to 8 μM ruthenium or rhodium complex, with overnight incubation at 37 °C. Control reactions were identical to samples, but contained no ruthenium or rhodium complex. The total reaction volumes were 30 μl. The cleavage reactions not vortexed until after the completion of the overnight incubations so as to minimize the DNA precipitation from solution caused by the positively charged, hydrophobic complexes. Exposure of the reaction mixtures to room light was reduced but not eliminated by covering the reactions with aluminum foil during the incubations. After the overnight incubations were complete, the Figure 4.5 and Figure 4.6 reactions were quenched by the addition of 3 μl 10% SDS, and vortexed; 7 μl of a solution containing 50% sucrose, 0.5% bromophenol blue, and 100 mM EDTA were then added, and the reactions were vortexed again. The Figure 4.9 reactions were quenched by the addition of 10 μl of a solution containing 29% sucrose, 0.29% bromophenol blue, 58 mM EDTA, and 2.5% SDS, and then vortexed. A 1% agarose gel was prepared in 100 mM trizma-borate and 2 mM EDTA. 30 to 33 μl of the

quenched reactions were loaded onto the gel. The gel was run at 75 V for 140 to 180 minutes. The gel was stained in ethidium bromide for 5 to 15 minutes, destained overnight at +4 °C, and illuminated from below with 302 nm UV light from a Spectroline™ Transilluminator Model TR-302. The gel was then photographed with a Polaroid 600 camera equipped with a red filter and Polaroid 655 Positive/Negative Instant Pack Film.

The data on the negative of the gel photograph were quantitated with an LKB Ultroscan XL Enhanced Laser Densitometer. For each cleavage reaction sample, the percentage of supercoiled, nicked, and linearized plasmid was determined. Small amounts of DNA cleavage of the controls were detected. The "total cleavage" is defined as the percentage nicked in each reaction sample plus twice the percentage linearized plasmid. The total cleavage in the control sample which contained the least total cleavage was subtracted from the total cleavage of all samples to give the "% Cleavage" in Figures 4.5, 4.6, and 4.9. For example in Figure 4.5, 44.9% total cleavage was detected in the $ZnSO_4$ control and 52.3% in the $CoSO_4$ control, so 44.9% was subtracted from all samples, to give a "% Cleavage" of 7.4% for the $CoSO_4$ control and 0% for the $ZnSO_4$ control. This calculation procedure slightly differs from that used in chapter 3; the procedure was changed to take into account the larger amounts of linearized plasmid in the controls of this chapter.

Cleavage and Product Analysis of the Radiolabeled DNA Oligonucleotide 5'-CTGGCATACCGGTATGCCAG-3'. The above oligonucleotide was synthesized on a Pharmacia Gene Assembler using phosphoramidite chemistry and purified by reverse-phase HPLC. 2 picomoles of the oligonucleotide were then ^{32}P 5'-radiolabeled using T4 polynucleotide kinase, or 3'-radiolabeled using terminal deoxynucleotidyl transferase. The oligonucleotide was then purified by Nensorb™ (Du Pont). The labeled

oligonucleotide used for Figures 4.7 and 4.8 was further purified using a preparative 20% polyacrylamide gel, isolated by electroelution, and desalted by Nensorb™. 100% labeling efficiency was assumed for the purposes of oligonucleotide quantitation.

The reaction conditions for the cleavage of the 5'-radiolabeled oligonucleotide by ruthenium complexes (Figure 4.7) were as follows: Samples A, B, and E-H had 10 μM base pairs ^{32}P 5'-radiolabeled oligonucleotide and 100 μM $ZnSO_4$, in a total volume of 20 μl. Samples A and B had 3.1 mM of the sodium salts of MES, HEPES, CHES and CAPS, partially neutralized with 2.5 mM H_2SO_4 to pH 8.4. Samples E-H had 12.5 mM trizma·H_2SO_4 (pH 7.8), and 2.5 mM Na_2SO_4 . Samples A and E had 13 μM $Ru(phen)_2$(DSTM-AP), sample F had 13 μM $Ru(phen)_2$(DSTM-AE), and sample G had 13 μM $Ru(phen)_2$DSTM. Samples A, B, and E-H were incubated at 37 °C for 24 hours in the dark, and then dried *in vacuo*. Samples C and D were the A+G and C+T Maxam-Gilbert reactions, respectively. Samples I and J were the A+G and C+T reactions treated with T4 polynucleotide kinase in the absence of ATP in order to produce 3'-hydroxyl termini.[16] These dephosphorylation reactions were done in 10 mM $MgSO_4$, 12.5 mM MES, 5 mM NaOH, and 5 mM dithiothreitol, in 20 μl total volume. Samples I and J were incubated for 1 hour with 8 units T4 polynucleotide kinase at 37 °C, and then dried *in vacuo*.

The reaction conditions for the cleavage of the 3'-radiolabeled oligonucleotide (Figure 4.8) were as follows: Samples A-L had 12.5 mM trizma·H_2SO_4 (pH 7.8), 2.5 mM Na_2SO_4, and 2.54 μM base pairs ^{32}P 3'-radiolabeled oligonucleotide in a total volume of 20 μl. Samples A, C, E, G, I, and K had 5 μM $Ru(phen)_2$(DSTM-AP). Samples A, B, I, and J had 100 μM $ZnSO_4$; samples E and F had 100 μM $EuCl_3$; samples G and H had 100 μM $NiSO_4$; and samples C, D, K, and L had 100 μM EDTA rather than divalent metal ion. All pipetting of samples A-D was done in the darkroom

under greatly reduced light. Samples E-L were exposed to room light for 20-25 minutes. All samples were incubated at 37 °C for 20 hours in the dark, and then dried *in vacuo*.

The reaction conditions for the cleavage of the 5'-radiolabeled oligonucleotide by rhodium complexes (Figure 4.10) were as follows: Samples C-S had 12.5 mM trizma·H_2SO_4 (pH 7.8), 2.5 mM Na_2SO_4, and 16 μM base pairs ^{32}P 5'-radiolabeled oligonucleotide in a total volume of 20 μl. Samples C and F had 3 μM $Rh(phi)_2bpy^{3+}$, and samples J and O had 5 μM $Rh(phi)_2bpy^{3+}$. Samples D and G had 3 μM $Rh(phi)_2$(DSTM-AP), samples K and P had 2 μM $Rh(phi)_2$(DSTM-AP), samples L and Q had 5 μM $Rh(phi)_2$(DSTM-AP), and samples M and R had 12 μM $Rh(phi)_2$(DSTM-AP). Sample H had 12 μM 1,10-phenanthroline. Samples F, G, and I had 9 μM $CuSO_4$, sample H had 3 μM $CuSO_4$, samples J-N had 200 μM $ZnSO_4$, and samples O-S had 200 μM $CoSO_4$. Samples C-E were irradiated with a 1000 W Hg/Xe lamp at 310 nm for 6 minutes, and then dried *in vacuo*. Samples F-I were reacted with 200 μM 2-mercaptoethanol and 200 μM H_2O_2 for 5 minutes at 37 °C; the reaction was then quenched by the addition of 2 μl EDTA, and the samples were dried *in vacuo*. Samples J-S were incubated at 37 °C for 22 hours in the dark, and then dried *in vacuo*. Samples A and B were the A+G and C+T Maxam-Gilbert reactions, respectively. Samples T and U were A+G and C+T reactions dephosphorylated to give hydroxyl ends in a manner similar to that described above for the Figure 4.7 experiment.

The dried samples were resuspended in either 80% formamide loading dye (Figures 4.7 and 4.8; 10 mM NaOH, 0.025% xylene cyanol, and 0.025% bromophenol blue in TBE) or 98% formamide loading dye (Figure 4.10; 10 mM EDTA, 1% xylene cyanol, and 1%. bromophenol blue). The samples were then heated at 90 °C for 3 minutes, chilled on wet ice for 3 minutes, and loaded onto 20% denaturing polyacrylamide sequencing gels which were run at approximately 1700 V for

approximately four hours. The gels were exposed to x-ray film with intensifying screens at approximately -70 °C, and then developed.

4.3. Results

Comparisons of the DNA Cleavage Efficiency of $Ru(DIP)_2DSTM$, $Ru(phen)_2DSTM$, $Ru(phen)_2$(DSTM-AE), and $Ru(phen)_2$(DSTM-AP). The DNA cleavage efficiency of the four ruthenium complexes in the presence and absence of additional labile metal ions has been assayed by agarose gel electrophoresis. DNA cleavage is observed which varies with the concentration of the ruthenium complexes and of the added metal ions.

DNA cleavage of $Ru(DIP)_2DSTM$, $Ru(phen)_2DSTM$, $Ru(phen)_2$(DSTM-AE), and $Ru(phen)_2$(DSTM-AP) as a function of ruthenium complex concentration (Figure 4.5). The comparison of $Ru(phen)_2DSTM$ to $Ru(DIP)_2DSTM$ (graph A of Figure 4.5) shows that neither complex promotes substantial DNA cleavage in the presence of added Zn^{2+}. In the presence of added Co^{2+}, both complexes promote increasing DNA cleavage with increasing complex concentration, with $Ru(phen)_2DSTM$ promoting more efficient cleavage. The small amount of negative cleavage by $Ru(DIP)_2DSTM$ in the presence of Zn^{2+} (i.e., there is less cleavage in the absence of $Ru(DIP)_2DSTM$ than in its presence) is within the uncertainty of the experiment (± 7%) and should be interpreted as zero cleavage.

The complexes $Ru(DIP)_2DSTM$ and $Ru(phen)_2DSTM$ were each designed with a pair of unfunctionalized ligands that would be involved in a binding interaction with DNA, and a pair of tethered metal chelates that would promote DNA cleavage. The intent was that in the presence of additional labile metal ions, the metal chelates might promote DNA phosphodiester hydrolysis by either a charge neutralization and/or a

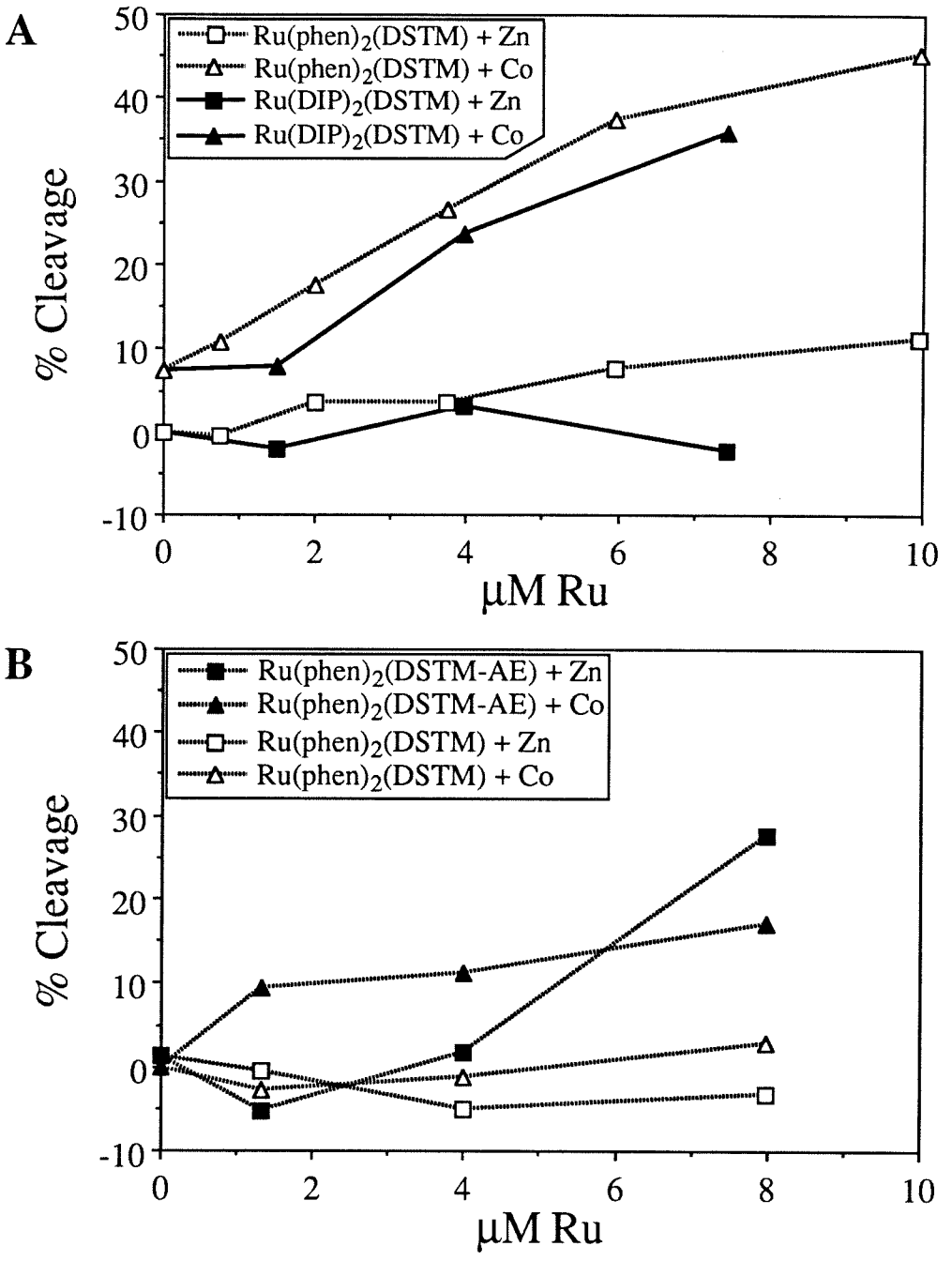

Figure 4.5. Comparison of DNA Cleavage of $Ru(DIP)_2DSTM$, $Ru(phen)_2DSTM$, $Ru(phen)_2(DSTM\text{-}AE)$, and $Ru(phen)_2(DSTM\text{-}AP)$ as a Function of Ruthenium Complex Concentration. Conditions for **A** and **B**: 12.5 mM trizma·H_2SO_4, 2.5 mM Na_2SO_4, 1% TRITON X-100, 30 μM base pairs pBR322, 300 μM $ZnSO_4$ or $CoSO_4$.
A: $Ru(phen)_2DSTM$ compared to $Ru(DIP)_2DSTM$, 22 hours at 37 °C.
B: $Ru(phen)_2(DSTM\text{-}AE)$ compared to $Ru(phen)_2DSTM$, 18 hours at 37 °C.

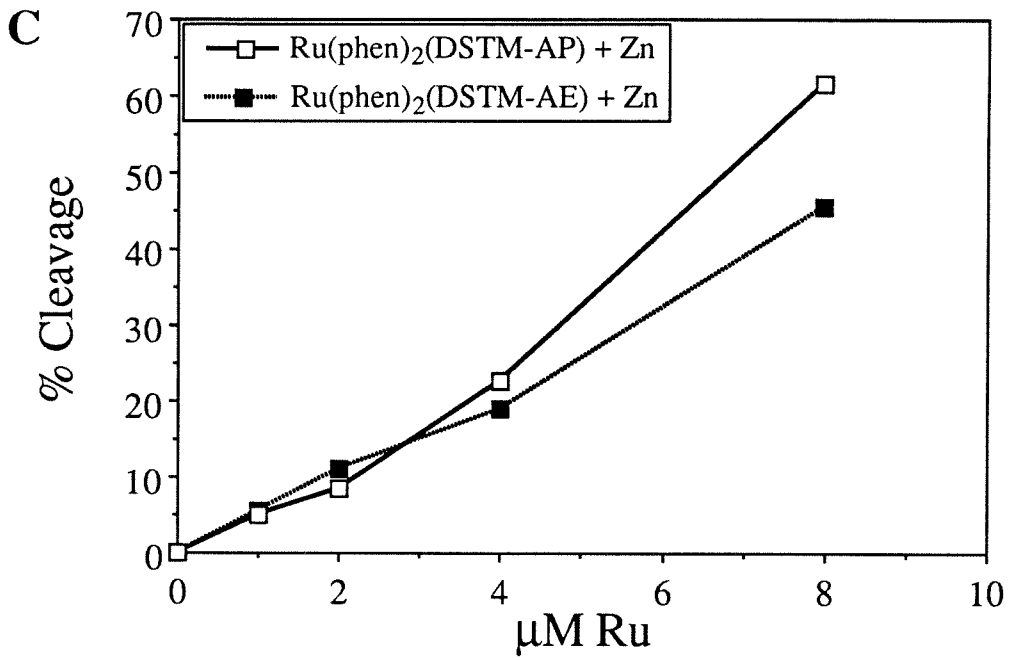

Figure 4.5. (cont.) Comparison of DNA Cleavage of $Ru(DIP)_2DSTM$, $Ru(phen)_2DSTM$, $Ru(phen)_2$(DSTM-AE), and $Ru(phen)_2$(DSTM-AP) as a Function of Ruthenium Complex Concentration. Conditions for **C**: 12.5 mM trizma·H_2SO_4, 2.5 mM Na_2SO_4, 1% TRITON X-100, 30 μM base pairs pBR322, 100 μM $ZnSO_4$, 15 hours at 37 °C. $Ru(phen)_2$(DSTM-AP) was compared to $Ru(phen)_2$(DSTM-AE).

coordinated hydroxide mechanism. The greater DNA cleavage efficiency of $Ru(phen)_2DSTM$ can be explained in these terms, since the less bulky phenanthroline ligands might provide less hindrance for the approach of the metal chelates to the DNA phosphodiester bonds. Solubility is also likely to play a role in the greater DNA cleavage efficiency of $Ru(phen)_2DSTM$, since the hydrophobic $Ru(DIP)_2DSTM$ has a tendency to precipitate from aqueous solutions, and to cause DNA to do so. The greater DNA cleavage of both complexes in the presence of Co^{2+} rather than Zn^{2+} could be explained in terms of differences in the pK_a's of water molecules coordinated to Co^{2+} and Zn^{2+}. It should be noted that for the purpose of promoting hydrolytic rather than oxidative DNA cleavage, the less redox active Zn^{2+} might be a better choice. Unlike Zn^{2+}, Co^{2+} has an accessible +3 oxidation state: $[Co(NH_3)_6]^{3+} + e^- \rightarrow [Co(NH_3)_6]^{2+}$ has a reduction potential of +0.108 volts.[17]

$Ru(phen)_2$(DSTM-AE) is similar in structure to $Ru(phen)_2DSTM$, except $Ru(phen)_2$(DSTM-AE) was designed to have an additional pair of 2-dimethylaminoethyl groups that would be protonated at neutral pH and could provide general acid assistance to the leaving group in phosphate hydrolysis. The comparison of $Ru(phen)_2$(DSTM-AE) to $Ru(phen)_2DSTM$ (graph B of Figure 4.5) shows more efficient DNA cleavage by $Ru(phen)_2$(DSTM-AE) both in the presence of Co^{2+} and in the presence of Zn^{2+}. The greater DNA cleavage promoted by $Ru(phen)_2$(DSTM-AE) is promising for the purpose of the design of metal complexes that promote DNA hydrolysis.

The comparison of $Ru(phen)_2$(DSTM-AP) to $Ru(phen)_2$(DSTM-AE) (graph C of figure 4.5) in the presence of Zn^{2+} again shows increasing DNA cleavage with increasing ruthenium complex concentration. $Ru(phen)_2$(DSTM-AP) promotes more efficient DNA cleavage than $Ru(phen)_2$(DSTM-AE) and is therefore the most efficient DNA nuclease of the four ruthenium complexes. The only structural difference between the two complexes is the increased length of the tether between the dimethylamino group

and the sulfonamide from two carbons in the case of $Ru(phen)_2$(DSTM-AE) to three carbons in the case of $Ru(phen)_2$(DSTM-AP). This increased tether length was designed to facilitate leaving group assistance in phosphodiester hydrolysis by the protonated dimethylamino group. The length of the tether will be important when the leaving group is opposite to the nucleophile, and where the nucleophile is a hydroxide coordinated to the chelated Zn^{2+} ion. The greater DNA cleavage efficiency promoted by $Ru(phen)_2$(DSTM-AP) is therefore also promising.

DNA cleavage of $Ru(phen)_2$DSTM, $Ru(phen)_2$(DSTM-AE), and $Ru(phen)_2$(DSTM-AP) as a function of $ZnSO_4$ concentration (Figure 4.6). The effect of Zn^{2+} concentration on the DNA cleavage efficiency of $Ru(phen)_2$DSTM greatly differs from its effect on $Ru(phen)_2$(DSTM-AE) (graph A of Figure 4.6). $Ru(phen)_2$(DSTM-AE) promotes only 10% DNA cleavage in the absence of Zn^{2+}. 20 μM $ZnSO_4$ greatly increases the DNA cleavage efficiency of $Ru(phen)_2$(DSTM-AE), but further increases of the Zn^{2+} concentration, even up to 2 mM, increase the DNA cleavage only slightly. The binding affinity of $Ru(phen)_2$(DSTM-AE) for Zn^{2+} therefore appears to be great enough so that both its metal binding sites are mostly occupied at 6.6 μM $Ru(phen)_2$(DSTM-AE) and 20 μM $ZnSO_4$. The small amount of DNA cleavage by $Ru(phen)_2$(DSTM-AE) in the absence of $ZnSO_4$ could be due to trace divalent metal ions in solution.

In contrast, $Ru(phen)_2$DSTM promotes substantial DNA plasmid cleavage in the absence of Zn^{2+}, and little or no DNA cleavage over the control in the presence of Zn^{2+}. $Ru(phen)_2$DSTM does promote efficient DNA cleavage in the presence of Zn^{2+} when the substrate is an oligonucleotide rather than a supercoiled plasmid (Figure 4.7). The chemistry that is responsible for this effect is not understood.

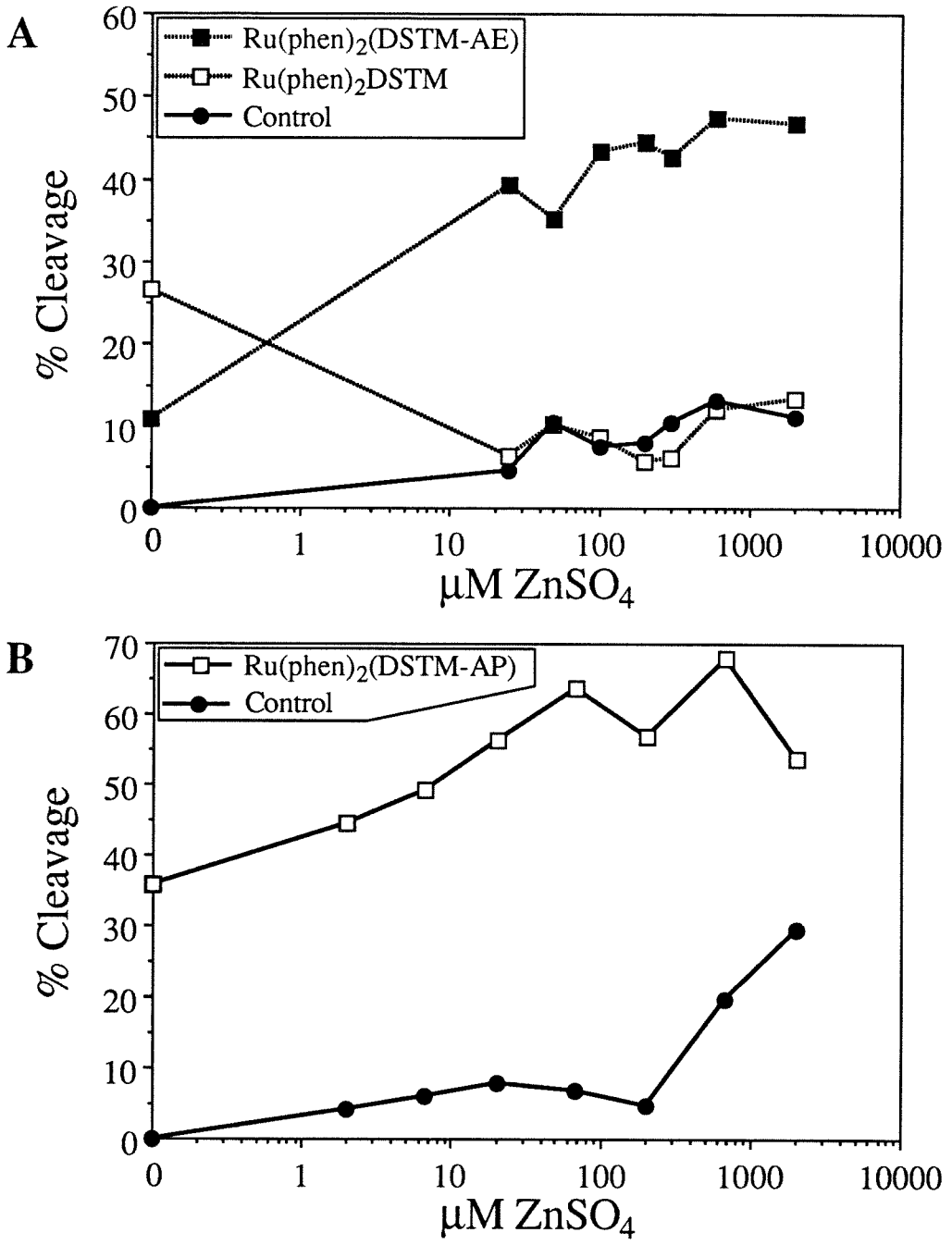

Figure 4.6. Comparison of the DNA Cleavage of $Ru(phen)_2DSTM$, $Ru(phen)_2(DSTM\text{-}AE)$, and $Ru(phen)_2(DSTM\text{-}AP)$ as a Function of $ZnSO_4$ Concentration. Conditions for **A** and **B**: 12.5 mM trizma·H_2SO_4, 2.5 mM Na_2SO_4, 1% TRITON X-100, 30 μM base pairs pBR322, 16 hours at 37 °C.

A: 6.6 μM $Ru(phen)_2(DSTM\text{-}AE)$, 6.6 μM $Ru(phen)_2DSTM$, and the no Ru control compared.

B: 7.5 μM $Ru(phen)_2(DSTM\text{-}AP)$ compared to the no Ru control.

The effect of Zn^{2+} concentration on the DNA cleavage efficiency of $Ru(phen)_2$(DSTM-AP) is similar to its effect on $Ru(phen)_2$(DSTM-AE) (graph B of Figure 4.6). DNA cleavage by $Ru(phen)_2$(DSTM-AP) over the control increases with increasing Zn^{2+} concentration, and reaches a maximum in the presence of 67 μM Zn^{2+}. DNA cleavage does not reach a maximum at 2 μM or 6.7 μM Zn^{2+} since at those concentrations there is insufficient Zn^{2+} to occupy both binding sites of 7.5 μM $Ru(phen)_2$(DSTM-AP). $Ru(phen)_2$(DSTM-AP) does promote more efficient DNA cleavage than $Ru(phen)_2$(DSTM-AE) in the absence of added Zn^{2+}.

In summary, DNA cleavage is promoted by different ruthenium complexes with tethered metal chelates. The order of the DNA cleavage efficiency of the four ruthenium complexes is $Ru(phen)_2$(DSTM-AP) > $Ru(phen)_2$(DSTM-AE) > $Ru(phen)_2$(DSTM) > $Ru(DIP)_2$(DSTM). Both $Ru(phen)_2$(DSTM-AP) and $Ru(phen)_2$(DSTM-AE) promote more efficient DNA cleavage in the presence of sufficient Zn^{2+} to occupy both metal binding sites. The greater DNA cleavage efficiency of $Ru(phen)_2$DSTM relative to $Ru(DIP)_2$DSTM may be due to the greater water solubility of $Ru(phen)_2$DSTM. The greater DNA cleavage efficiency of $Ru(phen)_2$(DSTM-AP) and $Ru(phen)_2$(DSTM-AE) relative to $Ru(phen)_2$(DSTM) may be due to the protonated dimethylamino groups providing general acid assistance to the leaving group in DNA hydrolysis. The order of DNA cleavage efficiency is therefore consistent with a hydrolytic mechanism for DNA cleavage, but is definitely not proof of such a mechanism.

DNA Cleavage and Product Analysis of the ^{32}P 5'-Radiolabeled Oligonucleotide 5'-CTGGCATACCGGTATGCCAG-3' by $Ru(phen)_2$DSTM, $Ru(phen)_2$(DSTM-AE), and $Ru(phen)_2$(DSTM-AP) (Figure 4.7). The DNA cleavage products of the above ^{32}P 5'-radiolabeled oligonucleotide have been analyzed by

high-resolution polyacrylamide gel electrophoresis in order to study the sequence-selectivity and the 3'-termini produced by the DNA cleavage reaction.

The products of hydrolytic DNA cleavage are either one 5'-phosphate terminus and one 3'-hydroxyl terminus, or one 5'-hydroxyl terminus and one 3'-phosphate terminus. The products of oxidative DNA cleavage are frequently one 5'-phosphate terminus, and either one 3'-phosphate, 3'-phosphoglycolate, or 3'-phosphoglycaldehyde terminus.[18] Since most oxidative DNA cleavage reactions produce a 5'-phosphate terminus, detection of such a terminus is not evidence for DNA hydrolysis. However, since oxidative DNA cleavage is not known to produce hydroxyl termini, the detection of hydroxyl termini *is* strong evidence for hydrolytic cleavage. In this experiment, the Maxam-Gilbert A+G and C+T reactions (lanes C and D) were used as markers for 3'-phosphate termini, and the Maxam-Gilbert reactions treated with T4 polynucleotide kinase in the absence of ATP (lanes I and J) were used as markers for 3'-hydroxyl termini.[15] Hydroxyl termini clearly migrate slower in the gel matrix than their corresponding phosphate termini due to their lesser charge.

It can be seen in Figure 4.7 that $Ru(phen)_2$(DSTM-AP) (lane E), $Ru(phen)_2$(DSTM-AE) (lane F), and $Ru(phen)_2$DSTM (lane G) all promote DNA cleavage in the presence of added Zn^{2+} over the control containing Zn^{2+} alone (lane H). The reaction appears to be base-selective, with the most efficient DNA cleavage at guanine residues. The major cleavage products are 3'-phosphate termini, especially neighboring the guanine residues. Several cleavage products of the ruthenium complexes appear to be neither phosphate nor hydroxyl termini.

It is noteworthy, however, that a band produced by $Ru(phen)_2$(DSTM-AP) (lane E) appears to comigrate with the 3'-hydroxyl terminus at G-4. This 3'-hydroxyl terminus appears to be distinct from the nearby 3'-phosphate terminus at A-5, which migrates slightly faster. This band is produced more efficiently by $Ru(phen)_2$(DSTM-AP) than it

Figure 4.7. Cleavage of the ^{32}P 5'-radiolabeled DNA oligonucleotide 5'-CTGGCATACCGGTATGCCAG-3' by ruthenium complexes. **A:** 13 μM $Ru(phen)_2(DSTM\text{-}AP)$, 100 μM $ZnSO_4$, buffer containing MES, HEPES, CHES, and CAPS (pH 8.4). **B:** DNA only, same buffer. **C & D:** A+G and C+T Maxam-Gilbert reactions, respectively. **E:** 13 μM $Ru(phen)_2(DSTM\text{-}AP)$, 100 μM $ZnSO_4$, trizma buffer (pH 7.8) **F:** 13 μM $Ru(phen)_2(DSTM\text{-}AE)$, 100 μM $ZnSO_4$, trizma buffer. **G:** 13 μM $Ru(phen)_2(DSTM)$, 100 μM $ZnSO_4$, trizma buffer. **H:** 100 μM $ZnSO_4$, trizma buffer. **I & J:** Dephosphorylated A+G and C+T reactions, respectively (hydrolyl termini). Note that fragments with hydroxyl termini migrate slower than the corresponding fragments with phosphate termini.

G-4 OH: Fragment produced by cleavage at G-4, with a 3'-hydroxyl termini. A band produced by $Ru(phen)_2(DSTM\text{-}AP)$ in lane E appears to comigrate with G-4 OH.

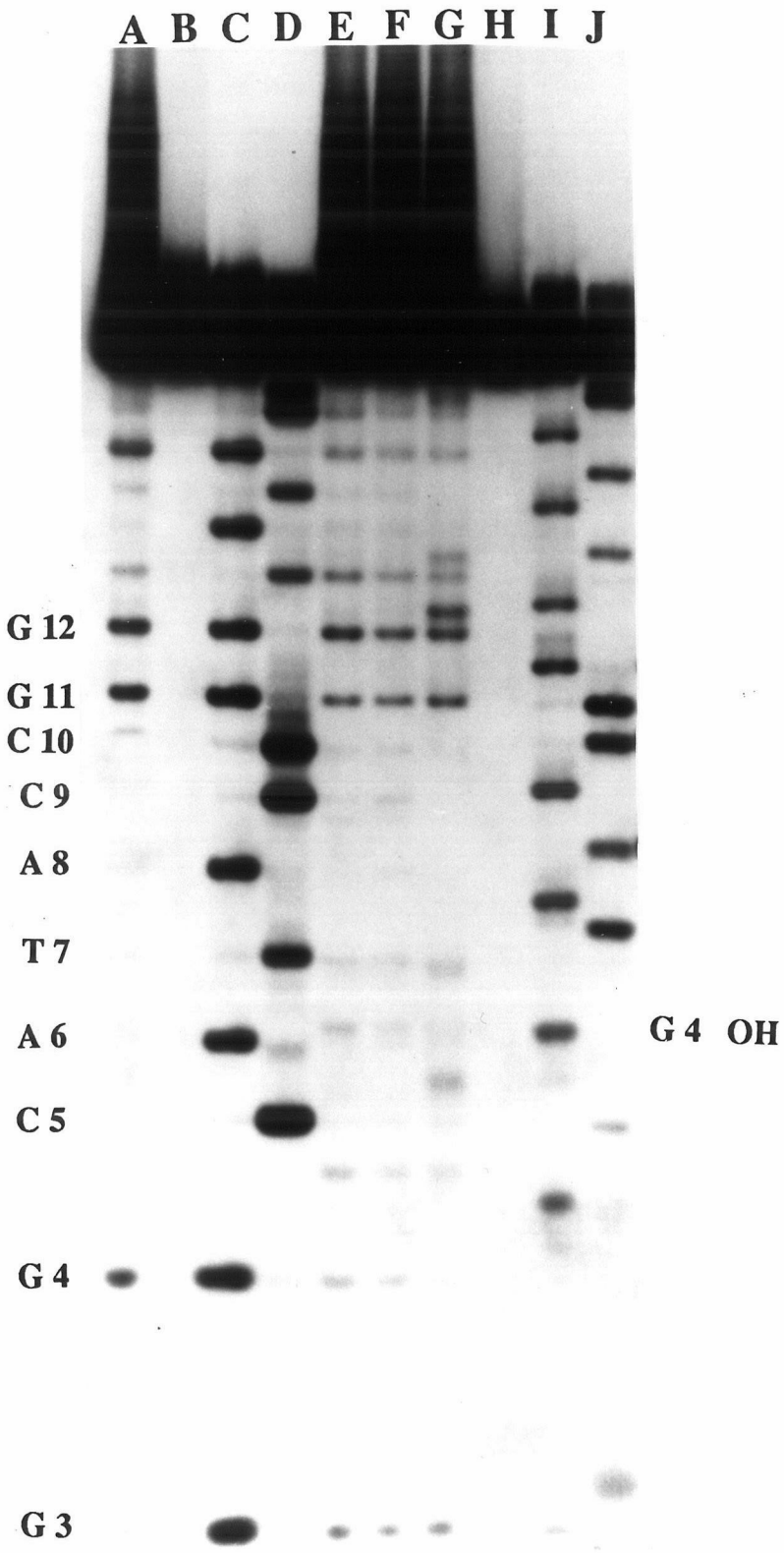
A B C D E F G H I J
G 12
G 11
C 10
C 9
A 8
T 7
A 6
C 5
G 4
G 3
G 4 OH

is by $Ru(phen)_2$(DSTM-AE) (lane F) or by $Ru(phen)_2$(DSTM) (lane G). The production of this band by $Ru(phen)_2$(DSTM-AP) appears to be sensitive to reaction conditions since in a different buffer system and at a slightly higher pH (8.4 rather than 7.8), less of this product can be detected (lane A). In lane A, 3'-phosphate termini at guanine residues are produced more efficiently, and all other termini are produced less efficiently. It should be noted that in reaction samples where ruthenium complex is present, the intense band at the top of the polyacrylamide gel due to intact oligonucleotide is partially retarded. This is also observed in Figure 4.8 .

The scarcity of 3'-hydroxyl termini indicates that unless a hydrolytic cleavage reaction is stereoselectively producing 5'-hydroxyl termini, the major cleavage reaction pathway is not hydrolytic. Since it is not likely that these ruthenium complexes would bind to DNA in a highly base-selective manner, the selectivity of the cleavage reaction for guanine residues indicates that the major reaction pathway involves chemistry at the DNA base, rather than at the DNA phosphate or the DNA sugar. The apparent production of a 3'-hydroxyl terminus at G-4, and the greater efficiency of its production by $Ru(phen)_2$(DSTM-AP) relative to $Ru(phen)_2$(DSTM-AE) and $Ru(phen)_2$DSTM indicates that phosphodiester hydrolysis may be a minor pathway of the DNA cleavage reaction. It should be stressed that this result is preliminary, and that further experiments would be needed to establish that phosphodiester hydrolysis is even a minor pathway.

DNA Cleavage and Product Analysis of the ^{32}P 3'-Radiolabeled Oligonucleotide 5'-CTGGCATACCGGTATGCCAG-3' by $Ru(phen)_2$(DSTM-AP) (Figure 4.8). The DNA cleavage products of the above ^{32}P 3'-radiolabeled oligonucleotide have been analyzed in order to study the sequence-selectivity and the 5'-termini produced by the DNA cleavage reaction. $Ru(phen)_2$(DSTM-AP) clearly promotes efficient DNA cleavage in the presence of Zn^{2+} (lane I) over the control

containing Zn^{2+} alone. $Ru(phen)_2(DSTM\text{-}AP)$ promotes less efficient DNA cleavage in the absence of Zn^{2+} (lane K) than in its presence. EDTA was present in the reaction sample loaded in lane K in order to reduce the possible binding of trace divalent metal ions to $Ru(phen)_2(DSTM\text{-}AP)$. $EuCl_3$ (lane E) and $NiSO_4$ (lane G) appear to inhibit DNA cleavage by $Ru(phen)_2(DSTM\text{-}AP)$. When the pipetting was done in the darkroom under greatly reduced light, $Ru(phen)_2(DSTM\text{-}AP)$ did not promote DNA cleavage in either the presence of Zn^{2+} (lane A) or the presence of EDTA (lane C). The products of the DNA cleavage reaction are almost exclusively 5'-phosphate termini. The reaction is highly base-selective, with the most efficient DNA cleavage at guanine residues, and the second-most efficient DNA cleavage at thymine residues.

The almost exclusive production of 5'-phosphate termini (coupled with the scarcity of 3'-hydroxyl termini detected in Figure 4.7) indicates that the major DNA cleavage reaction pathway is not phosphodiester hydrolysis. The high base-selectivity of the cleavage reaction indicates that DNA base chemistry is involved in the reaction pathway. The selectivity of the cleavage reaction for first guanine residues, and then thymine residues is consistent with a singlet oxygen mediated reaction, since the reactivity of DNA bases with singlet oxygen follows the order $G > T > C \approx A$.[19] Since ruthenium complexes are known to promote the formation of singlet oxygen in the presence of visible light,[20] the pipetting for the reactions loaded in lanes A-D was done in the darkroom. The reduced exposure of the samples to visible light resulted in the elimination of the DNA cleavage reaction. When DNA was exposed to visible light for 14 hours at 37 °C in the presence of $Ru(phen)_2(DSTM\text{-}AP)$ and Zn^{2+}, greatly increased DNA cleavage was observed (data not shown). These experiments confirm that the major DNA cleavage reaction pathway of $Ru(phen)_2(DSTM\text{-}AP)$ involves the production of singlet oxygen by ruthenium and visible light, followed by singlet oxygen

Figure 4.8. Cleavage of the ^{32}P 3'-radiolabeled DNA oligonucleotide 5'-CTGGCATACCGGTATGCCAG-3' by $Ru(phen)_2(DSTM\text{-}AP)$. **A-D:** Samples prepared in the darkroom under greatly reduced light. **E-L:** Samples exposed to room light for 20-25 minutes. **A & I:** 5 μM $Ru(phen)_2(DSTM\text{-}AP)$, 100 μM $ZnSO_4$. **B & J:** 100 μM $ZnSO_4$. **C & K:** 5 μM $Ru(phen)_2(DSTM\text{-}AP)$, 100 μM EDTA. **D & L:** 100 μM EDTA. **E:** 5 μM $Ru(phen)_2(DSTM\text{-}AP)$, 100 μM $EuCl_3$. **F:** 100 μM $EuCl_3$. **G:** 5 μM $Ru(phen)_2(DSTM\text{-}AP)$, 100 μM $NiSO_4$. **H:** 100 μM $NiSO_4$.

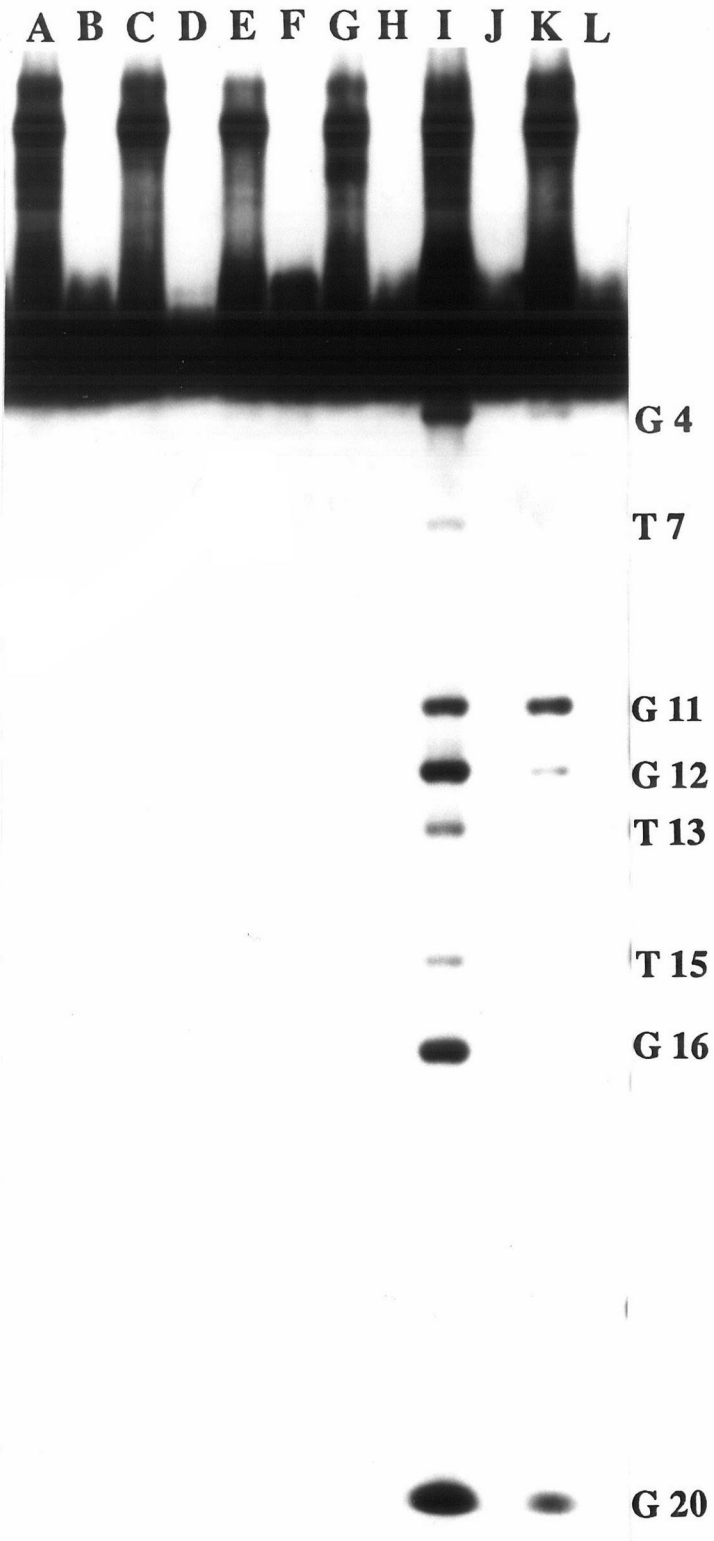
A B C D E F G H I J K L
G 4
T 7
G 11
G 12
T 13
T 15
G 16
G 20

mediated oxidation of the DNA base. However, hydrolytic DNA cleavage should not be ruled out as a possible minor pathway.

Generally, the efficiency of DNA cleavage promoted by ruthenium complexes and mediated by singlet oxygen is substantially enhanced by subsequent alkali treatment.[21] The DNA cleavage efficiency of the ruthenium complexes $Ru(phen)_2DSTM$, $Ru(phen)_2$(DSTM-AE), and $Ru(phen)_2$(DSTM-AP) observed here, however, is unusually large considering that the reactions were not treated with alkali. It is possible that the tethered metal chelates can substitute for alkali treatment by promoting DNA strand scission subsequent to the singlet oxygen mediated oxidative attack on the DNA base. Furthermore, in the case of $Ru(phen)_2$(DSTM-AE) and $Ru(phen)_2$(DSTM-AP), this strand scission is enhanced by the presence of Zn^{2+}. Possible mechanisms for this interesting chemistry are described in the discussion section.

Time Course of the DNA Cleavage Reaction of $Rh(phi)_2$(DSTM-AP) (Figure 4.9). The time course of the DNA cleavage reaction of $Rh(phi)_2$(DSTM-AP) has also been studied by agarose gel electrophoresis. $Rh(phi)_2$(DSTM-AP) in the presence of $ZnSO_4$ clearly promotes increasing DNA cleavage with increasing incubation time. The DNA cleavage percentages greater than 100 result from the production of significant amounts of linearized plasmid by $Rh(phi)_2$(DSTM-AP) at longer times (the calculation method for "% cleavage" is described in the experimental section). Overall, at long reaction times $Rh(phi)_2$(DSTM-AP) appears to promote far more efficient cleavage of plasmid DNA than the ruthenium complexes discussed previously. Preliminary results indicate that $Rh(phi)_2$(DSTM-AP) also promotes comparable DNA cleavage in the absence of added divalent metal ion or in the presence of $CoSO_4$, but not in the presence of $NiSO_4$ (data not shown). The DNA photonuclease $Rh(phi)_2bpy^{3+}$,[22] which does not have tethered metal chelates or dimethylamino groups,

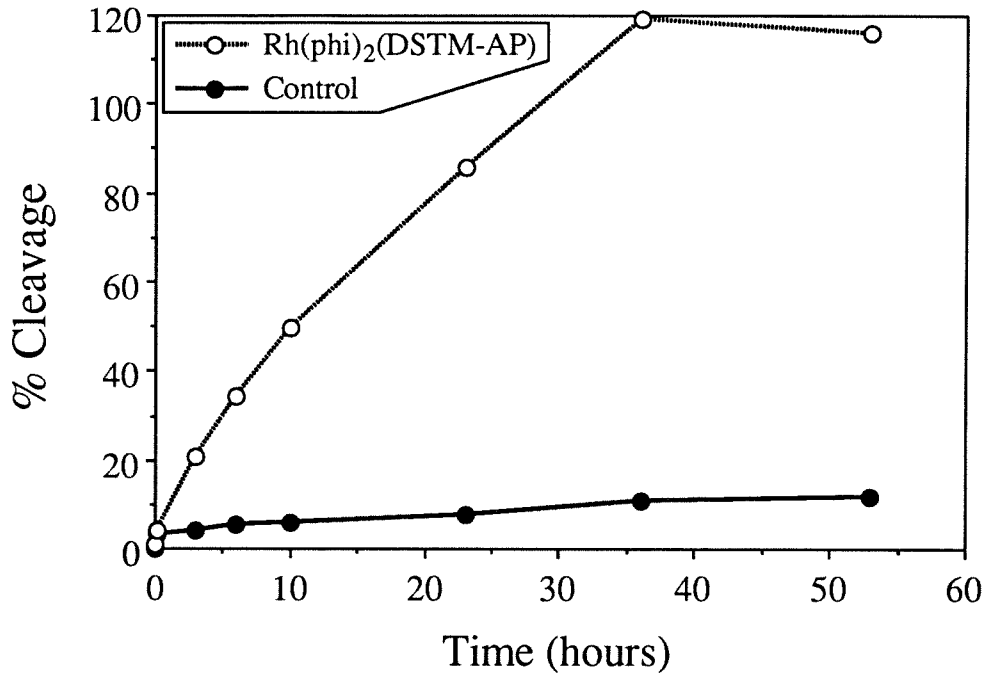

Figure 4.9. DNA Cleavage of $Rh(phi)_2(DSTM\text{-}AP)$ as a Function of Reaction Time. Conditions: 13 mM trizma·H_2SO_4, 2.6 mM Na_2SO_4, 20 μM base pairs pBR322, 200 μM $ZnSO_4$. 4 μM $Rh(phi)_2(DSTM\text{-}AP)$ was compared to controls without rhodium complex.

promotes no DNA cleavage when incubated under the same conditions as $Rh(phi)_2$(DSTM-AP) (data not shown).

The complex $Rh(phi)_2$(DSTM-AP) has two important differences from $Ru(phen)_2$(DSTM-AP). Firstly, the phenanthrenequinonediimine (phi) ligands of $Rh(phi)_2$(DSTM-AP) tightly bind to DNA by intercalating between the DNA base pairs.[23] Secondly, rhodium complexes are not known to promote singlet oxygen chemistry with photolysis. The DNA cleavage reaction of $Rh(phi)_2$(DSTM-AP) is clearly a gradual reaction that takes place in the dark at 37 °C over the course of 1 to 2 days. $Rh(phi)_2$(DSTM-AP) therefore appears to be a highly promising candidate with respect to the development of molecules that promote DNA hydrolysis. A similar reaction profile as a function of incubation time was not observed with the ruthenium complexes, where the exposure of the reactions to room light during sample preparation was the more important variable.

DNA Cleavage and Product Analysis of the ^{32}P 5'-Radiolabeled Oligonucleotide 5'-CTGGCATACCGGTATGCCAG-3' by $Rh(phi)_2$(DSTM-AP) (Figure 4.10). The DNA cleavage reactions of $Rh(phi)_2$(DSTM-AP) have been studied by high-resolution polyacrylamide gel electrophoresis, and compared to the DNA cleavage reaction of $Rh(phi)_2bpy^{3+}$. Upon irradiation with UV light, $Rh(phi)_2bpy^{3+}$ (lane C) and $Rh(phi)_2$(DSTM-AP) (lane D) both promote efficient DNA cleavage when compared to DNA irradiated alone (lane E). In the presence of copper, 2-mercaptoethanol, and H_2O_2, $Rh(phi)_2$(DSTM-AP) (lane G) and 1,10-phenanthroline (lane H) promote efficient DNA cleavage, while $Rh(phi)_2bpy$ (lane F) and copper alone (lane I) do not. However, $Rh(phi)_2$(DSTM-AP) promoted no DNA cleavage (lanes K-M and P-R) when incubated with the oligonucleotide for 22 hours under conditions comparable to those used to promote cleavage of plasmid DNA (Figure 4.9). Neither

Figure 4.10. Cleavage of the ^{32}P 5'-radiolabeled DNA oligonucleotide 5'-CTGGCATACCGGTATGCCAG-3' by $Rh(phi)_2(DSTM\text{-}AP)$. **A & B:** A+G and C+T Maxam-Gilbert reactions, respectively. **C:** 3 μM $Rh(phi)_2bpy^{3+}$, irradiated 6 minutes at 310 nm. **D:** 3 μM $Rh(phi)_2(DSTM\text{-}AP)$, irradiated 6 minutes at 310 nm. **E:** DNA only, irradiated 6 minutes at 310 nm. **F:** 3 μM $Rh(phi)_2bpy^{3+}$, 9 μM $CuSO_4$, 200 μM 2-mercaptoethanol, 200 μM H_2O_2. **G:** 3 μM $Rh(phi)_2(DSTM\text{-}AP)$, 9 μM $CuSO_4$, 200 μM 2-mercaptoethanol, 200 μM H_2O_2. **H:** 12 μM 1,10-phenanthroline, 3 μM $CuSO_4$, 200 μM 2-mercaptoethanol, 200 μM H_2O_2. **I:** 9 μM $CuSO_4$, 200 μM 2-mercaptoethanol, 200 μM H_2O_2. **J:** 5 μM $Rh(phi)_2(bpy)$, 200 μM $ZnSO_4$. **K:** 2 μM $Rh(phi)_2(DSTM\text{-}AP)$, 200 μM $ZnSO_4$. **L:** 5 μM $Rh(phi)_2(DSTM\text{-}AP)$, 200 μM $ZnSO_4$. **M:** 12 μM $Rh(phi)_2(DSTM\text{-}AP)$, 200 μM $ZnSO_4$. **N:** 200 μM $ZnSO_4$. **O:** 5 μM $Rh(phi)_2(bpy)$, 200 μM $CoSO_4$. **P:** 2 μM $Rh(phi)_2(DSTM\text{-}AP)$, 200 μM $CoSO_4$. **Q:** 5 μM $Rh(phi)_2(DSTM\text{-}AP)$, 200 μM $CoSO_4$. **R:** 12 μM $Rh(phi)_2(DSTM\text{-}AP)$, 200 μM $CoSO_4$. **S:** 200 μM $CoSO_4$. **T & U:** Dephosphorylated A+G and C+T Maxam-Gilbert reactions, respectively.

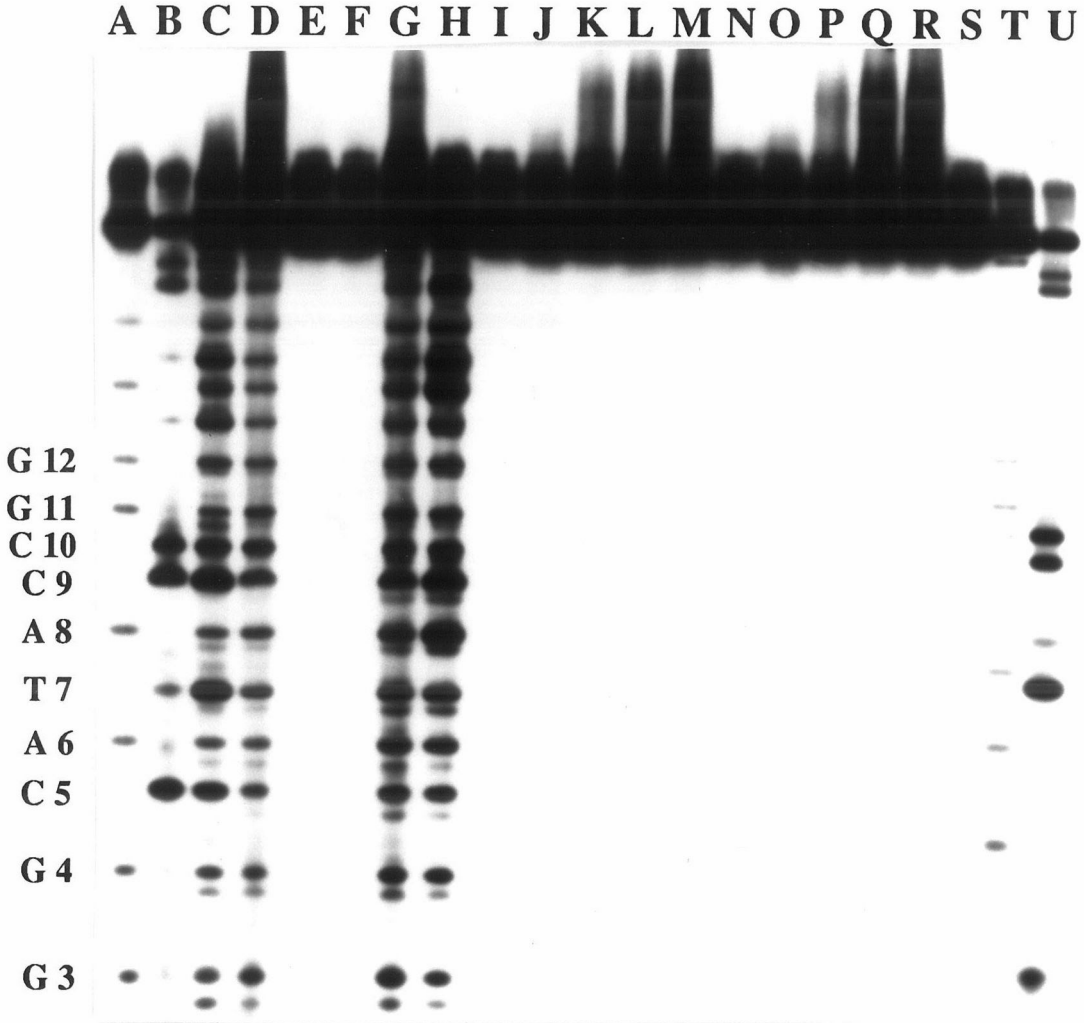
A B C D E F G H I J K L M N O P Q R S T U
G 12
G 11
C 10
C 9
A 8
T 7
A 6
C 5
G 4
G 3

high concentrations of $Rh(phi)_2(DSTM\text{-}AP)$ (12 μM; lanes M and R), the presence of $ZnSO_4$ (lanes K-M), nor the presence of $CoSO_4$ (lanes P-R) resulted in any DNA cleavage.

The DNA cleavage chemistry of $Rh(phi)_2(DSTM\text{-}AP)$ is entirely consistent with the structure of the complex. $Rh(phi)_2(DSTM\text{-}AP)$ promotes DNA photocleavage with efficiency comparable to that of its structural analogue $Rh(phi)_2bpy^{3+}$. The mechanism of photocleavage of DNA by $Rh(phi)_2bpy^{3+}$ is thought to be the attack of a phi-centered cation radical on the DNA sugar.[22] $Rh(phi)_2(DSTM\text{-}AP)$ promotes copper-activated oxidative DNA cleavage in a manner similar to that of its structural analogue $Ru(DIP)_2DSTM$, which also has a pair of tethered bis(2-picolyl)amine chelating groups. The copper-activated DNA cleavage reaction of $Ru(DIP)_2DSTM$ is described in chapter 3. $Rh(phi)_2bpy^{3+}$, which does not have tethered chelating groups, does not promote copper-activated DNA cleavage. The efficiency of the copper-activated DNA cleavage reaction of $Rh(phi)_2(DSTM\text{-}AP)$ appears to be greater than that of $Ru(DIP)_2DSTM$ under comparable conditions. This is consistent with the tighter, intercalative binding mode of the phi ligands of $Rh(phi)_2(DSTM\text{-}AP)$, which would be expected to reduce the entropic penalty required for the approach of the reactive copper to the DNA substrate. However, the gradual cleavage of plasmid DNA by $Rh(phi)_2(DSTM\text{-}AP)$ in the presence of Zn^{2+} appears to be almost entirely absent under similar reaction conditions when the DNA substrate is changed to an oligonucleotide.

When the reaction temperature was increased to 51 °C, $Rh(phi)_2(DSTM\text{-}AP)$ did promote cleavage of the above DNA oligonucleotide in both the presence and the absence of $ZnSO_4$ over the course of 1-3 days (data not shown). The higher reaction temperature resulted in the reaction samples drying out over the course of the incubation. The DNA cleavage was sequence neutral, and the products of the DNA cleavage reaction appeared to be a mixture of 3'-phosphate and 3'-phosphoglycolate termini. The sequence neutral

nature of the DNA cleavage indicates that the DNA bases are not the target of the cleavage reaction. Since 3'-hydroxyl termini were not observed, the cleavage reaction is not likely to be phosphodiester hydrolysis unless the hydrolysis is stereoselective and results in the production of 3'-phosphate and 5'-hydroxyl termini only. The target of the cleavage reaction is therefore likely to be the DNA sugar, although it is difficult to understand the nature of the reactive species, since the reaction samples were not irradiated with UV light, nor were redox-active metals (such as copper) or reagents (such as thiols or H_2O_2) present in the reaction mixture. It should be stressed that the above analysis of the products of the DNA cleavage reaction of $Rh(phi)_2$(DSTM-AP) is preliminary, and the mechanism of the reaction should be investigated further.

4.4. Discussion

DNA hydrolysis is a difficult reaction to achieve under mild conditions due to the negative charge and resonance stabilization of the phosphate, and the poor alkoxide leaving group. In the development of synthetic molecules that promote DNA hydrolysis, the catalytic amino acid residues and the divalent metal ions utilized by nucleolytic enzymes should be modeled. The function of reactive groups involved in promoting DNA hydrolysis can be divided into four categories: (i) Binding to the DNA substrate; (ii) Neutralization of the negative charge on the phosphate to allow nucleophiles to approach the phosphorus; (iii) Providing a coordinated nucleophile to attack the phosphorus and gain an intramolecular entropic advantage; and (iv) General acid assistance to the alkoxide leaving group.

The five complexes $Ru(DIP)_2$DSTM, $Ru(phen)_2$DSTM, $Ru(phen)_2$(DSTM-AE), $Ru(phen)_2$(DSTM-AP), and $Rh(phi)_2$(DSTM-AP) have been designed with these four categories in mind. All five complexes have a high binding affinity for DNA due to

their hydrophobicity, high positive charge, and intercalative potential. The affinity of the complexes for DNA would be further increased by the presence of additional labile divalent metal ions bound to the bis(2-picolyl)amine chelating groups. $Rh(phi)_2$(DSTM-AP) also has two phenanthrenequinonediimine (phi) ligands that bind tightly to DNA through intercalative stacking.[23] The DNA-binding moieties of these complexes serve to deliver functional groups to the DNA phosphate backbone to promote cleavage.

All five complexes have two tethered bis(2-picolyl)amine chelating groups. Additional labile metal ions bound to these groups have the potential to promote DNA hydrolysis by either providing a coordinated hydroxide nucleophile, neutralizing the negative charge on the phosphate, or both. A mechanism involving both a coordinated hydroxide and charge neutralization has been proposed for the hydrolysis of model phosphodiesters with good leaving groups by the simple metal complexes $Cu(bpy)^{2+}$, $Ni(tren)^{2+}$, and $Co(cyclen)^{2+}$.[1,5,6] However, the complexes $Ru(phen)_2$(DSTM-AE), $Ru(phen)_2$(DSTM-AP), and $Rh(phi)_2$(DSTM-AP) also have the potential to promote DNA hydrolysis through general acid assistance to the poor alkoxide leaving group by a protonated dimethylamino group. If the mechanism of phosphate hydrolysis is in-line nucleophilic displacement, then the leaving group needs to be opposite to the incoming nucleophile in the trigonal bipyramidal transition state.[24] If the mechanism is in-line nucleophilic displacement, and if the nucleophile is a hydroxide coordinated to a metal bound to the bis(2-picolyl)amine group, then $Ru(phen)_2$(DSTM-AP) and $Rh(phi)_2$(DSTM-AP) (with three methylene groups in the linker between the sulfonamide and the dimethylamino groups) might be expected to be better nucleases than $Ru(phen)_2$(DSTM-AE), where the linker of two methylene groups might be insufficient to reach the leaving group. Some possible routes for phosphodiester hydrolysis by these complexes are illustrated in Figure 4.11.

Figure 4.11. Possible Mechanisms for the Promotion of Phosphodiester Hydrolysis by Transition Metal Complexes in the Presence of Zn^{2+}

Coordinated hydroxide

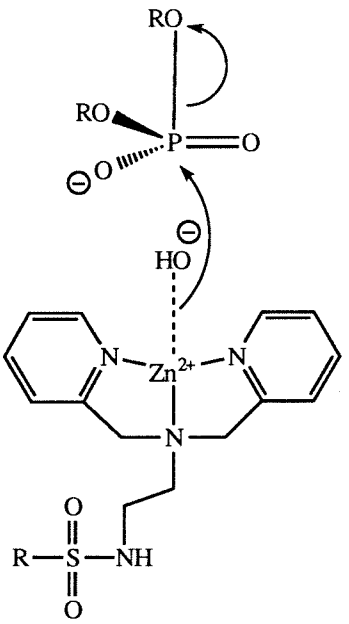

Charge neutralization

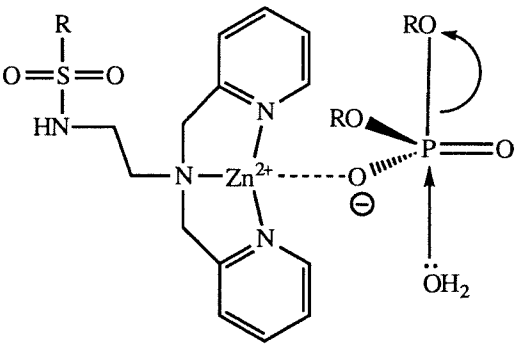

Coordinated hydroxide and charge neutralization

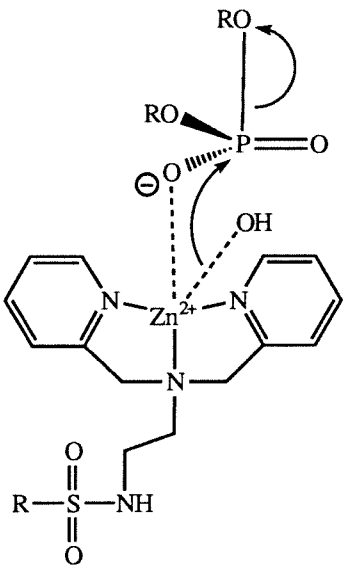

Coordination hydroxide, charge neutralization, and genaral acid assistance to the leaving group

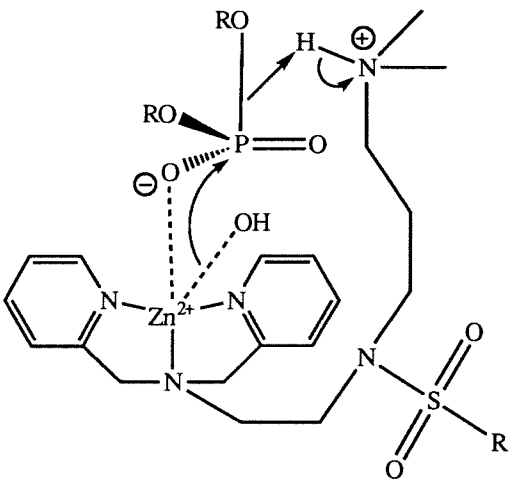

The cleavage efficiency of the five complexes on the DNA plasmid pBR322 in the presence of additional labile metal ions has been assayed by agarose gel electrophoresis. Zn^{2+} was used as the additional metal for many of the experiments since it is less likely to promote oxidative DNA cleavage, although Co^{2+}, Ni^{2+}, and no additional metal were also explored. The plasmid experiments have shown that the order of DNA cleavage efficiency is $Ru(phen)_2$(DSTM-AP) > $Ru(phen)_2$(DSTM-AE) > $Ru(phen)_2$(DSTM) > $Ru(DIP)_2$DSTM, and that DNA cleavage by $Ru(phen)_2$(DSTM-AP) and $Ru(phen)_2$(DSTM-AE) is enhanced by the presence of Zn^{2+}. The low aqueous solubility of $Ru(DIP)_2$DSTM and the dimethylamino groups of $Ru(phen)_2$(DSTM-AP) and $Ru(phen)_2$(DSTM-AE) and the observed order of DNA cleavage efficiency are consistent with a hydrolytic mechanism. However, the analysis of the cleavage of a DNA oligonucleotide has shown that primarily 3'- and 5'-phosphate termini are produced by the cleavage reaction, that the base-selectivity of the DNA cleavage is G > T > C ≈ A, and that little or no cleavage was observed when the samples were prepared in the darkroom (Figures 4.7 and 4.8). This indicates that the primary cleavage pathway of the oligonucleotide involves singlet oxygen mediated attack on the DNA base. The singlet oxygen was produced by the reaction of the ruthenium metal center with room light. Since the length of time that the samples were exposed to room light during their preparation varied from experiment to experiment, the different DNA cleavage efficiency of $Ru(phen)_2$DSTM observed in graphs A and B of Figure 4.5 is understandable.

It is important to recognize, however, that the DNA cleavage chemistry on an oligonucleotide may be fundamentally different from that on a plasmid. For example, the supercoiled stress present in plasmids may facilitate hydrolytic chemistry. Furthermore, technical differences between experiments may result in different cleavage reaction pathways. It is possible that the safety precautions used for work with radiolabeled

oligonucleotides result in longer exposure of the samples to light and therefore a greater degree of singlet oxygen mediated chemistry.

The efficiency of the DNA cleavage reaction of $Ru(phen)_2$(DSTM-AP) and $Ru(phen)_2$(DSTM-AE) appears to be high considering that the reaction samples were neither irradiated with light nor were they treated with alkali. The attack of singlet oxygen on the DNA base does not by itself produce strand scission. It may, however, produce an aldehydic abasic site that can be later cleaved by alkali treatment.[20] It is possible that the efficient DNA cleavage promoted by $Ru(phen)_2$(DSTM-AP) and $Ru(phen)_2$(DSTM-AE) is due to the functional groups of the ruthenium complexes substituting for alkali treatment. The bound Zn^{2+} could polarize the carbonyl of the aldehydic abasic site so as to increase the acidity of the C2' DNA sugar protons. The dimethylamino groups, which would be partially unprotonated even at pH 7.8, could act as a general base to facilitate DNA strand scission. These mechanisms are illustrated in Figure 4.12. These mechanisms are related to that of *E. coli* endonuclease III, except that the enzyme activates the abasic site for β-elimination by the formation of a Schiff base with the aldehyde carbonyl.[25] Higher reaction pH would increase the efficiency of strand scission by increasing the fraction of dimethylamino groups in the unprotonated state, but would decrease the ruthenium mediated formation of singlet oxygen itself.[21] These possible mechanisms could be investigated further by testing the cleavage reaction of $Ru(phen)_2$(DSTM-AP) on a pre-existing abasic DNA site. The cleavage experiment on the pre-existing abasic site could be conducted with $Rh(phi)_2$(DSTM-AP) in order to eliminate the singlet oxygen chemistry. Hence these complexes may offer interesting mimics of endonuclease III.

Figure 4.12. Possible Mechanisms for DNA Strand Scission Subsequent to the Formation of an Abasic Site

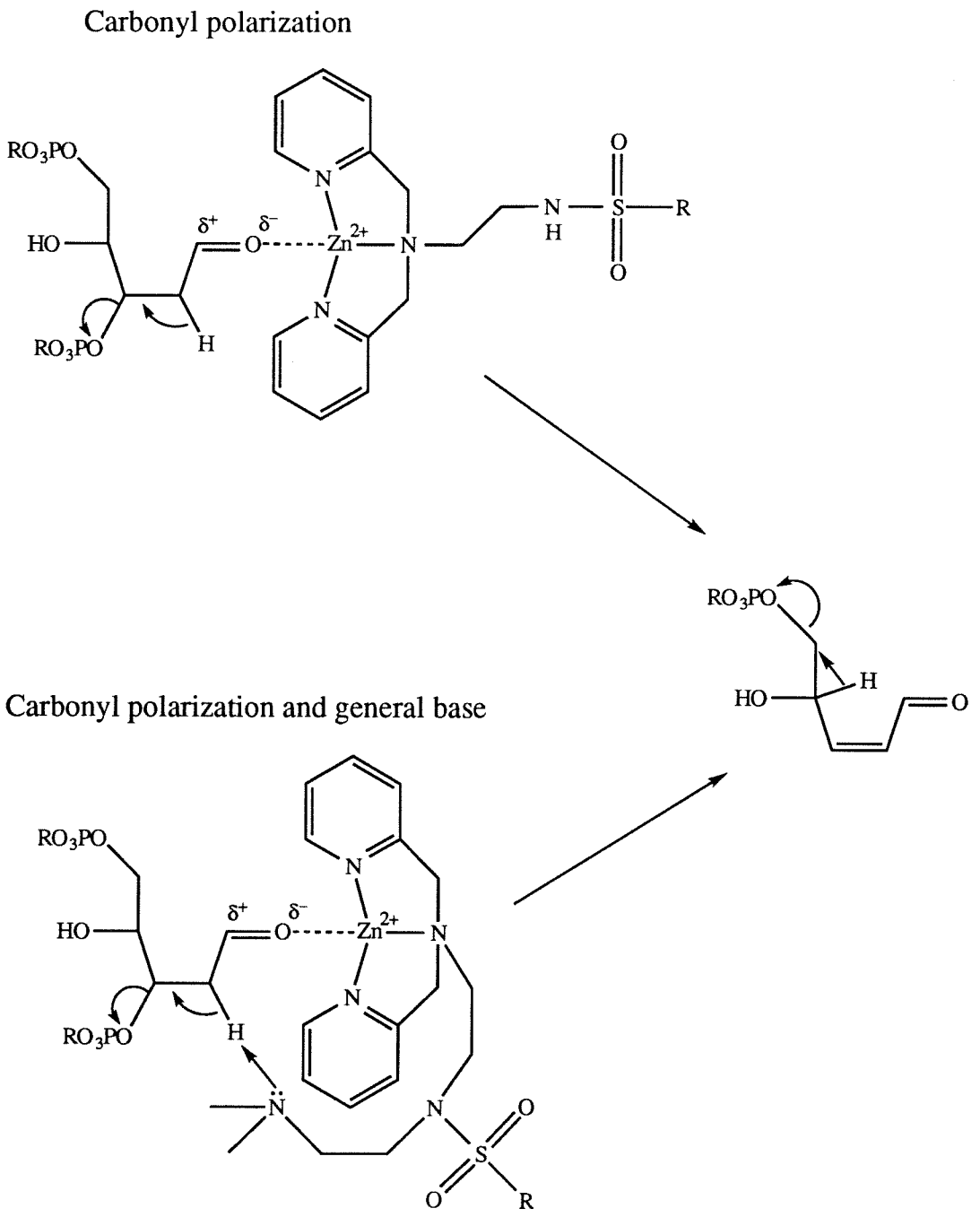

$Ru(phen)_2$(DSTM-AP) showed some promise for hydrolytic DNA cleavage (the apparent production of a 3'-hydroxyl terminus at G-4 in Figure 4.7), but any potential hydrolytic reaction was obscured by the more efficient singlet oxygen mediated reaction. $Rh(phi)_2$(DSTM-AP) was therefore investigated for its potential to promote DNA hydrolysis in the absence of singlet oxygen chemistry. The functional groups of the DSTM-AP ligand were retained, while the change of the metal center from ruthenium to rhodium eliminates the singlet oxygen reaction. The two phi ligands of $Rh(phi)_2$(DSTM-AP) also could provide a tighter intercalative binding mode that would tend to bring the reactive groups of the DSTM-AP ligand closer to the phosphate. The initial results showed that the complex promotes cleavage of the DNA plasmid pBR322 as a function of incubation time in the dark (Figure 4.9). This result is highly promising, although the lack of dependence of the cleavage on the presence of additional metal ions is puzzling. However, $Rh(phi)_2$(DSTM-AP) was surprisingly inefficient at promoting cleavage of a DNA oligonucleotide (Figure 4.10), even considering that DNA plasmid cleavage is a far more sensitive assay (the conversion of pBR322 from form I to form II only requires a single cleavage event in 4363 base pairs). A different reaction is perhaps being observed in the plasmid experiment compared to that in the oligonucleotide experiment. When incubated at a higher temperature, $Rh(phi)_2$(DSTM-AP) did promote DNA oligonucleotide cleavage, however. A preliminary experiment indicated that the cleavage reaction is sequence neutral, and produces a mixture of 3'-phosphate and 3'-phosphoglycolate termini. These products are consistent with oxidative attack on the DNA sugar, although it is difficult to understand how such chemistry could be initiated in the absence of added redox-active metals and reagents, and in the absence of irradiation with UV light. If $Rh(phi)_2$(DSTM-AP) does prove to promote oxidative DNA cleavage by a novel reaction pathway, then further investigation should be conducted in order to understand the nature of the pathway. Such investigation would include further product

analysis by HPLC and PAGE, and DNA plasmid cleavage assays to study more thoroughly the effect of additional labile metals and other reagents on DNA cleavage efficiency.

It is important to recognize that the mechanism of DNA cleavage by $Rh(phi)_2$(DSTM-AP) on plasmid DNA may be different from the mechanism of DNA cleavage on DNA oligonucleotides. It is possible that $Rh(phi)_2$(DSTM-AP) promotes efficient hydrolytic cleavage of DNA plasmids where supercoiled stress is present, and inefficient oxidative cleavage of DNA oligonucleotides, where supercoiled stress is absent. However, product analysis to establish a hydrolytic mechanism for DNA plasmid cleavage would be difficult unless the cleavage were site-selective. An alternate approach would be to design and synthesize rhodium complexes related to $Rh(phi)_2$(DSTM-AP), and study the effect of structure on DNA cleavage efficiency in a manner similar to that done for the ruthenium complexes.

4.5. Conclusions

The five complexes $Ru(DIP)_2$DSTM, $Ru(phen)_2$DSTM, $Ru(phen)_2$(DSTM-AE), $Ru(phen)_2$(DSTM-AP), and $Rh(phi)_2$(DSTM-AP) have been investigated for their potential to promote DNA hydrolysis. The four ruthenium complexes promote DNA cleavage in the presence of additional labile metal ions. The complexes $Ru(phen)_2$(DSTM-AP) and $Ru(phen)_2$(DSTM-AE) with tethered dimethylamino groups promote the more efficient DNA cleavage. The primary DNA cleavage pathway of the ruthenium complexes appears to be an attack by singlet oxygen on the DNA base, mediated by the ruthenium metal and visible light. The mechanism of strand scission subsequent to the attack of singlet oxygen on the DNA base may involve both the additional labile metal ions and the dimethylamino groups, and should be investigated

further. $Ru(phen)_2(DSTM\text{-}AP)$ may also promote DNA hydrolysis as a secondary pathway.

$Rh(phi)_2(DSTM\text{-}AP)$ promotes efficient cleavage of plasmid DNA at micromolar concentrations as a function of time. $Rh(phi)_2(DSTM\text{-}AP)$ promotes less efficient cleavage of oligonucleotide DNA. The chemical pathways responsible for these are not understood. $Rh(phi)_2(DSTM\text{-}AP)$ should be investigated further in order to understand the nature of its interesting DNA cleavage reaction, whether it be hydrolytic or a novel chemical pathway leading to oxidative DNA cleavage.

References

1. J. R. Morrow & W. C. Trogler (1988) *Inorg. Chem.* **27:** 3387-3394.
2. L. A. Basile & J. K. Barton (1989) "Metallonucleases: Real and Artificial" Sigel, H.; Sigel, A., eds. *Metal Ions in Biological Systems,* vol. 25 (Marcal Dekker, Inc.: New York) 31-103.
3. D. M. Kneeland, K. Ariga, V. M. Lynch, C.-Y. Huang, & E. V. Anslyn (1993) *J. Am. Chem. Soc.*, **115:** 10042-10055.
4. J. O. Edwards & R. G. Pearson (1962) *J. Am. Chem. Soc.* **84:** 16-24.
5. M. A. De Rosch & W. A. Trogler (1990) *Inorg. Chem.* **29:** 2409-2416.
6. J. H. Kim & J. Chin (1992) *J. Am. Chem. Soc.* **114:** 9792-9795.
7. A. Streitwieser Jr.& C. H. Heathcock (1981) "Introduction to Organic Chemistry, 2nd Edition" MacMillan, New York, 998.
8. F. A. Menger & M. Ladika (1987) *J. Am. Chem. Soc.* **109:** 3145-3146.
9. Breslow, R.; Singh, S. (1988) *Bioorganic Chemistry* **16:** 408-417.
10. J. Chin, M. Banaszczyk, V. Jubian, & X. Zou (1989) *J. Am. Chem. Soc.* **111:** 186-190.
11. G. L. Eichorn, E. Tarien, & J. J. Butzow (1971) *Biochemistry*, **10:** 2014-2027.
12. J. R. Morrow, L. A. Buttrey, V. M. Shelton, and K. A. Berback (1992) *J. Am. Chem. Soc.* **114:** 1903-1905.
13. J. Smith, K. Ariga, & E. V. Anslyn (1993) *J. Am. Chem. Soc.* **115:** 362-364.
14. L. A. Basile & J. K. Barton (1987) *J. Am. Chem. Soc.* **109:** 7548-7549.
15. A. M. Pyle (1989) Ph.D. Thesis, Columbia University, 122.
16. R. P. Hertzberg & P. B. Dervan (1984) *Biochemistry*, **23:** 3934-3945.
17. P. Vanysek (1986) "CRC Handbook of Chemistry and Physics, 67th Edition" R. C. Weast, M. J. Astle, & W. H. Beyer, eds., CRC Press, Inc., Boca Raton, Florida, D-151 to D-155.

18. J. Stubbe & J. W. Kozarich (1987) *Chem. Rev.* **87:** 1107-1136.

19. J. Cadet & R. Teoule (1978) *Photochem. Photobiol.* **28:** 661-667.

20. M. B. Fleisher (1988) Ph.D. Thesis, Columbia University, 165-167.

21. Ibid., 38-39.

22. A. Sitlani, E. C. Long, A. M. Pyle, & J. K. Barton (1992) *J. Am. Chem. Soc.* **114:** 2303-2312.

23. S. S. David & J. K. Barton (1993) *J. Am. Chem. Soc.* **115:** 2984-2985.

24. A. Fersht (1985) "Enzyme Structure and Mechanism, 2nd Edition" W. H. Freeman and Company, New York, 235-239.

25. S. Boiteux (1993) *J. Photochem. Photobiol. B: Biol.* **19:** 87-96.